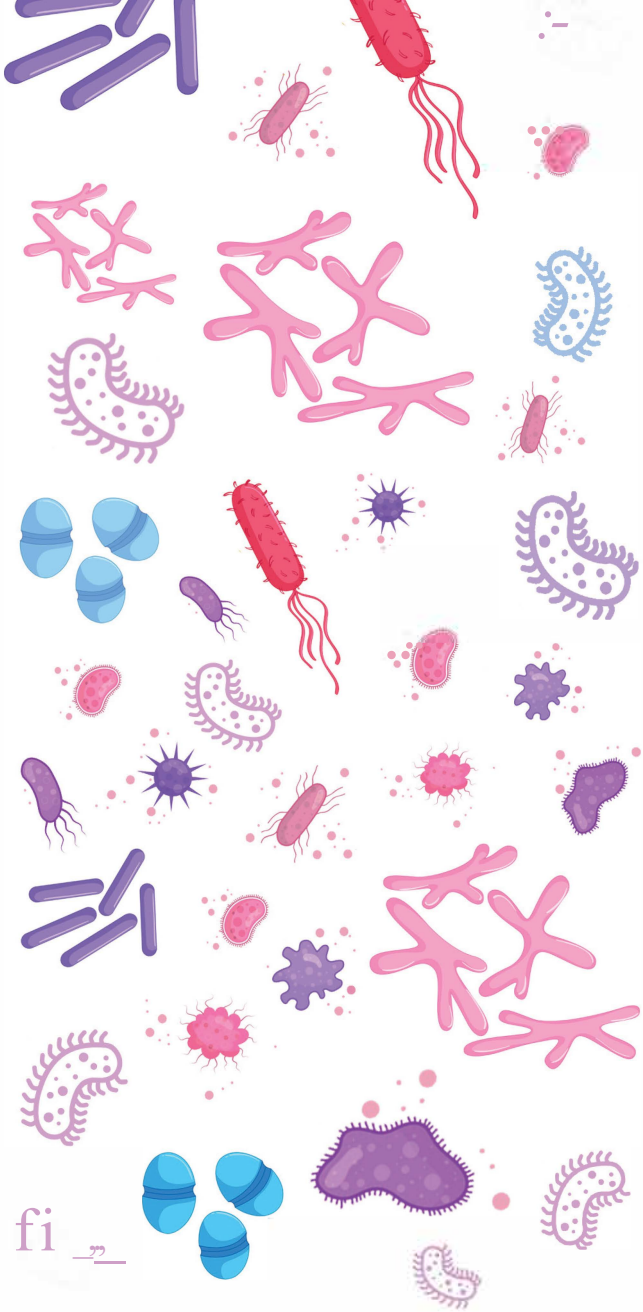

Doctoral Thesis

Deciphering the impact of the mitochondrial negative regulator MCJ on host-microbiota interactions in experimental ulcerative colitis

AINIZE PEÑA CEARRA

2021

eman ta zabal zazu

Universidad del País Vasco
Euskal Herriko Unibertsitatea

Deciphering the impact of the mitochondrial negative regulator MCJ on host-microbiota interactions in experimental ulcerative colitis

Doctoral thesis

Ainize Peña Cearra

Thesis directors:

Leticia Abecia, PhD

Asier Fullaondo, PhD

Universidad del País Vasco – Euskal Herriko Unibertsitatea

Center for Cooperative Research in Biosciences (CIC bioGUNE)

Leioa, 2021

Universidad del País Vasco Euskal Herriko Unibertsitatea

NAZIOARTEKO BIKAINTASUN CAMPUSA
CAMPUS DE EXCELENCIA INTERNACIONAL

TESI ZUZENDARIAREN BAIMENA TESIA AURKEZTEKO	AUTORIZACIÓN DEL/LA DIRECTORA/A DE TESIS PARA SU PRESENTACIÓN

Zuzendariaren izen-abizenak /Nombre y apellidos del/la director/a:
Leticia Abecia Aliende

IFZ /NIF: 72726993G

Tesiaren izenburua / Título de la tesis: Deciphering the impact of the mitochondrial negative regulator MCJ on host-microbiota interactions in experimental ulcerative coltis

Doktorego programa / Programa de doctorado:
Biología molecular y Biomedicina

Doktoregaiaren izen-abizenak / Nombre y apellidos del/la doctorando/a:
Ainize Peña Cearra

Unibertsitateak horretarako jartzen duen tresnak emandako ANTZEKOTASUN TXOSTENA ikusita, baimena ematen dut goian aipatzen den tesia aurkez dadin, horretarako baldintza guztiak betetzen baititu.	Visto el INFORME DE SIMILITUD obtenido de la herramienta que a tal efecto pone a disposición la universidad, autorizo la presentación de la tesis doctoral arriba indicada, dado que reúne las condiciones necesarias para su defensa.

Tokia eta data / Lugar y fecha: Leioa, 03/09/2021

ABECIA ALIENDE LETICIA - 72726993G

Firmado digitalmente por ABECIA ALIENDE LETICIA - 72726993G
Fecha: 2021.09.03 10:49:37 +02'00'

Sin. / Fdo.: Tesiaren zuzendaria / El/La director/a de la tesis

Universidad del País Vasco Euskal Herriko Unibertsitatea

NAZIOARTEKO BIKAINTASUN CAMPUSA
CAMPUS DE EXCELENCIA INTERNACIONAL

TESI ZUZENDARIAREN BAIMENA TESIA AURKEZTEKO	AUTORIZACIÓN DEL/LA DIRECTORA/A DE TESIS PARA SU PRESENTACIÓN

Zuzendariaren izen-abizenak /Nombre y apellidos del/la director/a:
Asier Fullaondo Elordui-Zapaterieche

IFZ /NIF: 30620719Z

Tesiaren izenburua / Título de la tesis: Deciphering the impact of the mitochondrial negative regulator MCJ on host-microbiota interactions in experimental ulcerative colitis

Doktorego programa / Programa de doctorado:
Biología molecular y Biomedicina

Doktoregaiaren izen-abizenak / Nombre y apellidos del/la doctorando/a:
Ainize Peña Cearra

Unibertsitateak horretarako jartzen duen tresnak emandako ANTZEKOTASUN TXOSTENA ikusita, baimena ematen dut goian aipatzen den tesia aurkez dadin, horretarako baldintza guztiak betetzen baititu.	Visto el INFORME DE SIMILITUD obtenido de la herramienta que a tal efecto pone a disposición la universidad, autorizo la presentación de la tesis doctoral arriba indicada, dado que reúne las condiciones necesarias para su defensa.

Tokia eta data / Lugar y fecha: Leioan, 2021eko Irailaren 3a

ASIER FULLAONDO ELORDUI-ZAPATERIECHE - 30620719Z

Firmado digitalmente por ASIER FULLAONDO ELORDUI-ZAPATERIECHE - 30620719Z
Fecha: 2021.09.03 12:08:55 +02'00'

Sin. / Fdo.: Tesiaren zuzendaria / El/La director/a de la tesis

Universidad del País Vasco Euskal Herriko Unibertsitatea

NAZIOARTEKO BIKAINTASUN CAMPUSA
CAMPUS DE EXCELENCIA INTERNACIONAL

AUTORIZACION DEL TUTOR/A DE TESIS

PARA SU PRESENTACION

Dr/a. Asier Fullaondo Elordui-Zapaterieche como Tutor/a de la Tesis Doctoral: Deciphering the impact of the mitochondrial negative regulator MCJ on host-microbiota interactions in experimental ulcerative colitis realizada en el Programa de Doctorado en Biología Molecular y Biomedicina por la Doctorando Doña. Ainize Peña Cearra, y dirigida por la Dra. Leticia Abecia Aliende y el Dr. Asier Fullaondo Elordui-Zapaterieche autorizo la presentación de la citada Tesis Doctoral, dado que reúne las condiciones necesarias para su defensa.

En Leioa a 3 de septiembre de 2021

EL/LA TUTOR/A DE LA TESIS

ASIER FULLAONDO ELORDUI-ZAPATERIECHE - 30620719Z

Firmado digitalmente por ASIER FULLAONDO ELORDUI-ZAPATERIECHE - 30620719Z
Fecha: 2021.09.03 12:09:19 +02'00'

Fdo.: _____

Universidad del País Vasco Euskal Herriko Unibertsitatea | NAZIOARTEKO BIKAINTASUN CAMPUSA CAMPUS DE EXCELENCIA INTERNACIONAL

AUTORIZACIÓN DE LA COMISIÓN ACADÉMICA DEL PROGRAMA DE DOCTORADO

La Comisión Académica del Programa de Doctorado en Biología Molecular y Biomedicina en reunión celebrada el día 1 de septiembre de 2021, ha acordado dar la conformidad a la presentación de la Tesis Doctoral titulada: Deciphering the impact of the mitochondrial negative regulator MCJ on host-microbiota interactions in experimental ulcerative colitis dirigida por la Dra. Leticia Abecia Aliende y el Dr. Asier Fullaondo Elordui-Zapaterieche y presentada por Dña. Ainize Peña Cearra adscrita al Departamento de Genética, Antropología Física y Fisiología Animal.

En Leioa a 3 de septiembre de 2021

EL/LA RESPONSABLE DEL PROGRAMA DE DOCTORADO

MIREN ITZIAR ALCORTA CALVO - 16037937Z

Firmado digitalmente por MIREN ITZIAR ALCORTA CALVO - 16037937Z
Fecha: 2021.09.03 17:51:30 +02'00'

Fdo.: Dra. Miren Itziar Alkorta Calvo

AUTORIZACIÓN DEL DEPARTAMENTO

El Consejo del Departamento de Genética, Antropología Física y Fisiología Animal en reunión celebrada el día ___ de Julio de 2021 ha acordado dar la conformidad a la admisión a trámite de presentación de la Tesis Doctoral titulada: Deciphering the impact of the mitochondrial negative regulator MCJ on host-microbiota interactions in experimental ulcerative colitis dirigida por la Dra. Leticia Abecia Aliende y el Dr. Asier Fullaondo Elordui-Zapaterieche y presentada por Doña. Ainize Peña Cearra ante este Departamento.

En _____ a _____ de _____ de _____

VºBº DIRECTOR/A DEL DEPARTAMENTO

SECRETARIO/A DEL DEPARTAMENTO

Fdo.: _____

Fdo.: _____

“The more I learn, the more I realize
how much I don't know”

Albert Einstein

Acknowledgements/Agradecimientos

Durante este largo periodo realizando la tesis doctoral he tenido el placer de contar con el apoyo de numerosas personas a las que debo gratitud. En primer lugar, gracias a mi directora Leticia A., por haberme dado esta oportunidad, brindando su gran apoyo y conocimiento a lo largo de este proceso. El esfuerzo prestado, la dedicación, criterio y la paciencia con la que cada día se preocupaba por el avance y desarrollo de esta tesis, es único y se refleja en la redacción de este trabajo. Además, agradecer su preocupación por mi y sobre todo su humanidad. También, quiero agradecer a Asier F., por haber aceptado tanto la codirección como la tutoría de esta tesis y por haber estado siempre disponible.

En segundo lugar, mostrar mi agradecimiento a todos los compañeros del JA LAB, que, sin lugar a dudas, el camino no hubiera sido el mismo sin vosotr@s. Reconocer a Juan A., por haberme aceptado en el laboratorio y haberme brindado los medios y consejos necesarios para la elaboración de la tesis doctoral. Mencionar a Miguel P., ya que fue la primera persona en guiarme en aquellos pasos iniciales. Asimismo, ha sido una pieza clave en este proyecto, transmitiendo tanto su pasión hacia este trabajo como sus ganas por seguir aprendiendo. Buen profesional y mejor persona, con la que he formado una buena amistad en esta etapa. A Itzi, por todos sus grandes consejos y por ayudarme cuando lo necesitaba. Tengo que reconocer que, aunque al principio me pareció un poco dura, ha acabado siendo un cacho de pan. A Estiti, casta bilbaína, en su caso, detrás de un caparazón se esconde un gran corazón y para mí ha sido un gran apoyo. A Leti S., nuestra pasión por el motor nos unió, pero más allá de esto, gracias por haber estado siempre dispuesta a echar una mano y por avisar con las duties. A Héctor, gracias por sus sabios consejos de microbiología que han sido de gran ayuda durante esta tesis. Además, con su bondad y su actitud positiva, hace que trabajar a su lado sea muy fácil. A Aize, vino una temporada de postdoc al laboratorio y nos dio muy buenos momentos y consejos. A Julen, nunca olvidaré esa noche que pasamos aislando macrófagos con foto incluida a la 1 am en el microscopio, gracias por haberme ayudado. A Ana, gracias por haberme transmitido su locura y por haberme hecho reír con tanta facilidad, estoy segura de que la fofo-religión traspasará las fronteras que haga falta. A Diego, mi gran aliado de animalario y doctorado, me ha hecho reír muchísimo a la vez que ayudado, gracias por todos esos buenos momentos. A Ainhoa, agradecer sus ganas de escuchar, compartir sus conocimientos y ayudar en los momentos más oportunos. A Janire, por haber estado siempre tan dispuesta a ayudarme y escucharme, por los croissants almendrados de la suiza tan ricos que me trajo para despedirme, eso

sí, nunca me olvidaré del robo de mi silla. A Sam, por haberme ayudado con su perfecto inglés cuando me bloqueaba y por haberme enseñado algo más de la cultura americana que tanto me llama la atención. A Saray, aunque pasamos poco tiempo juntas fue lo suficiente para conectar bien y ayudarnos mutuamente. A todos los miembros del AW LAB gracias por haber estado siempre tan cerca, Encarni, Marta, Laura, Leire, Miguel y Adri. También a toda esa gente del CIC bioGUNE que me han ayudado de manera más indirecta y con la que he compartido muchos momentos durante estos cuatro años.

Por otro lado, tengo mucho que agradecer a los bioinformáticos que me han ayudado durante la tesis. En primer lugar, a JL, por habernos ayudado tanto a Leticia como a mi cuando lo hemos necesitado. A Marc, por haberme enseñado los conceptos básicos de la bioinformática que necesitaba para adentrarme un poco en este mundo. Por último, a Urko, por haber estado siempre dispuesto a ayudarme y enseñarme cuando me bloqueaba con algún paso en RStudio. Además, tengo mucho que agradecer al equipo completo de la plataforma de genómica Ana M., Monika, Laura y Nuria, por toda la ayuda ofrecida para el desarrollo de la tesis.

I also need to thank Noah Palm for the stay I did in his laboratory. Thank you for receiving me with open arms, you made me feel one more in the lab since the first day and thank you for having provided me the resources I needed to progress with my thesis. Thanks to all the members of the Palm lab for having welcomed me so well. I would like to thank Deguang for being a great instructor and also, Agatha, Anjelica, Mytien, Nicole, Saleh, Shana, Shreya, Tyler, Yi, and Yiyun.

Gracias a las frikis Ainara, Gara, Gara L, Oiane y Shei, por haber estado siempre ahí apoyándome desde la ikastola hasta ahora, sois el resultado de una buena amistad.

A las compis de Biotecnología, Marina, Leire y Jone por haber sido un apoyo desde la carrera hasta la fecha.

Gracias a la Big Family por haber estado ahí siempre, por haberme entendido y ayudado cuando lo necesitaba. Sois un gran apoyo para mí, Mari, Antonio, Ari, Borja, Andoni y Aiala.

A Aita y Ama por haber confiado siempre en mí y por haberme apoyado en cada paso. Gracias por haber estado siempre conmigo y haberme dado los medios que necesitaba para cumplir mis objetivos. No tengo suficientes palabras de agradecimiento. ¡También quiero agradecer al resto de la familia que ha estado siempre conmigo, maite zaituztet!

Por último, gracias a ti caritxu, por creer y confiar tanto en mí. Gracias por haberme apoyado y valorado cada día, tranquilizado cuando lo necesitaba, por haberme acompañado en todas las etapas y sobre todo por haberme entendido y animado siempre a cumplir mis objetivos. Tus ánimos, cariño y amor me han hecho llegar a este punto y estoy segura de que juntos llegaremos muy lejos. I love you to the moon and back.

JA LAB & AW LAB

Table of content

List of figures

List of tables

Abbreviation list

Abx	Antibiotic
ACK	Ammonium-Chloride-Potassium
AK2	Adenylate Kinase 2
ALOX15	Arachidonate 15-lipoxygenase
AMPK	AMP-activated protein kinase
AMPs	Antimicrobial peptides
ANOSIM	Analysis of similarity
ANOVA	Analysis of variance
Anti-TNF	Tumor necrosis factor (TNF) inhibitor therapies
AP-1	Activator protein 1
ASAS	Aminosalicylates
ATG16L1	Autophagy-related 16-like 1
ATP	Adenosine triphosphate
BAM	Binary Alignment Map
BAs	Bile acids
BCA	Bicinchoninic Acid
BMM	Bone marrow-derived macrophages
BP	Biological processes
BSH	Bile salt hydrolase
CAPN10	Calpain 10
CARD9	Caspase Recruitment Domain Family Member 9
CC	Cellular components
CCR2/3/5/6	C-C Motif Chemokine Receptor 2/3/5/6
CD	Crohn´s disease
CD4/8/40/163	Cluster of differentiation 4/8/40/163
CDH1	Cadherin 1
cDNA	Complementary DNA
CLDN	Claudin
CLR	C-type lectin receptors
CpG-ODN	Cytosine-phosphorothioate-guanine oligodeoxynucleotides
CREM	CAMP Responsive Element Modulator
CRP	C-reactive protein
CST7	Cystatin F
CU	Colitis Ulcerosa

CXCL1/2/3/10	CXC chemokine ligand 1/2/3/10
CXCR4	C-X-C Motif Chemokine Receptor 4
DAB	3,3′-Diaminobenzidine
DAI	Disease activity index
DAMPs	Damage-associated molecular patterns
DAP	D-glutamyl-meso-diaminopimelic acid
DAPI	4′,6-Diamidino-2-phenylindole
DAVID	Database for annotation, visualization and integrated discovery
DE	Differential expression
DESeq2	Differential expression analysis for sequence count data
DHE	Dihydroethidium
DISC	Death-inducing signaling complexes
DNA	Deoxyribonicleic acid
dsRNA	Double-strand RNA
DSS	Dextran sulphate sodium
DTT	Dithiothreitol
ECM1	Extracellular matrix protein 1
EII	Enfermedad inflamatoria intestinal
ELF5	ETS-related transcription factor Elf-5
ELISA	Enzyme-linked immunosorbent assay
ENA	European Nucleotide Archive
ERG	Transcriptional regulator ERG
ESI	Electrospray ionization
ETC	Electron transport chain
F4/80 / ADGRE1	Mouse macrophage-restricted F4/80 protein / Adhesion G Protein-Coupled Receptor E1
FA	Formic acid
FBS	Fetal bovine serum
FC	Fold change
FCGR1	High affinity immunoglobulin gamma Fc receptor I
FCGR2A	Fc fragment of IgG receptor IIa
FCGR2B	Fc Fragment of IgG Receptor IIb
FCGR3	Low affinity immunoglobulin gamma Fc region receptor III
FcγR	Fcgamma receptor
FDR	False discovery rate
FITC	Fluorescein isothiocyanate
FMT	Fecal microbial transplantation

FOS	Fructooligosaccharide
FOXP3	Forkhead box P3
FXR	Farnesoid X receptor
F/B	Firmicutes/Bacteroidetes ratio
GAPDH	Glyceraldehyde 3-phosphate dehydrogenase
GALT	Gut-associated lymphoid tissues
GATA3	GATA Binding Protein 3 transcription factor
GEO	Gene expression omnibus
GF	Germ-free
GO	Gene ontology
GOS	Galactooligosaccharide
GPR65	G Protein-Coupled Receptor 65
GWAS	Genome wide association studies
HAIIA	Hierarchical All-against-All significance testing
HBSS	Hank's Balanced Salt Solution
HFD	High-fat-diet
HIF1A	Hypoxia-inducible factor 1-alpha
HMDB	The Human Metabolome Database
HNF4A	Hepatocyte nuclear factor 4-alpha
HOMER	Hypergeometric Optimization of Motif EnRichment
HRP	Horseradish peroxidase
IBD	Inflammatory bowel disease
IBS	Irritable bowel syndrome
ICI	IgA coating index
IF	Immunofluorescence
IFN-γ	Interferon gamma
IFX	Infliximab
IgA	Immunoglobulin A
IgG	Immunoglobulin G
IkBα	NFKB Inhibitor Alpha
IkBβ	NFKB Inhibitor Beta
IKK	IkappaB kinase
IL	Interleukin
IL1/12B	Interleukin-1/12 subunit beta
IL1R2	Interleukin 1 Receptor Type 2
IL2RA	Interleukin 2 Receptor Subunit Alpha
IL7/12/23R	Interleukin-7/12/23 receptor

IL8RA/CXCR1	Interleukin-8 receptor, alpha / C-X-C Motif Chemokine Receptor 1
IL8RB/CXCR2	Interleukin-8 receptor, beta / C-X-C Motif Chemokine Receptor 2
IRF3/5/7	Interferon regulatory factor 3/5/7
IRGM	Immunity related guanosine triphosphatase M
ITGAL	Integrin Subunit Alpha L
JAKs	Janus Kinase
KEGG	Kyoto encyclopedia of genes and genomes
KO	Knock-out
LAMB1	Laminin subunit beta-1
LC-MS	Liquid chromatography–mass spectrometry
LCN-2	Lipocalin-2
LEfSe	Linear discriminant analysis effect size
LPS	Lipopolysaccharide
LRR	Leucine-rich repeat
LRRK2	Leucine rich repeat kinase 2
LSP1	Lymphocyte Specific Protein 1
Ly6c1	Lymphocyte antigen 6 complex, locus C1
MACS	Magnetic-activated cell sorting
MAdCAM-1	Mucosal Addressin Cell Adhesion Molecule 1
MALT	Mucosal-associated lymphatic tissue
MAMP	Microbe-associated molecular patterns
MCJ/DNAJC15	Methylation-controlled J protein / DnaJ Heat Shock Protein Family (Hsp40) Member C15
MDDC	Monocyte-derived dendritic cells
MDPs	Muramyl dipeptides
MF	Molecular function
MHCII	Major Histocompatibility Complex Class II
MLNs	Mesenteric lymph nodes
MMP	Mitochondrial membrane potential
MPO	Myeloid-specific peroxidase
mRNA	Messenger ribonucleic acid
mtDNA	Mitochondrial DNA
mTNF	Membrane-associated tumor necrosis factor
MUC2	Mucin 2, Oligomeric Mucus/Gel-Forming
MUC3	Mucin 3, Cell Surface Associated
MYD88	Myeloid differentiation primary response 88
NADPH	Nicotinamide adenine dinucleotide phosphate

NF-kB	Nuclear factor kappa B
NGS	Next generation sequencing
NK	Natural killer
NLRP3	NOD-like receptor P3
NLRs	NOD-like receptors
NMDS	Non-multimetric dimensional scaling
NOD1/2	Nucleotide-binding oligomerization domain 1/2
NSAID	Nonsteroidal anti-inflammatory drugs
OCLN	Occludin
OSM	Oncostatin-M
OTUs	Operational taxonomic units
PAMPs	Pathogen-associated molecular patterns
PAS	Periodic acid-Schiff
PASEF	Parallel Accumulation–Serial Fragmentation
PB	Phosphate buffer
PBMCs	Peripheral blood mononuclear cells
PBS	Phosphate-buffered saline
PCA	Principal component analysis
PCoA	Principal coordinates analysis
PCR	Polymerase chain reaction
PDE5	Phosphodiesterase type 5
PGC-1α	Peroxisome proliferator-activated receptor gamma coactivator 1-alpha
PICRUSt2	Phylogenetic investigation of communities by reconstruction of unobserved states
pIgR	Polymeric immunoglobulin receptor
PIM3	Pim-3 Proto-Oncogene, Serine/Threonine Kinase
PLS-DA	Supervised partial least-squares discriminate analysis
PRRs	Pattern recognition receptors
PTGS2/COX2	Prostaglandin-endoperoxide synthase 2 / Cyclooxygenase 2
QIIME	Quantitative insights into microbial ecology
qPCR	Quantitative polymerase chain reaction or real-time polymerase chain reaction
RCT	Randomized controlled trials
RDP	Ribosomal database project
REG3B	Regenerating islet-derived protein 3-beta
REG3G	Regenerating family member 3-gamma

RFU	Relative fluorescence units
RIG-1	Retinoic acid-inducible gene 1
RIPA buffer	Radioimmunoprecipitation assay buffer
RLRs	Retinoic acid-inducible gene-I-like receptors
RNA	Ribonucleic acid
ROS	Reactive oxygen species
RPL19	Ribosomal Protein L19
RPM	Revolutions per minute
RPMI	Roswell Park Memorial Institute
rRNA	Ribosomal ribonucleic acid
RT-PCR	Reverse transcription polymerase chain reaction
RUNX	Runt-related transcription factor 1
S1PR	Sphingosine-1-phosphate receptor
SCFAs	Short-chain fatty acids
SCT	Stem cell therapy
SDS-PAGE	Sodium dodecyl sulfate polyacrylamide gel electrophoresis
SEM	Standard error of the mean
SFB	Segmented filamentous bacteria
SIgA	Secretory IgA
SIRT1	Silent mating type information regulation 2 homolog
SLC11A1	Solute Carrier Family 11 Member 1
SMAD3/7	Acronym from the fusion of *Caenorhabditis elegans* SMA genes ("small" worm phenotype) and the *Drosophila Mad* ("Mothers Against Decapentaplegic") 3/7
SP140	SP140 Nuclear Body Protein
SPF	Specific pathogen free
SPIB	Transcription factor Spi-B
ssRNA	Single-stranded RNA virus
STAMP	Statistical analysis of taxonomic and functional profiles
STAR	Spliced Transcripts Alignment to a Reference
STAT1/3/4	Signal transducer and activator of transcription 1/3/4
sTNF	Soluble tumor necrosis factor
Ta	Primer annealing temperature
TACE/ADAM17	Tumor necrosis factor alpha converting enzyme / A disintegrin and metalloprotease 17
TAPI-2	TNF-alpha protease inhibitor 2
TCA	Taurocholic acid

TCR	T cell receptor
TGF-β	Transforming growth factor beta
Th1	Type 1 T helper
Th2	Type 2 T helper
Th17	Type 17 T helper
TIMP3	Tissue inhibitor of metalloproteinases-3
Tip-DCs	TNF and nitric oxide producing dendritic cells
TIRAP	TIR domain-containing adaptor protein
TJP1	Tight Junction Protein 1
TLRs	Toll-like receptors
TMF	Trasplante de microbiota fecal
TNBS	2,4,6-Trinitrobenzene sulfonic acid
TNF	Tumor necrosis factor
TNFR1/2	Tumor necrosis factor receptor 1/2
TNFRSF9/14	Tumor necrosis factor receptor superfamily member 9/14
TNFSF11/15	Tumor necrosis factor superfamily member 11/15
TRADD	TNFR1-associated death domain protein
TRAF1/2/3/6	TNF receptor-associated factor 1/2/3/6
Tregs	Regulatory T cells
TREM1	Triggering receptor expressed on myeloid cells 1
TRIF	TIR-domain-containing adapter-inducing interferon-β
TYK2	Tyrosine Kinase 2
UC	Ulcerative colitis
VIP	Variable importance in projection
vs	Versus
WL	Weight loss
WT	Wild-type

Abstract

Inflammatory bowel disease (IBD) encompasses two types of idiopathic intestinal diseases, ulcerative colitis (UC) and Crohn's disease. Both are chronic, heterogeneous, and severe inflammatory disorders that primarily affect the intestine. Although the specific underlying cause of UC is unknown, it is considered the result of a complex interaction between the microbiota, immune system, host genetics and environmental factors. Recent evidence has demonstrated potential links between mitochondrial dysfunction and IBD. Indeed, mitochondrial function are decreased in active UC patients, in particular, the activity of complex I of the electron transport chain is heavily compromised. Furthermore, several studies have reported a bidirectional interaction between intestinal microbiota and mitochondria that seems to play a key role in the disease. In this thesis work, we use a mouse model deficient in MCJ (Methylation controlled J protein), which is a mitochondrial inner membrane protein identified as a natural inhibitor of respiratory chain complex I, to study the role of mitochondrial dysfunction within UC, thereby overcoming the clinical heterogeneity reported in the human patient population.

The induction of experimental acute colitis in MCJ-deficient mice resulted in a more severe disease phenotype by means of mitochondrial dysfunction and a distinct gut microbiota composition. MCJ-deficient mice showed upregulated *Timp3* expression, which led to the inhibition of TACE activity that likely inhibits *Tnf* shedding from the cell membrane in the colon confirming previous findings with bone marrow-derived macrophages. These mice also displayed higher expression of the proinflammatory cytokine *Il1b* and the *Tlr9*/*Myd88* signaling. Furthermore, the deficiency of MCJ resulted in distinct microbiota metabolism and composition, including a member of the gut community in UC patients, *Ruminococcus gnavus*. Importantly, gene expression analyses in UC patients showed decreased levels of *MCJ* and higher expression of *TIMP3*, suggesting a relevant role of mitochondrial genes and function among active UC.

In addition, the co-localization of MCJ within macrophages using colon samples from human colectomies related its effect to immune cells. Therefore, we conducted a murine colon macrophage transcriptome to assess the role of MCJ in this specific type of cells. MCJ deficiency mainly affected the expression of the FcγR signaling pathway. Some of the modified genes were linked to an anti-TNF refractory gene signature in IBD patients. Indeed, these mice were not able to respond to the therapy. Additionally, we used a fecal microbial transplantation (FMT) approach in mice to assess the contribution

of gut microbiota composition altered by MCJ levels in the therapeutic response. We further showed that antibiotic-induced dysbiosis increased experimental colitis severity and diminished microbial differences associated with the loss of MCJ. It seems that antibiotic treatment altered the microbiota and therefore, the production of anti-inflammatory cytokines in the inflamed tissue, resulting in increased experimental colitis severity in mice.

To further assess the potential role of MCJ-deficient gut microbiota composition, we performed three different approaches based on germ-free (GF) microbial colonization, FMT and finally, IgA-SEQ technology using a mouse model deficient in MCJ. We demonstrated that it was possible to transfer MCJ-deficient disease phenotype to GF mice with fecal transplants as they developed a more severe course of disease. Therefore, we designed a FMT experiment by cohousing to alter MCJ-deficient mice microbiota. It was observed that mitochondrial dysfunction phenotype was reverted through FMT after *Lactobacillus* acquisition, supporting the application of probiotics as a treatment. In these approaches, we detected other disease-driving bacteria such as *Oscillospira* and *Prevotella* related to mitochondrial dysfunction, suggesting the implementation of targeted and personalized antimicrobial therapies to selectively eliminate colitogenic bacteria. These bacteria might serve as predictive biomarkers of disease progression, permitting the stratification of UC patients. We also demonstrated through IgA-SEQ technology that IgA coating identified different intestinal bacteria in MCJ-deficient mouse model with a potential role in disease progression. In addition, we were able to determine impacted protein expression pathways due to MCJ deficiency and microbiota composition, providing valuable insights into pathophysiology.

Then, we used a mouse model of chronic colitis to understand the role of MCJ. The induction of chronic colitis resulted in a similar phenotype between control and MCJ-deficient animals. The increased TACE activity and the low levels of *Timp3* expression detected upon chronic colitis in MCJ-deficient mice supported the association of the soluble TNF form with the amelioration of the phenotype. Furhermore, the induction of experimental chronic colitis diminished microbial differences between WT and MCJ-deficient mice and in agreement with recent studies, a higher production of IL-6 and IL-1β cytokines in MCJ-deficient mice might be related to a higher presence of protective T cells, thereby improving the disease outcome. Therefore, it seems that the colon tissue adapts dynamically to changes in the environment as a way to adapt metabolically to new conditions.

The results in this thesis provide fundamental information about the complex regulatory relationship between the host mitochondria and microbiota affecting disease severity. Our results implicate both alteration of the microbial composition and the FcγR signaling pathway of gut macrophages in UC pathogenesis and non-responders to therapies due to mitochondrial dysfunction, opening new research lines to predict disease outcome and the response to anti-TNF therapy at baseline in UC patients. Furthermore, this study allowed us to identify potential microbial signatures in feces associated with disease progression and therapy response, which might serve as predictive biomarkers, permitting the stratification of UC patients into distinct clinical entities of UC spectrum.

Resumen

La enfermedad inflamatoria intestinal (EII) engloba dos patologías, la colitis ulcerosa (CU) y la enfermedad de Crohn. Ambas son trastornos inflamatorios crónicos, heterogéneos y complejos que afectan principalmente al intestino. Aunque la etiología de la enfermedad es desconocida, se considera que es el resultado de una interacción compleja entre la microbiota, el sistema inmune, la predisposición genética y los factores ambientales. En trabajos recientes se relaciona la disfunción mitocondrial con las EII. De hecho, los pacientes con CU activa, presentan una disminución de la función mitocondrial. En particular, se ha demostrado que la actividad del complejo I de la cadena transportadora de electrones está muy comprometida. Además, se ha descrito que existe una interacción bidireccional entre las mitocondrias y la microbiota, que parece jugar un papel clave en la enfermedad. Por todo ello, con el fin de reducir la heterogeneidad clínica de los pacientes en este trabajo, hemos utilizado un modelo de ratón deficiente en la proteína MCJ (Methylation-controlled J protein), una proteína localizada en la membrana interna de la mitocondria que actúa como un regulador negativo del complejo I de la cadena respiratoria, para estudiar el papel de la disfunción mitocondrial dentro de la CU.

La inducción de una colitis aguda en ratones deficientes en MCJ resultó en un fenotipo de enfermedad más grave, como consecuencia de la disfunción mitocondrial y una modificación de la composición microbiana. Los ratones deficientes en MCJ mostraron en el colon una expresión de *Timp3* sobre expresada, lo cual condujo a la inhibición de la actividad de TACE que es la enzima encargada de la liberación del *Tnf* unido a la membrana celular, confirmando los hallazgos descritos previamente en macrófagos derivados de médula ósea. Dichos ratones también presentaron una mayor expresión del gen proinflamatorio *Il1b* y de la vía de señalización *Tlr9*/*Myd88*. Asimismo, la falta de MCJ modificó tanto el metabolismo como la composición microbiana del contenido del colon, aumentando la presencia de *Ruminococcus gnavus* que es una especie comúnmente incrementada en la microbiota intestinal de pacientes con EII. Cabe destacar, que los análisis de expresión génica en pacientes que sufren CU también mostraron niveles reducidos de *MCJ* y una mayor expresión de *TIMP3* en el colon, lo que sugiere que la función mitocondrial juega un papel relevante durante la CU activa.

A continuación, determinamos la colocalización de MCJ en macrófagos intestinales de muestras de colon obtenidos mediante colectomías de pacientes y describimos que el efecto de la ausencia de MCJ no estaba relacionado con las células epiteliales si no con las células inmunes. Por lo tanto, realizamos un análisis transcriptómico de macrófagos murinos aislados del tejido del colon para evaluar el papel de MCJ en este tipo de células concreto. La deficiencia de MCJ afectó principalmente a la expresión de los receptores FcγR. Esta vía se asocia con una firma genética de pacientes con EII refractarios al tratamiento con agentes anti-TNF. De hecho, nuestros resultados confirmaron que estos ratones no fueron capaces de responder a la terapia. Para evaluar el efecto que tiene la microbiota asociada a niveles bajos de MCJ en la respuesta terapéutica al tratamiento con anti-TNF, estudiamos el impacto del trasplante de microbiota fecal (TMF) en ratones. Adicionalmente, mostramos que la disbiosis inducida por antibióticos aumentó la gravedad de la colitis experimental y disminuyó las diferencias microbianas asociadas con la pérdida de MCJ. Parece que el tratamiento antibiótico modificó la composición microbiana y, por consiguiente, la producción de citocinas anti-inflamatorias en el tejido inflamado, resultando en un aumento de la gravedad de la colitis en ratones.

Para evaluar el potencial papel de la microbiota intestinal asociada con la deficiencia de MCJ, utilizamos tres ensayos diferentes, la colonización de ratones libres de microorganismos (GF, "Germ-Free", en terminología inglesa) con la microbiota de ratones con daño mitocondrial, el trasplante de microbiota fecal a través de la cohabitación y la caracterización del recubrimiento específico de bacterias de la microbiota intestinal con la inmunoglobulina A (IgA-SEQ). Primero, observamos que era posible transferir el fenotipo de la enfermedad asociado a la deficiencia de MCJ a ratones GF, ya que los ratones colonizados a partir de ratones con daño mitocondrial desarrollaron un curso más grave de la enfermedad. Por esta razón, diseñamos un segundo experimento de TMF mediante cohabitación de ratones de distinto genotipo, con el objetivo de alterar la microbiota asociada a la deficiencia de MCJ. El fenotipo asociado a la disfunción mitocondrial se revirtió a través de TMF como resultado de la adquisición de bacterias tipo *Lactobacillus*, lo que apoya el uso de probióticos como tratamiento de la enfermedad. En estos experimentos, en condiciones de disfunción mitocondrial, también detectamos otras bacterias conocidas como causantes de la enfermedad, así como *Oscillospira* y *Prevotella*, lo que sugiere la implementación de terapias antimicrobianas personalizadas y dirigidas para eliminar de manera selectiva las bacterias colitogénicas. De hecho, estas bacterias podrían servir como biomarcadores predictivos del curso de la enfermedad, permitiendo la estratificación de

los pacientes con CU. La utilización de la técnica de IgA-SEQ nos permitió observar un alto recubrimiento de bacterias con IgA en el modelo de ratón deficiente en MCJ, siendo algunas de ellas bacterias intestinales con un papel potencial en la progresión de la enfermedad. Además, determinamos las vías de expresión de las proteínas afectadas debido a la deficiencia de MCJ y la composición microbiana, lo que proporcionó información valiosa sobre la fisiopatología de la enfermedad.

Utilizamos también un modelo murino de colitis crónica para estudiar el papel de MCJ durante la fase crónica de la enfermedad. Es importante destacar que la inducción de la colitis crónica mostró un fenotipo similar entre los ratones deficientes en MCJ y los WT. El aumento de la actividad de TACE y los bajos niveles de expresión de *Timp3* detectados en ratones deficientes en MCJ apoyan la teoría de que la forma de TNF soluble podría estar asociada con la mejora del fenotipo. Además, la inducción de la colitis crónica experimental resultó en una disminución de las diferencias microbianas entre los ratones control y deficientes en MCJ. En línea con otros estudios recientes, una mayor producción de citocinas IL-6 e IL-1β en ratones deficientes en MCJ, podría estar relacionado con una mayor presencia de células T protectoras, lo que ayudaría a mejorar el resultado de la enfermedad. Por tanto, parece que el tejido del colon es capaz de adaptarse de una manera dinámica a los cambios del entorno adaptándose metabólicamente a las nuevas condiciones.

Los resultados de esta tesis proporcionan información fundamental sobre la compleja interacción que se produce entre las mitocondrias y la microbiota del hospedador. Nuestros resultados implican tanto la alteración de la composición microbiana como los receptores FcγR de los macrófagos intestinales en la patogénesis de la CU y en el fallo a la respuesta a terapias biológicas a causa de la disfunción mitocondrial. Nuestros datos permiten abrir nuevas líneas de investigación para predecir en estadios tempranos la evolución de la enfermedad y la respuesta a la terapia con agentes anti-TNF en pacientes con CU. Por otra parte, este estudio nos ha permitido identificar posibles firmas microbianas en las heces asociadas con la progresión de la enfermedad y la respuesta a terapias, que podrían servir como biomarcadores predictivos, permitiendo la estratificación de los pacientes.

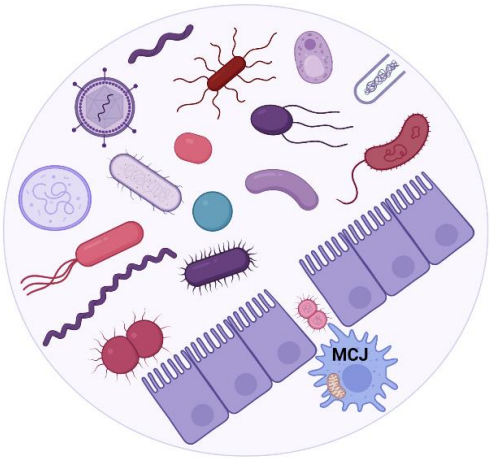

Introduction

1. Inflammatory Bowel Disease (IBD)

1.1 Forms and incidence

IBD is a group of idiopathic, chronic, relapsing and remitting inflammatory disorders of the gastrointestinal tract. Although the etiology remains unknown, the most accepted hypothesis is that an aberrant immune response to gut microbes is triggered by environmental factors in genetically susceptible hosts (Matsuoka and Kanai, 2015). The two major forms of IBD are Crohn's disease (CD) and ulcerative colitis (UC). CD is characterized by a discontinuous, patchy gut inflammation that affects all layers (transmural inflammation) and can be located in any segment of gastrointestinal tract including the distal ileum, cecum, perianal area and colon. Unlike CD, UC is limited to the colon and rectum, and presents a continuous and superficial inflammation, generally known as mucosal inflammation (Figure 1) (Guan et al., 2019).

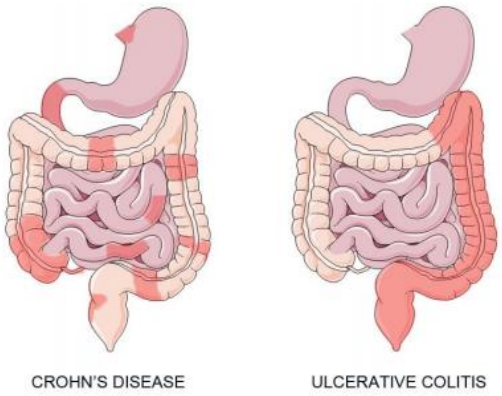

Figure 1. The location of inflammation in CD and UC. CD patients can present inflammation in any section of the gastrointestinal tract whereas patients with UC only present inflammation in the colon.

It is emerging as a global disease with a sharp increase in worldwide incidence and prevalence. Industrialization has largely affected human´s health by dramatically changing transportation, agriculture, manufacturing, urbanization and diet. Hence, shifts in manufacturing have led to increased air pollution, and fibers from diets started to be less plant-based (Windsor et al., 2019). Industrialization has accelerated IBD incidence in newly industrialized countries, principally occurring in the Western World, which includes Europe, North America and Australia. Remarkably, UC is more prevalent than CD and the first UC reports were detected in the 1800s in the Western World. Precisely, Samuel Wilks first described UC in 1859 (Gajendran et al., 2019). From the nineteenth century onward, the incidence of IBD has been rising continuously (Kaplan, 2015). Regarding the incidence of UC between 1990 and 2016, the highest incidence was recorded in developed countries such as Canada, USA, North Europe, Australia and

New Zealand (>7.71 per 100000) (Figure 2) (Kobayashi et al., 2020; Kaplan et al., 2019). Nevertheless, the incidence in Spain and other industrialized countries in Europe is also high and a rapid rise in newly industrialized countries including South America, Eastern Europe, Asia, and Africa has been reported (GBD 2017 Inflammatory Bowel Disease Collaborators, 2020).

Notably, the annual direct and indirect costs related to ulcerative colitis are estimated to be as high as €12.5–29.1 billion in Europe (Cohen et al., 2010). Furthermore, IBD incidence rates showed a bimodal age distribution being more pronounced in UC patients (Ordás et al., 2012; Hou et al., 2013). The first main onset peak was observed between ages 15 and 30 followed by a second smaller peak in the 50 to 70 years group (Ordás et al., 2012). Opposed to age distribution, gender-specific differences are conflicting, and not preferences have been clearly manifested.

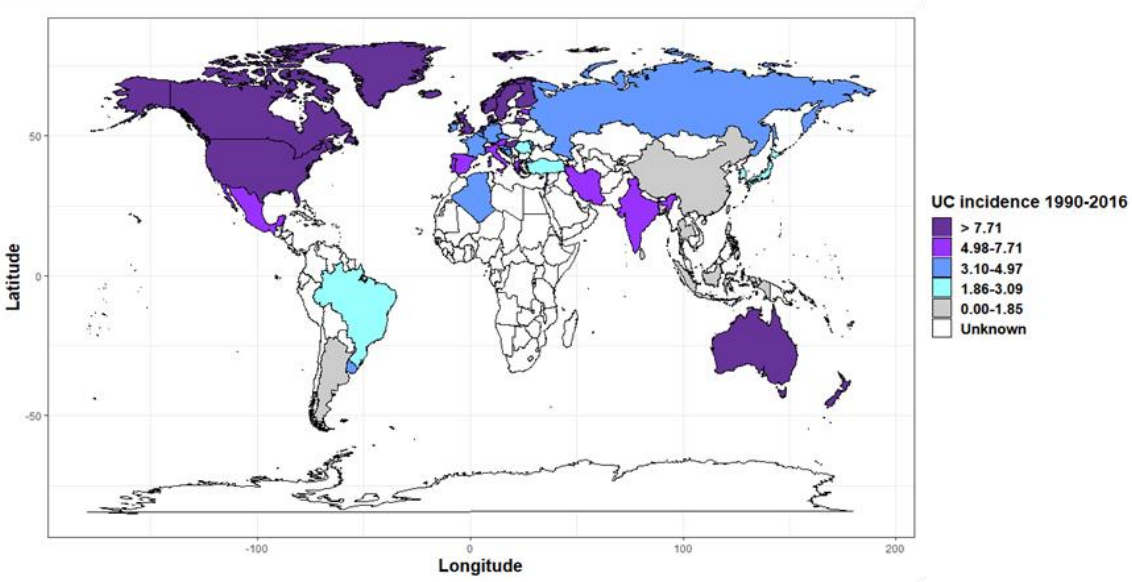

Figure 2. Global incidence of Ulcerative Colitis from 1990 to 2016. Data is shown as UC cases per 100.000 inhabitants and was adapted from Kaplan et al., (2019).

1.2 Risk factors

Although the etiology of IBD remains largely unknown, growing evidence has suggested that it arises from a combination of genetic predisposition, external environmental factors, dysregulated immune responses and gut microbiota (Figure 3) (Zhang et al., 2014).

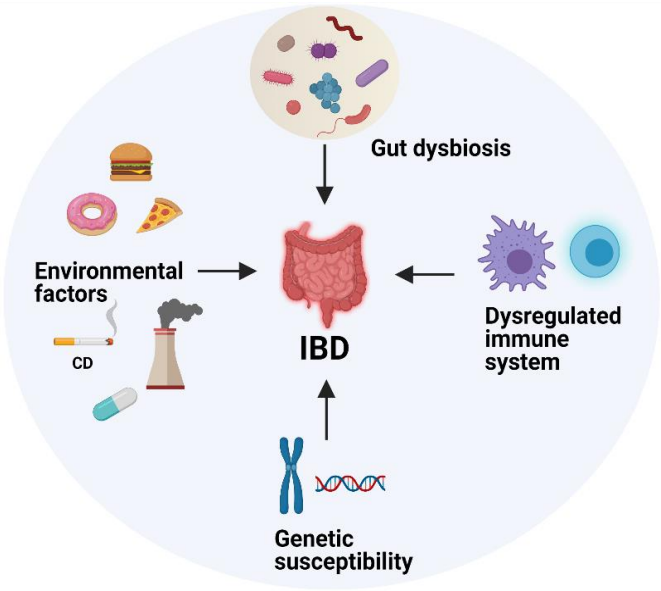

Figure 3. The multifactorial etiology of IBD. Environmental factors, genetic predisposition, dysregulated immune responses and gut dysbiosis have been considered as the major risk factors of IBD.

1.2.1 Genetic susceptibility

Advances in genomic technologies such as genome-wide association studies (GWAS), has allowed the identification of many IBD-associated gene loci. Hence, over 240 genetic risk loci have been identified in IBD patients and 30 are shared between CD and UC (Guan et al., 2019). Interestingly, many of the gene mutations are known to be involved in mediating host responses to gut microbes (Pickard et al., 2017). In 2001, a mutation in the intracellular receptor *NOD2* was first linked to CD patients, occurring in around one-third of the patients (Hampe et al., 2001) (Figure 4). Patients with the *NOD2* gene mutated usually present a much more severe disease than other CD patients. This gene is of particular interest in host innate immune responses to bacterial muramyl dipeptides (MDPs). In a caspase-1 dependent manner activates NF-kB signaling pathway leading to the secretion of pro-inflammatory cytokines. Furthermore, NOD2 is known to induce autophagy by interacting with ATG16L1, an essential factor for canonical autophagy. Autophagy maintains cellular homeostasis through the degradation of damaged or aged cytoplasmic components within lysosomes. Apart from that, autophagy seems to be a crucial process of the innate defense against intracellular

pathogenic insults, which is induced by bactericidal effects. Hence, xenophagy has been described to play a key role in macrophages to kill pathogens that evade conventional phagosome maturation (Yuk et al., 2012). *IRGM* gene is also associated with autophagy and mutations in both *ATG16L1* and *IRGM* genes are linked to CD. Moreover, polymorphisms in *ATG16L1*, *NOD2* and *LRRK2* resulted in reduced secretion of antimicrobial peptides by Paneth cells, affecting intestinal microbiota composition. In fact, variants in *NOD2* were linked to increased abundance of *Escherichia* and decreases in *Faecalibacterium* species and impaired ATG16L1 signaling was associated with increased production of IgG and IgA, losing tolerance to gut microbes (Cohen et al., 2019). Various studies have identified UC-specific gene variants related to epithelial functions (*HNF4A*, *CDH1* and *LAMB1*). Genes associated with the immune function and cytokines production such as *IL23R*, *IL12B*, *JAK2*, *STAT3*, *IL10* and *SMAD3* have been described in both CD and UC. *TNFSF15*, a gene involved in the TNF signaling pathway was also detected in both forms of IBD (Ek et al., 2014; Kaunitz and Nayyar, 2015).

The heritability model of IBD is still unclear. Nonetheless, IBD geneticists have found that some of the causative genes are transmitted through Mendelian inheritance (Liu et al., 2016). Of note, population-based studies have detected an 8- to 10-fold greater IBD risk among relatives of UC and CD and, most importantly, exists concordance between twins (Loddo and Romano, 2015; Cho and Brant, 2011).

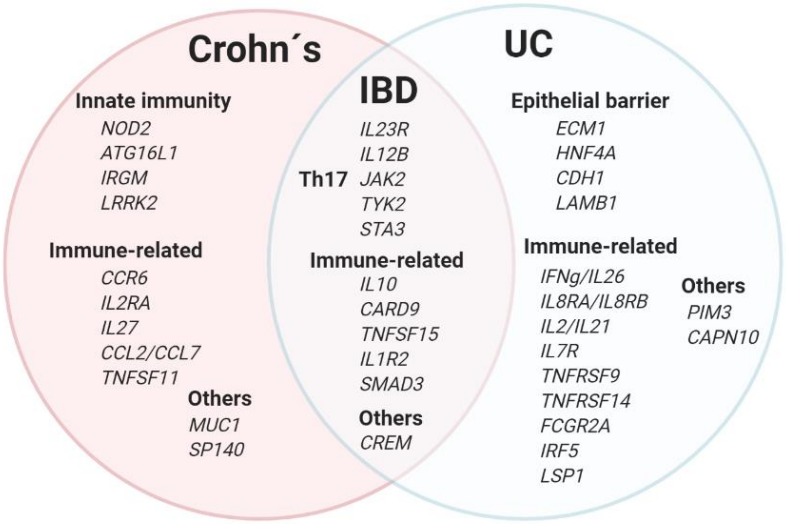

Figure 4. Some of the IBD risk loci identified by GWAS. Loci associated with CD are shown inside the orange circle, IBD inside both circles and UC inside blue circle. Adapted from Ek et al., (2014).

1.2.2 Environmental factors

Environmental factors also play an important role in the development of IBD. Piovani et al, (2019) identified 9 environmental factors that were associated with a greater risk of developing IBD: smoking (CD), urban living (CD and IBD), appendectomy (CD), tonsillectomy (CD), antibiotic exposure (IBD), oral contraceptive use (IBD), consumption of soft drinks (UC), vitamin D deficiency (IBD), and non–Helicobacter pylori–like enterohepatic Helicobacter species (IBD). Other factors such as diet, geography, social stress, and psychological element have also been reported (Zhang et al., 2014). Surprisingly, it was observed that smoking had a protective effect on the progression of UC with a lower relapse rate, although it increased the risk of CD (Cosnes, 2008). Currently, the increased exposure to air pollutants has led to augmented circulating levels of polymorphonuclear leukocytes, resulting in increased concentrations of plasma cytokines in IBD patients (van Eeden SF et al., 2001; Elten et al., 2020). However, air pollution and IBD association is still controversial, as some groups did not find to be consistently associated with IBD (Opstelten et al., 2016).

Remarkably, the widely used drugs like aspirin, nonsteroidal anti-inflammatory drugs (NSAIDs) and antibiotics are also known to increase the risk of CD and UC. Indeed, a large cohort study conducted with Danish infants showed that antibiotic users (one course) were 3.41 times more likely to be diagnosed with CD. The risk of CD was greater within 3 months at ages 3-11 months and 2-3 years compared to 1 year and more than 4 years ages. Notably, this ratio increased as the number of antibiotic courses increased and was significantly higher than UC subjects (Hviid et al., 2011). Therefore, antibiotic use during infancy can lead to the development of disease in later life.

In the past decades, considerable changes in food consumption have been documented and associated with the increased incidence of UC. However, available data are still inconsistent. Between 1976-80, it was first reported that CD patients consumed an excess amount of sugar and processed carbohydrates (Martini and Brandes, 1976; Mayberry et al., 1980; Legaki and Gazouli, 2016). Sucrose and fat consumption have been considered as a major risk factor for IBD, whereas intake of fibers, fruits, magnesium and vitamin C have been associated with reduced UC risk. The link between diet and UC development has been shown in distinct epidemiological studies. In fact, high consumption of mono- and polyunsaturated fat and vitamin B6 was related to increased risk of UC (Geerling et al., 2000). Thus, diets with high sucrose and fat intake correlate with a rapid increase in the incidence of IBD.

1.2.4 Immune response

Innate and adaptive immune responses are key factors in the pathogenesis of IBD. Intestinal mucosa is continuously exposed to food and commensal bacterial antigens. In homeostasis, the immune system is able to discriminate between commensal and potential pathogenic microorganisms. However, dysfunctions in the immune system can contribute to the aberrant intestinal inflammatory response reported in IBD patients.

The innate immune system provides a first line of defense against pathogens, characterized by a non-specific and quick response (within hours) (Biron, 2016). Furthermore, the response is mediated by epithelial cells, neutrophils, dendritic cells, monocytes, macrophages and natural killer cells. Innate immune cells carry pattern recognition receptors (PRRs), permitting the recognition of PAMPs (Pathogen-associated molecular patterns) and DAMPs (Damage-associated molecular patterns), and triggering pro-inflammatory responses, required to eliminate or contain potential pathogens or tissue damage (Amarante-Mendes et al., 2018). There are four subfamilies of PPRs: Toll-like receptors (TLRs), NOD-Leucin Rich Repeats (LRR)-containing receptors (NLRs), the retinoic acid-inducible gene 1 (RIG-1)-like receptors (RLRs), and C-type lectin receptors (CLRs) (Amarante-Mendes et al., 2018; Iurescie et al., 2020). In the gut, microbial products are commonly sensed by TLRs and NLRs. Altered function of these receptors has been described in individuals with IBD (Cario, 2010; Feerick and McKernan, 2017). Since increased activation of TLRs and NLRs promote the activation of the NF-kB transcription factor, which leads to the induction of a variety of proinflammatory cytokines, most TLR and NLR signaling pathways participate in the progression of IBD (Figure 5) (Lu et al., 2018). TLRs comprise a family of 13 types of receptors, of which only TLR1-9 receptors are found in the intestines. Each TLR is activated by a specific PAMP, as shown in figure 5 and can be found in the plasma membrane or in the endosomal intracellular compartments. MyD88 is the essential adaptor of all TLRs except for TLR3, and the alternative pathway is dependent on TIR-domain-containing adapter-inducing interferon-β (TRIF). TIR domain-containing adaptor protein (TIRAP) functions as a sorting adaptor that links MyD88 to the plasma membrane (Fitzgerald and Chen, 2006). Besides the expression of TLRs on professional immune cells, they are also expressed by the large majority of non-hematopoietic cells, including epithelial cells (McClure and Massari, 2014). Several studies have shown correlation between IBD and TLRs either promoting or preventing the disease.

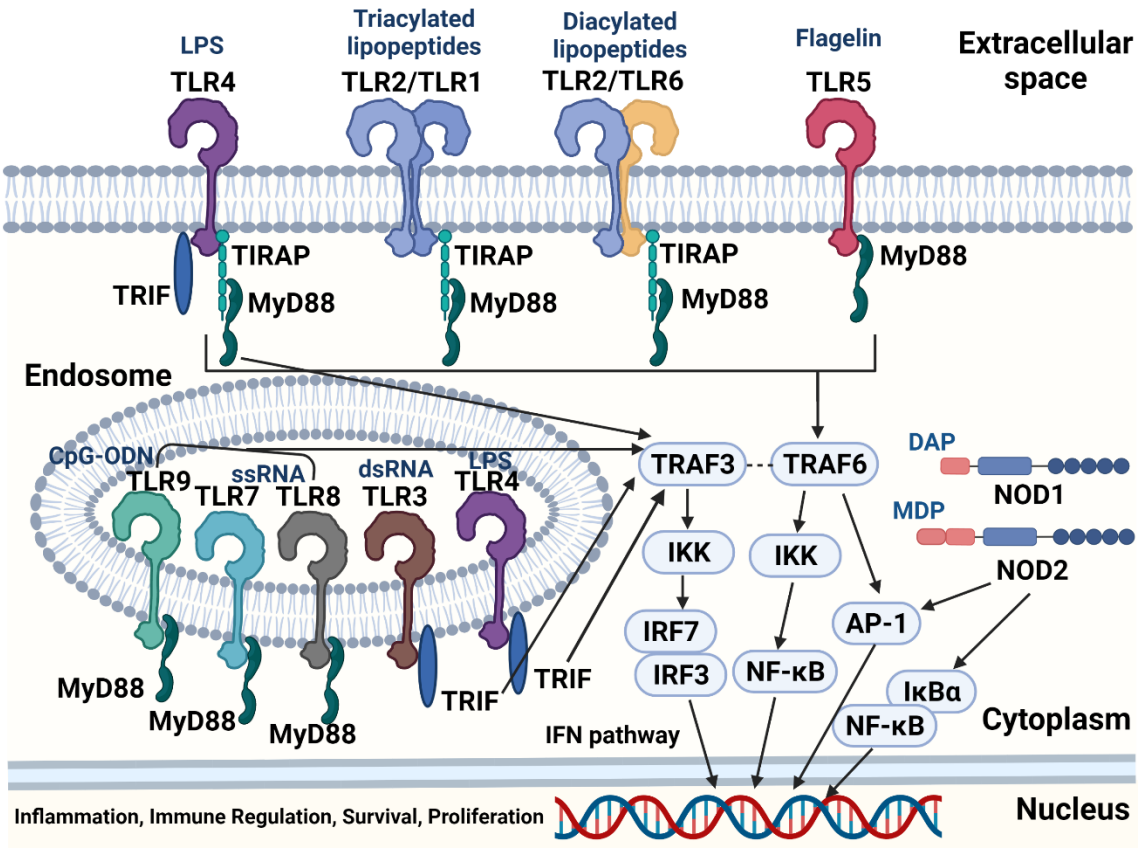

Figure 5. Toll-like receptors, NOD-like receptors and their signaling pathways. TLR1 and TLR6 recognize their ligands (Triacylated and diacylated lipopeptides respectively) as heterodimers with TLR2. TLR4 recognizes lipopolysaccharide (LPS) from gram negative bacteria. TLR3, TLR4, TLR5, TLR7, and TLR9 are currently thought to deliver their signal by forming homodimers after interacting with their ligands. TLR3, TLR7/8, and TLR9 are intracellular TLRs, located inside the endosome that recognize nucleic acids. NOD1 and NOD2 function as intracellular receptors for bacterial peptidoglycan fragments. While NOD1 activity is triggered by D-glutamyl-meso-diaminopimelic acid (DAP), NOD2 is activated by muramyl dipeptides (MDPs). Therefore, these receptors activate several transcription factors including the nuclear factor (NF)-kB and AP-1 by both TLRs and NLRs, and IRF3 and IRF7 (Interferon pathway) by TLRs, which results in the control of the inflammation, immune regulation, survival and proliferation. AP-1: activator protein 1; CpG-ODN: CpG oligodeoxynucleotides; dsRNA: double-strand RNA; IkBα: NFKB Inhibitor Alpha; IKK: IkappaB kinase; IRF3/7: interferon regulatory factor 3/5/7; NF-kβ: nuclear factor kappa B; ssRNA: single-stranded RNA virus; TIRAP: TIR domain-containing adaptor protein; TRAF3/6: TNF receptor-associated factor 3/6; TRIF: TIR-domain-containing adapter-inducing interferon-β.

Opposed to innate immunity, adaptive immunity is highly specific and responses are induced during the first weeks after infection (Biron, 2016). A dysfunctional interaction between gut microbiota and intestinal immune system may lead to an overreaction of effector T cells reacting against commensal microbiota (Silva et al., 2016). Classically, an aberrant Th1 response has been associated with CD, while UC patients are thought to exhibit an atypical Th2 response. Th1 cells, induced by IL-12 via interaction with IL-12R on undifferentiated T cells, produce high amounts of IFN-γ and IL-2, whereas Th2 cells are stimulated by IL-4 and release high amounts of IL-4, IL-5 and IL-13 cytokines (Figure 6). However, it was observed that UC was a "Th2-like" disease rather than a fully Th2 disease (Strober and Fuss, 2011). Strikingly, a new subset of effector Th cells, known as Th17, were later discovered to be involved in the pathogenesis of both forms of IBD (Round and Mazmanian, 2009). They were found in the mucosa of the GI tract of IBD patients, with a high production of IL-17, IL-21 and IL-22 cytokines, crucial for host defense against extracellular pathogens (Rovedatti et al., 2009; Monteleone et al., 2005). TGF-β and IL-6 are known to be the major inducers of Th17 producing IL-17 cells by naïve human CD4+ T cells, although IL-1β was also described to induce Th17 cells (Rovedatti et al., 2009; Ghoreschi et al., 2010). Furthermore, IL-23 was described as a key cytokine driving early responses to microbial insults, being its main function to interact with differentiated Th17 cells expressing the interleukin-23 receptor (IL-23R) and stabilize and/or expand Th17 cells (McGeachy et al., 2009). The lack of this receptor on naive CD4+ T cells supported the idea that IL-23 is not an inducer. Nonetheless, a study showed that IL-23 was essential to promote the production of pro-inflammatory cytokines by Th17 cells and, its absence led to the presence of Th17 cells producing IL-10 (McGeachy et al., 2007). Additionally, a polymorphism in the *IL-23R* gene was associated with reduced susceptibility to UC and CD, revealing the potential role of IL-23 and Th17 responses in IBD (Duerr et al., 2006). Collectively, an inappropriate mucosal immune response against common microorganisms may lead to the loss of immune tolerance, contributing to the imbalance of pro- and anti-inflammatory cytokines.

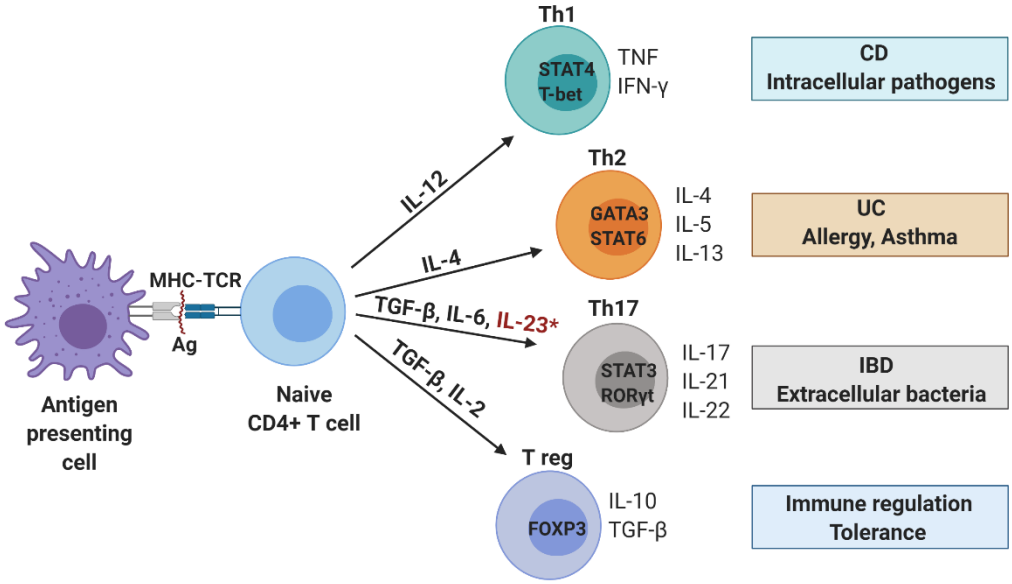

Figure 6. Differentiation of naïve T cells into effector Th cells during IBD upon antigen presenting cell stimulation. Naïve T cells recognize the presented antigen leading to cell division and differentiation. Differentiation is profoundly influenced by the cytokines present in the environment. Th1 response is induced by IL-12 and Th2 by IL-4. Moreover, Th17 differentiation is stimulated by TGF-β, IL-6 and IL-23* and T regs by IL10 and TGF-β. *IL-23 is not able to induce Th17 cells by itself. Adapted from Leung et al., (2010).

1.2.5 Gut microbiota composition

The advent of high-throughput next generation sequencing (NGS) technologies has enabled the identification of a disturbed microbiota composition and function, and a reduction of microbial diversity in IBD patients, which is termed as dysbiosis (Nishida et al., 2018). Obtained clinical and experimental data points dysbiosis as a key player in IBD pathogenesis, although is still unclear whether it is the cause of consequence of the disease.

The term microbiota refers to living microbial communities that inhabits a determined ecologic niche (Icaza-Chávez et al., 2013). Gut microbiota is a diverse ecosystem composed predominantly of bacteria, in addition to fungi, viruses, and other eukaryotes (Osakunor et al., 2020). The vast majority of microorganisms reside in the gut, consisting of approximately a total of 10^{14} enteric commensal microorganisms and around 500-1000 different bacterial species (Kim et al., 2017a). Bacteria present symbiotic interactions with the host being a mutualistic association. Whilst the host provides a stable environment with a permanent resource provision, gut microbes digest fiber, produce essential vitamins and nutrients for the host, have a central role in host development and provide protection against pathogen colonization (Gouba et al., 2019). After one year of age, gut microbiome remains stable, predominating Firmicutes and

Bacteroidetes phyla with more than the 90% of the total community (Gorkiewicz et al., 2018). Other subdominant phyla include Proteobacteria, Actinobacteria and Verrucomicrobia.

Factors, such as cesarian delivery, bottle feeding, genetics, environment, drugs and diet can induce changes in microbiota composition, highly impacting the incidence of IBD. These changes include increased oxidative stress and Gammaproteobacteria abundance and reduced levels of Firmicutes and Bacteroidetes (Ananthakrishnan et al, 2018). The resultant alterations can contribute to the development of intestinal inflammation in IBD. For instance, diet has shown to shape gut microbiota composition. A comparative study between the fecal microbiota of European children and children from a rural African village of Burkina Faso that have a diet based on high fiber intake, revealed significant shifts in gut microbiota composition (De Filippo et al., 2010). Children from Burkina Faso displayed a significant enrichment in Bacteroidetes, depletion in Firmicutes and a higher abundance of specific bacteria that contain genes for cellulose and xylan hydrolysis compared to European children. They also found significantly more short-chain fatty acids (SCFAs)-producing bacteria in the children of Burkina Faso. The polysaccharide-rich diet of the Burkina Faso individuals may allow them to maximize energy intake from fibers and might prevent the establishment of potentially pathogenic intestinal microbes such as *Enterobacteriaceae*, *Shigella* and *Escherichia* that were underrepresented in these children (De Filippo et al., 2010). Moreover, recent meta-analysis studies showed that soft drink and sucrose consumption were linked to a higher risk of developing UC (Nie and Zhao, 2017; Wang et al., 2017). Reduction in microbial richness might have been derived from the effect of globalization that has resulted in increased consumption of the Western diet, which is high in unhealthy fats, sugar, and animal proteins. In addition, babies born by caesarian section, deprived of contact with the maternal gut or vaginal microbiota, present decreased levels of facultative anaerobes such as *Clostridium*, but an association with IBD has not been demonstrated (Ananthakrishnan et al, 2018).

Gut inflammation in IBD is characterized by decreased microbial diversity. These microbial changes render the host more susceptible to pathogens colonization (Ananthakrishnan et al, 2018). However, patients with CD present a more pronounced reduction of microbial diversity than patients with UC (Pascal et al., 2017). In IBD patients, common changes in gut microbiome include an increase in facultative anaerobes from Proteobacteria phylum (Knights et al., 2014) and a reduction in obligate anaerobic producers of SCFAs from Firmicutes phylum (Morgan et al., 2012; Lloyd-Price

et al, 2019). In addition to bacterial dysbiosis, a distinct fungal microbiota dysbiosis has been also described in patients with IBD. Gut inflammation promotes fungi proliferation including the opportunistic fungal organism *Candida albicans*, associated with several human inflammatory conditions (Li et al., 2019). *Candida* is the most common member of the oral and intestinal mycobiota, but under certain circumstances it can cause infections (Mayer et al., 2013). In particular, IBD patients who present gut dysbiosis with a relatively low diversity of microbes are more likely to have increased abundance of *C. albicans* associated with active disease and delays in healing (Zwolińska-Wcisło et al., 2006; Zwolińska-Wcisło et al., 2009; Sokol et al., 2017). Furthermore, an increased Basidiomycota/Ascomycota ratio and a decreased proportion of *Saccharomyces cerevisiae* was reported in patients with inflammation compared to healthy individuals (Sokol et al., 2017).

Recent evidence suggested microbial composition to be associated with severity and therapeutic response (Haberman et al., 2019). Apart from understanding the role of gut microbiome in the pathogenesis in UC, research efforts are now focusing on the identification of disease-driving bacteria and specific microbial signatures related to IBD diagnosis and prognosis. In fact, fecal microbial signatures for CD or UC, could be utilized as a diagnostic tool to distinguish between IBD subtypes and IBD from other colonic diseases (Pascal et al., 2017). Additionally, the development of microbial-based treatments to modulate intestinal microbial composition might represent a promising and viable therapeutic strategy for IBD patients.

2. Pathophysiology of IBD

The intestinal epithelium, composed of a single layer of different cell types (enterocytes and specialized epithelial cells such as goblet cells and Paneth cells), is crucial for preserving gut homeostasis, thereby providing physical separation between host immune cells and luminal antigens derived from enteric microorganisms and food products (Allaire et al., 2018). Mucosal surfaces constitute a first line of defense against invading pathogens and represent the largest area of exposure of the body to external microbes. Mucins are likely to be the first molecules that invading microorganisms interact with at the cell surface, acting as a physical barrier and a trap for pathogens, as well as creating a matrix for other antimicrobial molecules (Linden et al., 2008). Mucin glycoproteins are secreted in large quantities by goblet cells and cover the apical epithelial surface of epithelial cells. There are two layers of mucus, an outer loosely adherent layer favorable for bacterial growth and an inner dense and firmly layer, adherent to the epithelial cells in order to prevent penetration of bacteria (Johansson et al., 2011). The mucus, especially the inner layer also contains immunoglobulin A (IgA) and antimicrobial peptides (AMPs) to limit access of commensal and pathogenic microorganisms to the lamina propria (Muniz et al., 2012). AMPs are produced naturally without stimulation, by intestinal epithelial cells, Paneth cells, and different immune cells. However, with the presence of external stimulation, they release larger amounts of AMPs including defensins, C-type lectins of the REG3 family and cathelicidins (Kim et al., 2014; Mukherjee and Hooper, 2015). The human secreted C-type lectin hREG3A functions as an antimicrobial protein and it is the homolog of murine Reg3b and Reg3g (Shindo et al., 2020). Whereas Reg3b exerts bactericidal activity against gram-negative bacteria by binding to lipopolysaccharide, Reg3g displays antibacterial activities against gram-positive bacteria by interacting with peptidoglycan carbohydrate (Darnaud et al., 2018).

On the other hand, secretory IgA (SIgA) plays a central role in the homeostatic maintenance of the intestinal microbiota. IgA coats a particular subset of microorganisms either pathogens or commensals blocking their attachment to epithelial cells and minimizing bacterial translocation, what is generally known as immune exclusion, acting as a neutralizing agent. SIgA is the predominant antibody class (80-90%) on most mucosal surfaces. Unlike the monomeric IgA present in the serum, gut mucosal secretory IgA produced by plasma cells in the lamina propria are polymeric, dominantly as dimeric IgA (Pabst and Slack, 2020, Pietrzak et al., 2020). Dimeric IgA is formed by two molecules of IgA covalently linked and stabilized by a J chain. The polymeric Ig receptor (pIgR) present in the basolateral membrane of epithelial cells carries IgA to

cross intracellularly epithelial cells to the apical domain by transcytosis. Release at mucosa surface generates SIgA containing a secretory component derived from the pIgR (Corthësy, 2009). Despite the dominance of secretory IgA in mucosal defense, mucosal production of IgG is also increased to react against bacterial antigens (Guarner, 2008).

Nonetheless, there is strong evidence that epithelial barrier integrity and expression of antimicrobial peptides are normally disturbed in IBD patients. Thus, decreased mucus production and defective tight junctions have been typically observed. In this regard, increased expression of the tight junction protein claudin-2 (CLDN2) usually occurs in active IBD, whereas the expression of CLDN-4, -5, -8 and occludin (OCLN) decreases (Landy et al., 2016). Epithelial damage leads to increased permeability and enhances the translocation of luminal antigens to the lamina propria (Figure 7). However, it is not clear whether disturbed epithelial barrier precedes IBD or is a consequence of the chronic inflammation (Ordás et al., 2012). Luminal antigens entering the lamina propria are first recognized by innate immune cells such as macrophages and dendritic cells. These antigen presenting cells recognize PAMPs and commensal bacteria via complementary PRRs and depending on the antigen, change their functional status from tolerogenic to an activated phenotype. PPRs stimulation results in the activation of NF-kB signaling, a master regulator of the inflammatory response against external stimuli by innate immune cells, important for the activation and development of adaptive immune cells, as well as the development of secondary lymphoid organs (Dorrington and Fraser, 2019). When NF-kB dimers translocate to the nucleus, initiates the transcription of major proinflammatory genes including TNF, IL-1β, IL-6, IL-12, IL-18 and IL-23. Once the innate cells have processed the antigens, they present them via MHCII (major histocompatibility complex class II) molecules to TCRs (T cell receptors) of naïve CD4+ T cells, promoting their differentiation into Th1 (CD), Th2 (UC) and Th17 (IBD) effector cells. Recent studies also have found increased levels of intestinal mucosal natural killer (NK) cells in the inflamed mucosa of IBD patients, indicating that they may play a role in disease pathophysiology. NK cells are a key part of the innate immune response that respond to intracellular pathogens. Furthermore, the presence of some proinflammatory cytokines (e.g., IL-2, IL-15, IL-21, and IL-23) have been linked to the immune responses of NK cells in IBD (Yadav et al., 2011).

Gut homing T cells expressing α4β7 integrin are augmented during intestinal inflammation, allowing immune cells to undergo diapedesis, which results in increased levels of gut-specific T cells in the lamina propria causing inflammation (Woodland and Kohlmeier, 2009; Lord et al., 2018). Thus, lymphocytes migrate to the gut by binding to

MAdCAM-1 (mucosal vascular addressin cell adhesion molecule 1) on the endothelial cells of blood vessels. During active inflammation, levels of CXCL1, CXCL3 and CXCL10 chemokines increase and neutrophils are recruited in response to microbial infections which preserves the inflammation (Wang et al., 2009; Sawant et al., 2016). Upon activation of neutrophils, myeloperoxidase (MPO), is either released into the phagolysosomal compartment or the extracellular environment (Aratani, 2018). MPO is a heme-containing peroxidase, produced mostly by neutrophils and to a lesser degree by monocytes. It has been considered as a component of the intracellular microbicidal system of phagocytes, in other words, a major arm of oxidative killing. Thus, it is an important player of the innate host defense system against invading microorganisms (Klebanoff et al., 2013; Aratani, 2018).

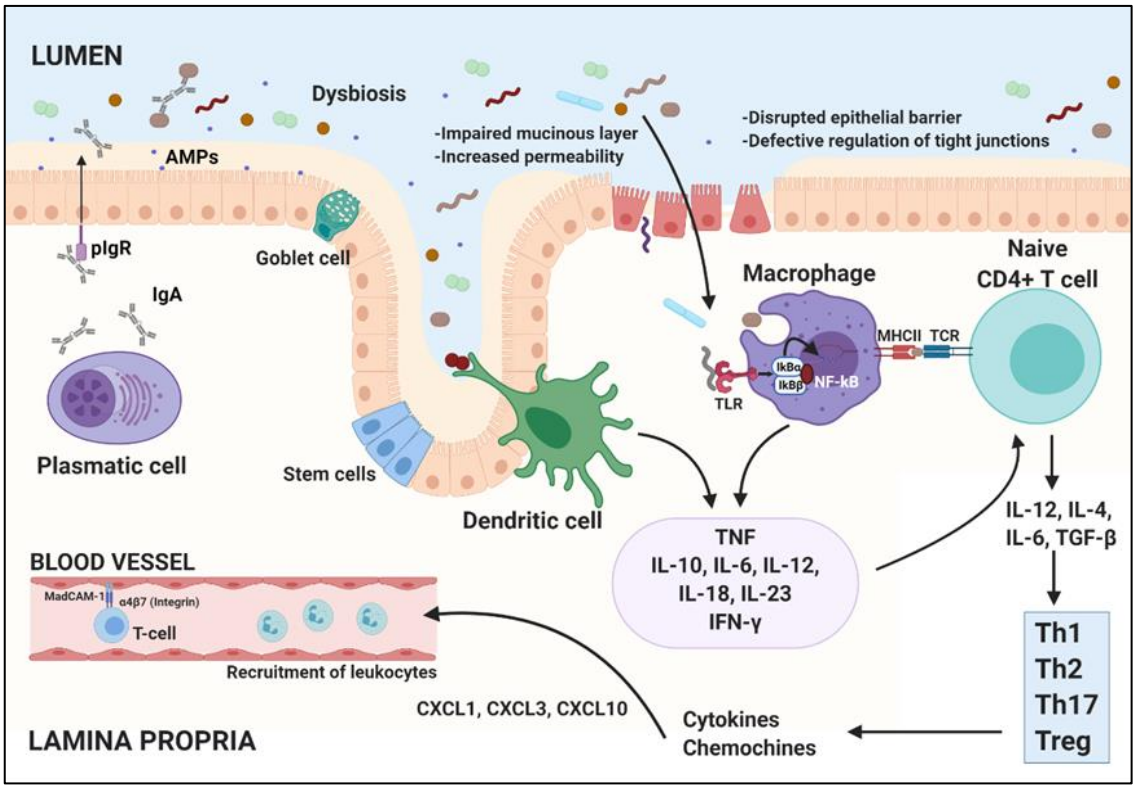

Figure 7. Pathophysiology of IBD. IBD is characterized by loss of epithelial barrier integrity due to defective regulation of tight junctions, impaired mucinous layer and increased epithelial permeability. Dysfunction of the epithelial barrier allows the translocation of bacteria that results in exaggerated mucosal immune responses. First, innate immune cells are activated in response to invading bacterial insults leading to the release of pro-inflammatory cytokines. Subsequently, antigen presenting cells activate naïve T cells by showing the antigen through MCHII-TCR complex, promoting differentiation into effector cells. Circulating T cells containing integrin α4β7 in the bloodstream can bind to MAdCAM-1, allowing lymphocyte diapedesis into the lamina propria. Augmented levels of chemokines attract circulating neutrophils enhancing intestinal inflammation. AMPs: antimicrobial peptides; IgA: immunoglobulin A; CXCL: chemokine; IkBα: NFKB Inhibitor Alpha; IkBβ: NFKB Inhibitor Beta; IL: interleukin; MAdCAM-1: mucosal addressin-cell adhesion molecule 1; MHCII: major histocompatibility complex class II; NF-κB: nuclear factor-κB; pIgR: polymeric immunoglobulin receptor; TCR: T-cell receptor; Th: T-helper; TLR: toll-like receptor; TNF: tumour necrosis factor; Tregs: regulatory T cell. Adapted from Ordás et al., (2012).

2.1 Gut microbiota

Advances in NGS technologies has allowed us to have a greater understanding of the role of the gut microbiome in the pathogenesis of IBD with unprecedented throughput depth and nucleotide resolution. Gut microbiota coevolves with humans in a symbiotic relationship, in which both human body and microbiota benefit, and these symbiotic interactions are required to maintain homeostasis (Nishida et al., 2018). While the host provides a habitat and nutrition to gut microbes, the gut microbiota contributes to several host physiological processes. Indeed, microbiota performs digestive and metabolic functions, promotes the intestinal epithelial barrier integrity and the development of immune system, and confers protection against pathogen colonization (Caruso et al., 2019).

Some bacteria are known to produce SCFAs as result of the anaerobic fermentation of undigested carbohydrates (Benharush et al., 2019). The three primary SCFAs include acetate, propionate and butyrate. SCFAs have been considered to play an important role maintaining homeostasis, since they are the primary energy source for colonocytes and exert important immunomodulatory functions (Parada Venegas et al., 2019). For instance, SCFAs have been reported to inhibit the activation of neutrophils (Ohbuchi et al., 2018). The main SCFA-producing bacteria in human gut belong to *Ruminococcaceae* family, in particular *F. prausnitzii* and *Clostridium leptum*, and *Lachnospiraceae* family including *Roseburia spp.* Indeed, *Faecalibacterium* is one of the most abundant genera of the human gut microbiome (Arumugam et al., 2011). Furthermore, it was shown that *F. prausnitzii* had anti-inflammatory properties in human peripheral blood mononuclear cells (PBMCs). The PBMCs stimulated *in vitro* by F. prausnitzii, produced significantly lower IL-12 and IFN-γ, and higher IL-10 (Sokol et al., 2008). However, SCFAs-producing bacteria are typically reduced in mucosa and feces of patients with IBD. Therefore, results suggest the use of *F. prausnitzii* as a probiotic is a promising strategy to treat CD (Sokol et al., 2008).

Despite not being a main SCFAs producer, *Akkermansia muciniphila* also produce both acetate and propionate, which are known to regulate host biological functions and improve host metabolic health (Derrien et al., 2004; Parada Venegas et al., 2019). It is an intestinal mucin-degrading bacterium that utilizes mucins as its sole carbon, nitrogen and energy source and resides in the mucus layer of the large intestine, where it is involved in maintaining intestinal integrity (Brodmann et al., 2017). Previous studies reported that both murine and human *A. muciniphila* strains improved chronic colitis disease severity parameters due to the exerted anti-inflammatory effects (Zhai et

al., 2019; Bian et al., 2019). Furthermore, although mucosa-associated bacteria such as *Ruminococcus gnavus* and *Ruminococcus torques* are typically increased in IBD to sustain nonmucolytic mucosa-associated bacteria, *A. muciniphila* levels significantly decreased compared to controls (Png et al., 2010). These findings suggested that *A. muciniphila* may be related to the health of the intestinal mucosa, conferring protection against intestinal injury. Remarkably, *A. muciniphila* was also shown to be safe when supplemented in humans (Depommier et al., 2019), as well as effective in controlling host metabolic disorders in mice (Everard et al., 2013), highlighting *A. muciniphila* value as a potential probiotic (Zhai et al., 2019). On the other hand, certain commensal species seem to trigger the induction of regulatory T cells via direct sensing of microbial products or metabolites (Guarner, 2008; Belkaid and Hand, 2014). These regulatory pathways are crucial for the host to tolerate microbial antigens without responding with inflammation.

2.1.1 Gut microbiota dysbiosis

The composition of fecal microbiota between subjects with IBD and healthy controls has been widely accepted to differ. The reported differences are heterogenous among the different studies. Nonetheless, a roughly 30-40% of dominant species within active IBD patients are uncommon in healthy individuals (Sokol et al., 2006; Guarner, 2008). This imbalance in the composition of the gut microbiota, so called dysbiosis, greatly affects host-microbiome interactions and is associated with a lower alpha diversity. Dysbiotic microbiota produces distinct metabolites and toxins having a profound effect on the intestinal immune system function, and therefore, influencing the course of the disease (Levy et al., 2017). Thus, dysbiosis has shown to disturb intestinal homeostasis and enhance intestinal inflammation. IBD patients are well-known to present decrease levels in obligate anaerobes of bacteria belonging to the class Clostridia in the Firmicutes phylum, including the butyrate-producing bacteria *F. prausnitzii* and *Roseburia hominis*, albeit an increase in *R. gnavus* has also been reported. In contrast, a substantial increase in the abundance of facultative anaerobic Proteobacteria, consisting mainly of *Escherichia coli,* has also been observed (Machiels et al., 2014; Pascal et al., 2017; Nishida et al., 2018; Lloyd-Price et al., 2019). Additionally, IBD patients are commonly associated with an increase in the abundance of Bacteroidetes phylum. Nevertheless, contradictory findings had shown reduced levels of Bacteroidetes mostly in patients with CD, but also in UC patients compared to healthy individuals (Maier et al., 2014; Zhou and Zhi, 2016; Lo Presti et al., 2019; Alam et al., 2020). Furthermore, the Firmicutes/Bacteroidetes (F/B) ratio is well known to be a key factor in maintaining gut homeostasis. Increased or decreased F/B ratio is regarded as

dysbiosis, whereby the former is usually associated obesity, and the latter with IBD (Stojanov et al., 2020).

The presence of interindividual variation within IBD subjects gut microbiota composition has hindered the identification of specific microbial signatures during IBD progression (Tyler et al., 2016). Thus, existing profiles of gut microbiome dysbiosis are inconsistent among studies. This could be in part the result of the presence of bias that can occur at any phase of research, including study design or data collection, as well as in the process of data analysis (Kim et al., 2017b). For instance, in microbiome studies it is highly important the sample collection and the choice of the *16S rRNA* gene region, among others. Therefore, to overcome the existing variability within technical differences, a consensus in the literature is needed (Smith et al., 2014). Furthermore, the diagnosis of IBD can be missed or delayed due to the presence of non-specific intestinal and extra-intestinal symptomatology (Dubinsky and Braun, 2015). In this regard, more research effort is needed to identify non-invasive, cost-effective, rapid and reproducible biomarkers that would be very helpful for physicians. On the other hand, there is growing evidence that certain members of the intestinal microbiota predispose individuals to disease, although the identification of disease-driving bacteria continues to be a challenge (Palm et al., 2014). These colitogenic bacteria might serve as predictors of disease progression or even therapy response, permitting the stratification of UC patients into distinct clinical entities of UC spectrum.

In recent years, deciphering the mucosal microbiota composition has become of great interest due to their close proximity to the host epithelium. Thus, it has been suggested that adherent microbes might play a key role in disease development. Despite the increased concentrations of mucosal adherent bacteria found in patients with active disease in either CD or UC, the diversity was found to be astonishing low (Swidsinski et al., 2015). Furthermore, these higher amounts of mucosal bacteria correlated with augmented disease severity. Mucosal microbiota profiles of IBD patients have been demonstrated to differ from those of healthy subjects. UC patients displayed enriched levels of Actinobacteria and Proteobacteria (*Enterobacteriaceae*, *Sutterellaceae*, *Veillonellaceae*), decreased Bacteroidetes and a specific reduction of *Lachnospiraceae* family belonging to Firmicutes phylum compared to healthy individuals (Lepage et al., 2011; Jalanka et al., 2020). These data suggested that mucosal microbiota shifts in UC resulted in increased proportions of pro-inflammatory and decreased proportions of anti-inflammatory bacteria, which may be associated with development and exacerbation of inflammation. Additionally, mucosa-associated bacteria community was found to be

significantly different from the fecal community suggesting that different populations are dominating in the mucosa and the feces (Zoetendal et al., 2002). Despite having distinct dominating species, mucosal-associated bacteria are of fecal origin. Microbial community from active UC patients' mucosal biopsies revealed the dominance of one or two bacterial orders, Lactobacillales and Enterobacteriales (Du et al., 2015). When these mucosa-associated bacterial communities were transferred to GF-mice, it was observed that they could increase sensitivity to DSS-induced colitis (Du et al., 2015). Hence, new research insight is required to further investigate host–microbiota interactions, which could help to develop novel strategies for mucosal restoration.

2.1.2 Intestinal microbial signatures

Emerging evidence has pointed towards gut microbiota to find a set of universal biomarkers for diagnosis, and prediction of disease severity and IFX treatment response in IBD patients. Although it is still challenging, it has been documented that the human fecal microbiota harbors promising and non-invasive biomarkers for this purpose, which emphasizes the potential ability that microbiota has to stratify IBD patients and apply personalized therapy for optimal outcomes (Zhou et al., 2018).

2.1.2.1 Diagnosis

A longitudinal study comparing healthy individuals with patients with CD, UC, irritable bowel syndrome (IBS) and anorexia was carried out in order to allow the identification of microbial signatures for CD and UC (Pascal et al., 2017). They found the most significant differences between CD and UC, and between CD and healthy controls, and they were able to discriminate CD from other diseases by analyzing eight groups of microorganisms. CD patients displayed reduced abundances of *Faecalibacterium*, an unknown *Peptostreptococcaceae*, *Anaerostipes*, *Methanobrevibacter*, an unknown *Christensenellaceae*, *Collinsella* groups and increased levels of *Fusobacterium* and *Escherichia* genera. Since the two forms of IBD and IBS share similar clinical and pathological features, in some cases, physicians do not have a clear diagnosis. Therefore, this specific microbial signature would be valid to distinguish CD from UC and IBS, allowing physicians to choose the proper treatment.

2.1.2.2 Prediction of disease severity

Specific members of the human intestinal microbiota have been associated with chronic inflammatory responses that could potentially be involved in IBD development and progression. Although most colitogenic bacteria itself cannot induce intestinal inflammation, they are associated with enhanced pathogenic inflammatory responses in genetically or environmentally predisposed patients (Palm et al., 2014). *Prevotellaceae* species have been demonstrated to drive intestinal inflammation and exacerbate DSS-induced colitis (Elinav et al., 2011, Brinkman et al., 2013, Iljazovic et al., 2020). In addition, *Prevotellaceae* species were found to be highly IgA coated in mice presenting gut dysbiosis through cohousing of animals prior to DSS administration compared to non-dysbiotic mice, suggesting that the high levels of IgA coating might have been derived from high-affinity, antigen-specific and T cell-dependent antibody responses (Palm et al., 2014). In addition, *R. gnavus* is widely accepted to be enriched in IBD patients with increased disease activity (Hall et al., 2017; Lloyd-Price et al, 2019). Henke et al. discovered that *R. gnavus* synthesizes an inflammatory polysaccharide that induces the production of inflammatory cytokines like TNF by dendritic cells, enhancing intestinal inflammation (Henke et al., 2019). Additionally, high abundance of this bacterium has been associated with lack of response to TNF inhibitor therapies (anti-TNFs) (Dovrolis et al., 2020). Therefore, *R. gnavus* is considered a possible biomarker of mucosal damage. Recently, low IgA coating of *Oscillospira* has been associated with earlier resection and has been considered a potential pathobiont without a potent IgA response (Shapiro et al., 2021). Furthermore, *Oscillospira* was part of the IgA+ consortium that was isolated from IBD patients, showing increased disease damage when it was inoculated to germ-free (GF) mice (Palm et al., 2014). Collectively, these microbial taxa might serve as predictors of disease severity and clinical outcomes in patients with IBD.

2.1.2.3 Prediction of anti-TNF response

Anti-TNF drugs have been shown to modulate gut microbiota composition. In fact, treatment with the anti-TNF antibody adalimumab has been suggested to restore the healthy microbiota composition, presenting high abundances of Firmicutes and Bacteroidetes phyla (Busquets et al., 2015). They confirmed that the microbiota of CD patients shifted towards a healthy like microbiota that consisted of reduced levels of *E. coli* and increased levels of *F. prausnitzii*. Therefore, monitoring of *F. prausnitzii* and *E. coli* species could serve as a fast and reliable indicator of mucosal healing in CD patients (Busquets et al., 2015). Furthermore, another study using Infliximab (IFX) revealed that

IFX diminished CD-associated gut microbial dysbiosis and the presence of opportunistic bacteria, whereas it promoted several SCFA-producing bacteria (Wang et al., 2018). Indeed, alpha diversity and the ratio *F. prausnitzii*/*E. coli* was found to be higher in responders compared to non-responders (Sanchiz-Artero et al., 2020).

Despite the high primary response rate (70-90%) to IFX, a moderate percentage of IBD patients lose response over time (40%). Thus, identifying predictors of response to anti-TNF antibodies would allow physicians to select patients who will response to the treatment. For this purpose, Wang et al. compared the fecal microbiota composition at baseline of CD patients who responded and patients who did not respond to IFX (Wang et al., 2018). Remarkably, they observed that responders were associated with enrichment of SCFA-producing bacteria, especially *Blautia*, *Faecalibacterium*, *Lachnospira*, and *Roseburia* (Wang et al., 2018). In UC the same tendency was observed, at baseline, anti-TNF responders displayed higher abundance of *F. prausnitzii* compared to non-responders (Magnusson et al., 2016). In line with these studies, dysbiosis, characterized by the reduction of *F. prausnitzii* at baseline, was a common feature in relapses suggesting that a deficit in *F. prausnitzii* could be used as a predictor of relapse after IFX administration in CD (Rajca et al., 2014). In this study, *Clostridium coccoides* was also found to be a valid candidate to predict CD relapse (Rajca et al., 2014). A recent study also compared microbial abundances before the initiation of the treatment in CD patients. Importantly, they observed *R. gnavus* enrichment in patients who will not respond, whereas *Roseburia* was more abundant in patients who will respond to IFX (Dovrolis et al., 2020). Therefore, *R. gnavus* might serve as a potential biomarker for non-response to anti-TNF treatment. Conversely, studies point *F. prausnitzii* as a predictive indicator of therapeutic response and mucosal healing in IBD patients. Apart from *F. Prausnitzii* other SCFA-producing bacteria have also been associated with treatment response suggesting the beneficial role of SCFAs.

Recent data suggest that metabolites and in particular, bile acids (BAs), might serve as predictors of anti-TNF response in IBD. In fact, different metabolic profiles have been detected between IBD patients with different IFX response (Bjerrum et al., 2015; Ding et al., 2020). Wang et al. showed that metabolic phenotypes associated with responders were linked to higher levels of glycine, linoleic acid, and L-lactic acid at baseline, compared to non-responders (Wang et al., 2021). Additionally, they concluded that the lower unconjugated/conjugated BAs ratio observed in CD patients could be the result of a reduction in bile salt hydrolase (BSH)-producing bacteria, including *Bifidobacterium* and *Clostridium* clusters IV and XIVb. Hence, enriching bacteria taxa

that produce SCFAs and BSH may promote IFX efficacy (Wang et al., 2021). These findings reinforce the important role of microbiome composition and its metabolites in the outcome of IFX therapy for IBD.

2.1.3 Gut microbiota manipulation techniques

Strategies for manipulating the gut microbiome might provide important insights into the link between microbiome and disease susceptibility and their use as a treatment approach for IBD patients. Hence, colonization of GF mice with fecal transplants and fecal microbial transplantation (FMT) by cohousing are the most used approaches.

2.1.3.1 Germ-free murine model

The use of GF mice has increased dramatically over the last decade, in part due to the growing interest in microbiome research. Currently, rodents are the most commonly used GF animal model, and most frequently mice, although other GF animals such as zebrafish can be used (Uzbay, 2019). The term germ-free or axenic refers to an animal demonstrably free of associated forms of life including bacteria, viruses, fungi, protozoa, and parasites, throughout its lifetime (Al-Asmakh and Zadjali, 2015). GF mice permit the study of murine physiology in absence of microbes and the generation of gnotobiotic animals after colonization by known microbes (Kennedy et al., 2018). Furthermore, GF animals are valid experimental models for studying host-microbial interactions in health and disease. This model is linked to extensive deficits in the development of the immune system and especially in gut-associated lymphoid tissues (GALT), presenting immature lymphoid tissues. In addition to numerous defects in antibody production, GF mice have fewer and smaller Peyer's patches and mesenteric lymph nodes (MLNs), and diminished levels of antimicrobial peptides compared to specific pathogen free (SPF) mice (Round and Mazmanian, 2009; Nishida et al., 2018). Therefore, microbiota is essential for the immune system development, indeed, colonization of GF mice with intestinal microbiota is sufficient to restore immune responses in germ-free mice (Nishida et al., 2018).

The use of GF mice allows the study of specific microbial communities from specific donors (human or other species) and analyze the impact of these microorganisms on the host immune system in health or in a certain disease. Monocolonization of GF mice with a single bacterial species provides a greater understanding of how that species affects host physiology. Nevertheless, the full effects of a single bacteria cannot be obtained due to the lack of a full microbial community context (Fritz et al., 2013). The key advantage of GF is that colonization with known

bacterial species permits to directly link a specific function to these bacteria, and this information could be valid to find a biomarker in risk prediction, a treatment or to find bacteria associated with therapy failure (Fritz et al., 2013). In conclusion, GF animals are an invaluable experimental tool to provide deeper insights into the effect of host–microbiota interactions between a host and its microbiota.

2.1.3.2 Fecal microbiota transplantation by cohousing of mice

Horizontal transmission of the microbiota between different mouse individuals is a fundamental tool for examining the contribution of microbes to health and disease. Currently, it is widely accepted that microbiota can be transferred from one mouse to another by simply cohousing the animals. During cohousing, animals may feed on feces (as a result of coprophagy) or ingest feces by self-grooming permitting the exchange of microorganisms (Laukens et al., 2016). The use of antibiotic to allow the introduction of donor microbiota is not necessary (Manichanh et al., 2010). Manipulation of gut microbial composition is recommended between the age of weaning and young adulthood (4-8 weeks of age). Later in life, it would be more difficult to change microbial composition due to the increased stability of microbiome homeostasis and the presence of a developed immunity (Laukens et al., 2016). Therefore, cohousing is a simple and convenient approach for microbial transference between non-related animals.

It has been observed that disease phenotypes can be transferred through animal cohousing. For instance, by using feces from obese human, obesity was transferred to lean mice that was characterized by decreased abundance of bacteria associated with the fermentation of SCFA and transformation of BAs (Ridaura et al., 2013). Furthermore, cohousing of lean and obese animals prevented the obese phenotype. Another study demonstrated that 4 weeks of cohousing was enough to transfer the colitogenic activity of the wild-type (WT) microbiota to the less susceptible Casp3/11$^{-/-}$ mice (Brinkman et al., 2013).

2.2 Bile acids

Numerous studies have pointed to BAs as a major regulator of the gut microbiota composition. BAs are the end product of cholesterol catabolism that facilitate intestinal fat digestion, nutrients absorption, and the biliary transport of lipids and toxic metabolic metabolites. Only primary bile acids are synthesized in the liver, namely cholic acid and chenodeoxycholic acid (Dawson and Karpen, 2015). Before being secreted via biliary ducts they are conjugated with taurine or glycine (glycocholic acid, glycohenodeoxycholic acid, taurocholic acid and taurochenodeoxycholic acid). Primary

BAs undergo distinct bacterial transformations including dihydroxylation, dehydrogenation, and epimerization that generate secondary BAs, such as lithocholic acid, deoxycholic acid and ursodeoxycholic acid (Changbumrung et al., 1990). BAs regulate the composition of gut bacterial communities with their strong antimicrobial activity and citotoxicity (Zheng et al., 2017; Grüner and Mattner, 2021). Indeed, excess BAs concentration seems to exert cytotoxicity and therefore, promote apoptosis and a pro-inflammatory environment (Zhan et al., 2020). Although the pathogenesis of diarrhea is still under debate, BAs malabsorption is widely accepted to play a major role. In fact, luminal BAs secrete water and electrolytes into the colonic lumen that may induce propagated contractions (Tiratterra et al., 2018). In addition, high bile acids in the colon have been shown to cause diarrhea (Johnston et al., 2011). In active IBD patients, while fecal-conjugated BAs are significantly higher, secondary BAs are commonly reduced (Duboc et al., 2013). This secondary BAs deficiency has been associated with impaired transformation activities of the microbiota and a pro-inflammatory state within the intestine (Sinha et al., 2020). Furthermore, increase in fecal primary BAs correlated with looser feces consistency in patients with IBS (Duboc et al., 2012).

Emerging evidence has pointed towards the critical role of microbial communities in the BA pool mitigating or contributing to disease development (Staley et al., 2017). Augmented levels of taurocholic acid (TCA, conjugated primary BA) have been described to favor the growth of the pathobiont *Bilophila wadsworthia*, which is associated with the induction of colitis (Zheng et al., 2017). Indeed, it was confirmed that *B. wadsworthia* needs taurocholate to proliferate (Devkota and Chang, 2013). Furthermore, *Oscillospira spp.* and *R. gnavus* abundances correlated positively with TCA as a result of the high-fat diet caused shifts in mouse cecal bacterial communities (Zheng et al., 2017). A recent study conducted with a large cohort of IBD patients, showed TCA and glycocholate augmented in dysbiotic samples from patients with active IBD when compared with non-dysbiotic samples (Lloyd-Price et al., 2019). Furthermore, SCFAs were reduced in dysbiosis, which is in line with the reduced levels of *F. prausnitzii* and *R. hominis* observed. An increasing number of studies have shown under-representation of *F. prausnitzii* in IBD patients with dysbiotic microbiota (Duboc et al., 2013). Interestingly, members of the *Roseburia* genus were metatranscriptionally as well as metagenomically associated with BAs suggesting that *Roseburia* might be involved in the BAs dysregulation observed in IBD (Lloyd-Price et al., 2019). This suggested that depletion of secondary BAs producing bacteria highly affects the concentration of secondary BAs in IBD patients. Therefore, BAs play a central role in IBD, in which impaired levels seem to sustain intestinal inflammation.

2.3 Mitochondria

2.3.1 Mitochondrial form and function

Mitochondria are double membrane-bound organelles found in most eukaryotic cells. Although they are regularly depicted as ovoid or bean-shaped, they continuously modulate their shape in response to physiological inputs. They usually oscillate between tubular and spherical morphology regulated by the dynamic processes of fusion and fission (Kondadi et al., 2019). Cristae, the invaginations protruding into the mitochondrial matrix, are functional dynamic compartments that undergo morphological changes, including elongation, shortening, fusion and division. However, under homeostatic conditions, mitochondria are known to contain normal tubular and lamellar cristae (Hu et al., 2020). In addition, mitochondrial quality control components are required to degrade and eliminate damaged mitochondria and aberrant mitochondrial proteins by autophagy (Tahrir et al., 2019).

Mitochondria have been long considered the “powerhouses of the cell” (McBride et al., 2006). They generate most of the cell´s energy supply, which is based on the production of the basic unit of cellular energy adenosine triphosphate (ATP) through oxidative phosphorylation. For this purpose, mitochondria contain the electron transport chain (ETC), which is composed of five large multiprotein complexes (I–V) and located in the inner mitochondrial membrane. The first four complexes (CI-CIV) are responsible for the transfer of electrons from electron donors to electron acceptors via redox reactions that contribute to the generation of the electrochemical proton gradient across the inner mitochondrial membrane (Tang et al., 2020). Between these complexes there are two mobile electron transporters, coenzyme Q (ubiquinone) and cytochrome. At the end of the ETC, ATP synthase (complex V) translocates the generated protons from the intermembrane space back into the matrix to catalyze the synthesis of ATP from ADP and phosphate (Tang et al., 2020). During this process, some electrons leak out from the electron transport system and interact with oxygen to produce superoxide or hydrogen peroxide. Indeed, CI and CIII (especially CI) are considered to be the main sources of reactive oxygen species (ROS) production in mitochondria (Zhao et al., 2019). Furthermore, mitochondria possess their own genome, the mitochondrial DNA (mtDNA), which is located in the mitochondrial matrix. MtDNA is a double-stranded and circular DNA, that both in mice and humans, harbors 37 genes coding for 2 rRNA subunits (12S and 16S rRNAs), 22 transfer RNAs and 13 polypeptides that are all involved in the oxidative phosphorylation. Mutations in these genes have been strongly implicated in a wide variety of clinical disorders such as neurodegenerative, cardiovascular,

gastrointestinal and skin diseases, aging, and cancer (Ro et al., 2013; Herst et al., 2017). Mitochondria apart from regulating the activation, differentiation and survival of immune cells, they can also release signals such as mtDNA and ROS to regulate transcription of immune cells (Angajala et al., 2018).

2.3.2 Mitochondrial dysfunction

Despite the causative role that mitochondrial dysfunction plays in IBD is not yet fully understood, it has been extensively described in IBD. In 1980, Roediger first reported that UC patient's colonocytes had decreased butyrate oxidation levels, suggesting that UC might be an energy-deficiency disease (Roediger, 1980). Mitochondria, apart from being the main energy producers of the eukaryotic cell, they are a major source of ROS and reactive nitrogen species (Bolisetty and Jaimes, 2013). This ROS production has been reported to contribute to mitochondrial damage in a broad range of pathological disorders. Indeed, ROS overproduction can cause oxidative damage to mitochondrial proteins, membranes, and mitochondrial DNA, finally resulting in mitochondrial injury and impeding to perform a wide range of metabolic functions (Murphy, 2009). Excess cellular levels of ROS also can lead to the activation of cell death processes such as apoptosis (Redza-Dutordoir and Averill-Bates, 2016). A rapid release of ROS in immune cells is known to degrade internalized pathogens through the oxidative burst mediated by NADPH oxidases in phagosomes (Sena and Chandel, 2012). Conversely, low levels of ROS serve as signaling molecules to regulate and maintain normal physiological functions (Sena and Chandel, 2012).

Recent studies showed evidence that support the relevance of mitochondria integrity in IBD (Ip et al., 2017). Dysfunctional mitochondria have been associated with augmented epithelial barrier dysfunction and inflammation. Furthermore, it has been shown that genetic variants within the mitochondrial genome, could affect mitochondrial function and therefore, the intestinal microbiota and composition (Clark and Mach, 2017). For instance, mutations in specific mitochondrial genes such as *ND5* and *CYTB* have been linked to the presence of the butyrate producers *Eubacterium* and *Roseburia* (Ma et al., 2014). Notably, reduced ATP levels within the intestine together with increased mtDNA damage, ROS production and swollen mitochondria with ultrastructural abnormalities have been observed in IBD patients (Figure 8) (Novak and Mollen, 2015). Recently, Boyapati et al. showed that mtDNA is released during active UC as a consequence of tissue injury and mitochondrial damage (Boyapati et al., 2018). They observed that mtDNA can act as a pro-inflammatory DAMP via activation of TLR9-Myd88 pathway, triggering NF-κβ signaling and perpetuating the inflammatory response.

Reduced activity of respiratory chain complexes II, III and IV (up to 60%) have been reported in UC patients (Sifroni et al., 2010). Remarkably, Haberman et al. used a large cohort of UC patients (408 patients) to study mitochondrial activity and they correlated disease severity with mitochondrial dysfunction (Haberman et al., 2019). Indeed, they observed 13 genes associated with reduced ATP production and reduced complex I activity in addition to the *PPARGC1A* (PGC-1α), the master regulator of mitochondrial biogenesis. Such mitochondrial perturbations resulted in increased epithelial permeability as a consequence of ROS production and promoted transcytosis of bacteria across the epithelial layer. Higher intestinal permeability was observed in active UC suggesting a role for mitochondrial dysfunction in the pathogenesis of IBD.

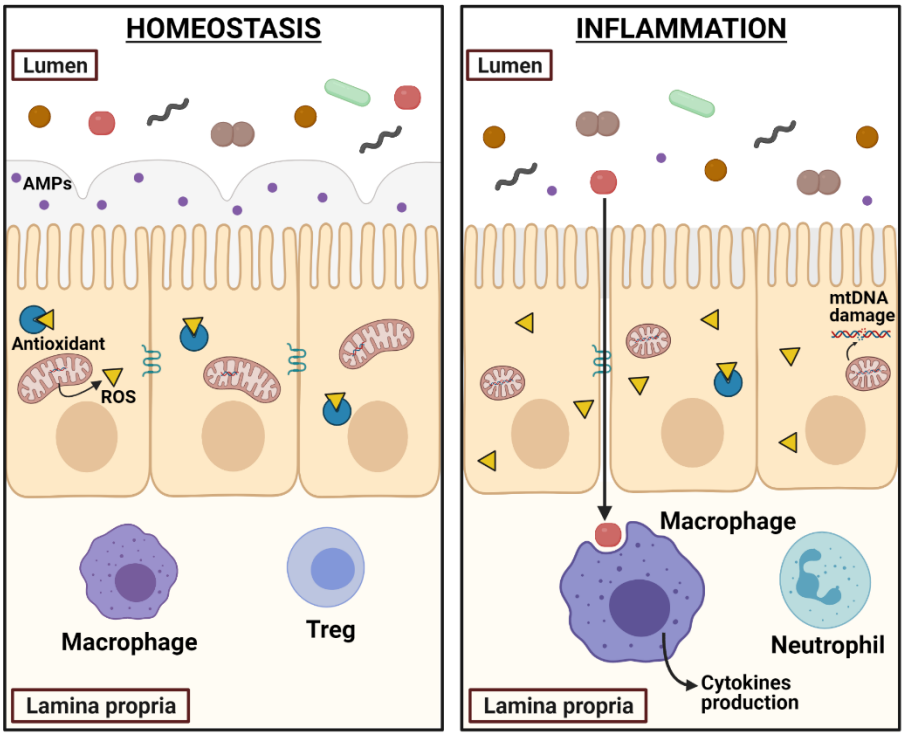

Figure 8. Mitochondrial dysfunction as a common feature during intestinal inflammation. Within intestinal homeostasis, gut barrier integrity is maintained by the proper functioning of tight junctions, by the presence of a thick layer of mucus produced by goblet cells and by the release of AMPs by Paneth cells. Under normal conditions, mitochondria contain well-formed cristae and ROS levels are suppressed by antioxidants. On the contrary, upon intestinal inflammation the mucus layer and the production of AMPs is reduced allowing the translocation of luminal antigens to the lamina propria. Additionally, the presence of defective tight junctions increases epithelial barrier permeability. Several studies revealed the association of IBD with decreased ATP levels and increased ROS production. Moreover, cellular antioxidants are decreased provoking augmented ROS levels. Mitochondrial morphology is abnormal and increased mtDNA damage has been reported during intestinal inflammation. AMPs: antimicrobial peptides; mtDNA: mitochondrial damage; ROS: reactive oxygen species; Treg: regulatory T cell. Adapted from Novak and Mollen, (2015).

2.3.3 Mitochondria-microbiota interaction

There is accumulating evidence for bidirectional interaction between mitochondria and microbiota (Clark and Mach, 2017). Mitochondria are believed to have descended from the ancestral α-proteobacteria symbiont leading to common features between eukaryotic mitochondrial and prokaryotic genomes (Jackson and Theiss, 2020). Therefore, mitochondria are capable of using mechanisms similar to bacteria and modulate immune responses. Microbiota participates in the regulation of key transcriptional co-activators, transcription factors and enzymes involved in mitochondrial biogenesis such as *PPARGC1A*, *SIRT1*, and *AMPK* genes. Additionally, the gut microbiota and its metabolites including SCFAs and secondary BAs, modulate host energy production processes, ROS generation and inflammation in the gut epithelial and immune cells. Gut microbiota has also been reported to attenuate TNF-mediated immune responses and inflammasomes such as NLRP3 (Clark and March, 2017). At the same time, mitochondria and ROS generation, have been shown to regulate gut microbiota via modulating intestinal barrier function and mucosal immune responses controlling pathogen invasion. Furthermore, the presence of genetic variants within the mitochondrial genome are suggested to impact mitochondrial function leading to changes in the intestinal microbiota composition and activity (Yardeni et al., 2019). Importantly, Mottawea et al. stated a disturbed host mitochondria-microbiota crosstalk in IBD. (Mottawea et al., 2016). Since defective mitochondria have been reported in IBD, the interplay between gut microbiota and host mitochondria is emerging as a significant area of research.

2.3.4 Methylation-controlled J protein (MCJ)

MCJ is a small mitochondrial protein (147 amino acids, 16 to 17 kDa) encoded by the *DNAJC15* gene that negatively regulates the ETC (Figure 9) (Hatle et al., 2013; Schusdziarra et al., 2013). While most of DNAJ proteins are soluble, MCJ contains a transmembrane domain and localizes in the inner mitochondrial membrane. Endogenous MCJ associates with complex I and acts as a natural inhibitor resulting in increased complex I activity, mitochondrial membrane potential and ATP production (Hatle et al., 2013). The activity of complex I is enhanced by its assembly into mitochondrial ‘‘respirasome’’, containing complexes I, III, and IV (Moreno-Lastres et al., 2012). Supercomplexes facilitate the efficient transfer of electrons minimizing the electron ‘‘leak’’ that results in reduced ROS production. *MCJ* was initially identified as a gene negatively regulated by methylation at CpG islands and expressed at very low levels in ovarian cancer (Shridhar et al., 2001), Wilms tumors (Ehrlich et al., 2002), brain

tumors (Lindsey et al., 2006) and melanoma (Muthusamy et al., 2006). Loss of *MCJ* gene expression in ovarian cancer cells together with a high rate of methylation in the CpG islands of *MCJ* gene, was associated with poor survival and poor chemotherapy response (Shridhar et al., 2001).

By using a murine model, MCJ has been found highly expressed in heart, liver and kidney and within the immune system it was detected in CD8+ T cells and macrophages, but not in CD4+ T cells and B cells (Hatle et al., 2013; Navasa et al., 2015a; Champagne et al., 2016). In the liver, decreased MCJ levels led to increased β-oxidation of fatty acids in hepatocytes and minimized lipid accumulation, resulting in decreased hepatocyte damage (Barbier-Torres et al., 2020). Later, IFNγ was identified as a repressor of *MCJ* gene transcription in macrophages by promoting the binding of the transcription factor Ikaros to MCJ promoter (Navasa et al., 2015b). Importantly, loss of MCJ in bone marrow-derived macrophages (BMM) results in increased mitochondrial respiration and elevated basal levels of ROS. Also leads to the upregulation of the TNF converting enzyme (TACE) inhibitor *Timp3* (tissue inhibitor of metalloproteinases-3), which effectively prevents the shedding of TNF from the membrane. Therefore, MCJ regulates the production of TNF by BMM in response to a variety of TLRs ligands and bacteria (Navasa et al., 2015a).

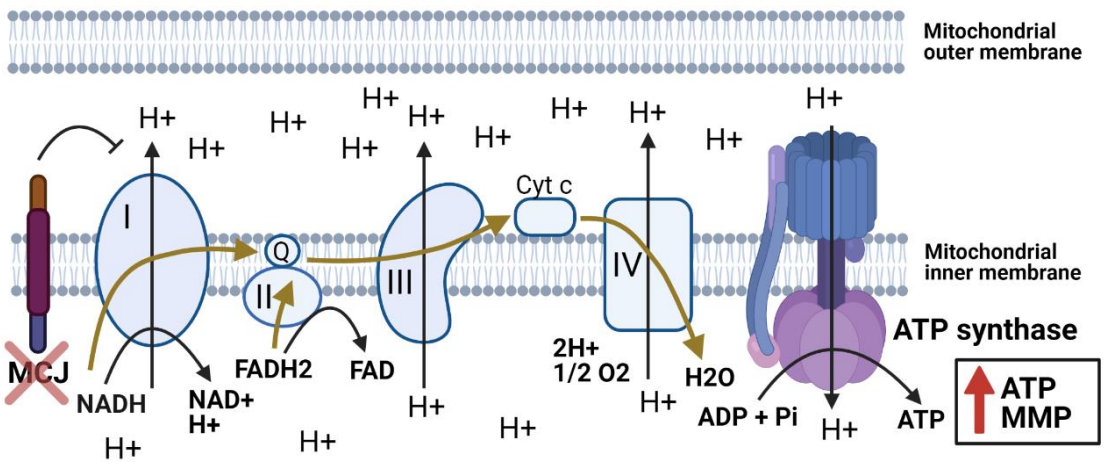

Figure 9. Impairment of mitochondrial electron transport chain by MCJ deficiency. As MCJ negatively regulates complex I, loss of this protein results in augmented ATP production and mitochondrial membrane potential. ETC includes complexes I-IV, the electron transporters ubiquinone and cytochrome c (cyt c), and ATP synthase (complex V). ATP: adenosine triphosphate; MCJ: methylation-controlled J protein; MMP: mitochondrial membrane potential.

2.3.4.1 *MCJ* expression in healthy human tissues and cells

The expression of *MCJ* in human tissue and cells was confirmed with the human protein atlas webtool. *MCJ* was found to be highly expressed in the gastrointestinal tract, especially in the small intestine and the colon (Figure 10). Additionally, it is also enriched in the brain, kidney, liver and muscle tissues. Regarding RNA expression in single cell types, high levels of *MCJ* expression are observed in enterocytes, monocytes and macrophages. Hence, *MCJ* is abundantly expressed in highly metabolic tissues that contain a larger content of mitochondria (Hatle et al., 2013).

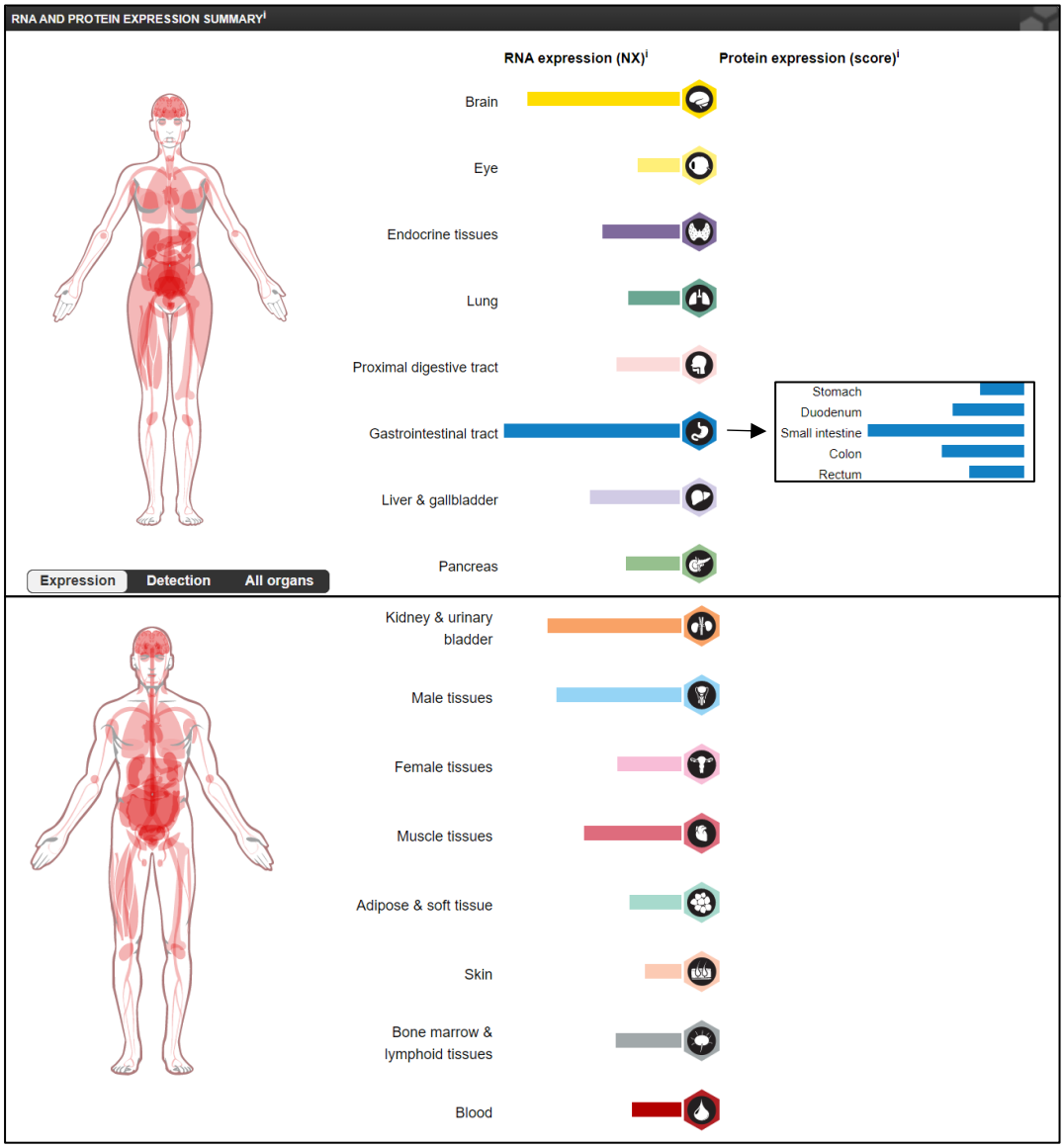

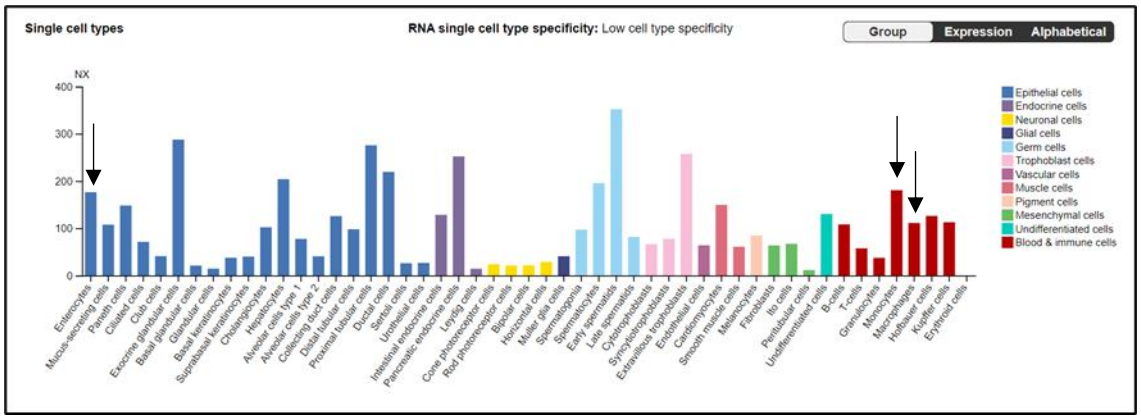

Figure 10. *MCJ* expression in healthy human tissues and cells. *MCJ* is highly expressed in the gastrointestinal tract and within the immune system, in monocytes and macrophages. Figures obtained from the Human Protein Atlas.

2.4 TNF signaling pathway

Apart from PRRs and cytokine receptors stimulation, NF-kB signaling is also governed upon stimulation of tumor necrosis factor superfamily receptors (TNFRs). TNF is a master pro-inflammatory cytokine involved in the pathogenesis of IBD, which not only promotes the pro-inflammatory response but also regulates cellular communication, differentiation and cell death (Brenner et al., 2015). TNF is mainly produced by macrophages, but also can be released by other tissues including lymphoid cells, mast cells and endothelial cells. This signaling pathway is composed of two receptors, TNFR1 and TNFR2. TNFR1 is expressed in most cell types, whereas TNFR2 is mainly expressed in immune cells and endothelial cells. Originally, TNF is produced as a membrane-bound TNF (mTNF). The soluble form of TNF (sTNF) is released via proteolytic cleavage of the mTNF by the metalloproteinase TACE (Wajant et al., 2003). However, the activity of TACE enzyme can be inhibited by its specific inhibitor TIMP3. While both forms of TNF can bind either to TNFR1 or TNFR2, sTNF cannot fully activate TNFR2 (Figure 11) (Holbrook et al., 2019). Furthermore, TNFR1 contains a cytoplasmatic death domain that enables the recruitment of TNFR1-associated death domain protein (TRADD), promoting apoptosis or necroptosis. Nonetheless, TNFR2 does not have this death domain and recruits TNFR-associated factor 1 (TRAF1) and TRAF2. Both TNFR1-TRADD and TNFR2-TRAF1/TRAF2 pathways can activate NF-kB transcription factors and promote the transcriptional activation of pro-inflammatory gene induction.

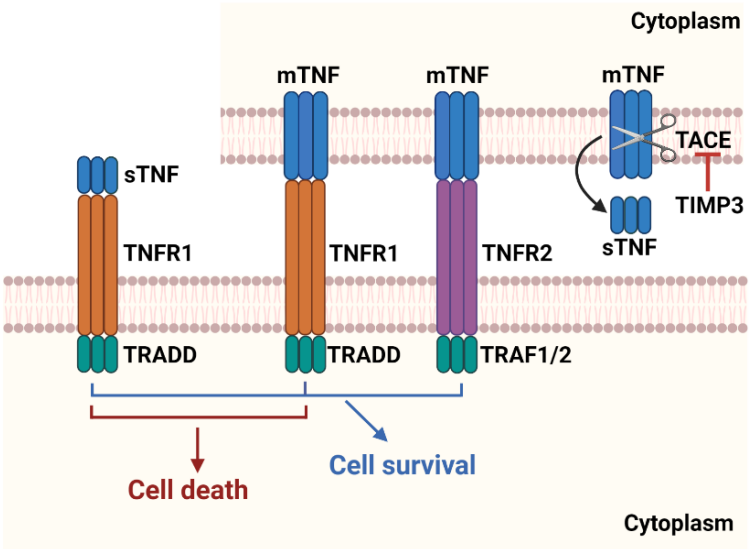

Figure 11. Soluble TNF production and TNF signaling through TNFR1 and TNFR2 receptors. mTNF is cleaved into sTNF by TACE enzyme, which function can be inhibited by TIMP3. mTNF can activate both receptors whereas sTNF only activates TNFR1. Both receptors promote cell survival but only TNFR1 has a death domain to induce cell death. mTNF: membrane-bound TNF; sTNF: soluble TNF; TACE: TNF alpha converting enzyme; TIMP3: tissue inhibitor of metalloproteinases 3.

3. Current and emerging IBD treatments

IBD is a lifelong disease and the main objective of available treatments is to induce and maintain remission in IBD patients, by reducing the inflammation and therefore the signs and symptoms of the disease. Specifically, the goal is to improve the patient´s quality of life. The main clinical manifestations of IBD are bloody stools, diarrhea, abdominal pain, fever, fatigue and weight loss (Low et al., 2013). Apart from the symptoms, histopathology is a potential diagnostic tool in IBD. Inflammation is characterized by the presence of an abnormal epithelium architecture including decreased crypt density, crypt distortion, reduced mucus surface and heavy diffuse transmucosal inflammation and lamina proprial infiltrate (Feakins, 2013; Gajendran et al., 2019). There are a wide variety of treatments depending on the extent and severity of the inflammation, although anti-TNF agents are the most used and effective ones in IBD (Figure 12). However, roughly one third of IBD patients do not respond to TNF inhibitor induction therapy and many lose response over time (Kennedy et al., 2019). Furthermore, serious adverse effects like severe infections have been reported (Gerriets et al., 2021).

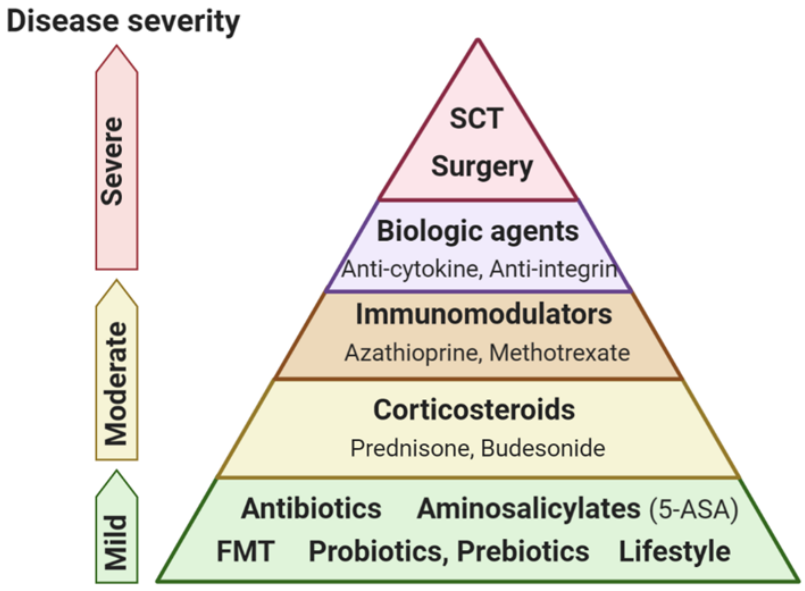

Figure 12. Therapeutic pyramid of available treatments for IBD patients depending on the disease severity level. To treat patients with mild IBD, antibiotics, aminosalicylates, fecal microbial transplantation (FMT), probiotics, prebiotics and changes in the lifestyle are recommended (shown in green). Immunomodulators and corticosteroids are used to treat patients with moderate disease severity (shown in yellow-orange). For critical IBD patients, biologics, surgery and stem cell therapy (SCT) are suggested (represented in purple-red).

3.1 Treatments for mild IBD: Aminosalicylates and gut microbiota modulation strategies

To treat patients with mild UC, treatments consist of aminosalicylates (ASAS), antibiotics, FMT, probiotics, prebiotics and diet. ASAS have remained the gold standard treatment for inducing and maintaining remission in patients with mild disease due to their cost, efficacy and safety profile (Chhibba and Ma, 2020). They act locally in the colon reducing the inflammation and promoting epithelial restitution. Moreover, antibiotics are recommended to restore the enteric microbiota by reducing pathogenic bacteria, either by killing or stopping their growth. However, the use of long-term oral antibiotics could cause resistance and become less effective, apart from killing commensal bacteria.

Restoration of enteric microbiota by the use of FMT from a healthy donor, probiotics and prebiotics are still under debate. Although FMT has proven extremely effective to treat *Clostridium difficile* infection, results concerning its usage are still inconclusive (Nicholson et al., 2020). The randomized controlled trials (RCT) of FMT conducted, suggested that CD patients were more likely to have a response (Lopez and Grinspan, 2016). Within CD, a meta-analysis including four cohort studies, which comprised 59 individuals, showed that approximately 63% of the patients achieved clinical response after FMT (Cui et al., 2015; Vermeire et al., 2016; Vaughn et al., 2016; Paramsothy et al., 2017a; Goyal et al., 2018). A meta-analysis of four RCTs of FMT performed on UC patients, which comprised a total of 140 FMT-treated individuals, revealed that FMT was significantly associated with clinical remission (Moayyedi et al., 2015; Rossen et al., 2015; Paramsothy et al., 2017a; Paramsothy et al., 2017b; Costello et al., 2019). Although emerging data support a potential increased role of FMT in IBD, many studies present several limitations. Therefore, more studies are needed to overcome the existing limitations including size, timing, frequency, mode of delivery, number of donors and the need for a single or repeated FMT (Sokol et al., 2020).

In the last years, several trials have been developed to assess probiotics potential to induce and maintain remission in IBD patients. Probiotics are defined as live microorganism that when administered in adequate amounts, confer a health benefit on the host (Hill et al., 2014). Such benefits include food digestion, modulation of the intestinal barrier and immune responses and secretion of potent AMPs such as bacteriocins. The fermentation of carbohydrates and indigestible dietary fibers by the intestinal microbiota produces SCFAs that have significant positive impacts on intestinal epithelial cell function. SCFAs acidify luminal pH, which is harmful for potential

pathogenic bacteria (Hardy et al., 2013). *Escherichia coli* Nissle 1917, *Bifidobacterium, Lactobacillus, Streptococcus* and VSL#3 are the most studied probiotics to date (Derwa et al., 2017; Nishida et al., 2018). VSL#3 is a commercial probiotic mixture of eight live freeze-dried bacterial strains including four strains of *Lactobacillus* (*Lactobacillus acidophilus*, *Lactobacillus plantarum*, *Lactobacillus casei*, and *Lactobacillus delbrueckii* subspecies *bulgaricus*), three strains of *Bifidobacterium* (*Bifidobacterium breve*, *Bifidobacterium longum*, *and Bifidobacterium infantis*), and one strain of *Streptococcus* (*Streptococcus salivarius* subspecies *thermophilus*) (Cheng et al., 2020). In the last years, inconclusive results have been obtained regarding probiotics efficacy. A large clinical trial made with the nonpathogenic *E. coli* strain Nissle 1917 showed that this bacterium obtained equivalent efficacy and safety outcomes in maintaining remission in UC patients compared to salicylates (Kruis et al., 2004). Nonetheless, VSL#3 mixture has yielded the most available evidence in IBD patients. Although VSL#3 probiotic has been demonstrated to have beneficial effects when inducing remission in active UC patients (56.2% failed to achieve remission with VSL#3 *versus* 75.2% in patients receiving placebo) (Derwa et al., 2017; Tursi et al., 2010; Sood et al., 2009), many trials made with distinct probiotics failed to determine effectiveness of probiotics either with UC or CD patients (Derwa et al., 2017). Many of the studies published to date about probiotics efficacy in UC failed due to the wrong duration of patient´s follow-up, study design, selection of patients or dose of the treatments (Iheozor-Ejiofor et al., 2020).

On the other hand, prebiotics are nondigestible oligosaccharides that confer benefits to the host including improvement of intestinal barrier integrity by the stimulation of protective bacteria (Davani-Davari et al., 2019). Moreover, they stimulate absorption of calcium and other minerals boosting bone mineralization and improving bowel function (Whisner and Castillo, 2018). They also provide defense against pathogens via decreased intestinal pH upon organic acids synthesis (Ashaolu, 2020). Currently, inulin-type fructans, oligofructose, fructooligosaccharide (FOS) and galactooligosaccharide (GOS) are the most researched prebiotics. Despite having reported efficacy with experimental colitis models, trials in human IBD are just emerging. While some studies reported decreased inflammation in IBD patients after inulin and FOS uptake (Welters et al., 2002; Lindsay et al., 2006), other studies did not observe any improvement (Looijer-van Langen and Dieleman, 2009). Understanding the mechanism of action of probiotics and prebiotics will improve their success.

3.2 Treatments for moderate IBD: Corticosteroids and immunomodulators

When mild treatments are not sufficient, treatments for moderate IBD patients such as corticosteroids/glucocorticoids (an anti-inflammatory solution) and immunosuppressives are used. Corticosteroids are drugs with anti-inflammatory properties that have been shown to be very effective in inducing remission in moderate flares. Nevertheless, they are not considered as a long-term or maintenance treatment due to the potential side effects (Salice et al., 2019). On the other hand, immunomodulators are employed to inhibit the immune response mediated by T lymphocytes. They are commonly used as a maintenance therapy to replace the use of corticosteroids. Conversely, there is poor evidence to support the use of immunomodulators as an induction therapy in UC (Chhibba and Ma, 2019).

3.3 Treatments for severe IBD: Biologics, surgery and stem cell therapy

Finally, to treat patients with severe UC or patients who failed to mild-moderate treatments, biologics such as anti-TNF agents and surgery are recommended. Emerging treatments including new biologics and small drugs are being developed by different companies. In regard to treatments that block immune cell migration, there are biologics such as anti-integrins that block the action of integrins, inhibiting the interactions between leukocytes and intestinal blood vessels (e.g., Natalizumab and Vedolizumab). Furthermore, anti-MAdCAM-1 antibodies also affect cell migration by obstructing ligands on vascular endothelium and seem to be effective in UC patients. Besides, there are sphingosine-1-phosphate receptor (S1PR) modulators (e.g., Ozanimod), which trap lymphocytes in lymph nodes. These S1PR modulators are effective with UC patients and they are being tested with CD patients in a phase III trial (Schreiner et al., 2019).

Regarding drugs that disturb immune cell communication, biologics are composed of small molecules including JAKs, SMAD7 and PDE5 inhibitors, and anti-cytokines. Anti-TNF is the most used treatment at the moment (e.g., IFX and Adalimumab). However, about 35% of patients poorly achieve clinical response to IFX over time (Feagan et al., 2013). Furthermore, this biologic is expensive, requires intravenous administration and has associated toxicities, such as infusion reaction and infectious complications (Parsi et al., 2002). IFX is a chimeric anti-TNF antibody (75% human, 25% murine) that is administered intravenously to block both TNF and TNFR. Due to the existing anti-TNF antibodies limitations and despite being the most used anti-

cytokine, other anti-cytokines have been developed as well as IL-6 and cytokines involved in the IL23/Th17 pathway. However, more studies are needed to prove efficacy of IL-6 and IL-17 cytokine inhibitors (Schreiner et al., 2019). Contrarily, inhibitors targeting IL-23 cytokine have been demonstrated to be effective in IBD patients (e.g., Ustekinumab and Mirikizumab).

Finally, surgery is recommended for critical patients that do not respond to other therapies and stem cell therapy (SCT) is under investigation to treat highly refractory patients that cannot undergo surgery. The objective of the latter treatment is to reset the immune system and restore immune tolerance (Shimizu et al., 2019).

Nonetheless, the cost associated with IBD treatments is increasing over time, mainly because of the costs associated with the biologic treatment itself. The identification of biomarkers with capacity to predict clinical response to biologic drugs is an area of great interest. This could allow the development of an individualized medicine where each patient would be treated with the most appropriate therapy given its unique profile in order to make a more rational use of resources. Achieving that goal will allow clinicians to indicate the most appropriate treatment to each individual, hence avoiding administering drugs to patients who will not respond.

4. Multi-omics in IBD

Considering that IBD is a multifactorial disease, the study of one specific aspect might not be enough to have a greater understanding in disease pathogenesis (Kumar et al., 2019). Multi-omics provide a global view of biological processes and molecular changes that underlie the development and progression of UC. Importantly, omic strategies are contributing to the process of biomarker development in precision medicine (Olivier et al., 2019). Therefore, multi-omics is based on the combination of omics including metagenomics, metatranscriptomics, metaproteomics and metabolomics. Currently, the integration of different 'omics' datasets is a challenging task that will enable the understanding of interactions between microbial functional aspects, host features and disease outcome (Metwaly and Haller, 2019). A recent study revealed multi-omics strength to identify specific species associated with BAs accumulation in a large cohort of IBD patients. Notably, these species could be used as new targets for therapeutic restoration (Lloyd-Price et al., 2019).

The clinical heterogeneity among patients has led to develop biomarkers that could distinguish the distinct clinical entities of UC spectrum and stratify UC patients (Czarnewski et al., 2019). Noninvasive, accurate, and inexpensive measures of intestinal inflammation would enable clinicians to select the best therapy for its patient in order to control the inflammation (Sands, 2015). Although there are some blood, stool and urine markers as indicators of IBD, few of them have at present clinical value.

In this sense, within transcriptomics, RNAs have been widely explored and have provided significant amount of information for a better understanding of IBD pathogenesis. Aberrant mRNAs have been demonstrated to contribute in molecular functions associated with immune response, mucosal inflammation, nutrients absorption, epithelial damage, oncogenesis and cell proliferation (Chan et al., 2018). This information could be utilized as targets in the development of diagnostic biomarkers or therapeutic agents in IBD treatments. However, more transcriptomic studies should be performed to further assess the molecular mechanisms and characterizations of RNAs in IBD by different study cohorts.

The study of the proteome, called proteomics, also seems to be crucial in the clinic to develop specific biomarkers. It comes together with the term personalized medicine, where the goal is to match each individual patient with the best therapy to ensure an optimal outcome (Duarte and Spencer, 2016). Since proteins are closely involved in nearly all physiological processes, they are very useful to discover novel

biomarkers or identifying potential drug targets. Therefore, they might serve as monitors of disease activity, as potential predictors of disease course and might be valid to decipher patients´ response to therapy. With regard to the limitations, a very small number studies have been performed and most of them have a small sample size with insufficient statistical power. Indeed, the vast majority of studies have been focusing on serum biomarkers. Furthermore, the methodology conducted in the studies is very heterogeneous (Gisbert and Chaparro, 2019).

Currently, the role that microbial dysbiosis plays in IBD pathogenesis is of particular interest. It is unclear whether gut dysbiosis is the cause or effect of the disease. Gut dysbiosis provokes an imbalance of commensal and pathogenic bacteria and their metabolites. Hence, the use of 'omic' profiling is increasing in order to improve the understanding of the pathophysiology of IBD. In addition, metagenomics illuminates gut microbiota composition which is indispensable to find specific microbial signatures associated with the disease. Metabolomics consist of the high throughput identification, characterization and quantification of small molecule metabolites within a biological system. Metabolites can be identified in different biofluids such as serum, urine or fecal samples (De Preter, 2015). Coupling metabolomics with metagenomics has great potential to unveil host-microbial interactions and the specific functions of the microorganisms (Chong and Xia, 2017). Nonetheless, the development of methods for the integrative analysis is still necessary to connect the heterogeneous matrices of the different omics.

Identifying which taxa are targeted by immunoglobulins can uncover important host-microbe interactions. Immunoglobulin binding of commensal and colitogenic taxa can be assayed by sorting bound bacteria from samples and using amplicon sequencing to determine their taxonomy, a technique most widely applied to study immunoglobulin A (IgA-SEQ) (Palm et al., 2014). This technology scores taxon binding in IgA-SEQ datasets by comparing abundances in the IgA bound and unbound sorted fractions, enabling accurate identification of commensal and disease-driving gut microbiota targeted by host immunoglobulins.

4.1 Identification of colitogenic bacteria by IgA-SEQ technology

The aim of this technique is to isolate bacterial populations coated by endogenous host IgA and identify IgA coated bacteria with the use of metagenomics, based on the *16S rRNA* gene sequencing. SIgA serves as first line of defense protecting the epithelium against enteric toxins and pathogen invasion, facilitating their clearance (Pabst and Slack, 2020; Pietrzak et al., 2020). Importantly, Palm et al. reported the ability of IgA-SEQ technology to identify colitogenic bacteria from both mice and human intestinal microbiota upon intestinal inflammation (Palm et al., 2014). They were able to differentiate IgA coating from disease-driving bacteria and indigenous members. While pathogen-induced IgA binding was considered to be of high-affinity and specificity in a T cell-dependent manner, commensal-induced IgA resulted in low-affinity and specificity T-cell independent response (Palm et al., 2020). Thus, IgA-SEQ might be a potential tool to identify specific members that are associated with enhanced susceptibility to IBD.

In mice subjected to inflammasome-mediated colitogenic dysbiosis, it was found that specifically disease-driving intestinal bacteria were highly coated with IgA such as an unclassified genus from the *Prevotellaceae* family (Palm et al., 2014). To test whether IgA coating would identify colitogenic bacteria in IBD patients, IgA coated and non-coated bacteria from IBD patients' feces were isolated and then, GF mice were colonized with these two consortia. GF mice colonized with highly IgA coated bacteria (UC *Bacteroides*, *Allobaculum* spp., *Oscillospira* spp., *Steptococcus* spp, etc.) displayed augmented disease severity after colitis induction compared to GF mice colonized with non-coated bacteria (*Bacteroides ovatus*, *Bacteroides uniformis*, UC *Lachnospiraceae*, *Bacteroides* spp., etc.) (Palm et al., 2014). Thus, relative levels of bacterial coating with IgA might predict disease course and might be associated with taxa that increases disease severity.

5. Experimental models of IBD

The high interindividual variability within human UC patients has led to develop murine models to induce colitis that display clinical characteristics that are similar to those of humans with IBD, to elucidate the connection between bacteria and the host (Wirtz and Neurath., 2007). Since research in human is expensive and ethically difficult to achieve, the use of animal models is widely accepted. Our understanding of the factors that contribute in the pathogenesis of IBD has relied on the use of various experimental models of IBD. Although experimental animal models do not exactly mimic the human condition, they are essential to provide new insights into the pathogenesis of the disease. Most of IBD models are based on chemical induction, although T cell transfer model of colitis or genetically engineered mouse colitis models are also used (Waldner and Neurath, 2009). Genetic manipulation has led to the creation of valuable mouse models such as IL-10-deficient mice. These mice spontaneously develop IBD and shares histological, physiological and biochemical features with human IBD (Kennedy et al., 2000). Nonetheless, most gene-targeted mouse strains also require chemical induction of colitis.

5.1 Chemically induced mouse models of colitis

Currently, chemically induced colitis models are the most widely used mouse IBD models, due to their rapid onset of inflammation and technical simplicity (Waldner and Neurath, 2009). However, chemically induced colitis models need to optimize concentration of chemicals depending on the animal facilities and mouse strains (Mizoguchi et al., 2020). The most commonly used chemically induced mouse models of colitis use TNBS (2,4,6-trinitrobenzene sulfonic acid), oxazolone, and dextran sulfate sodium (DSS). TNBS is administrated intrarectally dissolved in ethanol, which disrupts the mucosal barrier. Similar to TNBS, oxazolone is also administrated rectally to promote an inflammation of mucosal layers mainly in the distal colon of experimental animals. However, in DSS-induced colitis model, colitis is induced by dissolving the sulfated polysaccharide in the animals' drinking water (Waldner and Neurath, 2009). Notably, DSS colitis model is very popular in research due to its rapidity, simplicity, reproducibility, and controllability (Chassaing et al., 2014).

5.1.1 DSS-induced colitis murine model

Okayasu and colleagues first described this model in 1990 which is characterized by, significant body weight loss (WL), the presence of blood in the stool, altered feces

consistency, shortening of the intestine, mucosal ulceration, and neutrophils infiltration (Okayasu et al., 1990). DSS is a water-soluble, negatively charged sulfated polysaccharide that induces ulcerative colitis-like inflammation. It acts as a detergent disrupting the epithelial barrier by erosion/ulcer-type lesions with complete loss of surface epithelium, thereby increasing colonic mucosal permeability and permitting the entrance of luminal antigens to the lamina propria. Although it has a variable molecular weight ranging from 5 to 1400kDa, the most severe colitis is induced in the large bowel when a molecular weight of 40-50kDa of DSS is administrated in the drinking water (Chassaing et al., 2014). The variability between animals is due to the DSS (DSS intake, manufacturer and batch), genetic predisposition (strain and gender) and the composition of gut microbiota (Perše and Cerar, 2012).

To assess the extent and severity of inflammation, animals are monitored daily for disease activity index (DAI), which consists of weight loss, stool consistency and blood in the stool (Camuesco et al., 2004). Furthermore, semi-quantitative evaluation of the intestinal histopathology is performed to measure disease severity, in which higher histological scores indicate more severe inflammation (Koelink et al., 2018). Colonic shortening in DSS-induced mice is also an indicator of colonic inflammation and splenic enlargement is a common feature of this model. Since DSS makes erosions in the epithelial barrier leading to the infiltration of leucocytes, a much higher induction of MPO activity is regarded after colitis induction (Chassaing et al., 2014).

5.1.1.1 Acute and chronic colitis

Acute and chronic forms of the disease can be induced depending on the concentration, the duration and frequency of the DSS (Perše and Cerar, 2012). Acute DSS colitis has become a useful model to study the innate immune system contribution in the development of intestinal inflammation. This model is based on short-lasting barrier alterations and self-limiting inflammation. However, IBD in humans is characterized by a chronic relapsing and remitting inflammation of the gastrointestinal tract. Therefore, a mouse model of chronic colitis is required to assess the role of the adaptive immune system. This model of chronic colitis is characterized by signs of erosions and shortening of the large intestine, prominent regenerations of the colonic mucosa including dysplasia and frequent formation of lymphoid follicles (Okayasu et al., 1990). To cause a non-self-limiting chronic form of colitis, repeated epithelial damage and wound repair phases are induced by the administration of DSS in three cycles with a 2-week rest period between. Whereas experimental protocol of the acute colitis models can be performed within 1–2 weeks, chronic models may take between 2 and 4 months (Wirtz et al., 2017).

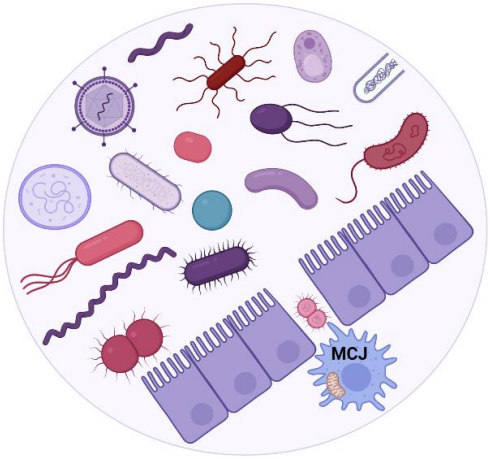

Hypothesis and objectives

In the last decade, alterations in mitochondrial function and gut microbiota composition have been demonstrated to be involved in the pathology of intestinal inflammation. Furthermore, recent evidence has shown a bidirectional interaction between mitochondria and microbiota that seems to be critical in numerous diseases including obesity, diabetes, intestinal inflammation and cancer. Although the role that this interaction plays in the IBD pathogenesis is still unclear, mitochondrial dysfunction characterized by a decreased mitochondrial electron transport chain (ETC) complex I activity and ATP production has been widely recognized as major contributor to the disease. Additionally, the mitochondrial protein MCJ (methylation-controlled J protein; also known as DnaJC15), natural repressor of ETC complex I function, has been described to be crucial to the production of TNF in bone-marrow derived macrophages. However, there is no data available about the role of MCJ in colon macrophages during intestinal inflammation.

The clinical heterogeneity observed among UC patient's disease course has led to the use of animal models in order to reproduce human IBD and avoid the variability. Although animal models do not recapitulate the disease completely, they are indispensable to investigate the contribution of distinct factors to IBD pathogenesis. In this regard, the use of a mouse model might serve as valuable tool for IBD biomarker discovery, allowing easy access to large numbers of samples from a uniform genetic background, a controlled environment and homogeneous sample collection. Thus, the identification of noninvasive, accurate, and inexpensive biomarkers of intestinal inflammation would enable clinicians to predict disease severity and treatment response. Although there are some blood, stool and urine biomarkers for IBD, few of them have clinical value.

With this concern, the hypothesis of this study is that a murine model deficient in the mitochondrial protein MCJ might be a viable tool to study the role of the mitochondria-gut microbiota interactions allowing the identification of potential biomarkers for UC disease progression and therapy response.

To demonstrate this hypothesis, the following specific objectives were proposed:

1. **To determine the role of MCJ in a murine model of acute experimental colitis**
   1.1 Phenotypic characterization of the DSS-induced colitis model
   1.2 Immune system determination
   1.3 Colonic gene expression detection
   1.4 Metagenomics of intestinal microbiota composition
   1.5 Metabolomic analysis of intestinal luminal content

2. **To characterize the impact of MCJ deficiency on intestinal macrophages during DSS-induced colitis**
   2.1 Phenotypic characterization, colonic gene expression study and metagenomic analysis of the gut microbial composition in mice subjected to antibiotic-induced gut microbiota dysbiosis
   2.2 Transcriptomic analysis of intestinal macrophages
   2.3 *In vivo* anti-TNF treatment response

3. **To ascertain the role of MCJ-deficient microbiota in the pathogenesis of UC using:**
   3.1 IgA-SEQ technology
   3.2 Colonization of germ-free mice
   3.3 Fecal microbiota transplantation as an alternative to anti-TNF treatment

4. **To assess the effect of MCJ in the DSS-induced chronic colitis murine model**
   4.1 Phenotypic characterization
   4.2 Immune system analysis
   4.3 Colonic gene expression study
   4.4 Metagenomic analysis of the gut microbial composition

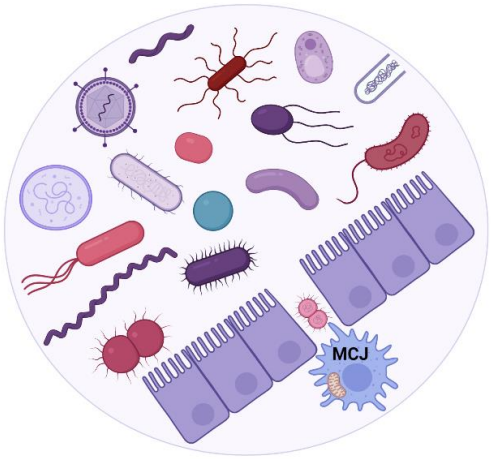

Material and methods

1. Animals and experimental design

1.1 Ethics statement and mouse husbandry

1.1.1 Wild-type and MCJ-deficient mice at CIC bioGUNE

Animal protocols were approved by the Animal Research Ethics Board of CIC bioGUNE (Spain; permit number CBBA-0615). MCJ-deficient mice (MCJ KO) on a C57BL/6 background and WT B6 mice (8–10 wk) were maintained under specific pathogen-free conditions with controlled temperature (21–23°C) and 12/12-hour light/dark cycles. Mice were fed ad libitum on standard mouse chow (Global diet 2914, Harlam, Madison, USA).

1.1.2 Germ-free mice at Yale University

All germ-free wild-type C57BL/6 male mice were bred and maintained at Yale School of Medicine and all treatments were made in accordance with Yale Animal Care and Use Committee guidelines. Strict husbandry protocols and stringent testing regimens were carried out to maintain and confirm the GF state. Mice were maintained in an uncontaminated environment and were fed ad libitum with sterile pellet-formulated diet on a 12h light/12h dark cycle and environmentally controlled rooms (23°C; 45% to 50% humidity).

1.2 Induction of acute colitis: experimental designs

Dextran sodium sulfate (DSS) (40-50 kDa; TdB Consultancy) was administered in the drinking water (3%) for 6 days; then, mice were given autoclaved water for 2 days. Control mice received autoclaved water. In all experiments, a blind technician evaluated daily, the disease activity index (DAI) of every mouse. This index is a score based on animal body WL, the presence of gross blood in feces and stool consistency. The criteria proposed by Camuesco et al. were used to assign scores (Table 1) (Camuesco et al., 2004). To assess the role of MCJ in acute colitis, we used 4 experimental groups consisting of WT and MCJ-deficient controls (WT DSS- and MCJ KO DSS-) and DSS-induced colitis groups (WT DSS+ and MCJ KO DSS+).

This experimental design was used to induce conventional acute colitis in healthy and in mice with antibiotic-induced dysbiosis. However, a different duration or concentration of DSS, or a different recovery period was used for other experiments. In all experimental designs, feces and tissues were collected at sacrifice and stored at -80ºC until use. In addition, colon lengths and spleen weights were measured at sacrifice.

Table 1. Disease Activity Index scoring system. (Camuesco et al., 2004).

Score	Weight loss (%)	Stool consistency	Rectal bleeding
0	None	Normal	Normal
1	1-5		
2	5-10	Loose stools	
3	10-20		
4	>20	Diarrhea	Gross bleeding

1.2.1 Antibiotic-induced dysbiosis

Dysbiosis was promoted by oral administration of 100 µl (715 mg ml^{-1}) of a broad-spectrum antibiotic (Abx) (Britapen, Reig Jofré laboratory Barcelona) to each mouse, twice per day during 7 days. Control groups received the same amount of water. Then, DSS (36-50 kDa; TdB Consultancy) was administered in the drinking water (3%) for 6 days followed by a two-day recovery period with autoclaved water. Mice not treated with DSS received autoclaved water. For this study, 8 experimental groups were used: WT and MCJ-deficient controls (WT_Abx-DSS- and MCJ KO_Abx-DSS-), antibiotic positive (WT_Abx+DSS- and MCJ KO_Abx+DSS-), DSS positive (WT_Abx-DSS+ and MCJ KO_Abx-DSS+) and antibiotic and DSS positive (WT_Abx+DSS+ and MCJ KO_Abx+DSS+).

1.2.2 Response to anti-TNF therapy

To evaluate the response to anti-TNF treatment, all experimental mice were administered 2% of DSS *ad libitum* in the drinking water for 6 days, followed by three days of recovery period. Mice were divided into two groups per genotype, with one group receiving an intraperitoneal administration of Inflectra (7.5 mg kg^{-1}), an Infliximab biosimilar (IFX+) proven to be effective for induction and maintenance of remission in moderate to severe UC. The mouse/human chimeric monoclonal IgG1 antibody to TNF, was provided from day 3 to 6 during DSS administration while the second group received saline solution (IFX-). Therefore, we had 4 different groups including colitis-induced and IFX negative WT and MCJ-deficient mice (WT_IFX- and MCJ KO_IFX-) and WT and MCJ-deficient mice treated with DSS and IFX (WT_IFX+ and MCJ KO_IFX+).

1.2.3 Germ-free mice colonization

For microbial transplantation, 4–6-week-old male germ-free C57BL/6 mice were colonized via oral gavage with 200mL of WT and MCJ KO bacterial consortia (50mg-200mg feces). After 2-4 weeks, 2% of DSS was administrated to mice during 6 days followed by two days of water. All gnotobiotic mice were maintained in Techniplast P Isocages and manipulated aseptically for the duration of the experiment. The V4 region of the 16S rRNA gene was sequenced from mice feces at day 0 (before DSS administration, WT_d0 and MCJ KO_d0) and at day 8 (2 days after DSS administration, WT_d8 and MCJ KO_d8) to confirm colonization and microbial composition.

1.2.4 Fecal microbiota transplantation by cohousing

For cohousing experiment, WT and MCJ-deficient female mice between 3-5 weeks of age WT and MCJ-deficient were mixed during 4 weeks prior to colitis induction. Colitis was induced administrating DSS in the drinking water (2%) for 7 days followed by a recovery period of three days with autoclaved water. Control mice received autoclaved water. In this study, 6 experimental groups were employed that included WT and MCJ-deficient controls (WT_An and MCJ KO_An), housed alone and DSS-treated WT and MCJ-deficient mice (WT_Ap and MCJ KO_Ap) and cohoused and DSS-treated WT and MCJ-deficient mice (WT_Cop and MCJ KO_Cop).

1.2.5 Cohousing and anti-TNF response

To evaluate the anti-TNF response in mice with altered microbial composition, a previous microbiota transplantation was made. For this purpose, WT and MCJ-deficient female mice between 3 and 5 weeks of age were cohoused for 4 weeks before inducing colitis. Then, colitis was induced by administrating 3% of DSS in the drinking water for 6 days to all mice, followed by three days of recovery period. The IFX mouse/human chimeric monoclonal IgG1 antibody against TNF, was provided intraperitoneally from day 3 to 6 during the DSS administration period to all mice. Hence, all groups received DSS and IFX, and we had 4 experimental groups that consisted of WT and MCJ-deficient mice housed alone (WT_Ap_IFXp and MCJ KO_Ap_IFXp) and cohoused WT and MCJ-deficient mice (WT_Cop_IFXp and MCJ KO_Cop_IFXp).

1.3 Induction of chronic colitis

Chronic experimental colitis was induced by three cycles of 2% DSS that consisted of 7 days of DSS administration in the drinking water followed by 14 days of water in the first and second cycles. After the third cycle of DSS we let mice 3 days to recover (1st cycle of DSS: from day 0 to day 7, 2nd cycle: from day 21 to day 28 and 3rd cycle: from day 42 to 49). A group of mice receiving autoclaved water was included as a control. The DAI of every mouse was evaluated daily during DSS administration cycles and eventually in recovery periods by a blind technician based on Camuesco et al. proposed criteria (Camuesco et al., 2004). To assess the role of MCJ in chronic colitis, we used 4 experimental groups that included WT and MCJ-deficient controls (WT_N and MCJ KO_N) and DSS-induced chronic colitis groups (WT_P and MCJ KO_P).

1.4 *In vivo* approach to determine transepithelial permeability

Mice received oral gavage of 600 mg kg-1 body weight of fluorescein isothiocyanate (FITC)–dextran (4 kDa; TdB consultancy) and whole blood was collected by cardiac puncture 4 h after gavage. Blood serum was collected after centrifugation at 6000 rpm for 10 min. Serum fluorescence intensity was measured using a multi-detection microplate reader (Spectramax M2 Microplate Reader, Molecular Devices) with an excitation wavelength of 485 nm and an emission wavelength of 528 nm. FITC concentration (mg ml^{-1}) was calculated from a standard curve using serial dilutions of FITC–dextran.

2. Analysis of tissue samples

2.1 Myeloperoxidase activity assay

One centimeter length of the distal colon was homogenized with 0.5 mm zirconium oxide beads in 2-ml tubes containing a solution of 50mM phosphate buffer (PB) (pH 6.0) and 0.5% hexadecyltrimethylammonium bromide (Sigma-Aldrich) using a Precellys 24 homogenizer (Bertin Instruments). After 4 cycles of 90 seconds at 6000 rpm, 7 µl of supernatant was mixed with 200µl of 0.02% dianisidine (Sigma-Aldrich) in 50 mM PB, pH 6.0, and 0.0005% H2O2 (Sigma-Aldrich). Human myeloperoxidase (MPO) (Merck Millipore) was used as a standard to measure samples' activity. All activity assays were performed in triplicates on 96 well microtiter plates and analyzed with a microplate reader measuring absorbance at 450 nm (Spectramax M2 Microplate Reader, Molecular Devices).

2.2 Cell preparation and analysis for flow cytometry

Spleens and mesenteric lymph nodes (MLN) were dissected post-mortem and collected in phosphate buffered saline (PBS). For splenocyte and lymph node cells preparation, organs were mashed through a 70 µm cell strainer (Falcon), and erythrocytes from spleens were lysed using ACK (Ammonium-Chloride-Potassium) lysis Buffer. Cells from the DSS-induced acute colitis experiment were stained with the following anti-mouse fluorochrome-conjugated antibodies: CD11b APC (Miltenyi Biotech, M1/70); CD11c PE Cy7 (Miltenyi Biotech, N418); CD103 PE (Miltenyi Biotech, REA789); F4/80 FITC (Miltenyi biotech, REA126). However, two separate fluorescent stains of multiple fluorescently labeled antibodies were performed with cells from the DSS-induced chronic colitis experiment. The first staining consisted of CD45R (B220) PE (Miltenyi Biotech, REA755); CD4 FITC (Miltenyi Biotech, GK1.5); CD8 PerCP-Vio 700 (Miltenyi Biotech, 53-6.7); CD69 APC-Vio 770 (Miltenyi Biotech, H1.2F3); CD44 APC (Miltenyi Biotech, IM7.8.1); CD62L PE-Vio 770 (Miltenyi Biotech, REA828). The second staining included CD11b APC (Miltenyi Biotech, M1/70); CD11c FITC (Miltenyi Biotech, N418); CD103 PE (Miltenyi Biotech, REA789); F4/80 PE-Vio 770 (Miltenyi Biotech, REA126); MHCII APC-Vio 770 (Miltenyi Biotech, REA813). Fc receptors were blocked with Anti-mCD16/CD32 (BD). Only events that appeared single in forward-scatter width were analyzed. A FACSCanto II and FACSDiva software (BD Biosciences) were used for flow cytometry and data were analyzed using FlowJo software (TreeStar).

2.3 Histology, immunohistochemistry and immunofluorescence

Colon tissues were harvested from mice and fixed in 10% formalin or Carnoy´s fixative, dehydrated, embedded in paraffin and cut into 5 µm-thick sections. For histopathology, sections were deparaffined, hydrated and stained with hematoxylin and eosin or periodic acid-Schiff (PAS) according to the standard protocol. Stained sections were analyzed and given a score by a pathologist blinded to mouse genotype and treatment. The histological score was based on edema, ulceration and infiltration of neutrophils and mononuclear cells in the different layers of the gastrointestinal wall: mucosal epithelium and lamina propria, crypts, submucosa and muscular layer. The number of goblet cells was determined on PAS stained slides and expressed as the percentage per intestinal epithelial cells.

For immunohistochemistry, segments of colon collected from mice were cut to 5 µm thickness, deparaffined, hydrated and subjected to antigen retrieval with proteinase K for 15 min at 37ºC. Subsequently, sections were incubated with an antibody specific for IgA and horseradish peroxidase (HRP)-conjugated (Sigma-Aldrich), developed by immersing in DAB (3,3′-diaminobenzidine) (Vector) solution for 2 min and counterstained in Mayer's hematoxylin for 30 seconds. For F4/80 staining, tissue sections were subjected to antigen retrieval using proteinase K for 15 min. Endogenous enzymes were first blocked with 3% hydrogen peroxide (H_2O_2) and, then with goat serum. Sections were incubated with rat anti-mouse F4/80 primary antibody (1:50, Biolegend) for 2 h at 37ºC, followed by 30 min incubation with ImmPRESS HRP Goat Anti-Rat IgG secondary antibody (Vector). Detection was performed with DAB substrate (Vector). Images were captured with a Zeiss Axioimager A1 microscope and analyzed with ImageJ software. At least 10 visual fields were captured randomly.

For immunofluorescence (IF) analysis, colon tissues harvested from mice were sectioned to 5 µm thickness, deparaffined, hydrated and subjected to antigen retrieval using proteinase K for 15 min at 37ºC. After blocking (3% H_2O_2), sections were incubated with primary antibodies for 1 h (F4/80, 1:50, Biolegend) or 2 h (Muc2, 1:100, Santa Cruz), at 37ºC followed by 30 min incubation with fluorescently labelled secondary antibody. Finally, DAPI (4′,6-diamidino-2-phenylindole) was added to stain nuclei. Photographs were taken with a fluorescence microscope (Axioimager.D1 Zeiss) and analyzed by two people blinded to the treatment. At least 10 visual fields were captured randomly.

2.3.1 Double immunofluorescence of human colonic tissue sections

Colon samples were obtained from human colectomies. Colocalization of MCJ with CD163 in inflamed and adjacent healthy colon tissues was determined by IF. Colon tissues were embedded in paraffin, cut, rehydrated and unmasked with proteinase K for 15 min. Then, tissues were incubated with mouse anti-human MCJ antibody (Fisher Scientific) at 4ºC overnight and a goat anti-mouse Cy3-conjugated secondary antibody (Abcam) was added for 30 min. After the first staining, tissues were incubated with rabbit anti-human CD163 antibody (Abcam) for 1hr at 37ºC followed by the addition of goat anti-rabbit FITC-conjugated secondary antibody (30 min, Abcam). Photographs were taken with a fluorescence microscope (Axioimager.D1 Zeiss). The area of each color was quantified using CellProfiler tool and the colozalization analysis of MCJ with CD163 was perfomed with Frida software.

2.3.2 Determination of ROS in mice colonic tissue sections

Samples were sectioned in a cryostat (8 µm) and incubated with MnTBAP 150 µM for 1 h at room temperature. They were then incubated with 5 µM of dihydroethidium (DHE) for 30 min at 37ºC. Sections were mounted with mounting media containing DAPI. Photographs were taken with a fluorescence microscope (Axioimager.D1 Zeiss) and analyzed by two people blinded to the treatment. At least 10 visual fields were captured randomly.

2.4 Transmission electron microscopy

Sections (2–3 mm) from mice distal colon were fixed in 2% glutaraldehyde in 0.12 M PB (pH 7.4), overnight at 4 °C. Then, samples were washed with 0.1 M PB (pH 7.4) and postfixed in 1 % OsO4 in 0.1 M PB (pH 7.4) overnight at 4ºC. After a washing step with distilled water, samples were stained with 0.5 % uranyl acetate during 45 min at 4ºC. Colon slices were washed again with distilled water, dehydrated in a graded ethanol series, and embedded in propylene oxide. Afterwards, samples were incubated 45 min in 1:1 propylene oxide and resin, and embedded in resin overnight at room temperature. Finally, samples were added to resin blocks and kept overnight at 60ºC. The 1 µm semi-thin and 60 nm ultra-thin sections were obtained on a Leica Ultracut UCT ultramicrotome. Ultra-thin sections were collected in 200-mesh copper grids and observed in a JEOL JEM 1400 Plus ETM at 100 kV.

2.5 Colon proteins extraction and quantification

Proteins from colonic tissue were extracted with radioimmunoprecipitation assay lysis buffer (RIPA buffer) with several protein inhibitors such as sodium fluoride (1 mM, Sigma-Aldrich), sodium orthovanadate (1 mM, Sigma-Aldrich), B-Glycerophosphate (1 mM, Sigma-Aldrich) and a protease inhibitor cocktail (1 tablet/50ml lysis buffer, Roche). Colonic tissues were put into 2-ml tubes containing lysis buffer and 0.5 mm zirconium oxide beads, and were grinded on Precellys tissue homogenizer (Bertin Instruments) using a protocol of 6000rpm with 2 cycles of 30 s. The lysate solution was centrifuged and the supernatant was saved at -80ºC.

Protein concentrations were measured with the Pierce™ Rapid Gold BCA Protein Assay Kit (Thermo Fisher Scientific) the following manufacturer's instructions.

2.6 Western blot

20 µg of protein were run on 12% sodium dodecyl sulfate-polyacrylamide gel electrophoresis (SDS-PAGE), transferred to nitrocellulose membranes and tested with antibodies specific for TIMP3 (Cell Signaling Technology), TNF bound to membrane (Cell Signaling Technology) and TNFR1 (Cell Signaling Technology). Equal loading was determined using antibodies against GAPDH from Santa Cruz Biotechnology.

2.7 Proteomic analysis

Samples were digested following the SP3 protocol described by Hughes et al. with minor modifications (Hughes et al., 2019). Trypsin was added to a trypsin:protein ratio of 1:10, and the mixture was incubated 2 h at 37ºC. Resulting peptides were dried out in a RVC2 25 speedvac concentrator (Christ), and resuspended in 0.1 % formic acid (FA).

Samples were analyzed in a novel hybrid trapped ion mobility spectrometry – quadrupole time of flight mass spectrometer (timsTOF Pro with parallel accumulation – serial fragmentation (PASEF), Bruker Daltonics) coupled online to a nanoElute liquid chromatograph (Bruker). This mass spectrometer takes advantage of a novel scan mode termed PASEF, which multiplies the sequencing speed without any loss in sensitivity (Meier et al., 2015) and has been proven to provide outstanding analytical speed and sensibility for proteomics analyses (Meier et al., 2018). Samples (200 ng) were directly loaded in a 15 cm Bruker nanoelute FIFTEEN C18 analytical column (Bruker) and resolved at 400 nl min^{-1} with a 30 min gradient. Column was heated to 50ºC using an oven.

Protein identification and quantification was carried out using PEAKS software with default settings. Searches were carried out against a database consisting of human protein entries (Uniprot/Swissprot), with precursor and fragment tolerances of 20ppm and 0.05 Da. Only proteins identified with at least two peptides at FDR<1% were considered for further analysis. Data was loaded onto Perseus platform 24 (Tyanova et al., 2016) and further processed (log2 transformation, imputation).

Gene ontology (GO) enrichment was tested using the ClusterProfiler bioconductor package (Yu et al., 2012), and comparative graphics were obtained via dot plot function.

2.8 TACE activity

Colon protein extracts were incubated with 10 µM of TACE FRET Substrate I (Anaspec, Fremont, CA) in black NUNC polystyrene 96-well microtiter plates (Fisher Scientific). Colon protein extracts were treated with the TNF Protease Inhibitor 2 (TAPI-2, 50 µM; Enzo Life Sciences) to determine non-specific TACE activity. For samples from the anti-TNF response experiment, fluorimetric SensoLyte 520 TACE (α-Secretase) activity assay kit (AnaSpec) was used. Enzyme activity was monitored using a BioTek Synergy HT microplate fluorescence reader (BioTek, Winooski, VT) at an excitation wavelength of 355 nm and an emission wavelength of 500 nm. Results are expressed as specific activity resulting from subtracting nonspecific activity from total activity. For infliximab experiment, results are represented as relative fluorescence units (RFU) per mg of protein.

2.9 Enzyme-linked immunosorbent assay (ELISA)

TNF levels from murine colon protein extracts were determined using the Mouse TNF-alpha DuoSet ELISA kit (R&D Systems) and IL-10 using the Mouse IL-10 ELISA Set (RUO) (BD Biosciences) according to the manufacturer’s recommendations.

2.10 RNA extraction, cDNA synthesis and gene expression

RNAlater solution was added to colon samples and stored overnight at -20ºC. The following day, colon tissues were resuspended in 1 ml of TRIzol reagent (Invitrogen) and homogenized on a Precellys homogenizer (Bertin Instruments) using 0.5 mm zirconium beads in 2 ml tubes and a protocol of 6000 rpm, 2 cycles of 30 seconds each. Then, chloroform (Sigma-Aldrich) was added, mixed and centrifuged at 14000 rpm for 20 min at 4ºC, and the upper aqueous phase was transferred to a new tube. The protocol was continued in the step 4 of the Nucleospin RNA kit (Macherey-Nagel) according to the manufacturer´s protocol. M-MLV reverse transcriptase (Thermo Fisher Scientific) was used to synthesize cDNA. Real-time polymerase chain reaction (qPCR) was performed on 384 well plates in a QuantStudio 6 Flex Real-Time PCR system (Thermo Fisher Scientific) and PerfeCTa SYBR Green SuperMix Low ROX reagent (Quantabio, Beverly). Amplification was analyzed by QuantStudio Real-Time PCR software v1.3. Selected genes and optimized primers are listed in Table 2. To normalize colonic mRNA expression, the murine *Rpl19* gene was used as reference. mRNA relative quantification was calculated using the ΔΔCt method (Livak and Schmittgen, 2001). Efficiency of qPCR was always between 90 and 110%. RNA-Seq from murine intestinal macrophages was validated by qPCR with *Il10*, *Il1b*, *Lcn2* and *Reg3b* genes, which were chosen according to their log2 fold change (FC).

Table 2. Forward and reverse primer sequences (5′ to 3′), annealing temperature (Ta) and the purpose of the mouse primers used for murine qPCR analysis.

Gene	Forward primer sequence Reverse primer sequence	Ta (°C)	Purpose
Adam17	5´-TGGGACACAATTTTGGAGCA-3´ 5´-CCTCCTTGGTCCTCATTTGG-3´	60	Gene expression
Caspase-3	5´-ATGGAGAACAACAAAACCTCAGT-3´ 5´-TTGCTCCCATGTATGGTCTTTAC-3´	60	Gene expression
Cldn2	5´-AGGACTTCCTGCTGACATCCAG-3´ 5´-AATCCTGGCAGAACACGGTGCA-3´	58	Gene expression
Cldn5	5´-TGACTGCCTTCCTGGACCACAA-3´ 5´-CATACACCTTGCACTGCATGTGC-3´	60	Gene expression
Dnajc15	5´-ACGCCGACATCGACCACACAG-3´ 5´-AATCTTCCTTGCTGTTGCCGTG-3´	58	Gene expression
Hif1a	5´-AGATGACGGCGACATGGTTT-3´ 5´-AGCTCCGCTGTGTGTTTAGT-3´	60	Gene expression
Ifng	5´-TGGTGACATGAAAATCCTGCAGAG-3´ 5´-GCTTATGTTGTTGCTGATGGCCTG-3´	59	Gene expression
Il10	5´-TGGCCCAGAAATCAAGGAGC-3´ 5´-CAGCAGACTCAATACACACT-3´	58	Gene expression RNAseq validation
Il1b	5´-ACACTCCTTAGTCCTCGGCCA-3´ 5´-CCATCAGAGGCAAGGAGGAA-3´	60	Gene expression RNAseq validation
Il6	5´-ACCACGGCCTTCCCTACTTCAC-3´ 5´-TTCTCATTTCCACGATTTCCCAG-3´	60	Gene expression
Lcn2	5´-CAATGTCACCTCCATCCTGGT-3´ 5´-ACTGGTTGTAGTCCGTGGTG-3´	60	Gene expression RNAseq validation
Muc2	5´-GATAGGTGGCAGACAGGAGA-3´ 5´-GCTGACGAGTGGTTGGTGAATG-3´	58	Gene expression
Muc3	5´-CGTGGTCAACTGCGAGAATGG-3´ 5´-CGGCTCTATCTCTACGCTCTC-3´	58	Gene expression
Myd88	5´-CCGCCTATCGCTGTTCTTGA-3´ 5´-GCCAGGCATCCAACAAACTG-3´	59	Gene expression
Nos2	5´-GTTGAAGACTGAGACTCTGG-3´ 5´-GACTAGGCTACTCCGTGGA-3´	58	Gene expression
Ocln1	5´-TGGCAAGCGATCATACCCAGAG-3´ 5´-CTGCCTGAAGTCATCCACACTC-3´	58	Gene expression
Pigr	5´-CGAAGCTACAAGGGAGCCAA-3´ 5´-ACGGATAGTGGCAGGAAACG-3´	60	Gene expression
Ptgs2	5´-GGGTTGCTGGGGGAAGAAATG-3´ 5´-GGTGGCTGTTTTGGTAGGCTG-3´	58	Gene expression
Reg3b	5´-TACTGCCTTAGACCGTGCTTTCTG-3´ 5´-GACATAGGGCAACTTCACCTCACA-3´	60	Gene expression RNAseq validation
Reg3g	5´-TTCCTGTCCTCCATGATCAAAA-3´ 5´-CATCCACCTCTGTTGGGTTCA-3´	60	Gene expression
Rpl19	5´-GACCAAGGAAGCACGAAAGC-3´ 5´-CAGGCCGCTATGTACAGACA-3´	60	Gene expression
Smad3	5´-CATCGAGCCCCAGAGCAATA-3´ 5´-GTGGTTCATCTGGTGGTCACT-3´	60	Gene expression
Stat1	5´-TCTGAATATTTCCCTCCTGGG-3´ 5´-CGGAAAAGCAAGCGTAATCT-3´	60	Gene expression
Tgfb	5´-CACTGATACGCCTGAGTG-3´ 5´-GTGAGCGCTGAATCGAAA-3´	60	Gene expression
Timp3	5´-GGCCTCAATTACCGCTACCA-3´ 5´-CTGATAGCCAGGGTACCCAAAA-3´	60	Gene expression
Tjp1	5´-GTTGGTACGGTGCCCTGAAAGA-3´ 5´-GCTGACAGGTAGGACAGACGAT-3´	58	Gene expression
Tlr2	5´-GCAGAATCAATACAATAGAGGGAGACGC-3´ 5´-AAGTGAAGAGTCAGGTGATGGATGTCG-3´	60	Gene expression

Tlr4	5´-GCAATGTCTCTGGCAGGTGTA-3´ 5´-CAAGGGATAAGAACGCTGAGA-3´	60	Gene expression
Tlr5	5´-ATGGCATGTCAACTTGACTT-3´ 5´-GATCCTAAGATTGGGCAGGT-3´	55	Gene expression
Tlr9	5´-CAGCTAAAGGCCCTGACCAA-3´ 5´-GCGATCCACCGTCTTGAGAA-3´	58	Gene expression
Tnf	5´-AGCCCACGTCGTAGCAAACCAC-3´ 5´-ATCGGCTGGCACCACTAGTTGGT-3´	60	Gene expression
Tnfr1	5´-GCTGTTGCCCCTGGTTATCT-3´ 5´-ATGGAGTAGACTTCGGGCCT-3´	60	Gene expression
Tnfr2	5´-CTCTCCAAGCCCACCGAAAT-3´ 5´-GGACCACTGAGTTACAGCCC-3´	60	Gene expression
Trif	5´-GGACCCCACCTAGATGGCTA-3´ 5´-CCCAAGCTAAGTCCTCTGGC-3´	59	Gene expression
Conditions	Hold cycle 95°C for 2.30', and then 40x (95°C for 15", 60°C for 1´)		
Reagents	PerfeCTa SYBR® Green SuperMix (Quantabio)		
Instrument	QuantStudio 6 Flex Real-Time PCR System		
Expression	Normalized to *Rpl19* housekeeping gene using the Pfaffl equation and expressed relative to the mean of a relevant control group		

2.11 Isolation of colonic epithelial cells

After the induction of experimental acute colitis in mice, the large intestine of each mouse was removed. Colon tissues were cut into pieces (0.5 cm), opened longitudinally and washed with PBS. Segments were then washed twice by inserting them in 50-ml polypropylene tubes containing 25 ml of 20 mM HEPES in Hank´s balanced salt solution (HBSS) with calcium, magnesium and sodium bicarbonate. To isolate colonic cells, colon pieces were immersed in 25 ml of 5 mM EDTA, 2Mm dithiothreitol (DTT) (Sigma-Aldrich), 10% fetal bovine serum (FBS) in HBSS for 20 min at 37ºC while stirring (250 rpm). Then, supernatants were poured through 100 µm strainers in new 50-ml polypropylene tubes and kept on ice. For further isolation, pieces were put back into the 50-ml tube, added 25 ml of the latter solution and incubated shaking for 20 min at 37ºC. Supernatants were poured again through 100 µm strainers and filtrated cells were centrifuged. Colon pieces were incubated for the last time, then, supernatants were poured and centrifuged. In the following step, cells were resuspended in 5 ml of 40% Percoll (GE Healthcare) in PBS, and cell solution was overlayed slowly on a 15 ml-tube containing 3ml of 100% Percoll. Tubes were centrifuged at 2000 rpm for 20 min at 4ºC without brake and the upper interphase was collected. A final washing step was carried out to remove the residual Percoll and cells were resuspended in the lysis buffer of the RNA extraction kit (Macherey-Nagel) with mercaptoethanol and stored at -80ºC.

2.12 Colon macrophages RNA-Seq

Intestinal cells from murine colon tissues collected in the antibiotic-induced dysbiosis experiment were first extracted by three washing steps in 25 ml of HBSS and then, by two washing steps with the matrix degrading enzyme collagenase type IV-mediated cleavage (Gibco) in RPMI (Roswell Park Memorial Institute) medium with 2% of FBS. For macrophage isolation, extracted cells were labelled with 10 µl of anti-F4/80-Biotin antibody (Miltenyi Biotec) for 30 min followed by the addition of 10 µl of anti-biotin microbeads (Miltenyi Biotec). A multistand magnet and LS columns from Miltenyi Biotec were used to isolate macrophages by positive selection. RNA from eluted macrophages was purified using TRIzol™ Reagent (Thermo Fisher Scientific) and the pellet was resuspended in 10 µl of HyClone water (Thermo Fisher Scientific). Finally, off-column DNase treatment was performed with RNase-Free DNase Set kit from Qiagen and stored at -80ºC. The quantity and quality of the RNAs were evaluated using Qubit RNA HS Assay Kit (Thermo Fisher Scientific) and Agilent RNA 6000 Nano and Pico Chips (Agilent Technologies), respectively.

Sequencing libraries were prepared using the NuGEN Universal Plus mRNA-Seq kit (PART NO. 0508, 9133, 9134) following the user's guide (M01442 v2). Libraries were visualized on an Agilent 2100 Bioanalyzer using Agilent High Sensitivity DNA kit (Agilent Technologies), quantified using Qubit dsDNA HS DNA Kit (Thermo Fisher Scientific) and sequenced in a HiSeq2500 with single-reads of 50 nucleotides.

Quality Control of sequenced samples was performed with FASTQC software (http://www.bioinformatics.babraham.ac.uk/projects/fastqc/). Reads were mapped against the mouse (mm10) reference genome with STAR (Spliced Transcripts Alignment to a Reference) (Dobin et al., 2013) program to account for spliced junctions. The resulting BAM (binary alignment map) for the samples were then used to generate a table of raw counts using Rsubread (Liao et al., 2013). The raw counts table was the input for the differential expression (DE) analysis, carried out by DESeq2 (differential expression analysis for sequence count data 2) package (Love et al., 2014) to detect differentially expressed genes among the different conditions. To further analyze the functional GO annotation enrichment of immunological and biological functions, and the pathways involved in colon macrophages, the Database for Annotation, Visualization and Integrated Discovery (DAVID) (Huang et al., 2009), ToppGene (Chen et al., 2009) and ToppCluster (Kaimal et al, 2010) were used. Visualization of networks were obtained using Cytoscape.v3.0.2 software (Saito et al, 2012). Related genes to immunological processes were mapped with the ClueGO tool (Bindea et al., 2009).

For enriched motif discovery in colon macrophages genomic regions, the Hypergeometric Optimization of Motif EnRichment (HOMER) software was used using the findMotifs.pl script (Heinz et al., 2010). Motifs of lengths between 10 and 12 nucleotides were considered in this analysis.

Raw sequences used to perform the transcriptomic analysis were uploaded to GEO (Gene Expression Omnibus) database under the project accession code GSE135033.

2.13 Human RNA-Seq samples

2.13.1 Public dataset of UC patients

Human samples were obtained from the GEO dataset related to the study of “UC Colon RNA-Seq subset analysis” released as part of the GSE107593 series (https://www.ncbi.nlm.nih.gov/gds), available since Apr 17, 2018. Raw read count table “GSE107593_raw_reads_BCHRNAseq” generated upon STAR alignments was downloaded and used as input for the DE analysis, carried out by DESeq2, aimed to detect differentially expressed genes.

2.13.2 Mucosal transcriptomes of UC pediatric patients

Rectal gene expression signature composed of 5296 genes differentially expressed (False discovery rate (FDR) <0.001 and FC ≥1.5) between UC and control individuals, were obtained from Supplementary Dataset 1 from Haberman et al., (2019). Corticosteroid response associated genes were presented by Haberman et al., (2019) and anti-TNF response data by West et al., (2017).

3. Analysis of fecal samples

3.1 DNA extraction and microbiome analysis

Colon content was collected at sacrifice. DNA was isolated from freeze-dried colon samples (40 mg) using the FavorPrep Stool DNA Isolation Mini kit (Vienna, Austria) following the manufacturer's instructions. In addition, the lysis temperature was increased to 95°C. However, DNA from fecal GF mice samples was extracted with DNeasy PowerSoil Kit following manufacturer's instructions. Samples were eluted with 50 ul of nuclease-free Hyclone water and assessed spectrophotometrically with a NanoDrop ND-100 Spectrophotometer (NanoDrop Technologies, Wilmington, DE, USA). Purified DNA samples were stored at −20ºC until use.

Using high throughput sequencing platforms and barcoded primer sets, phylogenetic-based methods targeting the *16S rRNA* gene were used to deeply characterize the microbial populations present in the colon of experimental mice (Figure 13). The *16S rRNA* gene is highly conserved between different species of bacteria and archaea. These conserved zones are alternated by hypervariable species-specific regions allowing bacterial identification. Universally primers are chosen as complementary to the conserved regions, with the variable region in between. Depending on the required level of taxonomic resolution, different regions can be chosen. Since both V2-V3 and V3-V4 have high resolution for the lower-rank taxa, we made a PCR-based amplification of the bacterial V3-V4 of the *16S rRNA* gene using a barcoded pyrotagging approach. Sequencing was performed by Illumina Miseq system with 2×250bp paired-end reads based on a standard protocol from the manufacturer.

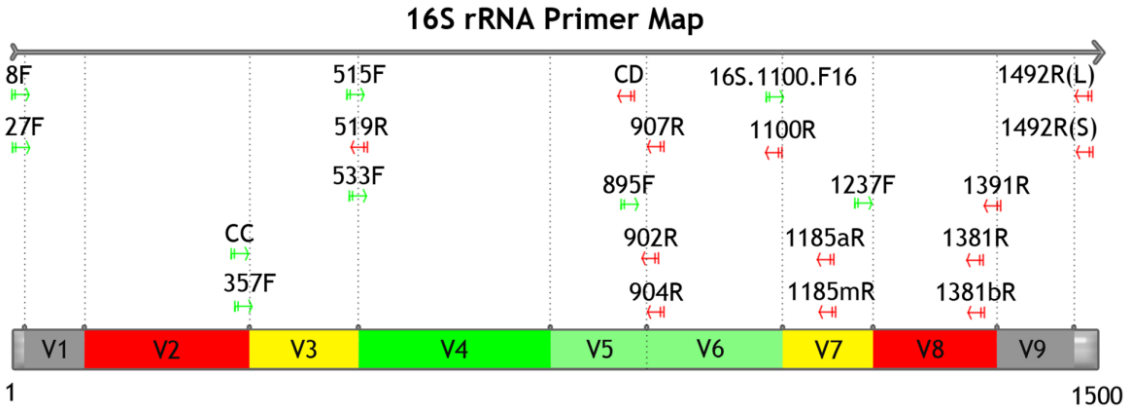

Figure 13: Illustration of variable regions within the *16S rRNA* gene and primer pairs for metagenomic sequencing. This schema shows most of the available primers. However, the primer 806R that was later discovered by Caporaso et al. and permits the amplification of the V4 region is missing (Caporaso et al., 2011). According to Yang et al. red regions (V2 and V8) are responsible for maintaining the structural stability and have a poor phylogenetic resolution at the phylum level (Yang et al., 2016). Yellow regions (V3 and V7) function is still understudied. Green regions (V4, V5 and V6) directly take part in the translation and therefore, they should be the most conservative regions, which suggests that they may be a good choice for phylogeny-related analyses. The figure refers to the primer map from Lutzonilab (http://lutzonilab.org/16s-ribosomal-dna/) and it was obtained from Yang et al., 2016.

Data processing was performed using QIIME (v.1.9.0): Quantitative Insights Into Microbial Ecology software package (Caporaso et al., 2010). Sequences were clustered as operational taxonomic units (OTUs) of 97% similarity using UCLUST (Edgar, 2010). OTUs were checked for chimeras using ribosomal database project (RDP) gold database and assigned taxonomy using the Greengenes database (version 4feb2011 for all experiments, except for GF mice colonization and IgA-SEQ that we used version Aug2013) (McDonald et al., 2012). Richness (number of observed species) and alpha and beta diversity metrics (Chao1, Shannon index, and phylogenetic Diversity whole tree) were calculated using the QIIME pipeline. MetaCoMET was used to visualize core microbiome (Wang et al., 2016). We further performed statistical analyses to detect differences in microbial composition between groups with the Vegan and DESeq2 (Love et al., 2014) packages for R and LEfSe (linear discriminant analysis effect size) tool (Segata et al., 2011). Within the Vegan package, the analysis of similarity (ANOSIM) was used to test the significances of grouping in the Principal Coordinates Analysis (PCoA) and non-metric multidimensional scaling (NMDS) plots. By using the DESeq2 package, the significant fold changes of OTU's were analyzed. Charts were plotted using several R packages, including phyloseq, ggplot2, ggpubr, reshape2 and qplots, among others.

Bioinformatic software PICRUSt2 (Phylogenetic Investigation of Communities by Reconstruction of Unobserved States 2) was used to investigate functional differences between groups. After normalizing the OTU table through Cumulative Sum Squares (CSS), KEGG (Kyoto encyclopedia of genes and genomes) pathways were predicted by PICRUSt algorithm (level 3) (Langille et al., 2013). Figure represents differential PICRUSt predicted KEGG pathways between bacterial communities found in the colon content of MCJ-deficient mice compared to WT detected by statistical analysis of taxonomic and functional profiles (STAMP) software (Parks et al, 2014).

Raw sequences from all experiments were deposited in the European Nucleotide Archive (ENA) under the project number detailed in table 3.

Table 3. The distinct project numbers of the sequences deposited in the ENA.

Experiment	Project number
Acute colitis	PRJEB19385
Antibiotic-induced dysbiosis	PRJEB33422
Anti-TNF response	PRJEB41595
IgA coated bacteria	PRJEB43545
Germ-free mice colonization	PRJEB43544
Cohousing of mice	PRJEB43553
Chronic colitis	PRJEB44741

3.2 IgA-SEQ technology

Feces were homogenized in PBS and duplicates were made for each sample. Presorting samples were centrifuged and stored at -80ºC. Then, homogenates were blocked with rat serum, stained with PE-conjugated Anti-Mouse IgA (eBioscience clone mA-6E1) and subsequently, anti-PE Miltenyi microbeads were added. To separate cells, we used magnetic activated cell sorting (MACS) with a custom-built 96 well magnetic separator (https://www.kjmagnetics.com/proddetail.asp?prod=D28-N52) for positive selection, followed by negative selection using multi-96 columns in combination with MultiMACS M96 Separator (Miltenyi Biotec) (Figure 14). All samples were kept at -80ºC until use.

DNA from presorting, IgA positive and IgA negative samples was isolated using MagAttract Microbial DNA isolation Kit (Qiagen). Samples were lysed by adding glass beads together with the lysis solution and were beat beaten for 5 min. After, supernatants were transferred to a new plate and DNA was extracted following manufacturer's instructions. IgA coated and non-coated samples were eluted in 20 ul. For microbial sequencing and analysis, the pipeline described in the microbiome analysis was followed. IgA coating index (ICI) for each individual bacterial taxon was determined dividing the relative abundance of IgA coated bacteria (IgA+) by the relative abundance of non-coated IgA bacteria (IgA-). Since we tested each sample in duplicate, we made the mean of the duplicates for the analysis.

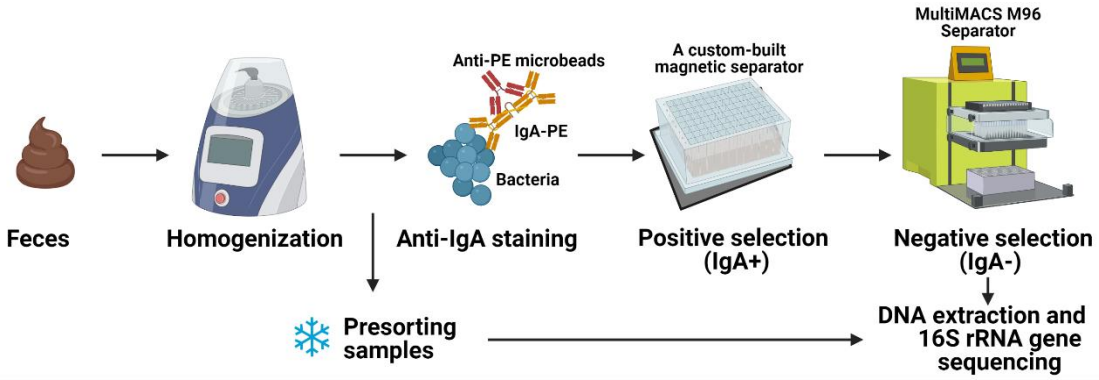

Figure 14: Overview of IgA−based cell sorting of fecal bacteria combined with *16S rRNA* gene sequencing (IgA−SEQ).

3.3 Quantification of live and dead and IgG-coated fecal bacteria by flow cytometry

Feces of each mouse were collected and homogenized in sterile PBS at a concentration of 100 mg ml^{-1}. Fecal debris was removed after several centrifugations and pellets were resuspended in sterile PBS and stained with anti-mouse IgG-FITC (Sigma-Aldrich) or LIVE/DEAD™ BacLight™ Bacterial Viability Kit (Thermo Fisher scientific) to check bacterial viability. BD FACSCanto II flow cytometer and BD FACSDiva software were used to obtain data that were analyzed with FlowJo software (TreeStar).

3.4 Metabolomic analysis

Colon content was collected at sacrifice and for each 20 mg of freeze-dried tissue, 300 µL of cold methanol-water (2:1, v/v) and 200 µL of chloroform with internal standards were sequentially added and mixed for 10 s with a vortex. Tree cycles of freezing/thawing and mechanical homogenization were performed. Samples were centrifuged at 3000 g for 10 min at 10 °C, and the methanol-water upper phase was stored at −80ºC until liquid chromatography–mass spectrometry (LC-MS) analysis. LC-MS was used for broad metabolite profiling (Esteban-Fernández et al., 2018). Metabolomic analyses were performed in a Waters Acquity UPLC system hyphenated to a Bruker maXis II UHR-QTOF mass spectrometer. Chromatographic separation was performed using an ACQUITY UPLC BEH C18 (2.1 mm × 50 mm, 1.7 µm) column. Mobile phase A was 0.1 % formic acid in water, and the mobile phase B was 0.1% formic acid in acetonitrile. Mass detection was run in the MS scan mode from m/z 20 to 2000 using electrospray ionization in positive (ESI^+).

Samples were analyzed in randomized order and in duplicate. Results were processed with MZMine v.2.3 (Pluskal et al., 2010) and univariate and multivariate statistical analysis was performed with MetaboAnalyst3.0 (Xia et al., 2016). Metabolite tentative identification was performed by the query of the exact mass of the detected features against online databases (The Human Metabolome Database (HMDB), and Metlin) within a ± 10 ppm mass range.

4. Statistical analysis

GraphPad software was used for statistical analysis (GraphPad Sofware, San Diego, CA, USA). Data was represented using line graphs, bar graphs and boxplots. Line and bar graphs showed the mean and the standard error of the mean (SEM), and box and whisker plots displayed median, quartiles, and range. The significance was assessed by two-way analysis of variance (ANOVA) followed by FDR post-test correction. In GF experiment, ANOVA was conducted for DAI and WL values, and the nonparametric Mann–Whitney U test was used for colonic length and qPCR results. A *p* value of less than 0.05 was considered significant (*p value < 0.05, **p value < 0.01, ***p value < 0.001, and ****p value < 0.0001).

4.1 Analysis of statistical differences between experimental groups

4.1.1 Chapter 1

Statistical differences in line graphs are shown by an asterisk "*" above the line for MCJ KO DSS-induced acute colitis (MCJ KO_DSS+) *versus* WT DSS-induced acute colitis (WT_DSS+).

The significance of a result in boxplots and bar graphs is shown by an asterisk or asterisks upside or inside the box to indicate differences within the same genotype in different experimental conditions: DSS treatment (DSS+) *versus* control (DSS−). Differences between genotypes in the same experimental group are presented as a line with an asterisk or asterisks above.

4.1.2 Chapter 2

Statistical significance in line graphs is shown by an asterisk or asterisks above the line for antibiotic- and DSS-treated MCJ KO (MCJ KO_Abx+DSS+) *versus* antibiotic- and DSS-treated WT (WT_Abx+DSS+); IFX and DSS positive MCJ KO (MCJ KO_IFX+) *versus* IFX and DSS positive WT (WT_IFX+); IFX and DSS positive MCJ KO housed alone (MCJ KO_Ap_IFXp) *versus* IFX and DSS positive WT housed alone (WT_Ap_IFXp). Furthermore, an asterisk or asterisks below line indicated the following comparisons; antibiotic negative and DSS-treated MCJ KO (MCJ KO_Abx-DSS+) *versus* antibiotic negative and DSS-treated WT (WT_Abx-DSS+); IFX and DSS positive WT (WT_IFX+) *versus* IFX negative and DSS positive WT (WT_IFX-); WT housed alone treated with DSS and IFX (WT_Ap_IFXp) *versus* WT cohoused treated with DSS and IFX (WT_Cop_IFXp).

The significance of a result in boxplots is shown by an asterisk or asterisks upside the box to indicate differences within the same genotype in different experimental conditions: antibiotic- and DSS-treated (Abx+DSS+) *versus* antibiotic negative and DSS positive (Abx-DSS+); DSS-treated IFX positive (IFX+) *versus* DSS-treated IFX negative (IFX-); cohoused DSS- and IFX-treated (Cop-IFXp) *versus* alone DSS- and IFX-treated (Ap-IFXp). Differences between genotypes in the same experimental group are presented as a line with an asterisk or asterisks above.

In antibiotic-induced dysbiosis experiment, DSS negative groups, both healthy (Abx-DSS-) and antibiotic-induced gut dysbiosis (Abx+DSS-) were used as controls and they were included in the statistical analysis.

4.1.3 Chapter 3

Statistical differences in line graphs are shown by an asterisk or asterisks above the line for GF MCJ KO DSS-treated (GF_MCJ KO) *versus* GF WT DSS-treated (GF_WT); MCJ KO DSS-treated alone (MCJ KO_Ap) *versus* cohoused (MCJ KO_Cop). An asterisk or asterisks below line indicated MCJ KO cohoused and DSS-treated (MCJ KO_Cop) *versus* WT cohoused and DSS-treated (WT_Cop) comparison.

In the cohousing study, the significance of a result in boxplots is shown by an asterisk or asterisks upside the box to indicate differences within the same genotype in different experimental conditions: GF DSS-treated (d8) *versus* GF DSS negative (d0); MCJ KO DSS positive groups (DSS+) and cohoused groups (cohoused DSS+) *versus* control (DSS-). Significant differences within the same-genotype mice between DSS-treated housed alone and cohoused groups are represented with an asterisk or asterisks inside the box of WT and MCJ-deficient mice that were housed alone (DSS+). Differences between genotypes in the same experimental group are presented as a line with an asterisk or asterisks above.

4.1.4 Chapter 4

Statistical differences in line graphs are shown by an asterisk or asterisks above the line for MCJ KO DSS-induced chronic colitis (MCJ KO_DSS+) *versus* WT DSS-induced chronic colitis (WT_DSS+). Statistical significance in boxplots is shown by an asterisk or asterisks upside the box to indicate differences within the same genotype in different experimental conditions: DSS-induced chronic colitis (DSS+) *versus* control (DSS-). Differences between genotypes in the same experimental group are presented as a line with an asterisk or asterisks above.

4.2 Pearson correlations

HAIIA (Hierarchical All-against-All significance testing) tool was used to find significant associations in high-dimensional and heterogeneous datasets (https://huttenhower.sph.harvard.edu/halla). Significant correlations (p.adj = 0.001) were represented either in blue or red. The size and intensity of color for each circle represents the strength of the correlation (the larger and darker circles demonstrate a strong correlation), blue colors illustrate positive correlations and red colors illustrate negative correlation coefficient. We made several correlations that will be described next.

4.2.1 Microbial community and host gene expression

A Pearson correlation of microbial community and host gene expression in the colon from WT and MCJ-deficient mice, treated or not with DSS was performed.

4.2.2 Bacterial community and macrophages gene expression

In this correlation, we made the 50 strongest correlations between genes differentially expressed due to MCJ deficiency in macrophages infiltrated during colonic inflammation and OTUs present in the 4 experimental groups that were not treated with antibiotics previously (Abx- and DSS - and DSS +).

4.2.3 Microbial community and colonic proteins

We sought to find significant associations in the cohousing experiment between proteins that were statistically different according to WT and MCJ-deficient genotypes upon intestinal inflammation and all microbial OTUs.

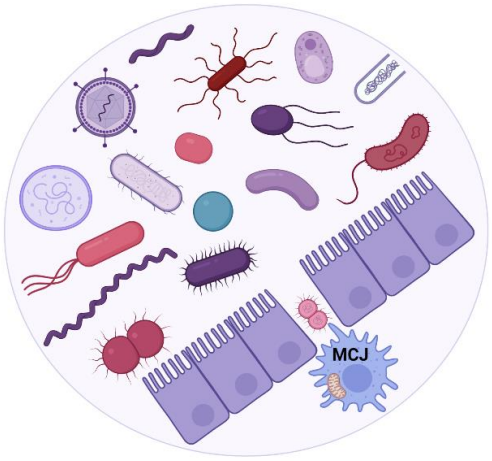

Results

1. MCJ impact on host-gut microbiota crosstalk during acute ulcerative colitis

Publication

Pascual-Itoiz MA*, **Peña-Cearra A***, Martín-Ruiz I, Lavín JL, Simó C, Rodríguez H, Atondo E, Flores JM, Carreras-González A, Tomás-Cortázar J, Barriales D, Palacios A, García-Cañas V, Pellón A, Fullaondo A, Aransay AM, Prados-Rosales R, Martín R, Anguita J, Abecia L. The mitochondrial negative regulator MCJ modulates the interplay between microbiota and the host during ulcerative colitis. Sci Rep. 2020;10:572. *These authors contributed equally.

Conference

Spanish Society of Immunology
Pascual-Itoiz MA*, **Peña-Cearra A*,** Martin-Ruiz I, Atondo E, Anguita J, Abecia L. Study of mitochondrial modulator MCJ on lymphoid populations present in MLN during murine experimental colitis. *These authors contributed equally.
Poster communication. (Zaragoza, May 25-27, 2017)

1.1 Results

The first aim of this thesis work was to assess the role of the mitochondrial gene *Mcj* in a mouse model of acute experimental colitis. Although it is widely known that it plays an important role in in the production of TNF in bone marrow-derived macrophages and it is higly expressed in metabolic active tissues, the impact of *Mcj* on UC remains unknown. For this purpose, we used an MCJ-deficient murine model.

HYPOTHESIS	Mitochondria and the natural negative regulator of mitochondrial respiration, MCJ (methylation-controlled J protein), might play a critical role in the inflammatory processes of the gut.

1.1.1 MCJ attenuates the severity of DSS-induced colitis and decreases colonic tissue

To assess the role of the mitochondrial negative regulator MCJ in the regulation of intestinal inflammatory responses, we studied a model of DSS-induced colitis. MCJ-deficient mice showed increased disease severity than WT mice, as reflected by an increased disease activity index (DAI; Figure 15A). In agreement with previous studies, the entire colon of DSS-treated mice showed histopathological changes, with loss of crypt regions. Strikingly, MCJ-deficient mice showed higher histopathology score (18.3 ± 1.38), compared to DSS-treated WT (12.8 ± 1.57) mice (p value ≤ 0.01) (Figure 15B).

To further assess the severity of colitis, colonic length, mucus layer thickness and the number of goblet cells were measured in all experimental groups. Both DSS-treated groups showed a marked reduction in colon length (Figure 15C), mucus layer thickness (Figure 15D; Supplementary Figure S1A) and number of goblet cells (Figure 15E; Supplementary Figure S1B), and higher permeability to the paracellular tracer FITC-dextran (Figure 15F; Supplementary Figure S1C), with no differences between WT and MCJ-deficient mice. Furthermore, analysis of ROS measured by DHE staining in colon sections showed increased levels in both genotypes (Figure 15G). Moreover, mitochondria shape observed by TEM showed that in MCJ-deficient mice changed from tubular to circular form with inflammation (Figure 15H; Supplementary Figure S1D). These results suggest that MCJ function helps to temper the tissue damage upon colon injury, supporting the hypothesis that an inhibition in mitochondrial respiratory contributes to histopathological changes during colitis disease aggressiveness.

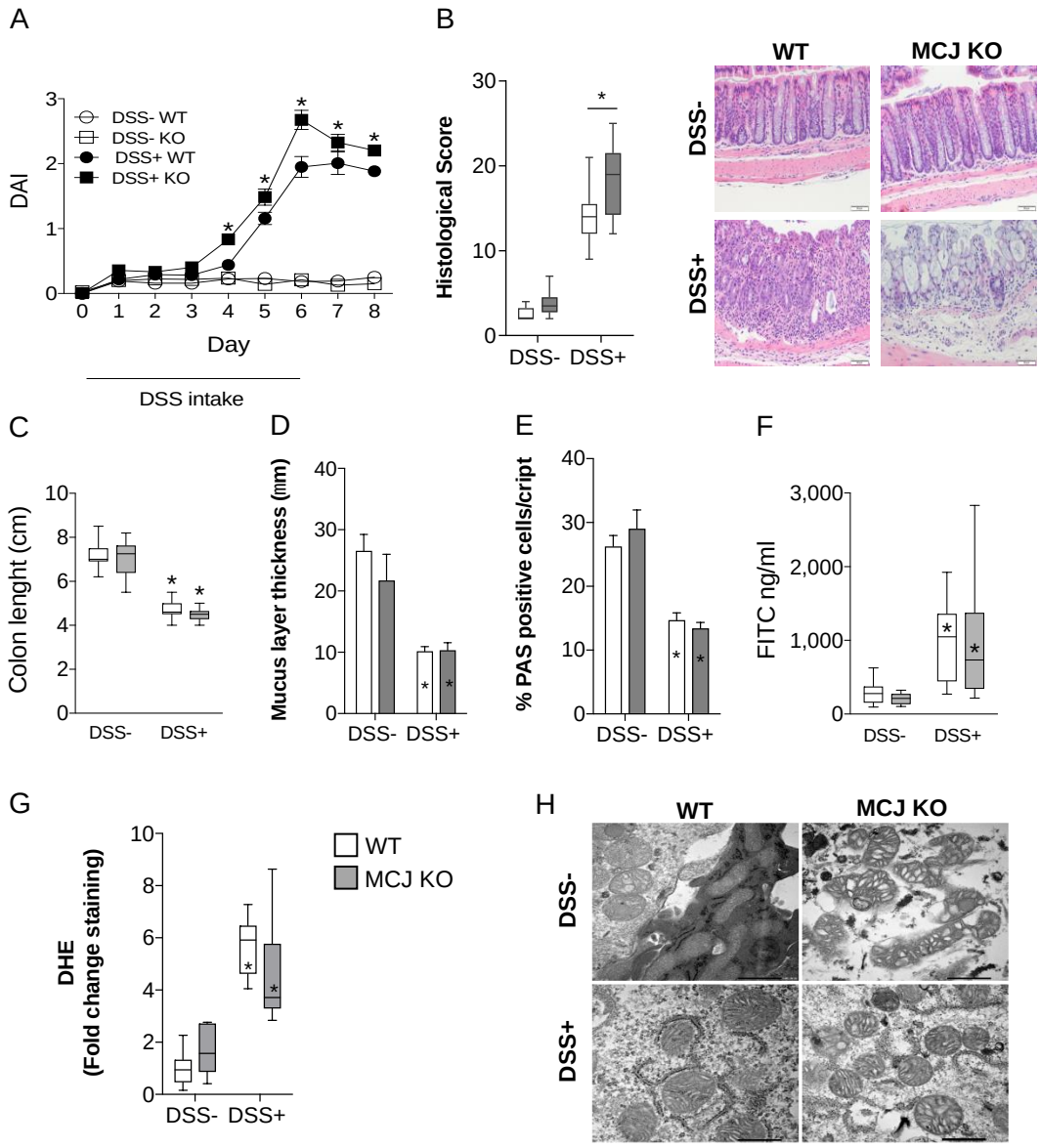

Figure 15. Evaluation of MCJ impact on acute colitis. Experimental design: WT and MCJ-deficient mice received 3% DSS in drinking water for 6 days, followed by 2 days of regular drinking water. (**A**) DAI values over the experimental period; data are expressed as means ± SEM (n=20). (**B**) Histological scores. Error bars indicate SEM. Representative images. (**C**) Colon length (cm). (**D**) Mucus layer thickness (µm). (**E**) Goblet cells: % of positive cells stained with PAS. (**F**) Permeability to the tracer FITC-dextran (ng/ml). (**G**) ROS measured by DHE staining in colon sections. (**H**) Electron microscopy showing mitochondrial morphology in DSS induced colitis groups (Scale bar: 500nm). White: wild-type; grey: MCJ-deficient. Box and whisker plots of median, quartiles and range, n=10 mice per group at a minimum. Statistical analysis: two-way ANOVA. In line graphs, statistical differences are represented by an asterisk or asterisks "*" above the line for MCJ-KO DSS-induced acute colitis (KO_DSSp) *versus* WT DSS-induced acute colitis (WT_DSSp). In boxplots and bar graphs, an asterisk "*" upside or inside boxes *versus* control, and an asterisk above line indicates differences between genotypes in the same experimental group. KO: MCJ KO.

1.1.2 MCJ increases colonic MPO activity and CD11c+CD103+ cells in mesenteric lymph nodes

We then analyzed the cellular composition and cell activation status in the presence or absence of MCJ. First, we evaluated the infiltration and activation of neutrophils in the local inflammatory colonic sites by measuring MPO activity. MPO levels were significantly increased (p value ≤ 0.0001) in both WT and MCJ KO mice treated with DSS. However, DSS-treated MCJ KO mice showed (p value ≤ 0.05) lower MPO activity than WT mice (Figure 16A), suggesting a reduced infiltration of neutrophils. Macrophages infiltrated in lamina propria and submucosa were also examined by expression of the cell surface marker F4/80 in serial colon sections. The number of F4/80+ cells was significantly higher in the inflamed mucosa of DSS fed mice, compared to untreated mice and no obvious difference was observed between genotypes (Figure 16B). Then, colon macrophages were isolated from tissue and TNF was determined by flow cytometry (Figure 16C). Results showed that TNF bound to membrane levels in both DSS+ groups and MCJ-deficient DSS- group were higher than WT DSS- one.

We also determined cellular populations in the spleen and MLN by flow cytometry. We identified an increased population of $CD11b^{high}$ and F4/80 double positive cells (monocyte-derived dendritic cells: MDDC) in spleen from mice deficient in MCJ treated with DSS (Figure 16D). In contrast, the population of cells that were positive for CD11b and CD11c (TNF and nitric oxide producing dendritic cells, Tip-DCs) decreased. In MLN, the CD11c and CD103 (dendritic cells) positive population did not change as a result of the treatment with DSS, although we noted a small, albeit significant decrease in MCJ KO DSS-treated mice compared to DSS-treated WT mice (Figure 16E). Overall, these results showed that innate immune populations are not dramatically changed in the absence of MCJ during colitis.

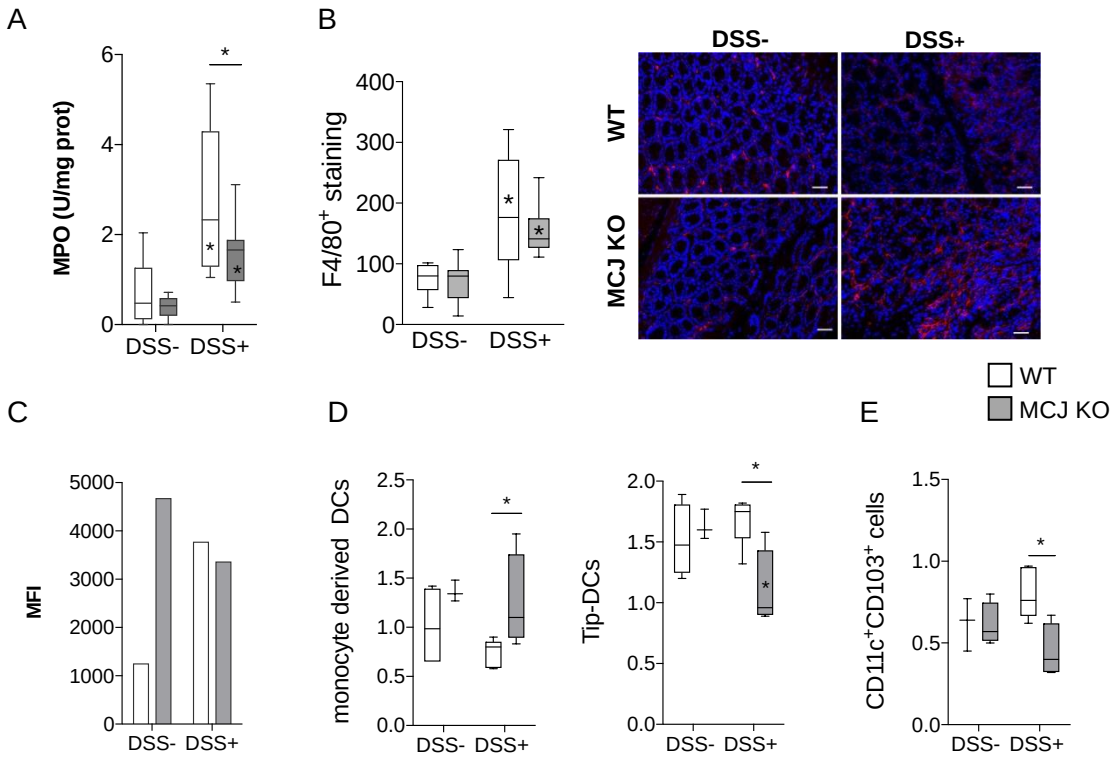

Figure 16. Assessment of immune system activation and immune cell composition in colonic tissue and mesenteric lymph nodes. (**A**) MPO activity (U/mg protein). (**B**) Macrophage infiltration in the colon of DSS-treated mice. Representative immunofluorescence sections of colonic macrophages by F4/80 marker. Bar represents 50 µm. (**C**) The average of the mean fluorescence intensity (MFI) determined by flow cytometry showing the expression of TNF bound to membrane present in macrophages isolated from colon tissue. The values presented correspond to one experiment of two with similar results. (**D**,**E**) Flow cytometry analysis of lymphoid populations in MLNs. White: wild-type; grey: MCJ-deficient. Box and whisker plots of median, quartiles and range, n=7 mice per group at a minimum. Statistical analysis: two-way ANOVA. An asterisk "*" in boxes *versus* control, and an asterisk above line indicates differences between genotypes in the same experimental group.

1.1.3 MCJ affects gene expression in murine colonic tissue

In order to measure the potential effect of MCJ on the inflammatory output in the colonic tissue during DSS-induced colitis, we quantified mRNA levels of several genes by quantitative PCR. The expression levels of *Tlr2*, *4*, *5* and *9*, the primary mucosal receptors of bacterial components, were analyzed. In untreated mice, the expression levels of *Tlr5* and *Tlr9* were not different in WT and MCJ-deficient mice, while *Tlr2* and *Tlr4* expression levels were significantly lower in the absence of MCJ (Figure 17A). The treatment with DSS did not result in significant changes in the expression level of *Tlr2* or *Tlr5* regardless of the genotype. On the other hand, the treatment resulted in decreased expression of *Tlr4* that was not affected by the lack of MCJ. However, *Tlr9* expression levels increased in WT mice that had been treated with DSS, and the absence of MCJ resulted in a further significant increase of its expression levels (Figure 17A). Although the expression levels of *Trif* did not change along the different conditions and genotypes, we found a significant increase in the expression levels of *Myd88* both as a consequence of the treatment with DSS and the genotype of the mice (Figure 17B). Overall, these data suggest that the absence of MCJ implies an increased expression of key genes regulating the inflammatory output in the colon, including *Tlr9-MyD88*.

We then measured the cytokine and proinflammatory gene expression profile of colonic tissue. The expression levels of *Il6*, *Il1b*, *Ptgs2*, *Nos2*, *Tnf*, *Tgfb* and *Il10* were significantly increased as a result of the treatment with DSS both in WT and MCJ-deficient mice (Figures 17C-E). The absence of MCJ caused significantly higher expression of genes such as *Nos2*, *Il1b*, *Tgfb*, *Il10*, and *Tnf*. In this regard, inflammation was confirmed by the ratio IL10/TNF measured by ELISA. The upregulation of *Tnf* and *Il1b* genes expression in the absence of MCJ were particularly intriguing due to its role in epithelial barrier disruption during IBD. In particular, membrane-bound *Tnf* is associated with more severe inflammatory conditions when interacting with *Tnfr1.* Therefore, we investigated the expression of both *Adam17* and *Timp3*. As reported in bone marrow-derived macrophages, the absence of MCJ resulted in significantly increased expression levels of *Timp3*, while the levels of *Adam17* remained invariable (Figure 17E). However, TACE activity was significantly reduced in MCJ-deficient group indicating a functional control of the enzyme by MCJ (Figure 17F). In accordance with slightly lower level of soluble TNF measured by ELISA (Figure 17F). In addition, the levels of *Tnfr1* expression remained constant in WT mice when treated with DSS, as opposed to the observed increase in *Tnfr2* levels. Of note, the absence of MCJ specifically resulted in an augmented expression of *Tnfr1* (Figure 17E). On the other hand, mRNA abundance of *Ifng* and *Stat1* was increased only in the absence of MCJ in

DSS treated mice (Figure 17G). These data support the augmented production of *Tnf* and the signaling through *Tnfr1* in the absence of MCJ. In addition, MCJ seems to be implicated in the regulation of *Ifng* and *Stat1* expression levels during inflammatory processes. Representative western blot reflecting TIMP3, TNFR1 and TNF bound to membrane protein levels in colon were presented in Supplementary Figure S1E.

Studies in rodents indicate that innate recognition of bacteria or bacterial components triggers epithelial expression of secreted C-type lectins *Reg3g* and *Reg3b*. As expected, the expression level of *Reg3b* and *Reg3g* raised with DSS treatment (Figure 17H). Interestingly the absence of MCJ in colitis-induced mice resulted in lower expression of both genes, indicating lower protective role against intestinal translocation which might be associated with the severity of the disease.

We also tested the expression of genes related to the integrity of the epithelial cell barrier, by analyzing the genes *Muc2*, *Muc3*, *Tjp1*, *Cldn2*, *Cldn5*, *Ocln* and *Pigr*. As anticipated, the expression of *Muc2* and *Muc3* were significantly repressed upon DSS treatment, but no effect was observed by the lack of MCJ (Figures 17I, J). No differences were observed in the expression of *Tjp1* (encoding the protein tight junction protein 1). Tight junction associated genes such as *Ocln*, *Cldn2* and *Cldn5* (encoding the proteins Occludin, Claudin 2 and Claudin 5, respectively) did not show differences due to DSS treatment in WT mice (Figure 17J). However, MCJ deficiency in DSS-treated mice resulted in the decreased expression of *Cldn2* and increased levels of *Cldn5* transcripts in the colon, suggesting an effect on tight junction permeability, although results should be interpreted with caution as only differences in concentration and not in localization have been determined.

In order to determine whether our findings in the murine model resemble human disease conditions, we analyzed a public dataset of UC patients (total of 48 samples) for the expression levels of *MCJ*. *DNAJC15* expression levels were found to be significantly lower in inflamed tissue compared to non-inflamed tissue (Figure 17K). Importantly, the expression of the genes *TIMP3* and *TNF* was increased in inflamed compared to non-inflamed tissue from UC patients, strongly suggesting that *MCJ* expression and the subsequent regulation of downstream genes are intimately related to the inflammatory output during colonic inflammation.

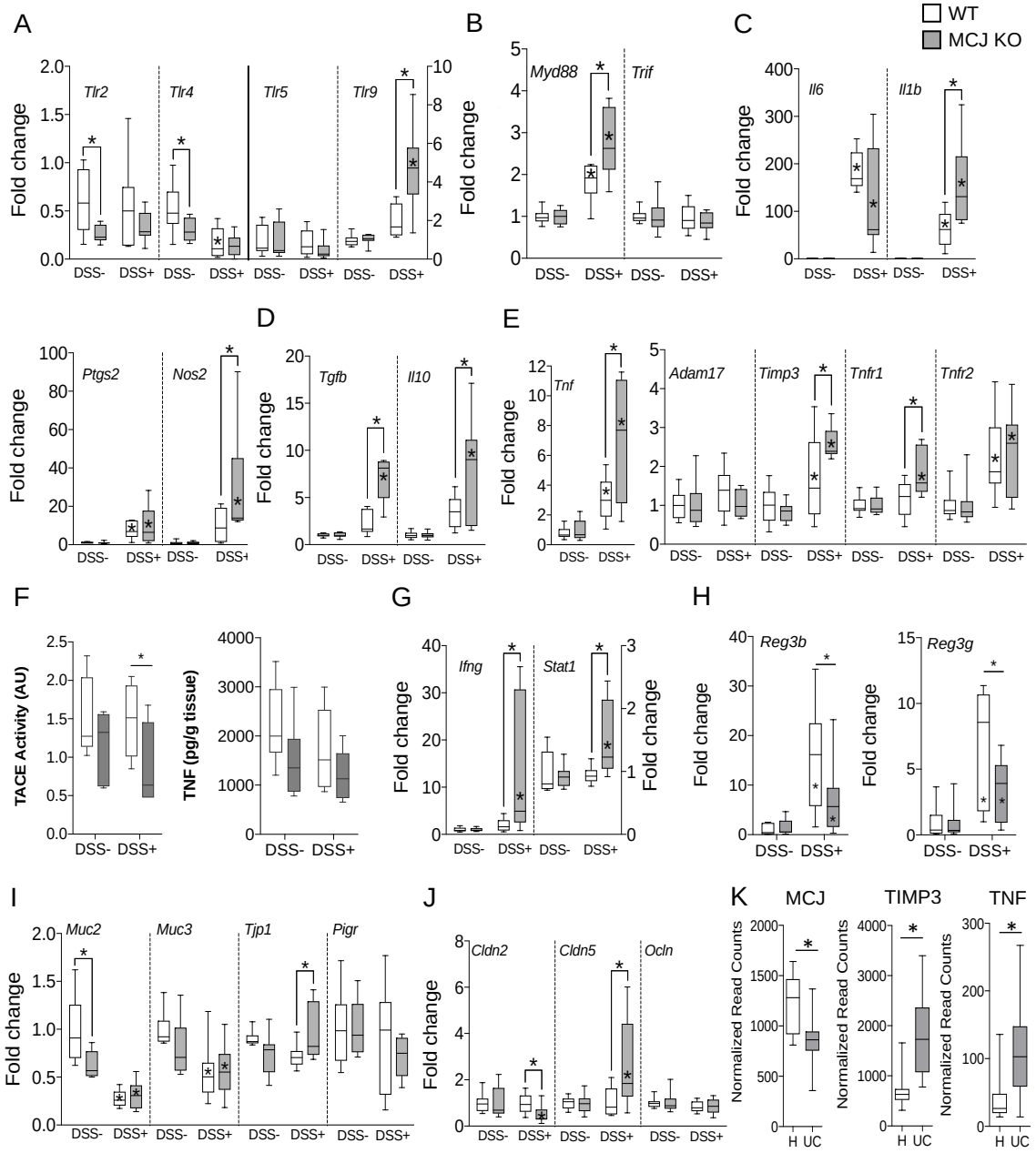

Figure 17. Gene expression levels in colon tissue in a DSS-induced colitis model. mRNA fold change normalized to *Rpl19* gene. (**A**) *Tlr2*, *Tlr4*, *Tlr5* and *Tlr9*. (**B**) *Myd88* and *Trif*. (**C**) *Il6*, *Il1b*, *Ptgs2* and *Nos2*. (**D**) *Tgfb* and *Il10*. (**E**) *Tnf*, *Adam17*, *Timp3*, *Tnfr1* and *Tnfr2*. (**F**) TACE activity and TNF concentration (**G**) *Ifng* and *Stat1*. (**H**) *Reg3b* and *Reg3g* were determined by qPCR. Results are fold change normalized to *Rpl19* gene to WT (white). (**I**) *Muc2*, *Muc3*, *Tjp1* and *Pigr*. (**J**) *Cldn2*, *Cldn5* and *Ocln*. Box and whisker plots of median, quartiles, and range, n=7 mice per group at a minimum. Statistical analysis: two-way ANOVA. An asterisk "*" in boxes *versus* control, and an asterisk above line indicates differences between genotypes in the same experimental group. (**K**) Gene expression levels of MCJ, TIMP3, and TNF in a public human dataset (H=non inflamed; UC=inflamed tissue). Sample size: H=24; UC=24.

1.1.4 Epithelial cells are not impacted by MCJ levels

Next, we asked whether MCJ deficiency would influence colonic epithelial cells, thereby affecting the pathways observed in the whole colon tissue. For that, we induced acute experimental colitis in mice and we tested the expression levels of some of the genes modified in the colon tissue. Remarkably, *Mcj* expression decreased in DSS-treated WT mice compared to healthy animals (Figure 18A). Although both *Tnf* and *Timp3* levels were upregulated in MCJ-deficient mice inflamed colon tissue, the levels of these genes in epithelial cells remained unchanged between the different genotypes (Figure 18B). Conversely, we detected an opposite regulation of *Tnfr1* and *Myd88* genes in the epithelial cells of MCJ-deficient mice upon intestinal inflammation compared to the whole colon tissue (Figures 18C, D). In addition, no differences were observed regarding *Tlr9, Reg3b* and *Reg3g* expression between DSS-treated genotypes (Figures 18E, F). Collectively, results suggest that *Mcj* deficiency effect is not associated with colonic epithelial cells, but with immune cells.

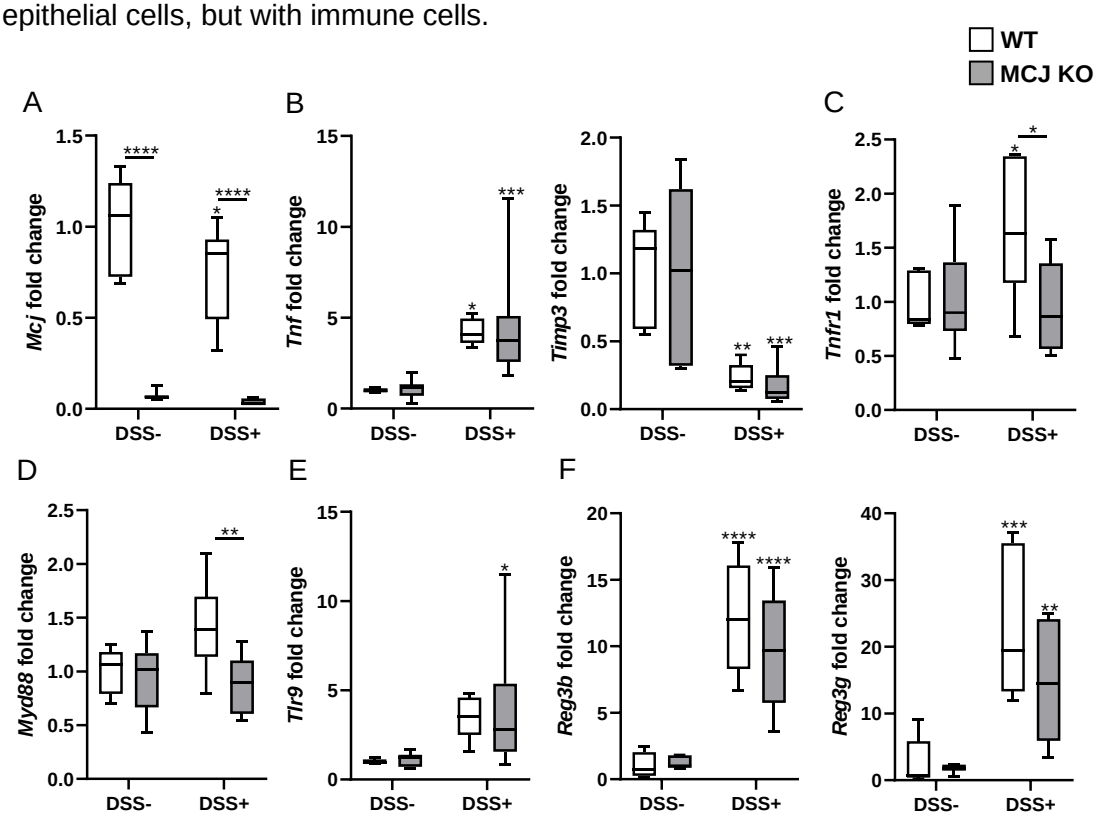

Figure 18. Gene expression levels of epithelial cells from an experimental model of acute colitis. (**A**) *Mcj.* (**B**) *Tnf* and *Timp3*. (**C**) *Tnfr1*. (**D**) *Myd88.* (**E**) *Tlr9.* (**F**) *Reg3b* and *Reg3g*. Results are fold change normalized to *Rpl19* gene, and to WT (white) control. Box and whisker plots of median, quartiles, and range, n=5 mice per group at a minimum. White boxplots indicate wild-type and grey boxplots MCJ-deficient mice. Statistical analysis: two-way ANOVA. An asterisk or asterisks "*" upside boxes *versus* control, and an asterisk or asterisks above line indicate differences between genotypes in the same experimental group.

1.1.5 MCJ impacts the composition of the host microbiome

Secretory IgA plays a role in the homeostatic maintenance of the intestinal microbiota, primarily by preventing mucosal inflammation through immune exclusion, removal of antigen-antibody complexes in the lamina propria and neutralization of inflammatory mediators. Therefore, we measured IgA levels in the colon wall by immunohistochemistry. A marked increase of IgA was found in colitis-induced MCJ-deficient mice compared to WT animals (Figure 19A), suggesting that the absence of MCJ could shape intestinal microbiota in the inflamed colon. Therefore, we evaluated microbiota composition in animals that were induced colitis compared to healthy control mice. Illumina sequencing of the V4 region of the *16S rRNA* gene of colonic bacterial communities yielded a total of 3.161.263 paired and merged sequences after quality filtering ranging from 56.302 to 162.730 sequences per sample. A Good's coverage average of 96.7% (range 95.3–98.2%) indicated that there was sufficient community coverage using this dataset so that the effects on the community structure of the microbiota could be assessed. Diversity indices decreased after DSS treatment presenting two indices (Observed species and Shannon) significantly lower diversity in the MCJ-deficient group (Figure 19B). Differences were detected using PCoA of non-phylogenetic (Bray Curtis) and phylogenetic distances (weighted and unweighted Unifrac), showing changes in particular OTUs abundances. The health status of the mice provided the strongest effect on microbiota composition, followed by the presence or absence of MCJ (e.g., Bray Curtis distances; Figure 19C). ANOSIM (analysis of similarities) detected significant (p.adj = 0.01) differences between colitis-induced groups. Core microbiota was represented in a Venn diagram (Figure 19D).

The comparison of taxa proportions among experimental groups identified a number of them that could be contributing to the differences observed in the microbial community. In homeostasis, the relative abundance of the phylum Verrucomicrobia was significantly higher (*p* value = 0.008) in MCJ-deficient mice (7.1 ± 0.09%) compared to WT animals (0.05 ± 0.0001%) (n=8 per genotype) (Figure 19E). The examination at the genus level showed that within the phylum Verrucomicrobia only *A. muciniphila* was represented. In addition, *Ruminococcus* and a small group belonging to the *Lachnospiraceae* family that has yet to be assigned to a genus, were significantly increased in healthy MCJ-deficient mice (Figure 19F). In MCJ-deficient colitis-induced mice, the analysis indicated a reduction in Bacteroidetes phylum based on the decreased levels of unclassified genus from Bacteroidales *S24–7* family, *Bacteroides* and *Prevotella*, and the increase in the presence of members of the Firmicutes phylum such as *Lactobacillus* and *R. gnavus* (Figure 19G). The *Enterobacteriaceae* family enlarged

its percentage from 10 in WT to 20% in MCJ-deficient mice. The disproportionate increase in mucolytic bacteria in MCJ-deficient mice could contribute to bacterial translocation and severity of the disease.

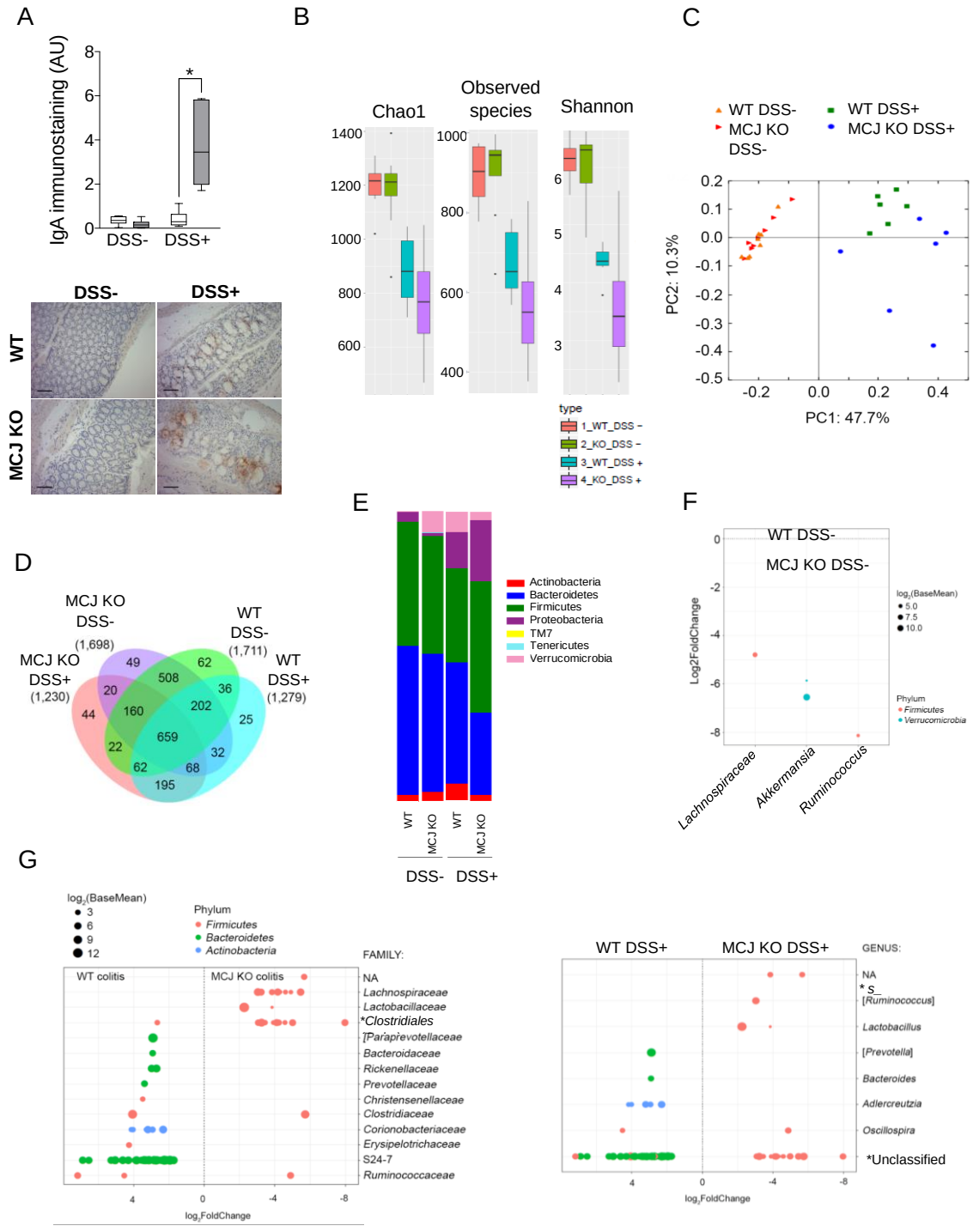

Figure 19. Composition of host microbiome in acute colitis. (**A**) Determination of IgA levels by immunohistochemistry in colon tissue from WT and MCJ-deficient mice during DSS-induced colitis. Error bars indicate SEM. Box and whisker plots of median, quartiles and range, n=7 mice per group at a minimum. Statistical analysis: two-way ANOVA. An asterisk "*" above line indicates differences between genotypes in the same experimental group. (**B**) Alpha diversity measures for colon microbiomes across different experimental groups: Total observed taxonomic units, Chao1 estimates, and Shannon diversity index. (**C**) PCoA of β-diversity comparison revealed a significant separation of microbial community based on genotype in DSS experimental colitis. P.adj = 0.01 using ANOSIM. (**D**) Venn diagram with OTUs in the colon microbiome within each experimental group. (**E**) Phylum level microbial composition. (**F**) OTUs significantly difference between WT and MCJ-deficient control groups at the family and genus level. (**G**) OTUs significantly different (p.adj < 0.05) between the colon content from WT and MCJ-deficient DSS-induced colitis groups. The left side represents OTU's with a log2 fold positive difference for WT colon contents relative to the MCJ-deficient, while the right side is the negative fold change of the WT colon relative to the MCJ-deficient contents. Each point represents a single OTU colored by phylum and grouped by taxonomic family or genus level, size of point reflects the log2 mean abundance of the sequence data.

We then analyzed the functionality of the microbiome present in the colon of all experimental groups by the application of an LC-MS-based metabolomics approach. Principal component analysis (PCA) analysis of the data showed a difference between samples from mice as a result of the treatment with DSS (Figure 20A) with two clearly differentiated clusters: non-treated and DSS-treated mice. Supervised partial least-squares discriminate analysis (PLS-DA) was applied to further differentiate the contributions of particular metabolites to the separations between metabolite levels from WT and MCJ-deficient mice during DSS-induced colitis. Those metabolites with variable importance in projection (VIP)>1 were considered as potential biomarker candidates for group discrimination. The list of identified metabolites (fold changes over 1.7) was entered into the pathway analysis module from MetaboAnalyst.

The results reflected significant alteration in BA metabolism in the digestive tract (Figure 20B). Interestingly, MCJ-deficient mice were characterized by the higher presence of BAs in the inflamed mucosa. More specifically, taurocholic acid and taurohyocholate were increased in MCJ-deficient mice under inflammatory conditions (Figure 20C). High BA concentration in the colon leads to aqueous stool and erratic bowel function, exacerbating diarrhea (stool consistency) which contributes to DAI. Moreover, higher levels of fecal BAs have been identified to worsen the severity of colitis in DSS-treated mice (Stenman et al., 2012).

In summary, these data show significant shifts in the microbiota of WT and MCJ-deficient mice under inflammatory conditions, suggesting a regulatory relationship between mitochondrial function and microbiota, and a disturbance of this relationship in colitis. Moreover, our data support an association between the metabolism of BAs, microbiota and inflammation.

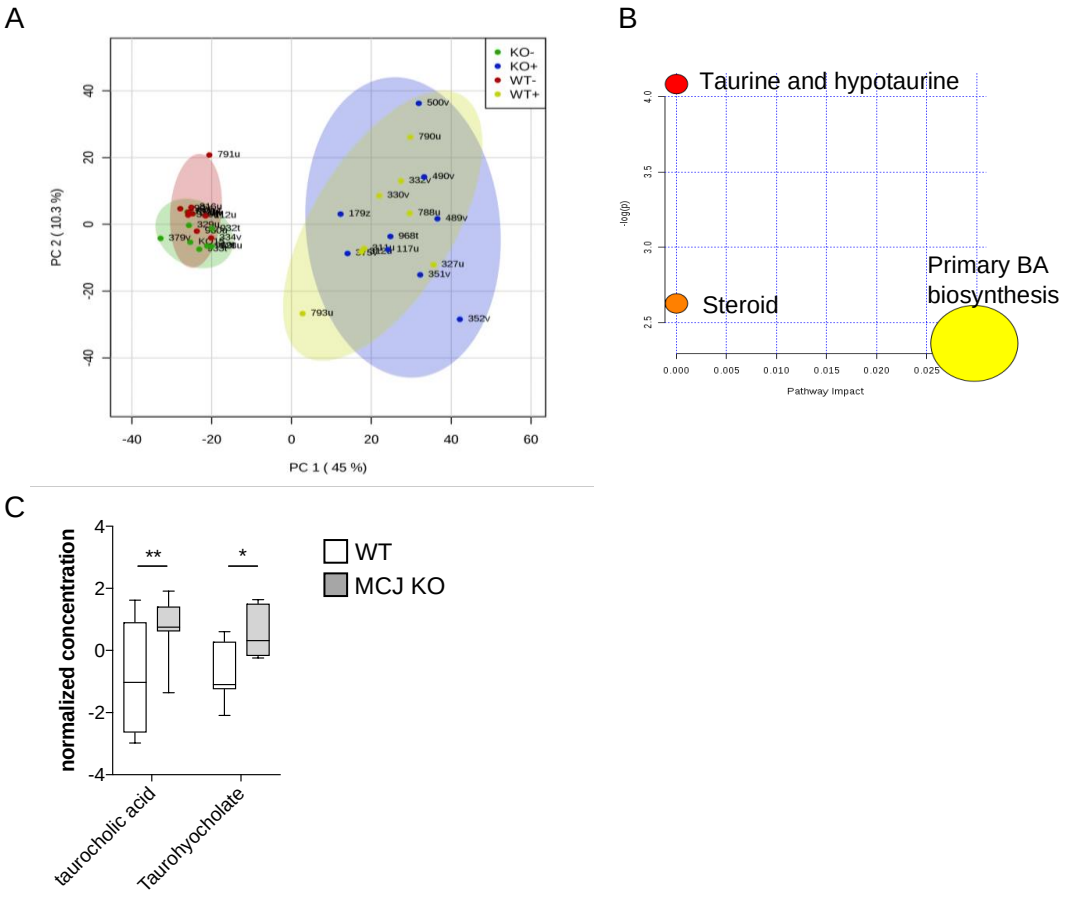

Figure 20. Metabolomic profiling of fecal samples in DSS-Induced colitis. (**A**) Score plot for PCoA model with PC1 plotted against PC2 with 95% confidence ellipses around the experimental groups (KO DSS-, KO DSS+, WT DSS- and WT DSS+). (**B**) Metabolic pathway analysis. The metabolic pathways are represented as circles according to their *p* values from enrichment analysis (Y-axis) and pathway impact values (X-axis) using MetaboAnalyst 4.0. Darker circle colors indicate more significant changes of metabolites in the corresponding pathway (*p* values). The size of the circle corresponds to the pathway impact score and is correlated with the centrality of the involved metabolites. (**C**) Boxplots of the abundances of important bile acids significantly differed among the groups. The center line of each box represents the median, and the top and bottom of the box represent the 75th and 25th percentiles of the data, respectively. The top and bottom of the error bars represent the 95th and 5th percentiles of the data, respectively. n=8 mice per group. Statistical analysis: two-way ANOVA. An asterisk or asterisks "*" above line indicate differences between genotypes in the same experimental group. BA: Bile acid.

1.1.6 Correlation between bacterial community and gene expression in the colon under experimentally-induced colitis

To understand whether the observed changes in microbiota composition were related to the response to colonic damage or the absence of MCJ, we performed Pearson correlation analyses. The variation in bacterial community composition and gene expression from colon wall interaction showed a significant correlation (Figure 21). The presence of *Akkermansia* correlated (p.adj ≤ 0.001) with *Ifnγ* expression while *Parabacteroides* correlated with the genes differentially expressed in the absence of MCJ (*Adam17*, *Timp3* and *Tnf* receptors). Even more important was the positive correlation observed between *Enterococcus* and the *Enterobacteriaceae* bacterial group with *Myd88* and *Tlr9* expression. Those bacterial groups were also correlated with the expression of cytokines such as *Il1b*, *Il6*, *Tgfb*, and *Il10*, as well as to *Ptgs2* and *Nos2* expression indicating a critical role during inflammation especially in MCJ-deficient mice. On the other hand, the presence of one unclassified genus belonging to the *Rikenellaceae* and *S24-7* families showed a negative correlation with the expression of genes associated with antigen presenting cells, pointing to a potential beneficial role of both groups of bacteria during inflammatory conditions.

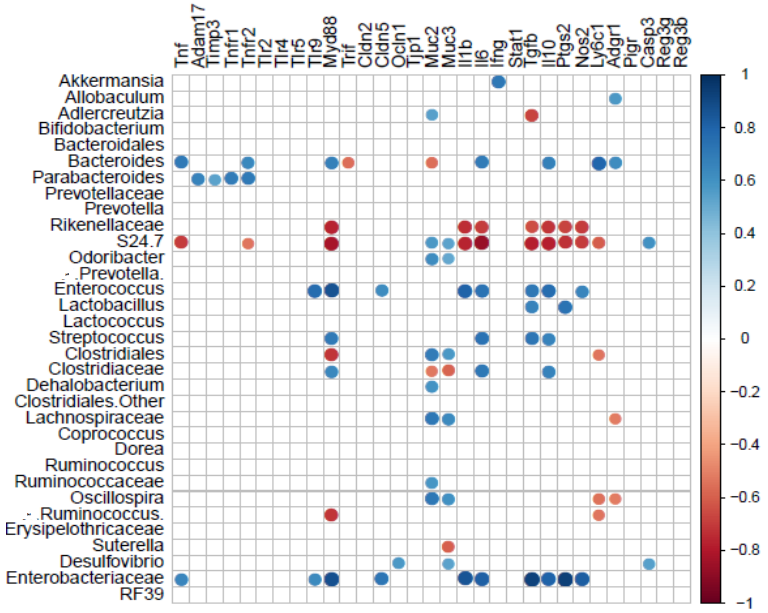

Figure 21. Pearson correlation of microbial community and host gene expression in the colon from WT and MCJ-deficient mice, treated or not with DSS. Pearson correlation analysis indicated that the variation in bacterial community composition and gene expression from the colon wall interaction had significant correlations (p.adj = 0.001). The size and intensity of color for each circle represents the strength of the correlation (the larger and darker circles demonstrate a strong correlation), blue colors illustrate positive correlations and red colors illustrate negative correlation coefficient.

1.2 Discussion

Mitochondrial dysfunction may play an important role in the pathogenesis associated with UC. MCJ is an endogenous negative regulator of the ETC that regulates mitochondrial function in response to altered metabolic conditions. We found that the loss of MCJ results in more severe colitis, suggesting that ETC function needs to be tightly controlled to regulate the pathological consequences upon the initiation of inflammation. We also show that the absence of MCJ results in changes upon the initiation of colonic damage, which may be related to variations in intestinal microbiota-host mitochondria crosstalk and the ensuing expression levels of key genes associated with the initiation and progression of the disease.

We have identified a pathway coordinated by MCJ at gut level. MCJ absence during colitis results in the upregulation of the TACE inhibitor *Timp3*, which probably affects TNF shedding from the cell membrane. Indeed, it has been reported that the loss of MCJ in macrophages inhibits TNF shedding from the plasma membrane (Navasa et al., 2015a). Similarly, both TNF receptors are TACE substrates (Black, 2004). In addition, transmembrane TNF induces the formation of STAT1-dependent death-inducing signaling complexes (DISC) and apoptosis through its interaction with TNFR1 (Jiang et al., 2017). These data suggest that MCJ deficiency contributes to disease severity at least partly due to the regulation of membrane TNF and its ability to signal through TNFR1 (Kalliolias and Ivashkiv, 2016). More importantly was that our MCJ-deficient mouse model resembled gene expression levels of *MCJ* and *TIMP3* observed in patients with UC. However, protein levels were distinctly regulated, probably by post-translational modifications. These results indicate that the kinetics of the response is important in defining the level of disease and that two levels of functional regulation at least (transcriptional and posttranslational) are key during the development and progression of IBD.

MCJ deficiency also increased production of some cytokines related to intestinal permeability such as *Il1b*, under DSS-induced inflammatory conditions. This cytokine is a known contributor to paracellular leakage within the epithelium and the consequent breakdown of the epithelial barrier (Lissner et al., 2015). The production of proinflammatory cytokines results from the interaction of innate immune cells with bacteria translocated to the intestinal submucosa upon disruption of the epithelial barrier (Rautava and Walker, 2007). Upon recognition of pathogens, TLR signaling induces transcription of *Il1b*, after ROS generation and following the release mtDNA (Fukata and

Ardidi, 2013). In contrast to what it was previously described in macrophages, *MCJ* deficiency did not affect ROS production during the inflammatory process reflecting the complex cellular interplay that takes place in colon tissue. However, our data show that not only *Tlr9* but also TLR signaling intermediate *Myd88* were augmented under disease conditions. These data are in line with those reported in the biopsy from active UC patients, in which *Tlr9* expression increased and positively correlated with the severity of intestinal inflammation as well as with inflammatory cytokine production (Sánchez-Muñoz et al., 2011; Fan and Liu, 2015). The TLR9 cellular responses to bacterial DNA in the gut are dependent upon both the site of stimulation (apical and basolateral membrane of epithelial cells) as well as CpG sequences. Therefore, bacterial DNA from luminal bacteria that pass a leaky epithelial barrier might be an important proinflammatory agent that would contribute to the perpetuation and progression of chronic intestinal inflammation. Emerging data indicate that MyD88 and TLR9 signaling of bacterial DNA is essential for induction of apoptosis and immune cell infiltration in colonic inflammation (Fűri et al., 2013; Everard et al., 2014). Moreover, also TLR9 responds to mtDNA, which shares many similarities with immunogenic bacterial DNA due to the common evolutionary origins, contributing to inflammation (Boyapati et al., 2018). Overall, these data suggest an increased susceptibility of innate immune cells to respond to invading microorganisms and the amplification of the inflammatory response. They also indicate that the absence of MCJ in mitochondria influences the production of proinflammatory cytokines such as *Il1b* through TLR9/MyD88 signaling after activation by translocated bacteria and mtDNA leaked from altered mitochondria. The activation of TLR9/MyD88 was reported to upregulate the expression of a key regulator of BA synthesis, FXR (Farnesoid X receptor) (Renga et al., 2013). It is known the capacity of the gut microbiota to alter physicochemical properties of bile acids, generating high affinity ligands to host nuclear receptors such FXR (Ridlon et al., 2014). In addition, previous studies suggested that taurocholate inhibits neutrophils infiltration in the inflamed colon tissue which may help to explain the decreased activity accumulation of MPO found in MCJ-deficient mice (Yang et al., 2015). We further tested the contribution of MCJ in epithelial cells and we observed that the expression of *Mcj* decreased in WT animals after acute colitis induction. In addition, the gene expression changes observed within the whole colon tissue during intestinal inflammation dissapeared, suggesting that MCJ deficiency effect might be primarily associated with intestinal immune cells.

We found that the absence of MCJ induces changes in gut microbial community. This modulation could be related to the higher levels of BAs described in DSS-treated MCJ-deficient mice. Their concentration regulates microbiota in the intestine inducing negative effects on Bacteroidetes and Actinobacteria, while they exert beneficial effects on Firmicutes and Proteobacteria in agreement with our results (Nie et al., 2015). Therefore, the proliferation of some BA-tolerant microbes such as *E. coli* can be facilitated by the heightened presence of these compounds (David et al., 2014). In this sense, *R. gnavus* and *Lactobacillus* (phylum Firmicutes) that were augmented in colitis-induced MCJ-deficient mice, also express bile salt hydrolase indicating tolerance to BAs (Begley et al., 2005; Zheng et al., 2017). Moreover, *R. gnavus* was proposed as an important member of the altered microbial community in IBD patients that can cope with increased oxidative stress. The increased abundance of this microorganism is often related with increased disease activity and it is also possible that contributes to the excessive immune response to microbiota (Hall et al., 2017).

On the other hand, the defective MUC2 mucin barrier, typical in a proinflammatory milieu, favor fast-growing bacteria that take advantage of increased sugar and oxygen concentrations induced by inflammation and tissue damage. In general, the overgrowth of *Enterobacteriaceae* was detected in both groups of colitis mice, with a higher increment in MCJ-deficient mice. The antimicrobial peptides (AMPs) and the secretory IgA balance microbial composition limiting penetration of commensal bacteria in the intestine. IgA coated bacteria in IBD were associated to unclassified genus of the family *S24-7* and *Erysipelotrichaceae*, and *Lactobacillus* (Macpherson, 2004). All of them altered due to MCJ levels in DSS+ groups. In addition, *Enterobacteriaceae* abundance correlated with higher levels of IgA and lower abundance of AMPs measured in the colon of MCJ-deficient group. According to Mirpuri et al. lamina propria CD11c+ antigen-presenting cells preferentially sample *Enterobacteriaceae* to produce specific IgA (Mirpuri et al., 2014). All this may help to explain our results, since we detected a significant reduction in dendritic cells (CD11c+CD103+) in MLN from colitis-induced MCJ-deficient mice. This suggests that there is a higher mobilization of cells to the lamina propria to selectively uptake this group of bacteria and produce higher amounts of specific IgA in the colon of those mice.

In conclusion (Figure 22), we observed that the loss of MCJ increased the levels of *Timp3* resulting in the inhibition of TACE activity and the shedding of membrane-bound *Tnf* and *Tnfr1*, leading to amplified *Tnfr1*-induced signaling in colon. *Tlr9/Myd88*-mediated signals augmented during intestinal inflammation by translocated bacteria in the absence of MCJ, with intensified proinflammatory cytokine production and a greater loss of the integrity of the colon tissue. Importantly, MCJ effect was mainly linked to intestinal immune cells. In addition, MCJ deficiency affected BAs levels, which modulate gut microbiota composition in colitis presenting a higher abundance of Firmicutes and Proteobacteria and lower levels of Bacteroidetes and Actinobacteria. All these factors contribute to the higher severity of the disease suggesting that dysfunctional mitochondria lead to mtDNA release potentiating inflammation in UC. Therefore, MCJ regulation is a new potential mechanism to evaluate in the disease. We propose that MCJ level links mitochondrial activity to the innate immune response and the integrity of the epithelial barrier in the gut, which indirectly regulates microbiota composition and BAs metabolism. The differential microbiota composition together with the mtDNA leaked from mitochondrial dysfunction drives proinflammatory signaling provoking the increase in the severity of the disease. Therefore, understanding the role that MCJ plays in homeostatic and pathological conditions in the gut may open new venues for the treatment of intestinal inflammation.

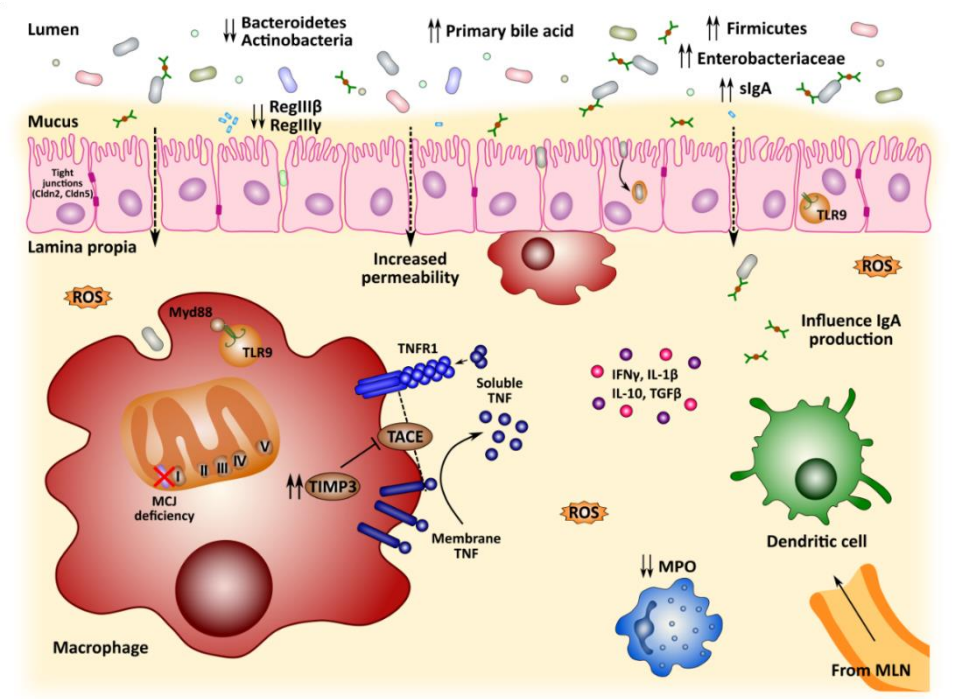

Figure 22. Graphical representation of potential microbiota-host interplay in DSS-induced colitis mice model deficient in MCJ.

2. MCJ deficiency and antibiotic-induced gut dysbiosis in colon macrophages transcriptome

Publication

Peña-Cearra A, Pascual-Itoiz MA, Lavín JL, Gonzalez-Lopez M, Castelo J, Fuertes M, Gutiérrez de Juan V, Bárcenas L, Martín-Ruiz I, Pellón A, Barriales D, Palacios A, Fullaondo A, Rodríguez-Lago I, Martinez-Chantar ML, Aransay AM, Rodriguez H, Anguita J, Abecia L. Colon macrophage transcriptome changes associated with mitochondrial dysfunction impacts pathogenesis and the response to therapy during ulcerative colitis. *Under revision*.

Conference

European Federation of Immunological Societies
Peña-Cearra A; Pascual-Itoiz MA; Fullaondo A; Anguita J; Abecia L. Immunoglobulin G coating shows earlier microbiota-host interaction in MCJ-Deficient model during murine experimental colitis.
Poster communication (Amsterdam, September 2-5, 2018)

2.1 Results

During UC, macrophages are activated by translocated pathogenic bacteria and are associated with the increased proinflammatory status characteristic of the disease (Peloquin et al., 2016). Accumulating evidence strongly supports the idea that enforcing a pre-resolving phenotype in macrophages might be a novel therapeutic approach to control intestinal inflammation and restore tissue function (Na et al., 2019).

Therefore, we performed an RNA-Seq study from inflamed murine intestinal macrophages to characterize the effect of mitochondrial dysfunction on the colon macrophage transcriptome. Additionally, dysbiosis was included to evaluate the regulation of mitochondria and microbiota during colitis.

HYPOTHESIS	Colon macrophages, as pivotal immune cells coordinating processes in the gut, play a critical role dealing with gut microbiota composition in the inflamed intestine of mice deficient in MCJ

2.1.1 Antibiotic-induced dysbiosis increases experimental colitis severity

To determine the influence of an altered microbiota composition on colitis in the MCJ-deficient mouse model, DAI and WL parameters were evaluated. MCJ-deficient mice presented higher DAI scores at day 7 compared to the respective WT groups, regardless of antibiotic treatment (Figure 23A). However, no differences were observed at WL level between the different genotypes in DSS treated mice at day 7 (both Abx- and Abx+) (Figure 23B), indicating that feces consistency determined the higher DAI scores associated with MCJ deficiency.

To study microbiota-host interactions along the DSS-induced colitis period, live bacteria and IgG coated fecal bacteria were quantified by flow cytometry. Starting at day 2 after the initiation of DSS treatment, the percentage of live bacteria was similar in all experimental groups (Figure 23C). In the antibiotic-treated groups, basal levels were recovered after 6 days of antibiotic treatment (Figure 23D). MCJ-deficient DSS-treated mice (Abx-DSS+) exhibited higher IgG-coated fecal bacteria than WT experimental group (Abx-DSS+) indicating earlier microbial-host cross-talk and a faster activation of the immune system. Among all colitis groups, mice treated previously with antibiotic (Abx+DSS+) presented the highest IgG coating at the beginning of DSS treatment (day 0). This percentage decreased gradually until day 8, while MCJ-deficient mice without antibiotic-induced dysbiosis (Abx-DSS+) increased progressively the IgG percentage reaching antibiotic-induced dysbiotic groups at day 6. All these data suggest that MCJ modifies the kinetics of the immune response.

2.1.2 MCJ level impact on immune responses in a dysbiotic scenario resembling disease

To further assess the role of MCJ in the regulation of the intestinal inflammatory response, colon length, number of goblet cells, spleen weight, and histological scores were evaluated. As expected, DSS-treated groups showed a marked reduction in colonic length compared to DSS negative groups (5.1 ± 0.1 cm *versus* 7 ± 0.07 cm) and similar results were found for goblet cell numbers (10.3 ± 0.61% *versus* 21.43 ± 0.01%) independently of the genotype (Supplementary Figure S2A, B). Remarkably, the colitis experimental groups exhibited higher spleen weights compared to healthy mice, with the Abx+DSS+ MCJ-deficient mice showing the highest spleen weights (Figure 23E). Lower histological scores were observed in the same group of mice (Abx+DSS+) (Figure 23F).

Macrophage infiltration in colonic tissue increased in mice treated with DSS compared to the healthy groups, as a response to the translocation of luminal antigens to the lamina propria (Figure 23G). After dysbiosis (Abx+), WT colitis mice presented higher macrophage infiltration than the other three groups with colitis (DSS+). Macrophage infiltration variability suggests that microbiota composition affects the recruitment of macrophages. These results confirm that microbiota disruption highly contributes to immune response and disease severity.

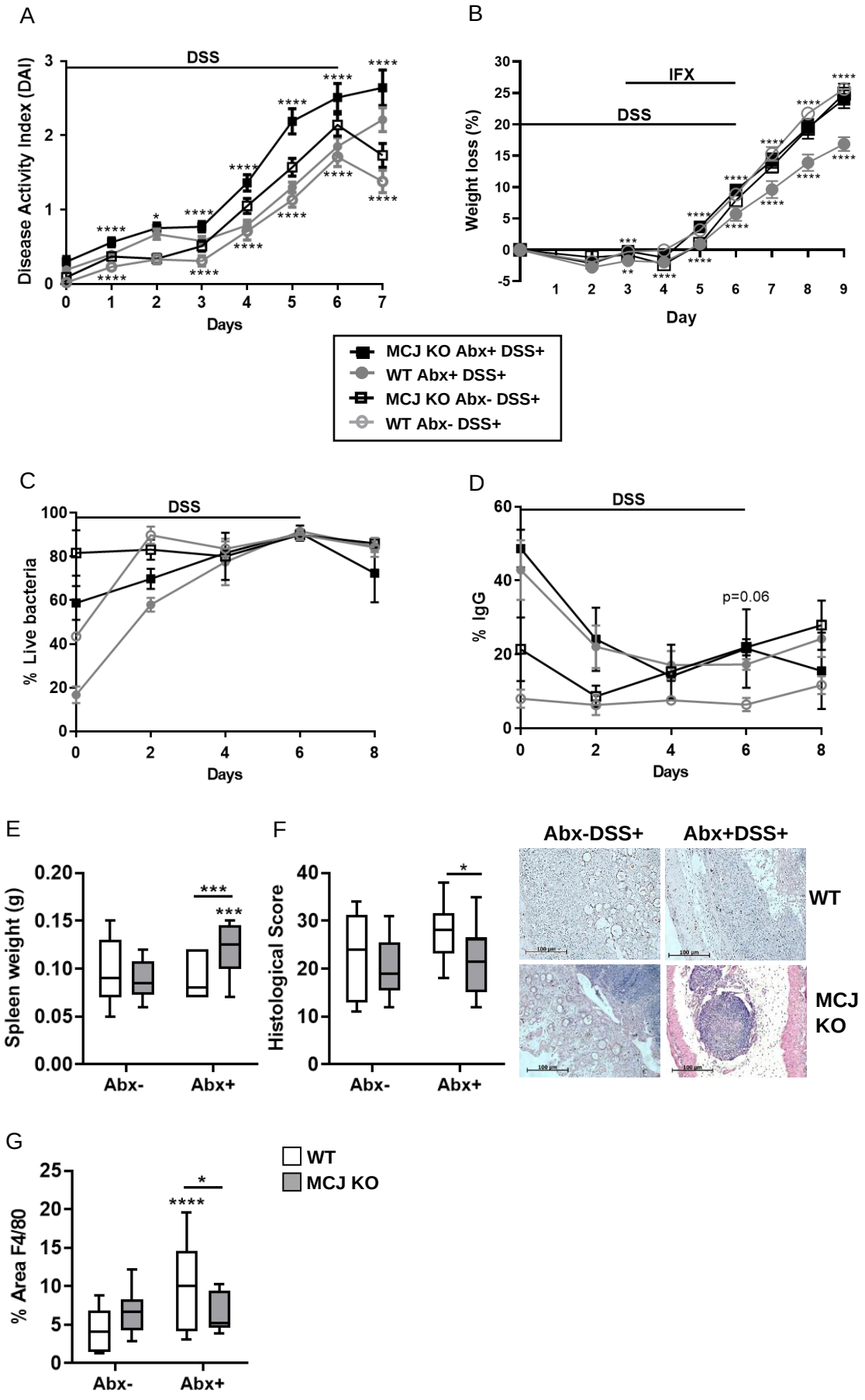
A
DSS
Disease Activity Index (DAI)
Days
B
IFX
DSS
Weight loss (%)
Day
MCJ KO Abx+ DSS+
WT Abx+ DSS+
MCJ KO Abx- DSS+
WT Abx- DSS+
C
DSS
% Live bacteria
Days
D
DSS
p=0.06
% IgG
Days
E
Spleen weight (g)
Abx-
Abx+
F
Histological Score
Abx-
Abx+
Abx-DSS+
Abx+DSS+
WT
MCJ KO
G
WT
MCJ KO
% Area F4/80
Abx-
Abx+

Figure 23. Dynamics of different types of gut dysbiosis in the progression of UC. Experimental design: antibiotic or water were administered to WT and MCJ-deficient mice one week before DSS administration which lasted 6 days. (**A**) DAI, values are expressed as means ± SEM (n=10 mice per group at minimum). (**B**) WL percentage (%) (n=14 per group at minimum). (**C**) Fecal live bacteria percentage (n=3) and (**D**) Fecal IgG-coated bacteria percentage obtained by flow cytometer (n=3). (**E**) Spleen weight (g) (minimum sample size 13 per group). (**F**) Histological scores (n=10) and H&E staining of mice colonic tissues (scale bar size, 100µm). (**G**) Quantification of infiltrated macrophages (F4/80) in colon tissue by immunohistochemistry (n=10) (%). (**A**-**D**) Grey lines indicate wild-type and black lines MCJ-deficient mice. (**E**-**G**) White boxplots indicate wild-type and grey boxplots MCJ-deficient mice. For statistical analysis two-way ANOVA was used. Only DSS+ groups are represented. In line graphs, statistical significance is shown by an asterisk or asterisks "*" above the line for antibiotic- and DSS-treated MCJ-KO (KO_Abx+DSS+) *versus* antibiotic- and DSS-treated WT (WT_Abx+DSS+) and below for antibiotic negative and DSS-treated MCJ-KO (KO_Abx-DSS+) *versus* antibiotic negative and DSS-treated WT (WT_Abx-DSS+). An asterisk or asterisks "*" above boxes *versus* control genotype (Abx+DSS+ *versus* Abx-DSS+), and an asterisk or asteriks above line *versus* different genotypes in the same experimental group. Abx: antibiotic.

2.1.3 Gene expression analysis and TACE activity at colon tissue level

Several gene expression levels related to the inflammatory output in UC were measured to study the impact of dysbiosis in MCJ-deficient mice. *Tnf, Timp3, Il1β* and *Hif1α* were upregulated in MCJ-deficient mice treated with DSS compared to WT mice under both antibiotic-induced dysbiosis (Abx+DSS+) and UC dysbiosis (Abx-DSS+) conditions (Figure 24A). Furthermore, MCJ-deficient mice presented reduced TACE activity in both groups of DSS-induced colitis. However, the previous induction of dysbiosis diminished the differences between genotypes (Figure 24B). On the other hand, *Tnfr1* and *Myd88* gene expression augmented only in colitis MCJ-deficient mice compared to WT mice without antibiotic treatment (Figure 24C). The anti-inflammatory response, as assessed by the expression of *Il10*, *Tgfβ* and its downstream canonical signaling mediator, *Smad3*, revealed an increase in MCJ-deficient mice upon treatment with DSS; however, after previous treatment with antibiotics the differences related to *Mcj* expression disappeared (Figure 24D). Our results indicate a relevant role of MCJ levels in genes regulation in response to bacterial translocation according to microbial composition in colon content.

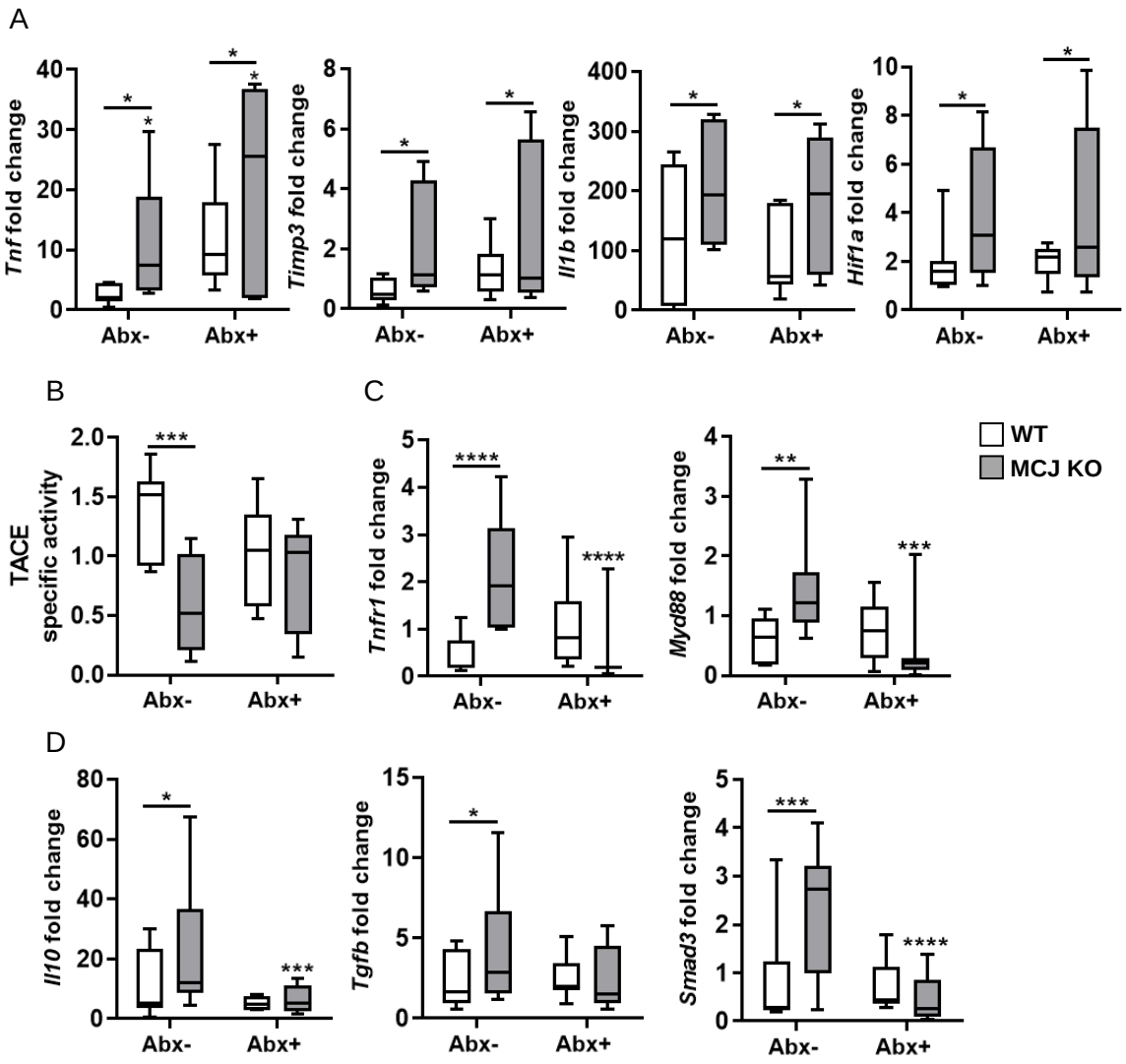

Figure 24. Evaluation of dysbiosis impact in gene expression during UC. Gene expression analysis from mice colon tissue of (**A**) *Tnf, Timp3, Il1b* and *Hif1a,* (**C**) *Tnfr1* and *Myd88,* and (**D**) *Il10*, *Tgfb* and *Smad3* shown as mean fold change of treated experimental groups *versus* untreated WT group (Abx-DSS-) (n=7 mice per group at minimum). (**B**) TACE specific activity (n=5). White boxplots indicate wild-type and grey boxplots MCJ-deficient mice. For statistical analysis two-way ANOVA was used. Only DSS+ groups are represented. An asterisk or asterisks "*" above boxes *versus* control genotype (Abx+DSS+ *versus* Abx-DSS+), and an asterisk or asterisks above line *versus* different genotypes in the same experimental group. Abx: antibiotic.

2.1.4 Composition of the host microbiome upon UC dysbiosis and antibiotic-induced dysbiosis

To assess the contribution that the microbiome-mitochondrion axis has on UC pathology, Illumina sequencing of the V3-V4 region of the *16S rRNA* gene from colonic bacterial communities was performed. Sequencing yielded a total of 2.096.426 paired and merged sequences ranging from 21.859 to 104.552 sequences per sample after quality filtering. The average good's coverage was 96.3 ± 3.9%.

Diversity indices decreased significantly (*p* value < 0.001) after antibiotic treatment in both genotypes confirming the efficacy of the treatment (Figures 25A, B). Differences were detected using NMDS plot based on non-phylogenetic Bray Curtis dissimilarity, showing changes according to both antibiotic and DSS treatment. Antibiotic-induced dysbiosis provided the strongest effect on microbial composition (e.g., Bray Curtis distances) (Figure 25C). ANOSIM indicated significant differences between the colitis-induced groups (DSS+) due to antibiotic treatment independently of *Mcj* expression (p.adj = 0.001). Differences observed due to MCJ deficiency in the colitis-induced groups (ANOSIM, p.adj = 0.01) disappeared after antibiotic-induced dysbiosis (Figures 25D, E). Results at the family level indicated a reduction in *Bifidobacteriaceae* and *Paraprevotellaceae* within the colitis-induced MCJ-deficient mouse groups, while *Ruminococcaceae*, *Lachnospiraceae*, *Rikenellaceae*, and several OTUs from Firmicutes phylum and *S24-7* family (Bacteroidetes phylum) increased (Figure 25F, Supplementary Figure S3C). The analysis of the effect of dysbiosis in MCJ-deficient colitis-induced mice indicated an increase in the presence of members of the Firmicutes phylum based on *Turicibacteraceae*, *Lachnospiraceae*, *Ruminococcaceae*, and a family that needs to be assigned and the decrease in several members from the family *Bacteroidaceae* (Figure 25G, Supplementary Figure S3D). It is noteworthy to mention that several species that were described as relevant in IBD patients such as *R. gnavus* were increased in this group of mice. PICRUSt estimated the functional profile of communities based on *16S rRNA* gene sequence (Supplementary Figures S3E, G). For detailed differences between genotypes that were not treated with DSS see Supplementary Figures S3A, B.

In summary, our results show that a previous antibiotic-induced dysbiosis diminished microbial differences associated with *Mcj* expression. This suggests a critical role of the initial microbial composition before the inflammatory phase, and points to a potential regulatory relationship from mitochondrial function of the immune cells in the intestinal inflammation environment.

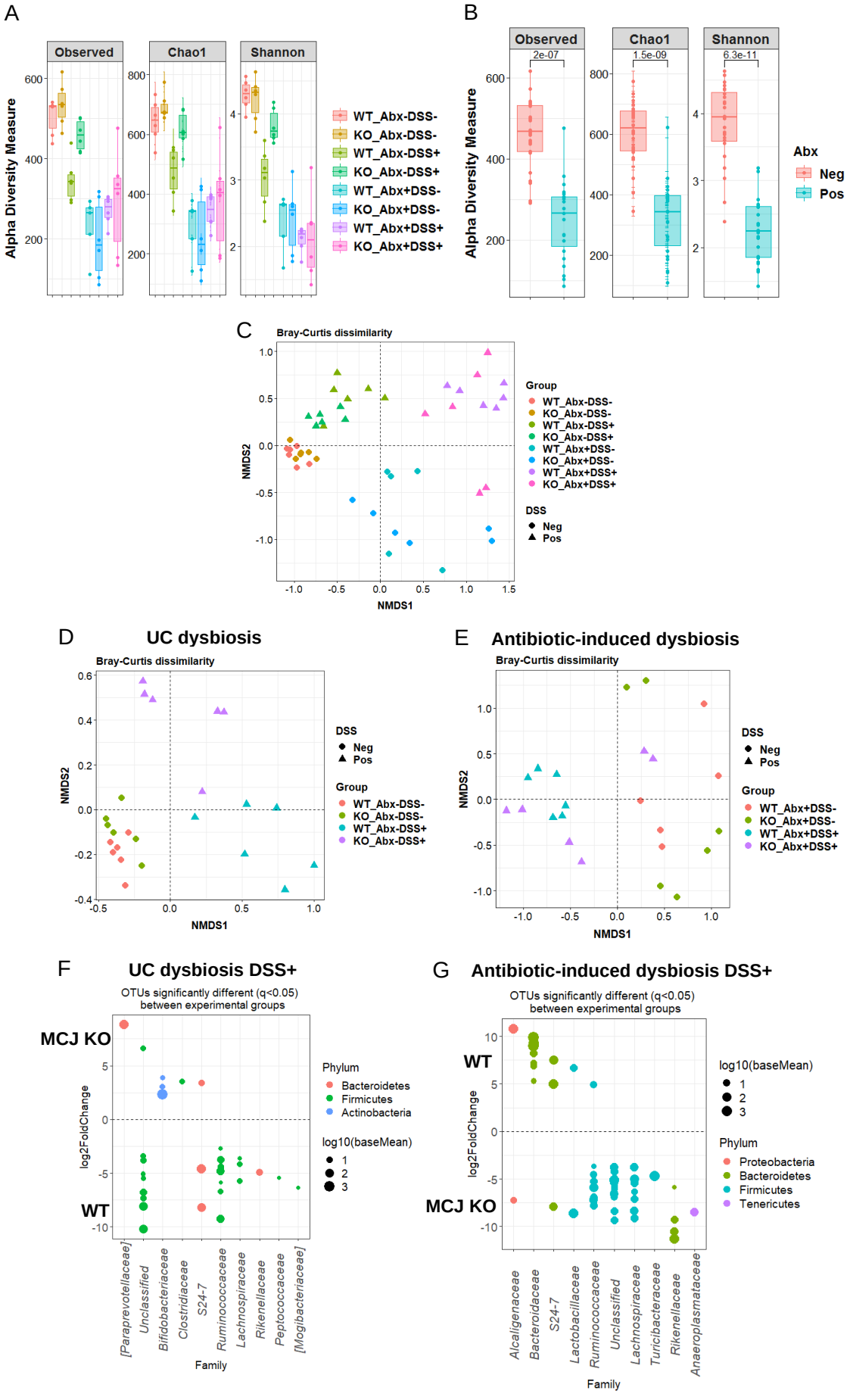
A
Observed
Chao1
Shannon
Alpha Diversity Measure
WT_Abx-DSS-
KO_Abx-DSS-
WT_Abx-DSS+
KO_Abx-DSS+
WT_Abx+DSS-
KO_Abx+DSS-
WT_Abx+DSS+
KO_Abx+DSS+
B
2e-07
1.5e-09
6.3e-11
Abx
Neg
Pos
C
Bray-Curtis dissimilarity
NMDS1
NMDS2
Group
DSS
D
UC dysbiosis
E
Antibiotic-induced dysbiosis
F
UC dysbiosis DSS+
OTUs significantly different (q<0.05)
between experimental groups
MCJ KO
WT
log2FoldChange
Phylum
Bacteroidetes
Firmicutes
Actinobacteria
log10(baseMean)
Family
[Paraprevotellaceae]
Unclassified
Bifidobacteriaceae
Clostridiaceae
S24-7
Ruminococcaceae
Lachnospiraceae
Rikenellaceae
Peptococcaceae
[Mogibacteriaceae]
G
Antibiotic-induced dysbiosis DSS+
Proteobacteria
Tenericutes
Alcaligenaceae
Bacteroidaceae
Lactobacillaceae
Turicibacteraceae
Anaeroplasmataceae

Figure 25. Composition of host microbiome in antibiotic-induced dysbiosis prior to colitis induction and UC derived dysbiosis. Alpha diversity analyses: total observed taxonomic units, Chao1 and Shannon diversity indices showing (**A**) all experimental groups and (**B**) antibiotic negative and positive groups. In (**B**) statistical analyses were performed using the nonparametric Wilcoxon rank sum test. (**C**) NMDS plot of bacterial beta-diversity based on Bray-Curtis dissimilarities presenting all experimental groups. ANOSIM (p.adj = 0.001) reveals differences between Abx-DSS+ and Abx+DSS+ groups independently of the genotype. (**D**) NMDS plot without antibiotic administration (UC dysbiosis) showing significant differences between genotypes within Abx-DSS+ group (ANOSIM, p.adj = 0.01). (**E**) NMDS plot displaying antibiotic-induced dysbiosis groups. Representation of OTUs that significantly (p.adj < 0.05) differ in colon content at family level among (**F**) WT and MCJ-deficient Abx-DSS+, and (**G**) WT and MCJ-deficient Abx+DSS+ groups. Each point represents a single OTU colored by phylum and grouped by taxonomic family, and point´s size reflect the mean abundance of the sequenced data. Abx: antibiotic; KO: MCJ KO.

2.1.5 Correlation between bacterial community and macrophages gene expression in the colon under experimentally-induced colitis

We then sought to find correlations between genes expressed in colon macrophages and specific microbial OTUs. Figure 26 shows the 50 strongest correlations between genes differentially expressed due to MCJ deficiency in macrophages infiltrated during colon inflammation and OTUs present in the 4 experimental groups that were not previously treated with antibiotics (Abx-DSS- and Abx-DSS+). Those included associations between *R. gnavus,* often increased with disease activity*,* and *Cst7* that may play a role in immune regulation through the hematopoietic system*. A. muciniphila* presence*,* often regarded as an immunomodulator*,* correlated with *Jak2* expression. JAK2 is involved in the production of key pro-inflammatory cytokines and consequently, JAK inhibitors are currently being investigated as therapeutic agents for UC*. Enterococcus* abundance, which is associated with disease severity, correlated with the expression levels of *Lsp1*, a gene involved in neutrophil transmigration. Different OTUs belonging to the genus *Bacteroides*, unbalanced in IBD patients, were linked to *Ly6c1* (marker of resident macrophages) and *Il1b* gene expression. On the other hand, the Bacteroidales *S24-7* family showed a negative correlation with *Il10* expression, which is related to gut homeostasis. These correlations suggest that the lack of MCJ provides the environmental conditions for specific bacteria that may act as immunomodulators contributing to UC severity and the response to specific treatments, such as anti-TNF therapy.

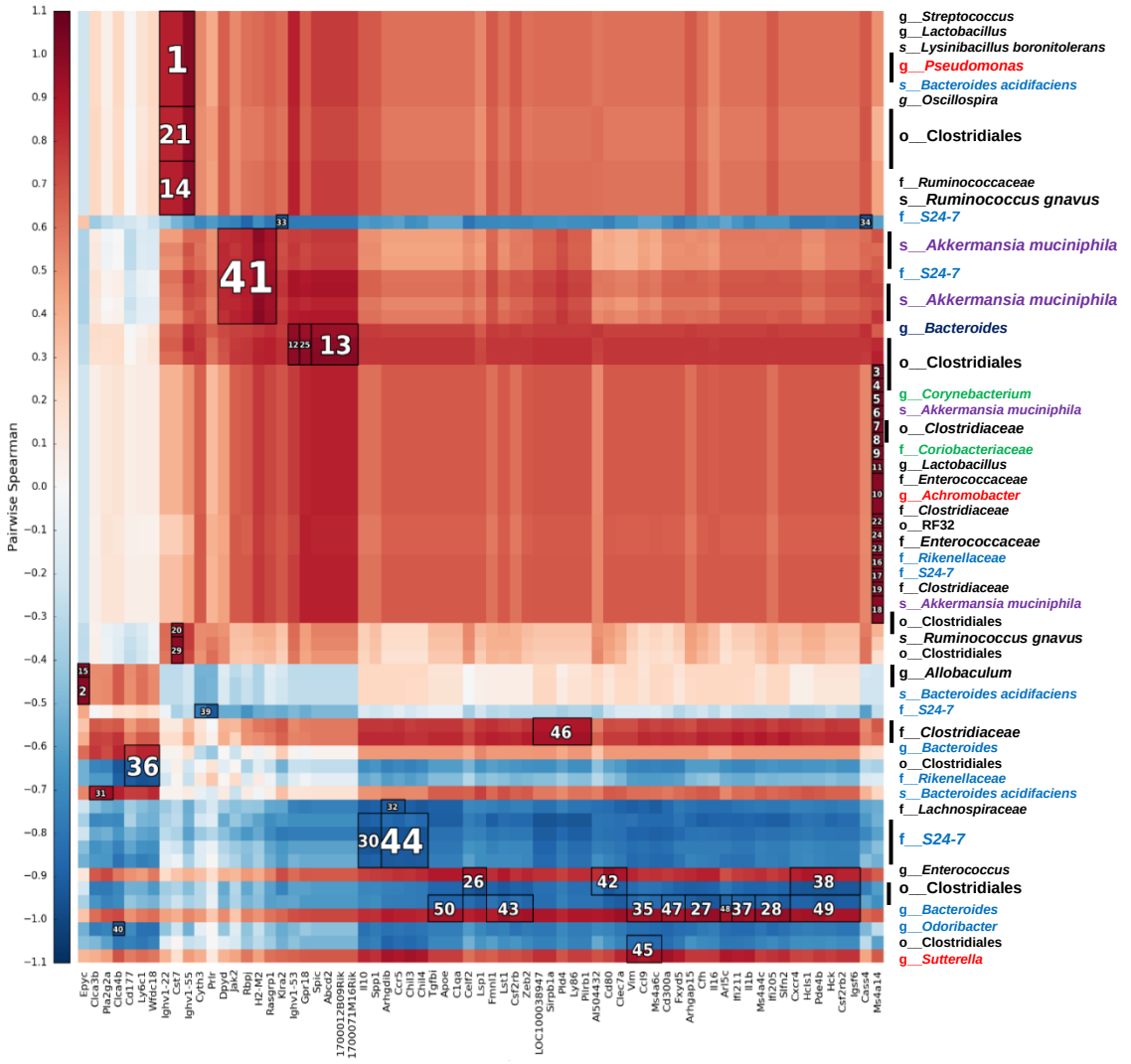

Figure 26. Heatmap of Spearman´s rank correlation coefficients. Bacterial abundances from the 4 experimental groups that were not treated with antibiotic and genes modified by the level of *Mcj* in colon macrophages upon intestinal inflammation (Abx-DSS+) were used. To find associations hierarchical all against all association (HAIIA) was performed. *A. muciniphila* correlates with *Jak2* and *R. gnavus* with *Cst7*. The numbers indicate the highest correlation between bacteria and gene expression, being number 1 the highest correlation. Red color illustrates positive correlation and blue negative. In the x axis each column shows a different gene and in the y axis each row shows different bacterial species; Firmicutes (Black font), Proteobacteria (Red), Bacteroidetes (Blue), Actinobacteria (Green) and Verrucomicrobia (Purple).

2.1.6 Localization of MCJ in colon from IBD patients

We first determined whether MCJ was expressed in inflamed colon tissue from IBD patients by immunofluorescence staining. Figure 27A shows that MCJ (in red) was readily detected in inflamed colon tissue. In order to assess MCJ location, the transmembrane scavenger receptor CD163 (green) associated to macrophages was used. The signal corresponding to MCJ colocalized with CD163 in active IBD patients (shown in yellow). Futhermore, MCJ and CD163 colocalization in healthy adjacent tissue was used as a control. Therefore, the impact of MCJ in IBD patients seems to be primarily associated to macrophages.

2.1.7 Transcriptional analysis of colon macrophages from MCJ-deficient mouse model

In order to reduce heterogeneity shown in human IBD samples, in this study a mouse model with MCJ deficiency was used. For this purpose, we examined the role of MCJ in the immune response and we delved into its relationship with microbial composition by performing a transcriptome analysis of colon macrophages in contact with two types of dysbiosis (UC and antibiotic-induced). PCA of the transcriptomic results showed changes according to both, antibiotic and colitis (Figure 27B). Antibiotic-induced dysbiosis provided the highest effect on macrophage transcriptional landscape. Clustering variation observed due to MCJ deficiency during colitis (Abx-DSS+) disappeared after the antibiotic treatment (Abx+DSS+). The analysis of the 50 most regulated genes under DSS-induced colitis without previous dysbiosis (Abx-DSS+) displayed different patterns of expression associated with distinct MCJ levels. In particular, MCJ deficiency in macrophages showed 305 upregulated genes. Among them, several confirmed susceptibility-related genes for UC such as *Irf5, Tnfrsf9, Fcgr2b Slc11a1, Itgal, Gpr65, Cd40,* and *Lsp1*, suggesting a relevant role of mitochondria dysfunction in immune cells such as macrophages during the course of the disease.

The HOMER package identified a set of transcription factors putatively responsible for the expression changes in macrophages from DSS-induced colitis animals (Abx-DSS+). The analysis of the genes upregulated in MCJ-deficient macrophages compared to WT mice identified several transcription factors (Figure 27C, Table 4). Two of them (*Spib* and *Elf5*) are related to *Fcgr2b* expression, *Runx* seems to be involved in *Irf5* expression and *Erg* in the expression of *Slc11a1* and *Tnfrsf9*. Moreover, *Elf5* and *Spib* possess motifs that regulate *Il1b* expression and *Erg* showed a motif that regulates the expression of *Tnf*, *Il10* and *Tgfbi*. Also, *Erg* and *Runx* may regulate *Cxcl3* expression

and therefore are involved in leucocyte recruitment. In order to discern whether transcriptional patterns associated with mitochondrial dysfunction in murine colon macrophages are also related to the disease in humans, UC transcriptomes from human rectal samples were compared to experimental colitis macrophage transcriptomes. Out of the 305 upregulated genes in this group of macrophages compared to DSS+ WT mice, 183 were also found overexpressed in the human UC cohorts (Figure 27D, Table 5), suggesting a critical role for mitochondrial function during disease progression.

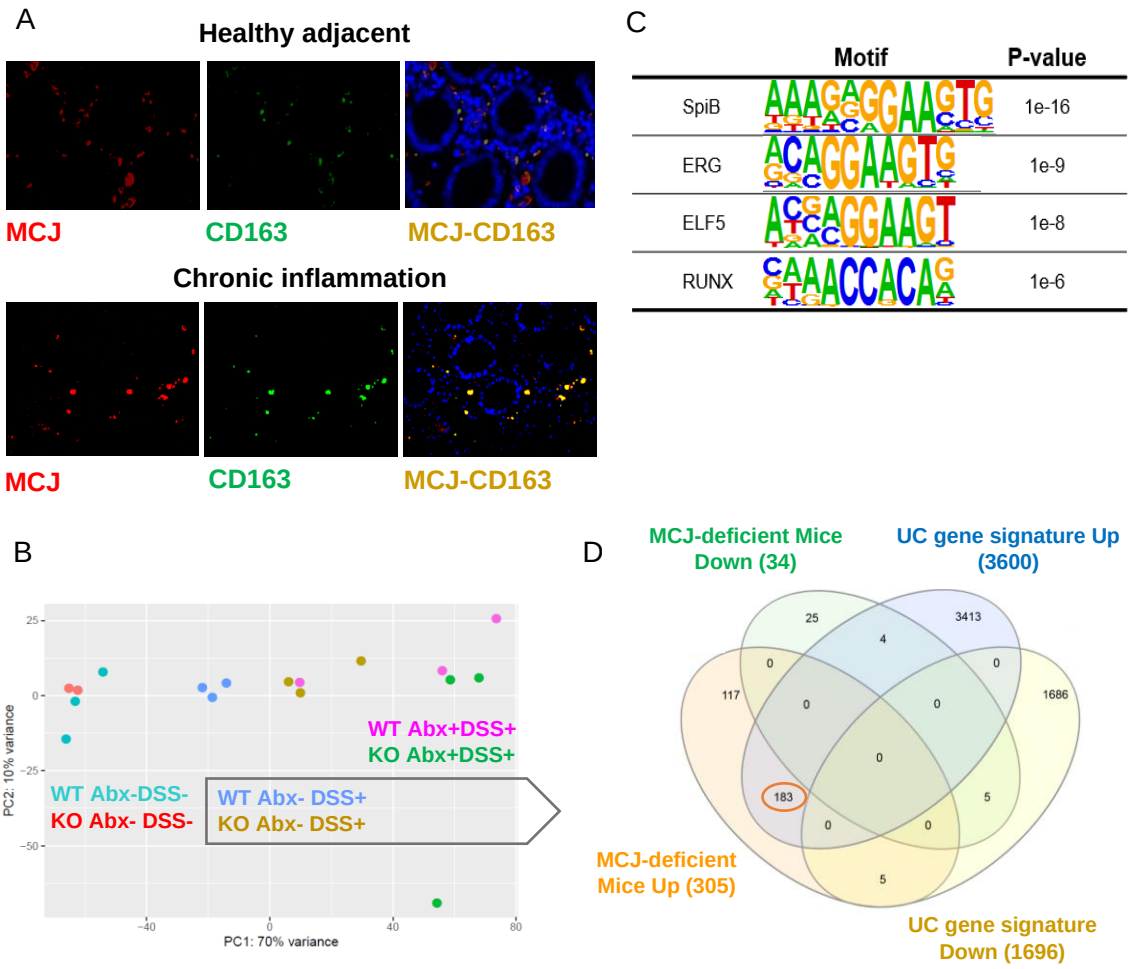

Figure 27. Transcriptomic analysis of intestinal tissue macrophages. (**A**) Immunofluorescence of MCJ (red) and CD163 (green) in inflamed colon tissue and healthy adjacent colon tissue from IBD patients. Colocalization is represented in yellow. (**B**) PCA showing differences between WT and MCJ-deficient DSS positive colon macrophages transcriptomes (Abx-DSS+). (**C**) HOMER identified several transcription factors enriched in DSS-treated MCJ-deficient colon macrophages (Abx-DSS+). (**D**) Venn diagram representing 339 differentially expressed genes found in colon macrophages due to MCJ deficiency and a human core rectal UC gene expression signature consisting of 5296 genes (Haberman et al., 2019). Out of 305 genes upregulated in MCJ-deficient colon macrophages, 183 were shared with the human UC gene signature. Abx: antibiotic; KO: MCJ KO.

Table 4. Transcription factors and its target genes. Genes upregulated in colon macrophages from MCJ-deficient mice treated with DSS compared to colitis WT that are putatively regulated by the transcription factors *Spib*, *Erg*, *Elf5* and *Runx.* Candidate genes associated to IBD risk are marked in bold.

Spib		***Erg***			***Elf5***		***Runx***	
AB124611	*Scimp*	*AB124611*	*Dok2*	*Ms4a4c*	*Alox5ap*	*Lcp2*	*1700012B09Rik*	*Scimp*
Alox5ap	*Slc15a3*	*Abcg3*	*Dpep2*	*Ms4a6d*	*Bcl2a1a*	*Lilra6*	*AB124611*	*Siglecf*
Ang4	*Spp1*	*Adgre4*	*Dram1*	*Msn*	*Bcl2a1b*	*Lrrc25*	*Adgre4*	*Spp1*
Arhgef6	*Tfec*	*Adgre5*	*Emilin2*	*Msr1*	*Bcl2a1d*	*Lyz1*	*Aoah*	*Srgn*
Bcl2a1a	*Tyrobp*	*Alox5ap*	*Evi2b*	*Myo1g*	*C1qa*	*Lyz2*	*Arhgap15*	*Tfec*
Bcl2a1b	*Vav1*	*Ang4*	*F13a1*	*Napsa*	*C1qb*	*Mcemp1*	*C1qc*	*Tnfsf1*
Bcl2a1d		*Aoah*	*Fcer1g*	*Ncf2*	*C1qc*	*Mmp13*	***Ccl3***	*Tyrobp*
C1qa		*Arg1*	***Fcgr3***	*Ncf4*	*Ccl3*	*Ms4a6d*	*Ccr1*	*Was*
C1qb		*Arhgap15*	*Fcrls*	*Nckap1l*	*Ccl4*	*Msn*	*Cd300c2*	
C1qc		*Arhgdib*	*Fmnl1*	*Pde4b*	*Ccr3*	*Msr1*	*Cd300lf*	
Ccr2		*Arhgef6*	*Fyb*	*Pik3ap1*	*Cd274*	*Myo1g*	***Cd40***	
Ccr5		*Bcl2a1a*	*Gm9733*	*Pik3r5*	*Cd300lf*	*Ncf2*	*Cd84*	
Cd300lf		*Bcl2a1b*	*Gng2*	*Pilra*	*Cd48*	*Ncf4*	*Cfh*	
Cd53		*Bcl2a1d*	*Gpr132*	*Pilrb1*	*Cd52*	*Nckap1l*	*Clec4a1*	
Cd84		*C1qb*	*Gpr18*	*Pilrb2*	*Cfp*	*Nrg1*	*Clec4e*	
Cfp		*C1qc*	*Gpr65*	*Plau*	*Chil3*	*Nxpe5*	*Clec5a*	
Chil3		*C3ar1*	*Gpr84*	*Pld4*	*Chil4*	*Pik3ap1*	***Cx3cr1***	
Clec4e		*Ccl4*	*Havcr2*	*Prg2*	*Clec4d*	*Pik3r5*	***Cxcl3***	
Clec5a		*Ccr1*	*Hcls1*	*Pstpip1*	*Clec4e*	*Pilra*	*Cybb*	
Csf2ra		*Ccr2*	*Hic1*	*Ptafr*	*Clec4n*	*Pilrb1*	*Cytip*	
Cst7		*Ccr3*	*Ifi204*	*Ptprc*	*Clec7a*	*Pilrb2*	*Dok2*	
Dcstamp		*Cd14*	*Ifi207*	*Retnlg*	*Csf2ra*	*Pira1*	***Fcer1g***	
Dok2		*Cd274*	*Ifi209*	*Rgs1*	*Csf2rb*	*Pira2*	*Fmnl1*	
Dpep2		*Cd300c2*	*Ifi211*	*Rsad2*	*Csf2rb2*	*Pirb*	*Gm9733*	
Fcgr2b		*Cd300lf*	***Il10***	*Runx3*	*Cst7*	*Pld4*	*Gpr132*	
Fcrls		*Cd4*	*Il1a*	*S100a4*	*Cxcl2*	*Prg2*	*Gpr18*	
Gfi1b		*Cd40*	*Il1rl1*	*Scimp*	*Cybb*	*Ptprc*	*Havcr2*	
Gm14548		*Cd44*	*Itgal*	*Serpinb*	*Emilin2*	*Rab7b*	*Hp*	
Gng2		*Cd48*	*Itgam*	*Slc11a1*	*Evi2b*	*Rsad2*	*Ifi204*	
Havcr2		*Cd53*	*Itgb2*	*Slc15a3*	*F13a1*	*S100a4*	*Ifi205*	
Hcls1		*Cd83*	*Itgb7*	*Slfn2*	***Fcgr2b***	*Scimp*	*Ifi207*	
Igsf6		*Chil3*	***Jak2***	*Spi1*	*Fcrls*	*Slfn2*	*Ifi211*	
Il1b		*Chil4*	*Klra2*	*Spic*	*Fgr*	*Spi1*	***Irf5***	
Itgb7		*Clec4a3*	*Lair1*	*Spp1*	*Gm14548*	*Spic*	*Itgax*	
Laptm5		*Clec4e*	*Laptm5*	*Srgn*	*Gng2*	*Spp1*	*Itgb2*	
Lilra6		*Clec4n*	*Lcp2*	*Tarm1*	*Gpr132*	*Trf*	*Laptm5*	
Ms4a6d		*Clec5a*	*Lilr4b*	*Tfec*	*Gpr65*	*Tyrobp*	*Lgmn*	
Myo1g		*Clec7a*	*Lpcat2*	***Tgfbi***	*H2-M2*	*Vav1*	*Lyz2*	
Ncf1		*Csf2ra*	*Lrrc25*	*Tiparp*	*Havcr2*	*Was*	*Milr1*	
Ncf2		*Cst7*	*Ly86*	*Tlr13*	*Hcls1*		*Mmp13*	
Nckap1l		***Cx3cr1***	*Lyve1*	*Tlr7*	*Ifi204*		*Napsa*	
Pik3ap1		*Cxcl2*	*Lyz1*	***Tnf***	*Ifi207*		***Osm***	
Pira1		***Cxcl3***	*Lyz2*	***Tnfrsf9***	*Ifi209*		*Pilra*	
Pira2		*Cyp4f18*	*Malt1*	*Tnfsf14*	*Ifi211*		*Pilrb1*	
Pirb		*Cyth3*	*Map4k4*	***Trem1***	***Il1b***		*Pilrb2*	
Pld4		*Cyth4*	*Mcemp1*	*Trf*	*Itgb2*		*Pirb*	
Plek		*Cytip*	*Mef2a*	*Tyrobp*	*Itgb7*		*Pstpip2*	
Rasgrp1		*Dcstamp*	*Mefv*	*Vav1*	*Klra2*		*Rgs1*	
S100a4		*Dock2*	*Milr1*	*Was*	*Laptm5*		*Runx3*	

Table 5. Comparison of human ulcerative colitis mucosal transcriptomes with MCJ-deficient and inflamed murine gut macrophages transcriptomes. Upregulated and downregulated genes are detailed below. Candidate genes associated to ulcerative colitis risk are marked in bold.

Mice Down	Mice Up		Mice & Human Up			Human & Mice Down
25	117		183			5
Clca4b	*1700071m16ri*	*Ifi207*	*Adgre1*	*Dpyd*	*Myo1g*	*Cd177*
Clca3b	*1700012b09rik*	*Ifi209*	*Adam8*	*Dram1*	*Napsa*	*Hspa1b*
Cphx1	*6530402f18rik*	*Ifi211*	*Ahr*	*Emb*	*Ncf1*	*Lsr*
Cphx2	*Ab124611*	*Ifnb1*	*Aif1*	*Emilin2*	*Ncf2*	*S100a14*
Cphx3	*Abcd2*	*Ighv1-22*	***Alox15***	*Emp3*	*Ncf4*	*Zg16*
Dnajc15	*Abcg3*	*Ighv1-53*	*Alox5ap*	*Evi2a*	*Nckap1l*	
Epyc	*Adamdec1*	*Ighv1-55*	*Anxa6*	*Evi2b*	*Ninj1*	
Gm5414	*Adgre4*	*Ighv1-64*	*Apoe*	*F5*	*Npl*	
Gm9780	*Adgre5*	*Igkv6-14*	*Arhgap15*	*Fcer1g*	*Nrg1*	
Hoxd13	*Adssl1*	*Klra2*	*Arhgdib*	***Fcgr2b***	*Olr1*	
Hspa1a	*Ai504432*	*Lgmn*	*Arhgef6*	***Fgr***	***Osm***	
Hsph1	*Ai662270*	*Lilr4b*	*Arl4c*	*Fmnl1*	*P2rx1*	
Klrd1	*Ang4*	*Lilrb4a*	*Basp1*	*Fpr2*	*Pde4b*	
Ly6a	*Antxr2*	*Loc10003894*	*C1qa*	*Fxyd5*	*Pik3ap1*	
Ly6c1	*Aoah*	*Lpcat2*	*C1qb*	*Fyb*	*Pik3r5*	
Ly6i	*Arg1*	*Lrrc8d*	*C1qc*	*Glipr1*	*Pilra*	
Na	*Arl5c*	*Lyve1*	*C3ar1*	*Gpr132*	*Pim1*	
Plac9a	*Bcl2a1a*	*Lyz1*	*Cass4*	*Gpr18*	*Pla2g7*	
Plac9b	*Bcl2a1b*	*Lyz2*	*Ccl3*	*Gpr65*	*Plau*	
S100a16	*Bcl2a1d*	*Mef2a*	*Ccl4*	*Gpr84*	*Pld4*	
Sfrp4	*Bcl2l11*	*Mmp13*	*Ccr1*	*Gsap*	*Plek*	
Slc5a4b	*Ccl9*	*Ms4a4c*	*Ccr2*	*Havcr2*	*Pstpip1*	
Snca	*Ccrl2*	*Ms4a6c*	*Ccr3*	*Hck*	*Pstpip2*	
Snrnp25	***Cd14***	*Ms4a6d*	*Ccr5*	*Hcls1*	*Ptafr*	
Wfdc18	*Cd300c2*	*Msr1*	*Cd244*	*Hic1*	*Ptgs2*	
	Celf2	*Nxpe5*	*Cd274*	*Hp*	*Ptprc*	
	Chil3	*Ofd1*	*Cd300a*	*Igsf6*	*Rab7b*	
	Chil4	*Pilrb1*	*Cd300lf*	***Il10***	*Rab8b*	
	Chil6	*Pilrb2*	*Cd4*	*Il10ra*	*Rac2*	
	Clec4a1	*Pira1*	***Cd40***	*Il16*	*Rasgrp1*	
	Clec4a3	*Pira2*	*Cd44*	*Il1a*	*Rassf4*	
	Clec4n	*Pira6*	*Cd48*	***Il1b***	*Rsad2*	
	Csf2rb2	*Pirb*	*Cd52*	*Il1rl1*	*Runx3*	
	Cx3cr1	*Prg2*	*Cd53*	*Irf5*	*S100a4*	
	Cxcr4	*Rab44*	*Cd68*	*Itga4*	*Scimp*	
	Cyp4f18	*Rap1b*	*Cd80*	*Itgal*	*Serpinb8*	
	Cyth3	*Rbpj*	*Cd83*	*Itgam*	*Sirpa*	
	Dcstamp	*Retnlg*	*Cd84*	*Itgax*	*Sla*	
	Dennd4a	*Rgs1*	*Cd86*	*Itgb2*	*Slc11a1*	
	F10	*Rgs10*	*Cdk5r1*	*Itgb7*	*Slc15a3*	
	F13a1	*Rgs2*	*Cfh*	***Jak2***	*Spi1*	
	Fcgr1	*Ric1*	*Cfp*	*Lair1*	*Spp1*	
	Fcgr3	*Serpinb2*	*Clec4d*	*Laptm5*	*Srgn*	
	Fcrls	*Siglecf*	*Clec4e*	*Lcp1*	*Tfec*	
	Fem1c	*Sirpb1a*	*Clec5a*	*Lcp2*	*Tgfbi*	
	Gfi1b	*Slfn2*	*Clec7a*	*Lilra6*	*Tgm2*	
	Gfod1	*Smim3*	*Coro1a*	*Limd2*	*Tm6sf1*	
	Gm10693	*Spic*	*Csf1r*	*Lrrc25*	***Tnf***	
	Gm13212	*Tarm1*	*Csf2ra*	*Lsp1*	***Tnfrsf9***	
	Gm14548	*Tgfbr1*	*Csf2rb*	*Lst1*	*Tnfsf14*	
	Gm15448	*Tiparp*	*Cst7*	*Ly86*	*Traf1*	
	Gm21190	*Tlr13*	*Cxcl2*	*Malt1*	***Trem1***	
	Gm6377	*Tlr7*	***Cxcl3***	*Map4k4*	*Trps1*	
	Gm9733	*Trem2*	*Cybb*	*Mcemp1*	*Tubb6*	
	Gng2	*Treml4*	*Cyth4*	*Mefv*	*Tyrobp*	
	H2-Ab1	*Trf*	*Cytip*	*Milr1*	*Vav1*	
	H2-M2		*Dennd5a*	*Mmp19*	*Vcam1*	
	Hmox1		*Dmxl2*	*Mpeg1*	*Vcan*	
	Id2		*Dock2*	*Ms4a14*	*Vim*	
	Ifi204		*Dok2*	*Ms4a4a*	*Was*	
	Ifi205		*Dpep2*	*Msn*	*Zeb2*	

Functional annotation enrichment analysis of the differentially regulated genes by MCJ deficiency using ToppGene, ToppCluster, and ClueGO mapped groups of related genes to immunological processes. Overview of the ClueGo-derived immune system related pathways (Figures 28A, B) comparing gene expression based on MCJ expression during DSS-induced colitis (Abx-DSS+) showed 46% enrichment for the FC-gamma receptor signalling pathway, followed by myeloid cell (13,1%), macrophage (6,7%) and dendritic cell activation (6,7%), regulation of adaptive immune response (6.7%) and leukocyte differentiation (6,7%), and downregulated chaperone cofactor-dependent refolding (50%) and regulation of microtubule polymerization (50%) pathways in DSS-treated MCJ-deficient animals compared to DSS-treated controls. *P* values for the top specific biological processes and pathways were obtained as an output from ToppGene and more detailed ToppCluster pathways analysis output is shown in figure 28C for the upregulated and figure 28D for the downregulated genes related to immunological and biological processes. MCJ-deficient mice presented higher immune system activation and therefore, higher production of cytokines and chemokines, and higher transendothelial migration of leukocytes. The validity of our analysis was phenotypically confirmed by the negative regulation of the mitochondrial electron transport in MCJ deficient mice. Importantly, IgA production was upregulated in MCJ-deficient colitis mice.

A

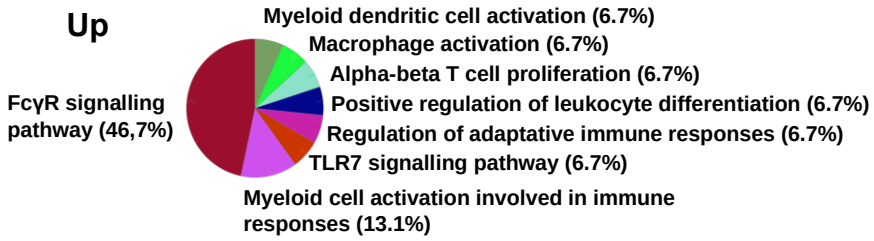

B

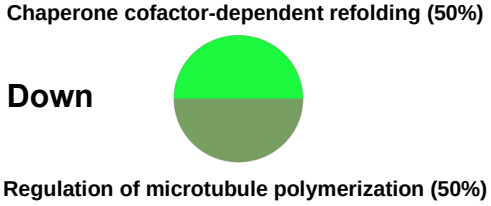

C

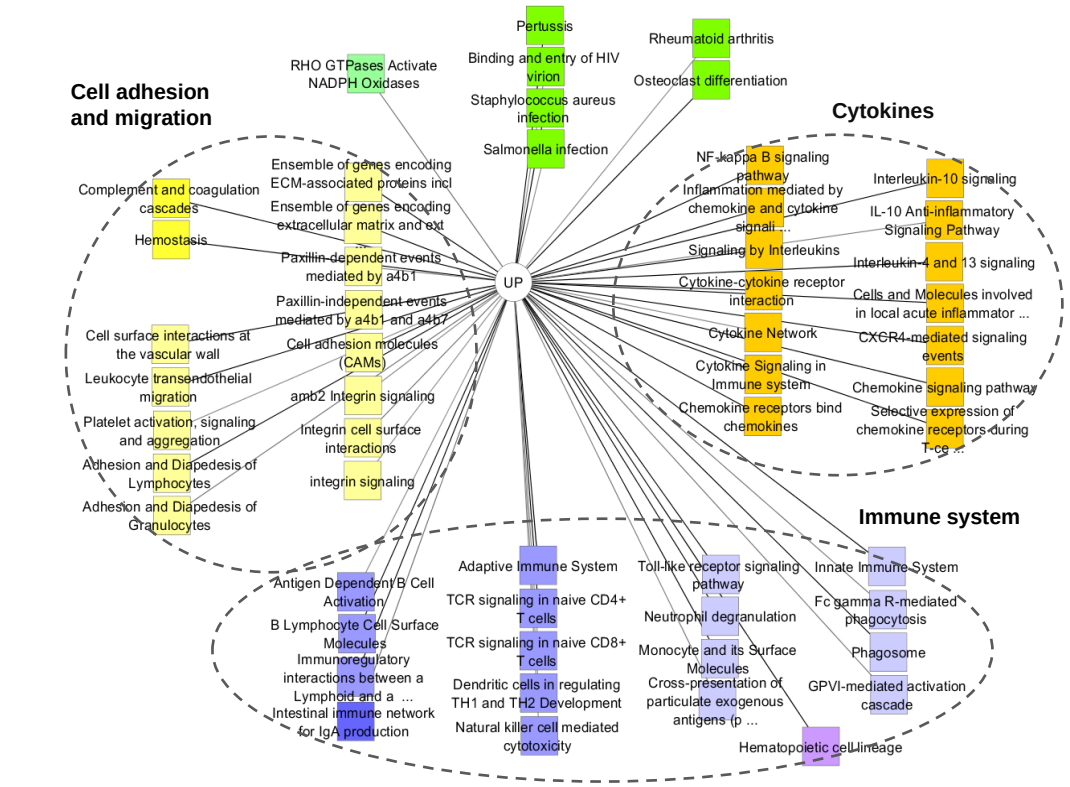

D

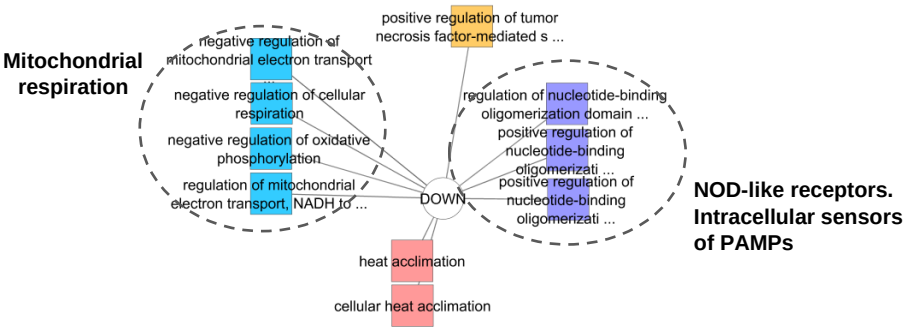

Figure 28. Functional annotation enrichment analysis of inflamed intestinal macrophages according to MCJ levels. RNA-Seq data analysis shows 305 upregulated and 34 downregulated genes in MCJ-deficient mice treated with DSS compared to WT colitis mice (Abx-DSS+) (FDR<0.05 and FC ≥ 1.5). ClueGO charts related to immunological function reveals (**A**) upregulation of FCγR signalling pathway (46,7%) and (**B**) downregulation of chaperone cofactor refolding (50%) and microtubule polymerization (50%) in MCJ-deficient colitis mice compared to WT colitis (Log2>2, p<0.05). Detailed functional annotation enrichment analyses of (**C**) 305 upregulated and (**D**) 34 downregulated genes in MCJ-deficient colitis mice using ToppGene, ToppCluster and Cytoscape are represented. (**C**) Pathways related to upregulated genes; immune system (purple), cytokines (orange), cell adhesion and migration (yellow) and other pathways (green). (**D**) Biological processes enriched by downregulated genes; mitochondrial respiration (blue), cytokines (orange), NOD-like receptors, the intracellular sensors of PAMPS (purple) and heat acclimation (red). Abx: antibiotic.

We then analyzed whether a drastic perturbation of microbial composition (antibiotic-induced dysbiosis) influences transcriptional macrophage response in inflamed tissue (Abx+DSS+). In these conditions, only 58 out of 314 genes (up- or down-regulated due to MCJ deficiency) were shared with inflamed macrophages that were not treated with antibiotics (Abx-DSS+ *vs* Abx-DSS+). ClueGO charts related to upregulated immunological processes revealed higher macrophage activation (37%), myeloid cell development (27%), and positive regulation of myeloid leukocyte mediated immunity (18%), complement activation, and T cell migration (9%) and lower antigen processing via MHCII (31%), humoral immunity by circulating immunoglobulins (21%), and B cell receptor signalling pathway (16%) in MCJ-deficient mice treated with antibiotic and DSS (Abx+DSS+) compared to WT animals (Abx+DSS+) (Figures 29A, B). *P* values for the top specific biological processes and pathways were obtained as an output from ToppGene. ToppCluster analysis represented by a cytoscape node chart showed upregulated oxidative stress, hormone levels, inflammatory response, response to bacterium and electrolytes homeostasis (Figure 29C). Among the pathways related to downregulated genes, included leukocyte migration, adaptive response, complement activation and the purinergic nucleotide receptor signalling pathway (Figure 29D).

A

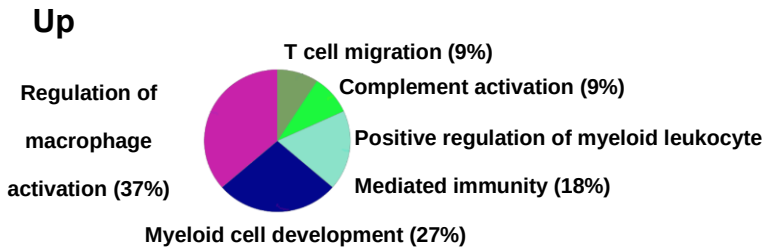

B

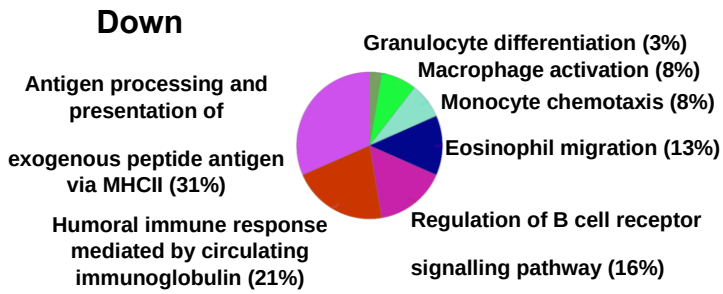

C

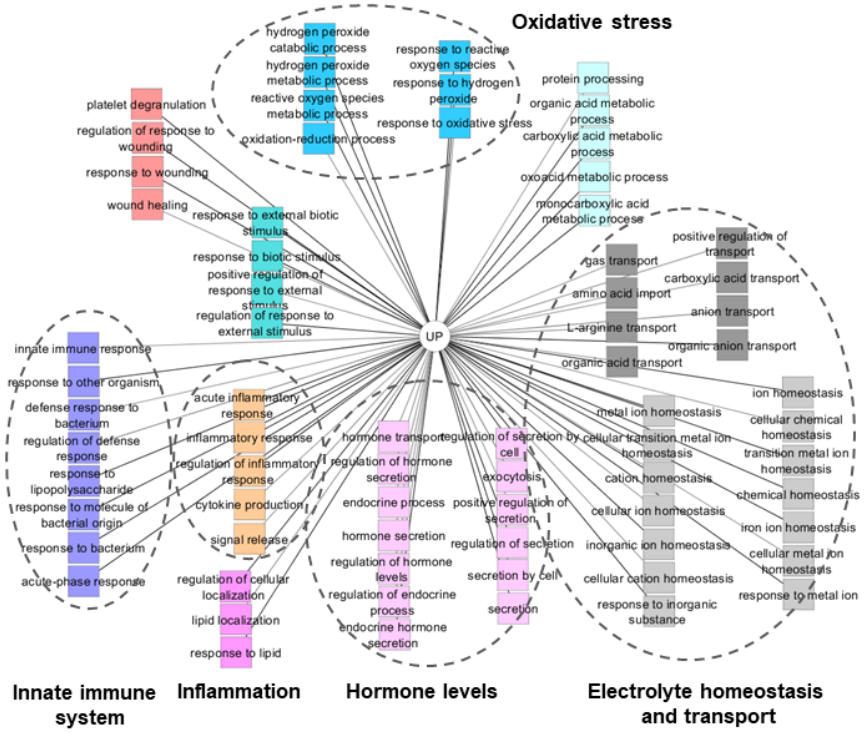

D

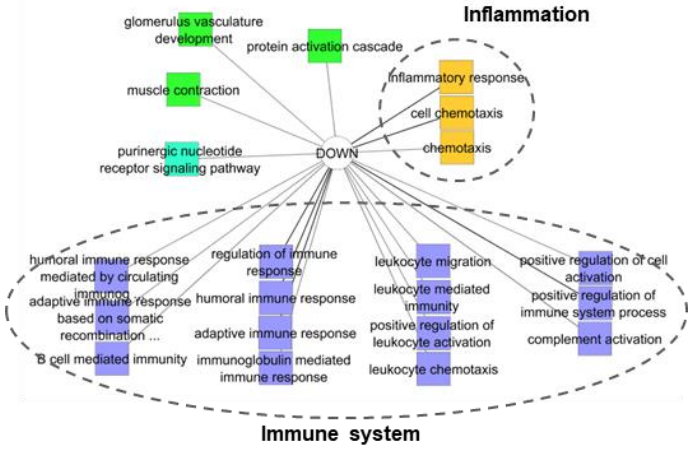

Figure 29. Functional annotation enrichment analysis of inflamed intestinal macrophages exposed to antibiotic-induced dysbiosis. RNA-seq data analysis shows 150 upregulated and 171 downregulated genes in MCJ-deficient mice with antibiotic-induced dysbiosis and DSS compared to WT mice (Abx+DSS+) (FDR<0.05 and FC ≥ 1.5). ClueGO charts related to immunological function reveals (**A**) upregulation of macrophage activation (37%) and myeloid cell development (27%), and (**B**) downregulation of antigen processing via MHCII (31%), humoral immunity by immunoglobulins (21%) and B cell receptor signalling pathway (16%) in dysbiotic and colitis MCJ-deficient mice compared to WT mice (p value < 0.05). Detailed functional annotation enrichment analyses of (**C**) 150 upregulated and (**D**) 171 downregulated genes in dysbiotic MCJ-deficient colitis mice using ToppGene, ToppCluster, and Cytoscape are represented. (**C**) Biological processes related to upregulated genes; immune system (purple), inflammatory response (orange), hormone levels (pink), electrolyte homeostasis and transport (grey), oxidative stress (dark blue), metabolic processes (light blue), response to wound healing (red) and response to biotic stimulus (turquoise). (**D**) Biological processes related to downregulated genes; inflammatory response (orange), immune system (purple) and other isolated processes in green and turquoise. Abx: antibiotic.

2.1.8 MCJ deficiency response to anti-TNF agents

A subset of genes obtained from transcriptional analyses were associated with mitochondrial dysfunction. Some of them were also linked to treatment response and shifts in microbial composition. In this regard, the 305 upregulated genes due to MCJ deficiency in macrophages from experimental colitis mice were compared to the list of genes proposed to identify patients that are refractory to TNF blockade (West et al., 2017) and corticosteroids (Haberman et al., 2019). Strikingly, 18 genes were shared with these 2 gene signatures (Figure 30A), in which *Trem1* and *Osm,* connected to decreased responsiveness to anti-TNF therapy, were shared between the three gene signatures. Besides, the high expression of activating *Fcgr1* and *Fcgr3* found in inflammatory MCJ-deficient macrophages, which are cell surface glycoproteins that bind to the Fc portion of IgG antibodies, and the high levels of colonic IgG found, suggested that the MCJ-deficient genotype might be associated with resistance to TNF blockade. Therefore, we evaluated the response of MCJ-deficient mice to anti-TNF therapy. Therapeutic efficacy of the infliximab biosimilar was diminished in MCJ-deficient mice, indicated by the absence of a significant improvement in body weight (Figure 30B) and histological score (Figure 30C) compared to WT mice, which successfully responded to anti-TNF therapy. Moreover, TACE levels within the colon only increased in treated WT mice independently of TNF, and infiltrated macrophage numbers that did not vary (Figure 30D, Supplementary Figures S4A, B). TACE activity is responsible for the final release of mature TNF protein from cells. Therefore, our results provide evidence that the different forms of TNF impact on anti-TNF therapy.

To assess the effect of anti-TNF agents on microbial composition and the impact on the therapeutic response, luminal bacterial communities were studied. They yielded a total of 1.189.812 paired and merged sequences, ranging from 56.923 to 101.477 sequences per sample after quality filtering. The good's coverage was over 98%. Remarkably, the taxa bar plot showed the enrichment of the Verrucomicrobia phylum and the reduction of Proteobacteria in WT mice treated with anti-TNF therapy compared to MCJ-deficient mice (Figure 30E). Although alpha diversity was not significantly altered, DESeq2 identified *Akkermansia* and OTUs from the *S24-7* family augmented in the WT group (Figure 30F, G) pointing to these microorganisms as critical in the primary response to the therapy. Overall, these data show that MCJ-deficient mice do not respond to anti-TNF agents. In this way, the microbial composition in this group was not affected by treatment, only specific changes rather than a global impact were induced. Meanwhile, the WT mice group responds to anti-TNF treatment and partially restores their gut microbiota which seems to play a critical role in therapy response.

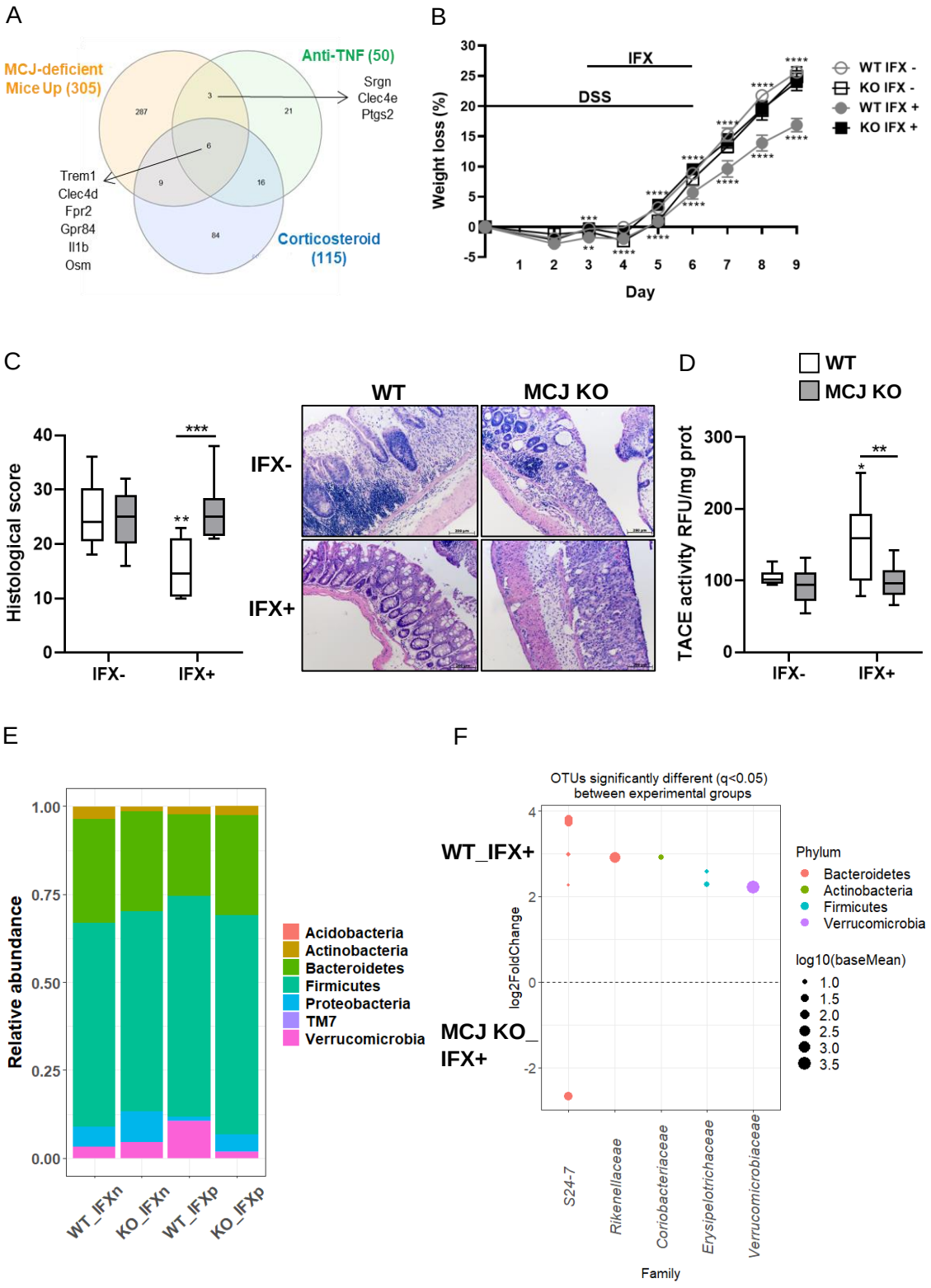
A
MCJ-deficient Mice Up (305)
Anti-TNF (50)
Corticosteroid (115)
Srgn
Clec4e
Ptgs2
Trem1
Clec4d
Fpr2
Gpr84
Il1b
Osm
287
3
21
6
9
16
84
B
IFX
DSS
Weight loss (%)
Day
WT IFX -
KO IFX -
WT IFX +
KO IFX +
C
Histological score
IFX-
IFX+
WT
MCJ KO
D
TACE activity RFU/mg prot
WT
MCJ KO
E
Relative abundance
WT_IFXn
KO_IFXn
WT_IFXp
KO_IFXp
Acidobacteria
Actinobacteria
Bacteroidetes
Firmicutes
Proteobacteria
TM7
Verrucomicrobia
F
OTUs significantly different (q<0.05) between experimental groups
WT_IFX+
MCJ KO_ IFX+
log2FoldChange
Phylum
Bacteroidetes
Actinobacteria
Firmicutes
Verrucomicrobia
log10(baseMean)
S24-7
Rikenellaceae
Coriobacteriaceae
Erysipelotrichaceae
Verrucomicrobiaceae
Family

G

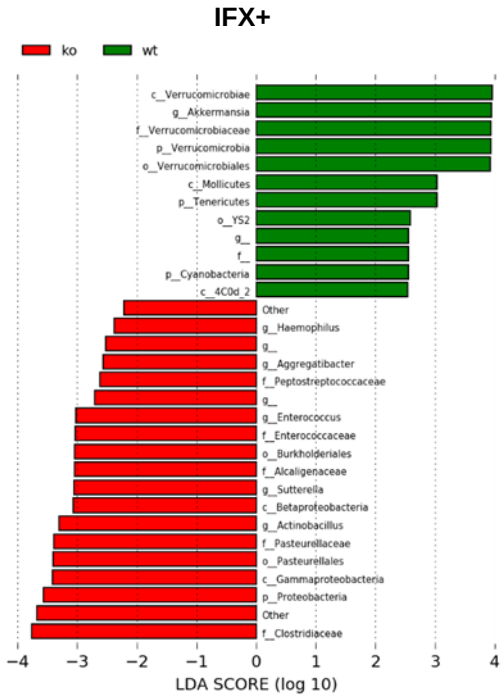

Figure 30. *In vivo* anti-TNF therapeutic response. Experimental design: mice were treated the first 6 days with DSS and infliximab (IFX) was administrated orally from day 3 to day 6, followed by 3 days of recovery period. All groups are positive for DSS. (**A**) Venn diagram showing shared genes between upregulated genes due to MCJ deficiency in Abx-DSS+ mice colon macrophages and patients refractory to anti-TNF and corticosteroid treatments. (**B**) WL (%) (n=8 mice per group at minimum). Statistical differences (*p* value < 0.05) were observed between WT IFX- and WT IFX+ from day 3 onward and between KO IFX+ and WT IFX+ at day 3 and from day 5 onward. (**C**) Histological scores and representative images of colon tissue (scale bar size, 100µm). (**D**) TACE activity in colonic protein extracts (RFU/mg protein). (**E**) Stacked bar plot representation of the relative abundances of colon content taxa at phylum level. (**F**) Differentially abundant OTUs identified through DESeq2 testing (p.adj < 0.05) between WT and MCJ-deficient mice treated with anti-TNF agents (WT_P vs KO_P). Each point represents a single OTU colored by phylum and grouped by taxonomic family, and point´s size reflect the mean abundance of the sequenced data. (**G**) LEfSe analysis showing the most differentially abundant taxons between WT and MCJ KO mice treated with anti-TNF agents, MCJ KO in red and WT in green. (**B**) Grey lines indicate wild-type and black lines MCJ-deficient mice. (**C**-**D**) White boxplots indicate wild-type and grey boxplot MCJ-deficient mice. For statistical analysis two-way ANOVA was used. In line graphs, asterisks **"*"** above line for IFX and DSS positive MCJ-KO (KO_IFX+) *versus* IFX and DSS positive WT (WT_IFX+), and below for IFX and DSS positive WT (WT_IFX+) *versus* IFX negative and DSS positive WT (WT_IFX-). In boxplots, an asterisk or asterisks upside boxes *versus* control genotype (IFX+ *vs* IFX-), and asterisks above line *versus* different genotypes in the same experimental group. WT_IFXn and KO_IFXn: WT and MCJ KO DSS positive and IFX negative; WT_IFXp and KO_IFXp: WT and MCJ KO DSS and IFX positive.

Then, we studied whether gut microbiota might be a key player in therapeutic response. Therefore, we cohoused WT and MCJ-deficient mice prior to DSS and IFX administration. We confirmed that only WT mice housed alone responded to IFX since they lost significantly less body weight (Figure 31A) and they had longer colons compared to the other experimental groups (Figure 31B). As reported, MCJ-deficient mice housed alone did not respond to IFX treatment. In this way, microbial transmission was not enough to improve treatment response in case of mitochondrial dysfunction. However, cohoused WT mice displayed greater WL percentages from day 7 onward (Figure 31A) and shorter colons (Figure 31B) compared WT housed alone. Therefore, cohoused WT mice did not respond to IFX suggesting that the acquired microbiota from MCJ-deficient mice might affect the anti-TNF agent response in individuals without mitochondrial impairment. Results indicate that MCJ-deficient mice gut microbiota composition might be related with an enhanced pro-inflammatory response, consequently reducing the efficacy of the treatment.

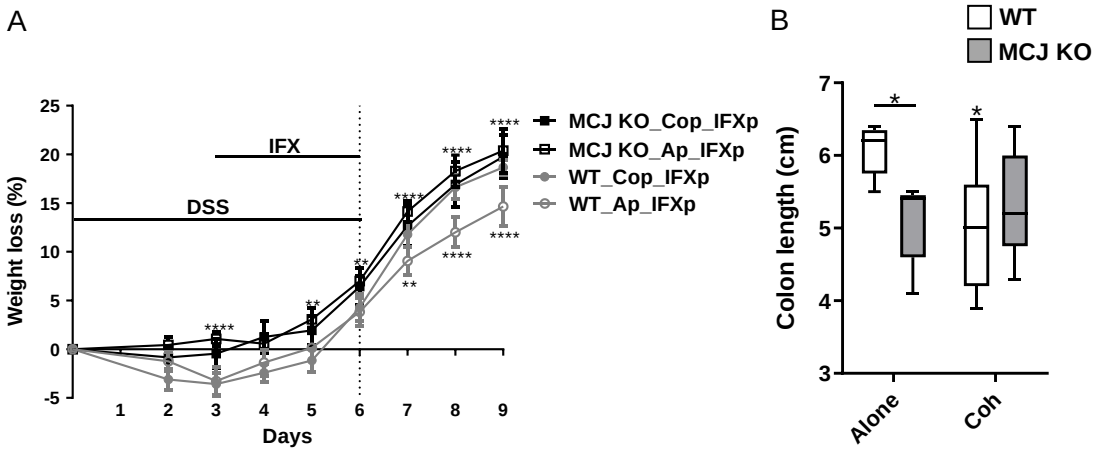

Figure 31. Evaluation of cohousing impact in the anti-TNF response in UC. Experimental design: to allow microbial transmission between genotypes, animals were cohoused during 4 weeks prior to colitis induction. (**A**) WL percentage shown as means ± SEM. (**B**) Colonic length shown as cm. Grey lines and white boxplots indicate WT, and black lines and grey boxplots MCJ KO mice. Box whisker plots of median, quartiles and range with at least 7 mice per group (in cohousing groups). For statistical analysis two-way ANOVA was used. In line graphs, asterisks "*" above the line for DSS positive MCJ-KO housed alone (KO_Ap_IFXp) *versus* IFX and DSS positive WT housed alone (WT_Ap_IFXp), and below for WT housed alone treated with DSS and infliximab (WT_Ap_IFXp) *versus* WT cohoused treated with DSS and IFX (WT_Cop_IFXp). An asterik above boxes *versus* control genotype (Alone IFX+DSS+ *versus* cohoused IFX+DSS+), and an asterisk above line *versus* different genotypes in the same experimental group. WT_Ap_IFXp and MCJ KO_Ap_IFXp: WT and MCJ KO housed alone, DSS and IFX positive; WT_Cop_IFXp and MCJ KO_Cop_IFXp: WT and MCJ KO cohoused, DSS and IFX positive.

Our results suggest that mitochondrial dysfunction play a critical role in anti-TNF therapy response due to the important impact of MCJ deficiency on TNF pathway. Noteworthy, MCJ levels modulate microbial composition in homeostasis, and through fecal microbial transplant key microorganisms were transmitted to WT mice affecting anti-TNF treatment response and pointing to microbiota as decisive contributor to the disease.

Taken together, our study indicates that the mitochondrial dysfunction in macrophages from DSS-induced colitis mice affect a wide range of signalling pathways critical in UC severity and the response to anti-TNF therapy. These data confirm a regulation of mitochondria and microbiota, and a pivotal role of the microbial community in macrophage immune responses during colitis. Our results show that around two thirds of genes impacted by MCJ deficiency are conserved between the murine model and human colitis. They also support the use of animal models to avoid the heterogeneity observed in patients and focus on those genes that are relevant and contribute to intestinal inflammation.

2.2 Discussion

Mitochondrial dysfunction has been related to disease severity and the response to treatment during UC, including the reduction of complex I activity in active patients (Haberman et al., 2019). Previously, other research groups showed evidence that support the relevance of the reduction in mitochondrial genes and associated energy production pathways during the disease (Cardinale et al., 2014; Mottawea et al., 2016; Ip et al., 2017). However, the impact of microbial composition in this context was still unclear. Here, we provide evidence of the regulatory role of mitochondrial dysfunction independently of the type of dysbiosis found in the colon, during UC disease progression.

2.2.1 Antibiotic induced dysbiosis

Epidemiological studies and data on antibiotic-induced alterations in gut microbiota indicate an increased risk of developing inflammatory bowel diseases, secondary to dysbiosis and bacterial translocation (Henao-Mejia et al., 2012; Knoop KA et al., 2016). Our data show that antibiotic-induced dysbiosis results in higher DAI, in agreement with the work by Shen et al. and Nishida et al. who showed that dysbiosis has a major impact on UC disease progression (Shen et al., 2018; Nishida et al., 2018). Although, antibiotic intervention diminished microbial differences observed between both genotypes after experimental colitis, specific bacterial taxa that included *R. gnavus* were enriched due to MCJ deficient environment. *R. gnavus* is augmented in IBD patients and promote intestinal inflammation through mechanisms of oxidative stress responses, adhesion, iron acquisition, and mucus utilization (Henke et al., 2019; Hall et al., 2017). Additionally, MCJ levels also affected DAI severity indicating that impaired mitochondrial function might play a relevant role modulating microbial environment, highlighting a direct role for mitochondria in sensitizing the intestine to commensal bacteria and exacerbating inflammation. After antibiotic-induced dysbiosis, our results agree with those observed in bone marrow-derived macrophages (Navasa et al., 2015a) pointing to these as critical cells. However, the differences observed in anti-inflammatory cytokine production were less evident, highlighting the role of microbial composition on their regulation. Collectively, these data show that antibiotic treatment altered microbiota and their metabolites (e.g., SCFAs) that specifically promote anti-inflammatory cytokines production by intestinal macrophages in inflamed tissue, thereby increasing experimental colitis severity (DAI) in mice.

2.2.2 Colon macrophages transcriptome

Tissue samples are highly heterogeneous, and the amount of different cell types in a biopsy will have a certain impact on gene expression profiles. Here, we determined that MCJ is expressed in gut macrophages from IBD patients. Therefore, we performed macrophage isolation from mice colon tissue in order to improve the quality of the results obtained by RNA-Seq technology and to characterize the role of MCJ in the early immune response. In agreement with a recent work from Czarnewski et al. that demonstrated a conserved transcriptomic profile between mouse and human colitis, our data show that the DSS mouse model is relevant to study mitochondrial dysfunction in UC patients (Czarnewski et al., 2019). MCJ deficiency in macrophages had a strong impact on the expression of susceptibility genes identified in UC. Previous studies analyzing mucosal transcriptomes revealed mitochondriopathy in a cohort of UC patients. Among the genes differentially regulated, they observed 13 genes associated with reduced ATP production and complex I activity in addition to the master regulator of mitochondrial biogenesis *PPARGC1A (PGC-1α)* (Haberman et al., 2019). Altogether, this evidence supports the implication of a colonic mitochondriopathy in the course of UC suggesting that approaches targeting the mitochondrial electron transport axis could represent potential therapeutic strategies improving the response to those currently in use.

Lamina propria macrophages are strongly phagocytic for live microorganisms (Smith et al., 1997). MCJ deficiency in colon macrophages revealed a high impact on Fc-gamma receptor signaling pathways. They recognize the Fc portion of IgG, triggering the engulfment and destruction of opsonized microorganisms. Our results are in agreement with previous reports (Castro-Dopico et al., 2019) using a chronic DSS mouse model and mirror observations in human UC patients. As described in the MCJ-deficient murine model, a higher proportion of luminal commensals bound by IgG were observed in UC stool samples, correlating with disease severity and pointing to anti-commensal IgG as a key player in the intestinal inflammatory response. This work shows that MCJ deficiency in macrophages isolated from the colon during colitis significantly increased the expression of *Fcgr3* and *Fcgr2b* in line with *Il1b* and *Cxcl2* levels. The former correlated with disease severity in patients with IBD (Peloquin et al. 2016). In addition, *Cxcl2* has been shown to control mucosal lymphocytes and neutrophil migration (Ohtsuka et al., 2001). Altogether, these data suggest that anti-commensal IgG might contribute to intestinal inflammation via FCGR-dependent induction of IL-1β.

Moreover, it was reported that elevated *FCGR2A* expression in mucosal UC biopsies taken prior to IFX intervention was associated with disease refractory to treatment and was predictive of subsequent resistance to TNF blockade (Castro-Dopico et al., 2019). Our results confirm that elevated *Fcgr* expression in colon macrophages associated to mitochondrial dysfunction and high colonic IgG levels predicted non-responder individuals to anti-TNF therapy. Noteworthy, the overlapping between upregulated genes in UC patients and alterations due to MCJ levels in colon macrophages including tumor necrosis factor receptor superfamily members (*Tnfrsf9*, *Tnfsf14*, *Cd40*), cytokines and chemokines (*Jak2*, *Cxcr4*, *Ccr5*, *Ccr3*, *Ccr2* and *Cxcl2*, *Cxcl3*), eosinophil-associated gene *Alox15* (linked to corticosteroid response), related to anti-TNF resistance such as oncostatin M (*Osm*), *Trem1* or cyclooxygenase-2 (*Cox2* [*Ptgs2*]), could provide a new research line to understand the basis of disease in order to guide trials of new strategies for treatment-resistant patients. Moreover, the presence of *R. gnavus* in MCJ-deficient mice, might serve as a potential biomarker for predicting the severity and non-response to anti-TNF treatment (Hall et al., 2017, Lloyd-Price et al, 2019; Dovrolis et al., 2020). On the contrary, the augmented abundance of *A. muciniphila* and several OTUs of the family S24-7 within the WT genotype indicated induction of healing gut microbiota. Microbial changes in patients with CD after IFX therapy displayed a significant gain in SCFA (Zhuang et al., 2020), the main metabolite of *A. muciniphila*. SCFA may mitigate intestinal inflammation through both intestinal epithelial barrier maintenance and immune regulation (Maslowski et al, 2009; Sina et al, 2009). Accordingly, previous studies reported that a murine *A. muciniphila* strain improved chronic colitis disease severity parameters probably due to the release of anti-inflammatory cytokines (Zhai et al., 2019). In this sense, the Bacteroidales *S24-7* family was negatively correlated with the expression of several proinflammatory genes in the colon, suggesting its beneficial role in inflammatory conditions (Pascual Itoiz et al., 2020). Interestingly, there seems to be a negative association between *R. gnavus* and *A. muciniphila* abundance although no molecular mechanisms to explain these correlations have been developed. While *A. muciniphila* resides in the mucus layer of the large intestine, where it is involved in maintaining intestinal integrity, *R. gnavus* colonizes the intestinal mucosal surface, where it can use sialic acid from mucin glycans as a carbon source. Therefore, since *A. muciniphila* utilizes mucin as the unique carbon, nitrogen and energy source, the presence of *R. gnavus* might affect *A. muciniphila* growth by limiting the mucus availability in MCJ-deficient mice. Indeed, a reduced abundance of *A. municiphila* was reported in IBD patients, while the total mucosa-associated bacteria including *R. gnavus* and *R. Torques,* increased (Png et al., 2010).

Recent studies have revealed the potential role of gut microbiota to affect and predict the anti-TNF response or relapse (Dovrolis et al., 2020). In this regard, in our mouse model of cohousing (WT and MCJ-deficient genotypes), we discovered that WT mice failed to respond to IFX treatment as a consequence of the acquired microbiota from MCJ-deficient mice. As previously described, MCJ deficiency regulate microbial composition and promote high levels of *Tnf* and *Il1b* expression during the course of UC (Pascual-Itoiz et al., 2020). The transmission of these pro-inflammatory bacteria to WT mice gut community may enhance pro-inflammatory cytokine production and counteract the effect of anti-TNF antibodies. Nevertheless, MCJ-deficient mice failed to respond to anti-TNF therapy after mice cohousing, suggesting that mitochondria dysfunction might be also a good predictor for anti-TNF failure independently of gut microbiota composition.

In summary, our results in the transcriptome of colon macrophages point to a relevant role of MCJ levels during colon inflammation. The high impact of MCJ levels on immune cell activation, Fc-gamma receptor signaling pathways, and colonic IgG indicate important implications in disease severity. Furthermore, the impact of MCJ deficiency on non-responsiveness to anti-TNF therapy was confirmed. Antibiotic-induced dysbiosis depleted the effects associated with MCJ deficiency in the colon environment. Our work supports a model in which dysbiosis and the subsequent modification of the microbiota-associated metabolites alter the induction profile of inflammatory cytokines, leading to higher disease severity. The data on MCJ-deficient mice implicates mitochondria dysfunction in UC pathogenesis mirroring the colonic mitochondriopathy described in UC patients that is also associated with anti-TNF therapy success. The conserved transcriptomic profile between mouse pathology and human disease opens new possibilities to predict disease severity and the responsiveness to therapy, which could be useful for the proper stratification of UC patients and the design of personalized therapies.

3. Role of the gut microbiota modulated by MCJ deficiency in the pathogenesis of UC

Publication

Peña-Cearra A, Song D, Pascual-Itoiz MA, Lavín JL, Castelo J, Azkargorta M, Elortza F, Fuertes M, Barriales D, Martin I, Fullaondo A, Aransay AM, Rodriguez H, Palm NW, Anguita J, Abecia L. Microbiota composition is a dominant determinant of ulcerative colitis development and progression as a result of mitochondrial dysfunction. *Under revision*.

Conference

International Human Microbiome Consortium Congress 2021

Peña-Cearra A, Palm NW, Pascual-Itoiz MA, Song D, Lavín JL, Fuertes M, Castelo J, Barriales D, Palacios A, Martin I, Fullaondo A, Aransay AM, Rodriguez H, Anguita J, Abecia A. Mitochondrial dysfunction phenotype can be transferred to germ-free mice but also reverted by fecal microbiota transplantation.

Poster communication (Virtual congress, June 27-29, 2021)

3.1 Results

There is accumulating evidence showing bidirectional interaction between mitochondria and microbiota, emerging as a significant area of research in health and disease.

Herein, we characterized the effect of mitochondrial dysfunction on gut microbiota composition and susceptibility to colitis. Our aim was to shed light on the role of microbiota-host mitochondria axis in UC. For this purpose, we performed three different approaches based on microbial colonization of GF mice, fecal microbial transplant (FMT) and IgA-SEQ technology using a mouse model deficient in MCJ.

HYPOTHESIS	MCJ impacted on host-gut microbiota crosstalk during ulcerative colitis. Thus, Gut microbiota modulated by MCJ levels is crucial in the pathogenesis of the disease. Thus, the specific role of the MCJ deficiency associated gut microbiota needs to be investigated.

3.1.1 MCJ-deficient mice microbial composition increased inflammatory profile in colonized germ-free mice

To investigate the colitogenic potential of MCJ-deficient mice gut microbial composition, GF mice were colonized with WT and MCJ-deficient mice microbiota. GF mice colonized with MCJ-deficient mice microbiota were significantly more susceptible to DSS colitis, as measured by DAI from day 4 to 6 and WL at days 2, 4 and 5, as compared to mice colonized with WT microbiota (Figures 32A, B). At day 8, a marked reduction of colonic length (*p* value = 0.018) was observed in GF mice colonized with MCJ-deficient mice microbiota (Figure 32C). The antimicrobial peptide *Lcn-2,* a biomarker of intestinal inflammation (Figure 32D), and the potent inflammatory cytokine *Il1β* (Figure 32E) were also upregulated in colonic tissues from MCJ-deficient microbiota colonized mice. Contrary to the antimicrobial peptide *Reg3b,* which was downregulated suggesting a less protective environment against MCJ-deficient luminal microbiota under inflammatory conditions (Figure 32F). Overall, these data suggest that the dysbiotic microbiota from MCJ-deficient mice exacerbated colitis independent of the direct effects of MCJ deficiency on the host immune system.

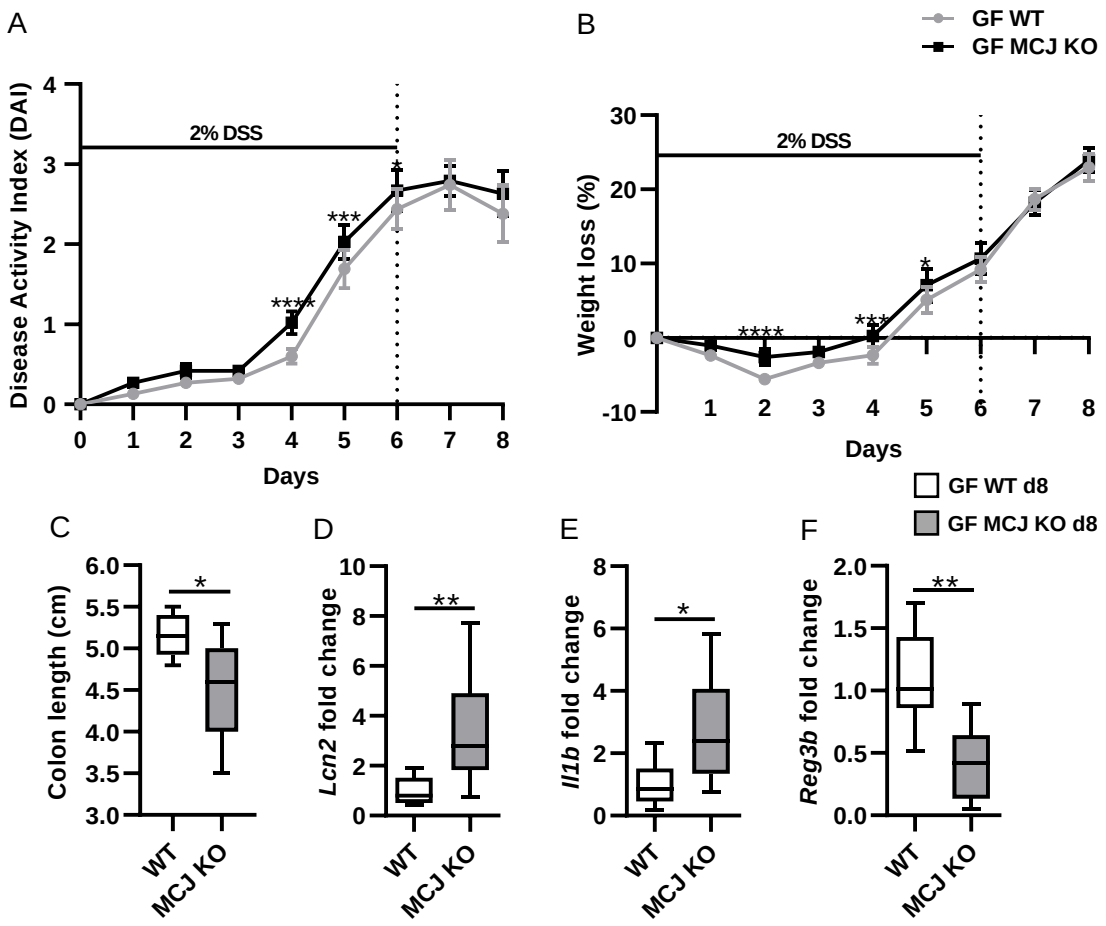

Figure 32. GF mice colonization with WT and MCJ-deficient mice microbial communities. Experimental design: to allow microbes to colonize, GF mice were gavaged 2 weeks prior to the 6 days of 2% DSS administration, followed by 2 days of recovery period with water. (**A**) DAI and (**B**) WL percentage; data are means ± SEM. (**C**) Colon length (cm). Gene expression analysis from mice colon tissue of (**D**) *Lcn2,* (**E**) *Il1b* and (**F**) *Reg3b* genes shown as mean fold change of GF mice colonized with MCJ-deficient microbial consortia compared to GF mice colonized with bacterial community from WT mice. Grey lines and white boxplots indicate WT and black lines and grey boxplots MCJ KO mice. Box and whisker plots of median, quartiles and range with at least 8 mice per group. For statistical analysis, two-way ANOVA and unpaired t-test were used. In line graphs, statistical differences are shown by an asterisk or asterisks "*" above the line for GF MCJ KO DSS-treated *versus* GF WT DSS-treated. In boxplots, an asterisk or asterisks above line *versus* control genotype at day 8 (GF_MCJ KO *vs* GF_WT). d8: day 8.

Next, we sought to identify specific groups of bacteria related to UC pathogenesis and impaired mitochondrial function that may serve as potential biomarkers of disease progression. Therefore, we sequenced the V4 region of the *16S RNA* gene from fecal content at day 0 (2 weeks after colonization, just before DSS treatment) and at day 8 (two days after DSS treatment stopped). We obtained a mean of 12.800 ± 2.962 counts per sample and the mean Good´s coverage percentage was 100%. PCoA based on Bray-Curtis dissimilarity displayed differences in homeostasis (day 0) between colonized microbial communities based on MCJ contribution (p.adj = 0.006) (Figure 33A). DSS treatment and MCJ deficiency at day 8 also were associated with distinct microbial compositions (p.adj = 0.042). As reported, alpha diversity indices decreased after DSS administration in both communities (Figure 33B). Strikingly, bacteria from the Actinobacteria phylum exhibited decreased relative abundance in MCJ-deficient microbiota at day 0 compared to WT (*p* value ≤ 0.0001) (8.81% *vs* 1%) (Figure 33C). In DSS treated groups, relative abundance of Actinobacteria (*p* value = 0.0044), *Bacteroides* (*p* value = 0.0257) and Verrucomicrobia (*p* value = 0.0075) phyla was significantly higher and Firmicutes (*p* value = 0.0025) lower, in GF mice colonized with MCJ-deficient microbial community compared to WT. In this regard, the dysbiosis index (Firmicutes/Bacteroidetes ratio) was significantly lower in GF mice colonized with MCJ-deficient mice microbiota compared to those colonized with WT gut microbes (Figure 33D) as usually observed in IBD. Moreover, DESeq2 identified the OTUs that were differentially abundant at day 0 and day 8 in colon content. Two weeks after colonization and just prior to DSS administration (day 0), *Bifidobacterium* and *Coprobacillus* were increased and *Staphylococcus, Bacteroides and Parabacteroides* decreased in GF mice colonized with MCJ-deficient mice microbiota (Figure 33K). Two days after DSS treatment (day 8), MCJ-deficient microbial community showed elevated levels of *Bifidobacterium* but also *Butyricicoccus*, *Akkermansia*, *Ruminococcus* and *Prevotella* were augmented (Figure 33F). Notably, measured *Ruminococcus* and *Prevotella* changes were confirmed with linear discriminant analysis effect size (LEfSE) (Supplementary Figure S5). Conversely, *Clostridium*, *Coprococcus* and *Odoribacter* were lower in GF mice colonized with MCJ-deficient microbiota as compared to mice colonized with WT microbiota. In conclusion, results suggest that mitochondrial dysfunction affected microbial environment and as a result, gut microbial composition could be transferred to germ-free mice (without mitochondrial impairment) and contribute to the development of the disease.

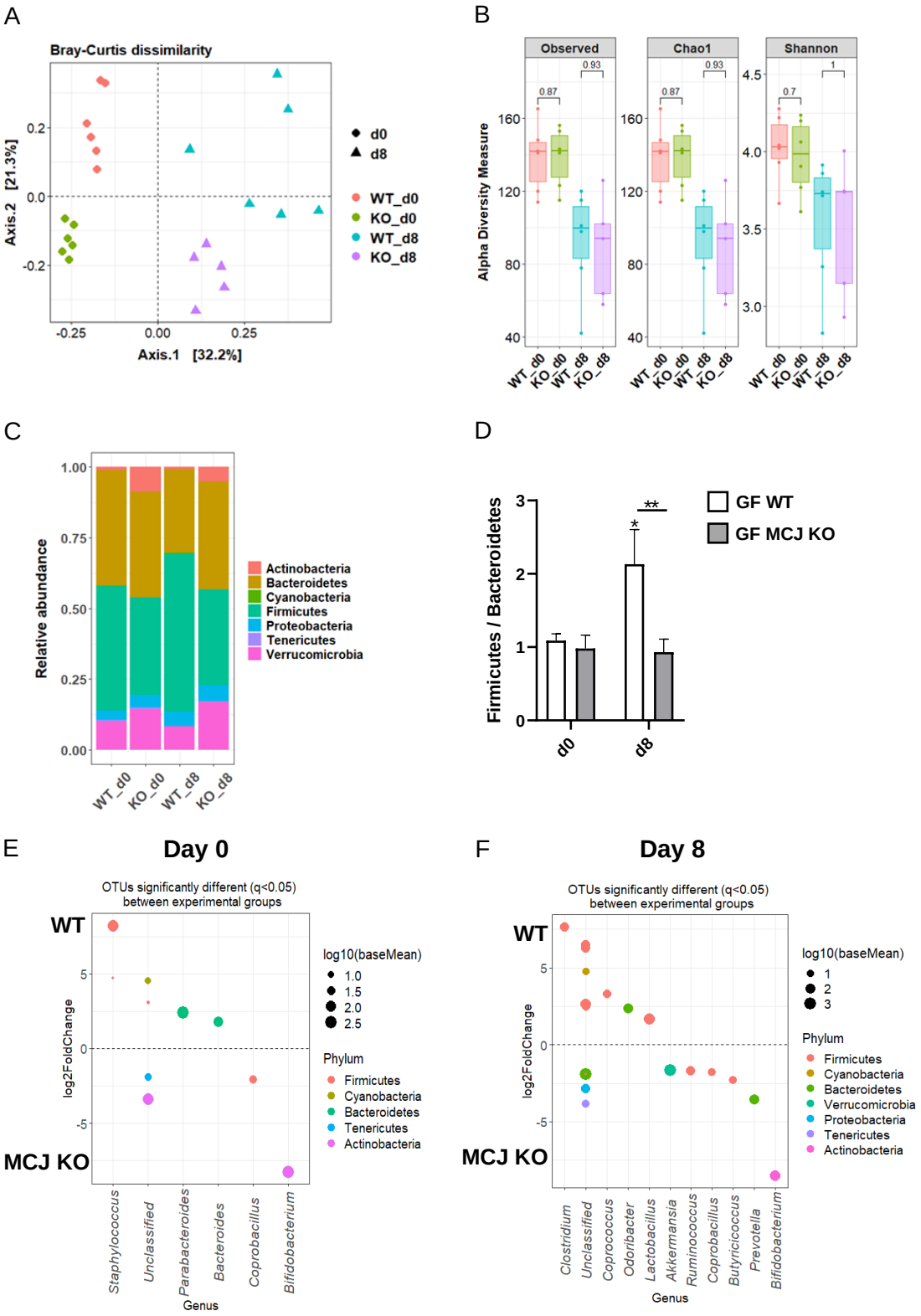
A
Bray-Curtis dissimilarity
Axis.2 [21.3%]
Axis.1 [32.2%]
d0
d8
WT_d0
KO_d0
WT_d8
KO_d8
B
Observed
Chao1
Shannon
Alpha Diversity Measure
0.87
0.93
0.7
1
C
Relative abundance
Actinobacteria
Bacteroidetes
Cyanobacteria
Firmicutes
Proteobacteria
Tenericutes
Verrucomicrobia
D
Firmicutes / Bacteroidetes
GF WT
GF MCJ KO
E
Day 0
OTUs significantly different (q<0.05) between experimental groups
WT
MCJ KO
log2FoldChange
log10(baseMean)
Phylum
Staphylococcus
Unclassified
Parabacteroides
Bacteroides
Coprobacillus
Bifidobacterium
Genus
F
Day 8
Clostridium
Coprococcus
Odoribacter
Lactobacillus
Akkermansia
Ruminococcus
Butyricicoccus
Prevotella

Figure 33. Colonized GF mice microbiota composition before and after DSS-induced colitis. (**A**) PCoA plot of bacterial beta-diversity based on Bray-Curtis dissimilarities showing experimental groups after bacterial colonization (WT_d0 and KO_d0) and after colitis induction (WT_d8 and KO_d8). ANOSIM revealed statistical differences within GF mice colonized with gut microbiota derived from distinct mice genotypes before DSS administration (p.adj = 0.006) and at the end of the experiment (p.adj = 0.042). (**B**) Bacterial alpha diversity analysis by means of observed Operational Taxonomic Units (OTUs), Chao1 and Shannon indexes. Statistical analyses were performed using the nonparametric Wilcoxon rank sum test. (**C**) Stacked bar plots showing the average relative abundance of bacterial phyla in the different experimental groups. (**D**) Boxplot representation of Firmicutes/Bacteroidetes ratio. The boxes represent the mean ± SEM. DESeq2 displayed OTUs that were differentially abundant between groups (**E**) before DSS administration (WT_d0 and KO_d0) and (**F**) at the end of the experiment (WT_d8 and KO_d8). Each point represents a single OTU colored by phylum and grouped by taxonomic genus. Point´s size reflect the mean abundance of the sequenced data. White bars indicate WT and grey bars MCJ KO mice. For statistical analysis, two-way ANOVA was used. In bar plots, an asterisk "*" above boxes *versus* control genotype (d8 *vs* d0), asterisks above line *versus* different genotypes in the same experimental group. KO: MCJ KO.

3.1.2 Cohousing altered microbial composition and reduced disease severity from MCJ deficient mice

To further determine the potential feasibility of microbial manipulation to treat DSS-induced damage (aggravated by mitochondrial dysfunction), we cohoused WT and MCJ-deficient mice for 4 weeks. First, disease activity index and histological score parameters were evaluated. MCJ-deficient mice treated with DSS presented the highest DAI scores at day 8 and 9 (Figure 34A). However, DAI from MCJ-deficient mice cohoused with WT mice and treated with DSS exhibited a significant reduction (*p* value < 0.05). It is worthy to mention that differences between WT groups were not observed. The histological analysis showed the same tendency presenting cohoused and DSS-treated MCJ-deficient mice significantly lower histological score compared to the WT group (*p* value = 0.05) (Figure 34B). Colon length and goblet cells were not affected by cohousing (Figures 34C, D). These results indicated that microbes acquired from the WT microbiota during cohousing ameliorate DSS colitis (and dysbiosis) in MCJ-deficient animals. Thus, microbial composition contributes to disease severity notably in case of mitochondrial impairment of the host.

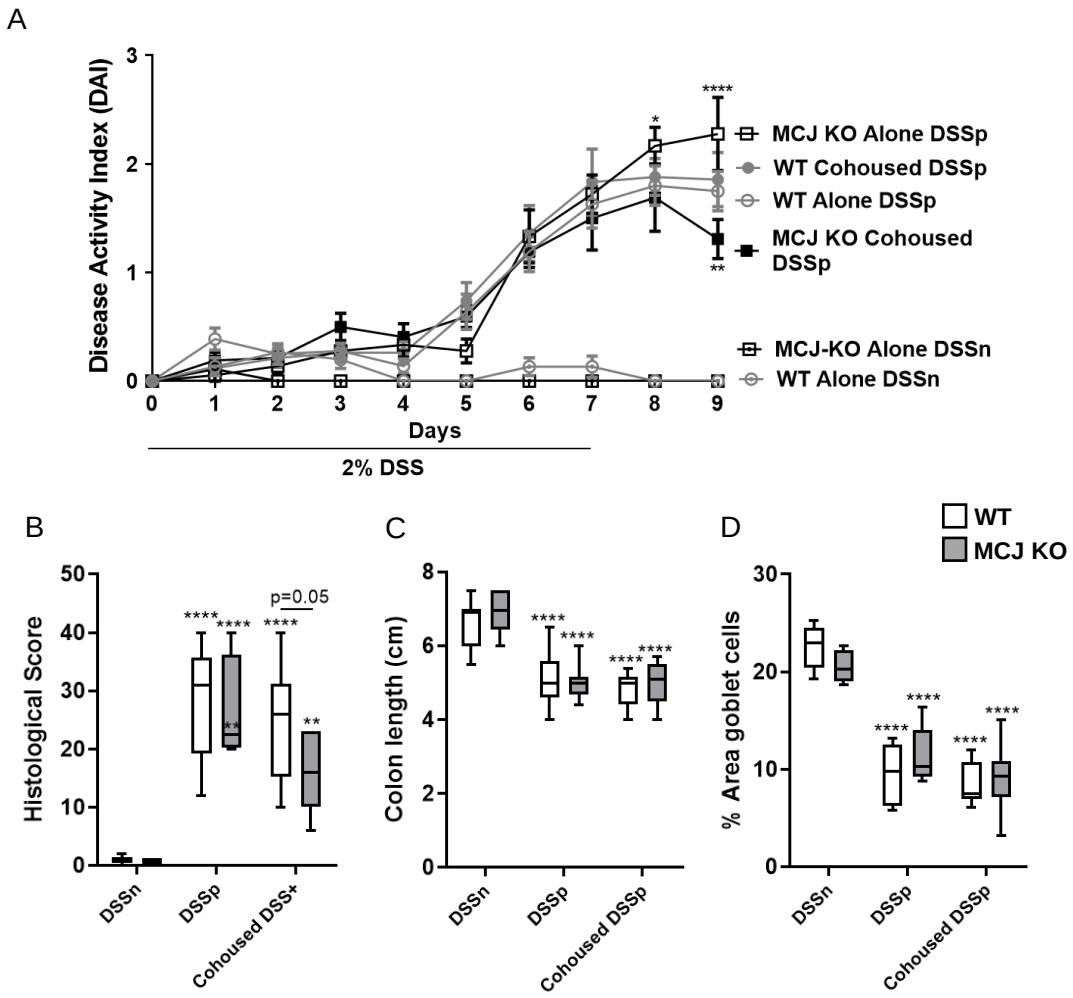

Figure 34. Fecal microbial transplantation via WT and MCJ-deficient animals cohousing. Experimental design: animals were cohoused during 4 weeks before colitis induction. (**A**) DAI expressed as means ± SEM. (**B**) Histological score. (**C**) Colonic length (cm). (**D**) Goblet cells: % of positive cells stained with PAS. Grey lines and white boxplots indicate WT and black lines and grey boxplots MCJ KO mice. Box and whisker plots of median, quartiles and range with at least 9 mice per group (in DSS-treated groups). For statistical analysis, two-way ANOVA was used. In line graphs, statistical differences are shown by an asterisk or asterisks "*" above the line for MCJ-KO DSS-treated alone (MCJ KO Alone DSSp) *versus* cohoused (MCJ KO Cohoused DSSp), and below line for MCJ-KO cohoused and DSS-treated (MCJ KO Cohoused DSSp) *versus* WT cohoused and DSS-treated (WT Alone DSSp) comparison. In boxplots, asterisks upside the box *versus* control genotype (DSS positive groups (DSSp) and cohoused groups (Cohoused DSSp) *versus* the control (DSSn)). Significant differences within the same mice genotype between DSS-treated housed alone and cohoused groups are represented with asterisks inside the box of WT or MCJ-deficient mice that were housed alone (DSSp).

To determine microbial shifts on WT and MCJ-deficient mice after cohousing and DSS-induced colitis, the V4 region of the *16S rRNA* gene from colonic bacterial communities was sequenced. This process generated a mean of 97.775 ± 16.765 counts per sample and the mean Good´s coverage percentage was 99%. Alpha diversity, determined by the number of observed OTUs, Chao1 and Shannon indices did not reveal differences between genotypes housed alone (Ap) or together (cohoused, Cop) during intestinal inflammation (Figure 35A). PCoA ordination plot based on Bray-Curtis dissimilarity (Figure 35B) detected differences between experimental groups. NMDS showed a clear cluster between homeostasis (DSSn, An) and DSS-induced colitis groups (DSSp, Ap). Although ANOSIM did not reveal statistical differences between genotypes (WT and MCJ KO) treated with DSS housed alone (Ap) or together (Cop), WT mice showed statistically different clustering between housed alone and cohoused conditions (p.adj = 0.001). After one month of cohousing, data confirms the reciprocal transmission of gut microbes between both cohoused genotypes impacting significantly in the WT cohoused group.

Taxonomic differences at phylum level revealed a significant enrichment (*p* value = 0.022) of the phylum Verrucomicrobia in the MCJ-deficient mice housed alone compared to WT upon intestinal inflammation. Of note, after cohousing, Verrucomicrobia abundance was significantly increased in WT mice compared to those DSS-treated and housed alone WT mice (*p* value = 0.017) (Figure 35C). Furthermore, the analysis of the top 10 most abundant genera showed substantial shifts between genotypes when they were cohoused (Figure 35D). Potential transmission of *Lactobacillus* and *Turicibacter* genera from WT to MCJ-deficient mice was observed. Subsequently, differential abundance analysis using DESeq2 was performed to test differences in microbial composition between WT and MCJ-deficient groups housed alone and together. *Oscillospira* genus augmented in MCJ deficient-mice microbiota both in healthy and inflammatory conditions (Figures 35E, F). After cohousing, WT cohoused mice showed an enriched abundance of *Oscillospira* genus compared to WT housed alone and MCJ-deficient mice cohoused (Figures 35G, I). In this regard, relative abundance of *Oscillospira* decreased after cohousing in MCJ-deficient mice (Figures 35F, I). Moreover, the increased abundance of *Prevotella* observed during acute colitis in MCJ-deficient mice housed alone, diminished after cohousing (Figure 35F, H) *Lactobacillus, Ruminococcus, and Adlercreutzia* genera showed higher abundances in the MCJ-deficient cohoused group compared to the group housed alone, indicating that these taxa could have been acquired as a consequence of fecal transmission (Figure 35H). Additionally, *Lactobacillus* also displayed a significant enrichment (p.adj < 0.05) in MCJ

KO cohoused mice compared to WT mice cohoused (Figure 35I). Furthermore, taxa from *Pasteurellaceae* and *Enterobacteriacea*e families were reduced in cohoused mice due to MCJ deficiency compared to MCJ-deficient mice housed alone (Supplementary Figure S6). Pearson´s correlation analysis revealed significant positive associations (p value < 0.05) between specific bacterial OTUs abundance and disease severity (DAI), including *Akkermansia muciniphila* (r=0.63), *Parabacteroides distasonis* (r=0.66), *Bacteroides acidifaciens* (r=0.63), *Turicibacter* (r=0.49), *Enterobacteriacea* (r=0.45) and *Prevotella* (r=0.44). Contrarily, the DAI correlated negatively with *S24-7* family (r=-0.64), *Lactobacillus* (r=-0.63), *Adlercreutzia* (r=-0.63) and *Bifidobacterium* (r=-0.60) among others.

Collectively, our data manifests significant microbial shifts after cohousing MCJ-deficient mice with WT for one month previously to disease induction. The elevated levels of the probiotic *Lactobacillus* established in MCJ-deficient cohoused mice suggest that the acquired taxa from the WT mice community protect against DSS-induced colitis. On the other side, the decreased relative abundance of *Prevotella* and *Oscillospira* genera points to a potential role of these taxa driving colitis susceptibility.

A

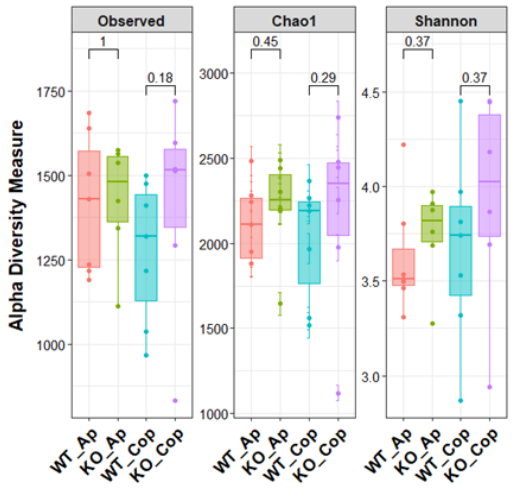
Observed
Chao1
Shannon
Alpha Diversity Measure
1
0.18
0.45
0.29
0.37
0.37
WT_Ap
KO_Ap
WT_Cop
KO_Cop

B

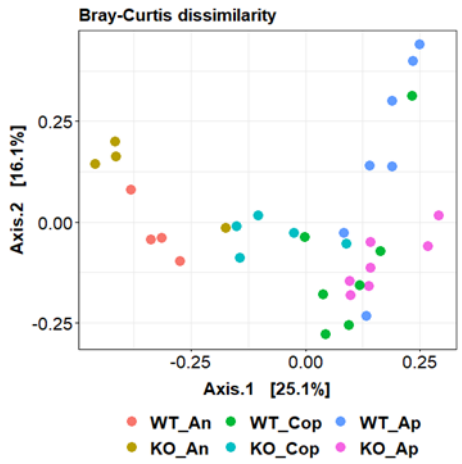
Bray-Curtis dissimilarity
Axis.2 [16.1%]
Axis.1 [25.1%]
WT_An
WT_Cop
WT_Ap
KO_An
KO_Cop
KO_Ap

C

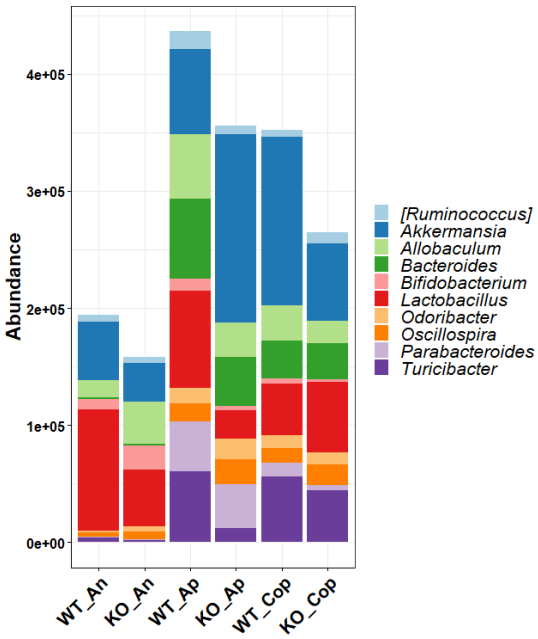
Abundance
[Ruminococcus]
Akkermansia
Allobaculum
Bacteroides
Bifidobacterium
Lactobacillus
Odoribacter
Oscillospira
Parabacteroides
Turicibacter
WT_An
KO_An
WT_Ap
KO_Ap
WT_Cop
KO_Cop

D

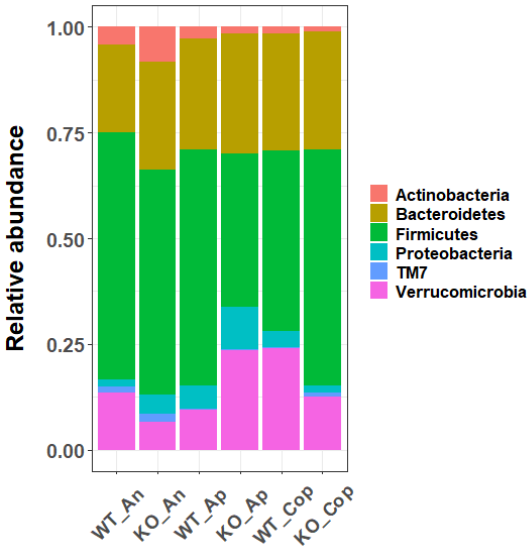
Relative abundance
Actinobacteria
Bacteroidetes
Firmicutes
Proteobacteria
TM7
Verrucomicrobia
WT_An
KO_An
WT_Ap
KO_Ap
WT_Cop
KO_Cop

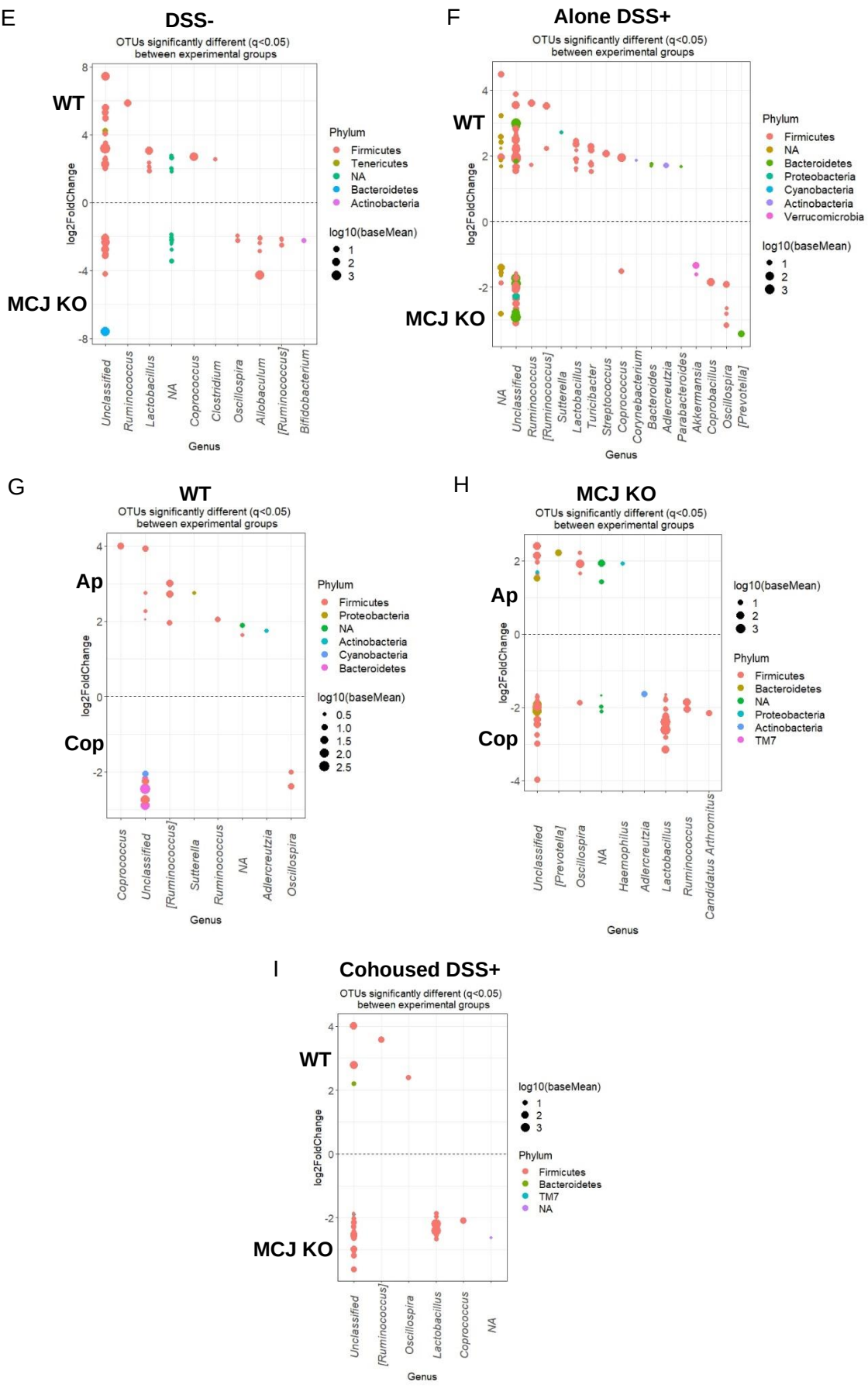
E
DSS-
OTUs significantly different (q<0.05) between experimental groups
WT
MCJ KO
log2FoldChange
Phylum
Firmicutes
Tenericutes
NA
Bacteroidetes
Actinobacteria
log10(baseMean)
Unclassified
Ruminococcus
Lactobacillus
NA
Coprococcus
Clostridium
Oscillospira
Allobaculum
[Ruminococcus]
Bifidobacterium
Genus
F
Alone DSS+
OTUs significantly different (q<0.05) between experimental groups
WT
MCJ KO
log2FoldChange
Phylum
Firmicutes
NA
Bacteroidetes
Proteobacteria
Cyanobacteria
Actinobacteria
Verrucomicrobia
log10(baseMean)
NA
Unclassified
Ruminococcus
[Ruminococcus]
Sutterella
Lactobacillus
Turicibacter
Streptococcus
Coprococcus
Corynebacterium
Bacteroides
Adlercreutzia
Parabacteroides
Akkermansia
Coprobacillus
Oscillospira
[Prevotella]
Genus
G
WT
OTUs significantly different (q<0.05) between experimental groups
Ap
Cop
log2FoldChange
Phylum
Firmicutes
Proteobacteria
NA
Actinobacteria
Cyanobacteria
Bacteroidetes
log10(baseMean)
Coprococcus
Unclassified
[Ruminococcus]
Sutterella
Ruminococcus
NA
Adlercreutzia
Oscillospira
Genus
H
MCJ KO
OTUs significantly different (q<0.05) between experimental groups
Ap
Cop
log2FoldChange
log10(baseMean)
Phylum
Firmicutes
Bacteroidetes
NA
Proteobacteria
Actinobacteria
TM7
Unclassified
[Prevotella]
Oscillospira
NA
Haemophilus
Adlercreutzia
Lactobacillus
Ruminococcus
Candidatus Arthromitus
Genus
I
Cohoused DSS+
OTUs significantly different (q<0.05) between experimental groups
WT
MCJ KO
log2FoldChange
log10(baseMean)
Phylum
Firmicutes
Bacteroidetes
TM7
NA
Unclassified
[Ruminococcus]
Oscillospira
Lactobacillus
Coprococcus
NA
Genus

Figure 35. Composition of host microbiome in cohousing experiment. (**A**) Observed OTUs, Chao1 and Shannon alpha diversity indices (*p* value < 0.05, Wilcoxon rank-sum test). (**B**) PCoA plot of bacterial beta-diversity based on Bray-Curtis dissimilarities revealed distinct grouping between healthy and DSS-treated experimental groups. Differences between WT genotype housed alone or cohoused after colitis induction were detected by ANOSIM (WT_Ap vs WT_Cop, p.adj = 0.001). (**C**) Stacked bar chart at phylum level showing significant shifts in gut microbiota composition from housed alone to cohoused groups. (**D**) Relative abundance of the top 10 most abundant genera confirmed the transmission of gut microbes in cohoused animals. DESeq2 identified OTUs that were differentially abundant between (**E**) healthy WT and MCJ-deficient mice (WT_An and KO_An), (**F**) DSS-treated WT and MCJ-deficient mice (WT_Ap and KO_Ap), (**G**) DSS-treated WT housed alone and cohoused (WT_Ap vs WT_Cop), (**H**) DSS-treated MCJ-deficient housed alone and cohoused (KO_Ap vs KO_Cop) and (**I**) DSS-treated cohoused groups (WT_Cop and KO_Cop). Each point represents a single OTU colored by phylum and grouped by taxonomic genus, and point´s size reflect the mean abundance of the sequenced data. WT_An: WT DSS negative; KO_An: MCJ KO DSS negative; WT_Ap: WT housed alone DSS positive; KO_Ap: MCJ KO housed alone DSS positive; WT_Cop: WT mice cohoused DSS positive; KO_Cop: MCJ KO mice cohoused DSS positive. KO: MCJ KO.

3.1.2.1 MCJ-deficient mice microbiota influences immune cell infiltration

Immune cell infiltration was tested by measuring monocytes, neutrophils MPO secretion, and quantifying macrophages and dendritic cells as part of UC histological feature. As expected, MPO levels increased with DSS treatment. Of note, significant differences (*p* value < 0.05) observed between WT and MCJ KO DSS treated groups, disappeared after 4 weeks of cohousing (Figure 36A). Infiltration of macrophages in the colon tissue was higher in DSS-treated mice although no differences were observed between genotypes in cohoused and alone groups (Figure 36B). The percentage of dendritic cells in MLNs decreased upon intestinal inflammation, suggesting the mobilization of these cells to the lamina propria (Figure 36C). Furthermore, the high percentage of dendritic cells observed in MCJ-deficient mice treated with DSS compared to WT genotype was not found in cohoused groups. These results indicate that dysbiosis in MCJ-deficient mice may modulate immune cell infiltration with potential implication in intestinal inflammation exacerbation.

3.1.2.2 Microbiota from the MCJ environment regulates the inflammatory response

Next, we studied colonic gene expression to examine whether specific microbial compositions affect inflammatory output. We found that *Tnf* expression was increased in MCJ-deficient mice treated with DSS as compared to WT DSS-treated mice. However, this difference was reduced after cohousing with WT, suggesting that the MCJ-deficient microbial community is linked to TNF production and can be modified after one month of cohousing (Figure 36D). Expression of TNF receptor 1, *Tnfr1*, the proinflammatory cytokine *Il1β* and the adaptor protein *Myd88* were also increased during experimental colitis in MCJ-deficient mice. However, this effect was eliminated when groups of mice were cohoused (Figures 36E-G). Overall, these results suggest that the transmission of microorganisms from WT mice to MCJ-deficient mice ameliorates intestinal inflammation.

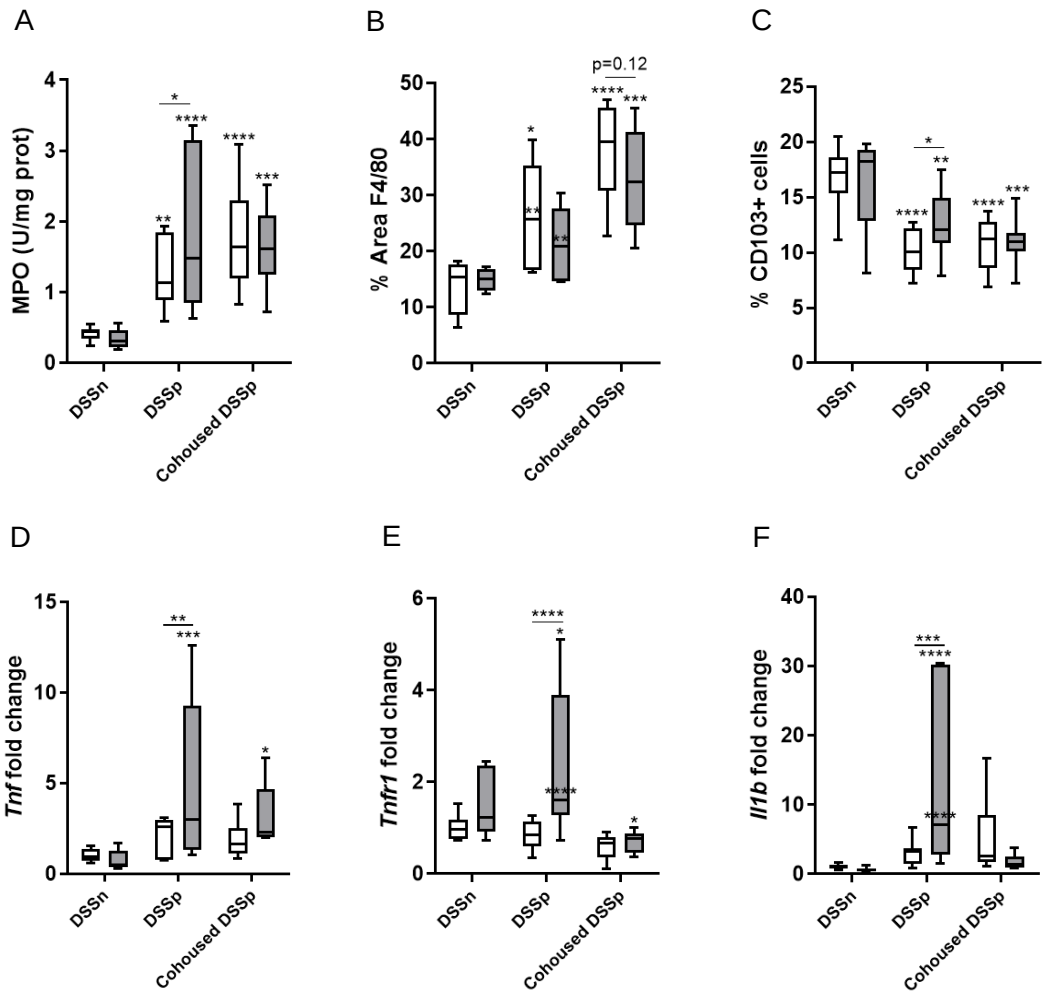

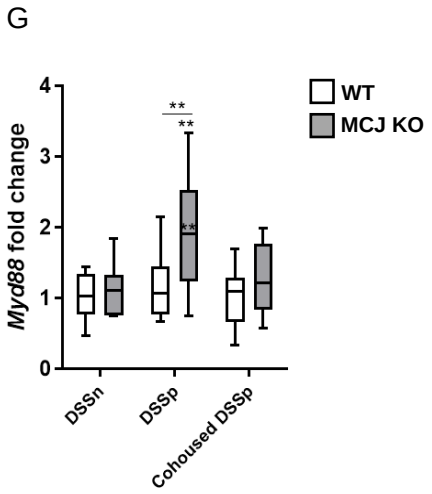

Figure 36. Evaluation of cohousing impact in colonic gene expression during UC. (**A**) Myeloperoxidase activity (U/mg prot). (**B**) Quantification of macrophage area (%) in colon tissue by immunohistochemistry (Anti-F4/80 antibody). (**C**) Flow cytometric detection of dendritic cells from mesenteric lymphoid nodes, shown as percentage (n=13 within cohoused groups). Gene expression analysis from mice colon tissue of (**D**) *Tnf*, (**E**) *Tnfr1*, (**F**) *Il1b* and (**G**) *Myd88*. Box whisker plots of median, quartiles and range with at least 8 mice per group (in DSS-treated groups), and at least 7 mice per group (in cohousing groups). White boxplots indicate WT and grey boxplots MCJ KO mice. For statistical analysis two-way ANOVA was used. An asterisk or asterisks "*" upside the box *versus* control genotype (DSS positive groups (DSSp) and cohoused groups (cohoused DSSp) *versus* the control (DSSn)). Significant differences within the same mice genotype between DSS-treated housed alone and cohoused groups are represented with asterisks inside the box of WT and MCJ-deficient mice that were housed alone (DSSp). Differences between genotypes in the same experimental group are presented as a line with an asterisk or asterisks.

3.1.2.3 Interaction between bacterial community and colonic protein levels

To delve into the impact that microbiota composition may have in the gut, we conducted a comprehensive proteomic analysis of the mouse colonic tissue. We identified and quantified a total of 4695 proteins. 153 proteins were differentially (*p* value < 0.05) expressed between WT and MCJ-deficient mice at steady state (no DSS treatment), 140 between separately housed DSS-treated groups, and 145 between cohoused DSS-treated groups. Functional annotation enrichment analysis revealed many pathways that were significantly different between WT and MCJ-deficient mice (Figure 37A). In homeostasis, proteins related to molecular function (MF) gene ontology (GO) pathways such as cofactor, nucleoside and actin-binding, and coupled ATPase activity were upregulated in the absence of MCJ. Notably, some proteins associated with MF pathways were enriched in MCJ-deficient mice compared to WT mice only when mice were cohoused, such as ATPase, helicase and enzyme activator activity, which demonstrates the potential of the microbiota to regulate the colonic proteome. Strikingly, separately-housed and cohoused MCJ-deficient DSS-treated mice exhibited significant (p.adj < 0.05) shifts in their proteomes, including both GO MF and biological processes (Figures 37A, 38A). Microbiota transmission during cohousing also eliminated some differences between separately-housed *versus* cohoused MCJ-deficient mice, such as proteins involved in cell adhesion. To decipher the biological complexity of colon proteomes, we assembled a protein interaction network of the upregulated proteins and pathways linked to MF GO in the cohoused DSS-treated MCJ-deficient mice compared to cohoused WT mice (Figure 37B). Remarkably, numerous proteins related to ATPase activity and helicase activity were connected. In the protein network that shows the significantly enriched proteins within the GO MF in MCJ-deficient DSS-treated mice housed compared to cohoused, we found multiple interactions between proteins with enzyme activator activity, actin-binding and cell adhesion molecule binding (Figure 37C). Furthermore, acquisition of the WT microbiota by MCJ-deficient mice during cohousing affected numerous metabolic processes and the establishment of cell polarity (Figure 38A).

As expected, we also observed increased oxidative phosphorylation in the absence of MCJ, both in healthy and DSS-treated housed alone conditions (Figure 38B). In addition, proteins associated with Cellular Component and KEGG pathways, suggested increased mitochondrial respiration (mitochondrial inner membrane, mitochondrial matrix and oxidoreductase complex) and metabolic pathways (carbon, pyruvate and propanoate metabolism, TCA cycle) in MCJ-deficient mice compared to WT mice in the absence of DSS (Figures 38B, C). Lastly, in MCJ-deficient mice, cohousing augmented microtubule plus-end binding compared to cohoused WT mice, an essential activity for cell motility, mitosis and intracellular transport (Figure 38B).

A

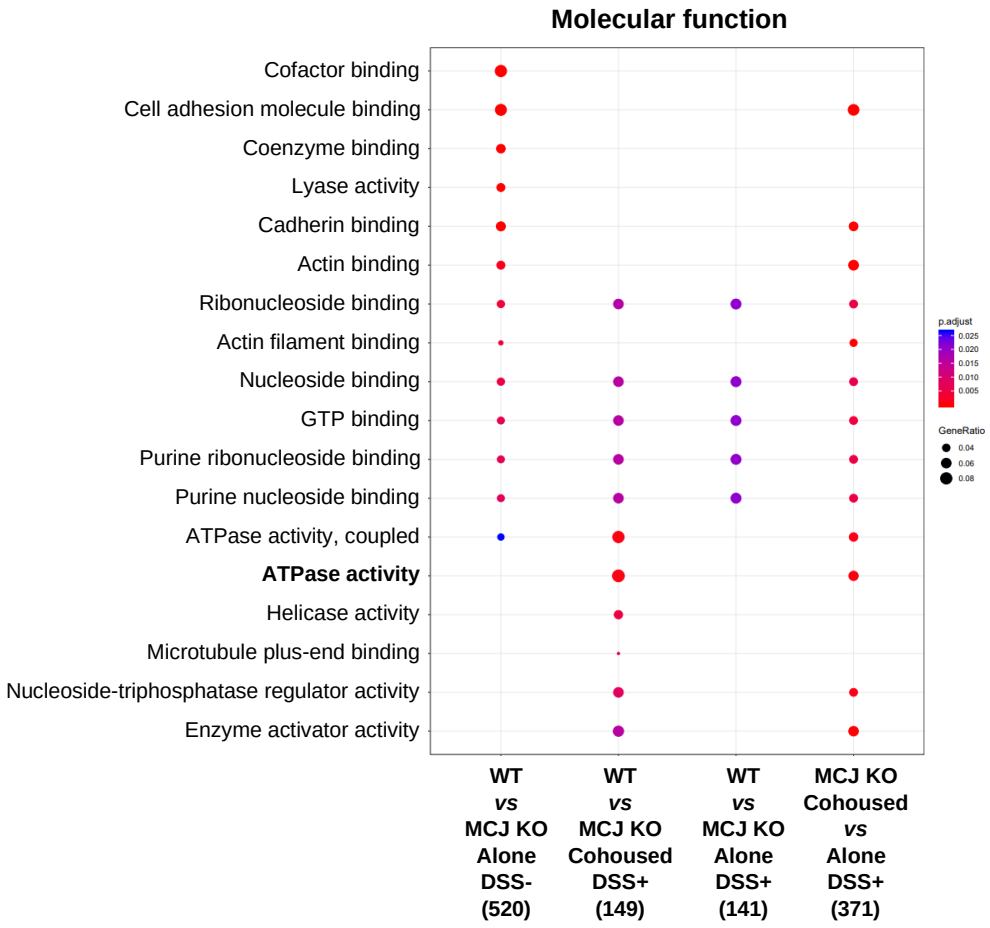

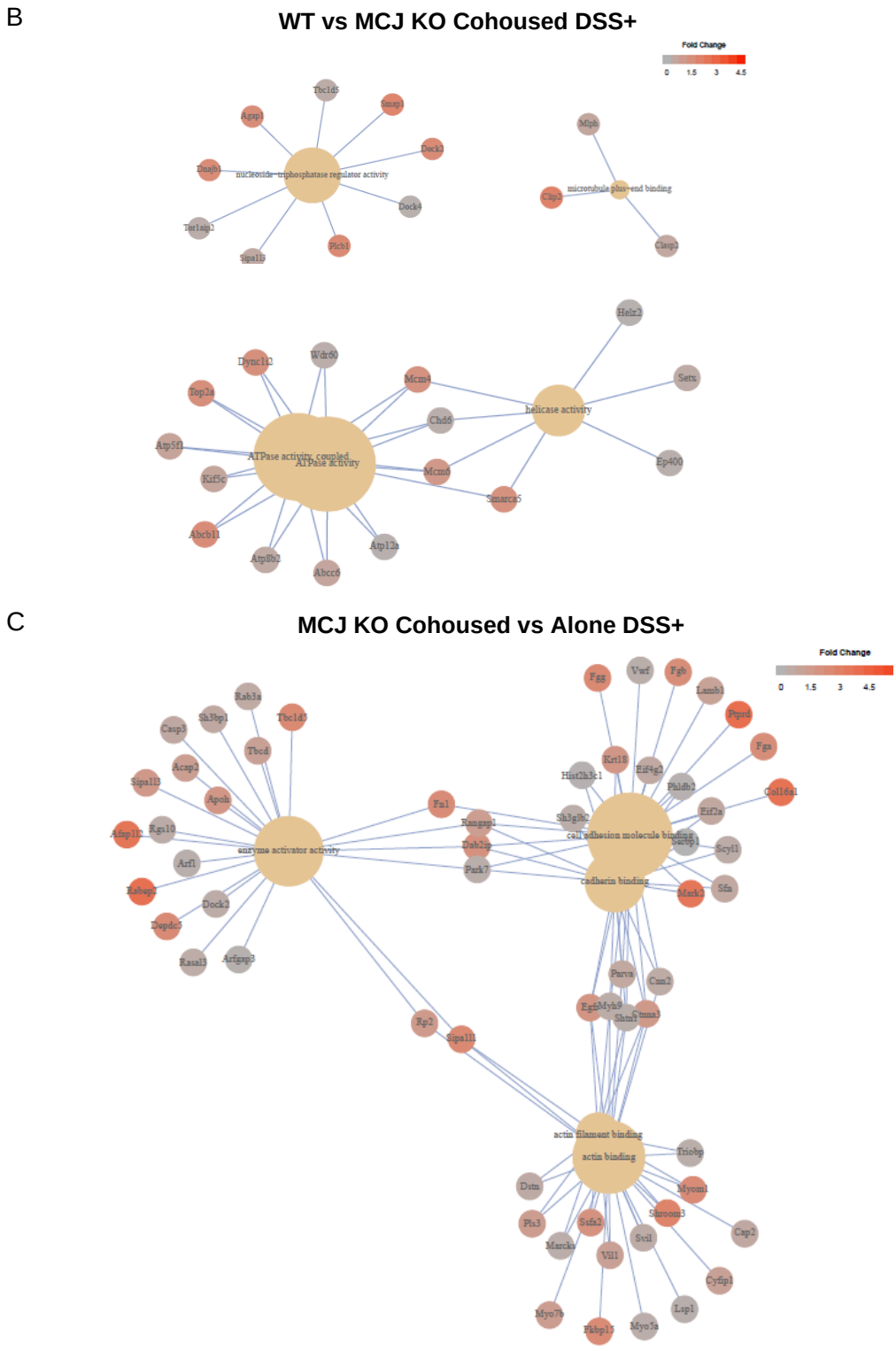

Figure 37. Differential proteome analysis of cohoused mice during acute colitis. (**A**) GO pathway enrichment analysis. Dot plot shows the upregulated proteins linked to molecular function (MF) GO pathways (FDR <0.05) in the different comparisons. Dot size reflects gene count enrichment in the pathway, and dot color displays pathway enrichment significance (p.adj), being red color the most significant. Proteins implicated in the most significant MF GO pathways in DSS-treated (**B**) cohoused (WT *vs* MCJ KO) and (**C**) MCJ-deficient (Cohoused *vs* Alone) mice conditions.

A

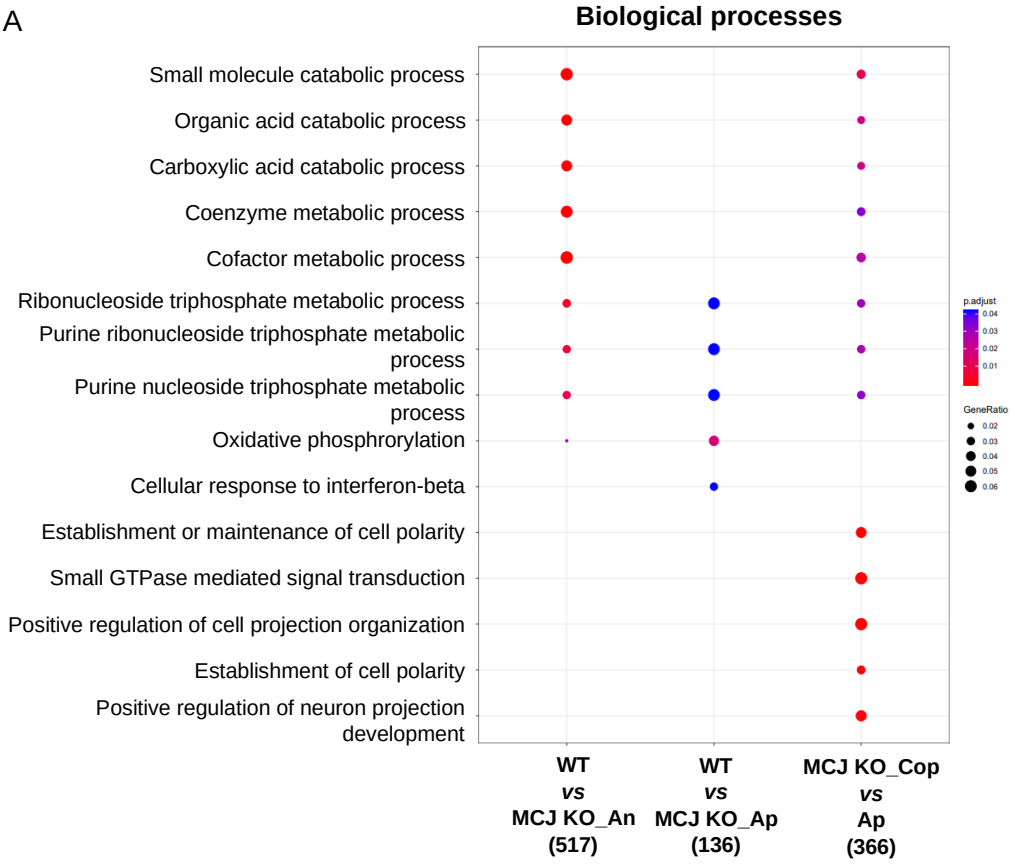
Biological processes
Small molecule catabolic process
Organic acid catabolic process
Carboxylic acid catabolic process
Coenzyme metabolic process
Cofactor metabolic process
Ribonucleoside triphosphate metabolic process
Purine ribonucleoside triphosphate metabolic process
Purine nucleoside triphosphate metabolic process
Oxidative phosphrorylation
Cellular response to interferon-beta
Establishment or maintenance of cell polarity
Small GTPase mediated signal transduction
Positive regulation of cell projection organization
Establishment of cell polarity
Positive regulation of neuron projection development
p.adjust
0.04
0.03
0.02
0.01
GeneRatio
0.02
0.03
0.04
0.05
0.06
WT vs MCJ KO_An (517)
WT vs MCJ KO_Ap (136)
MCJ KO_Cop vs Ap (366)

B

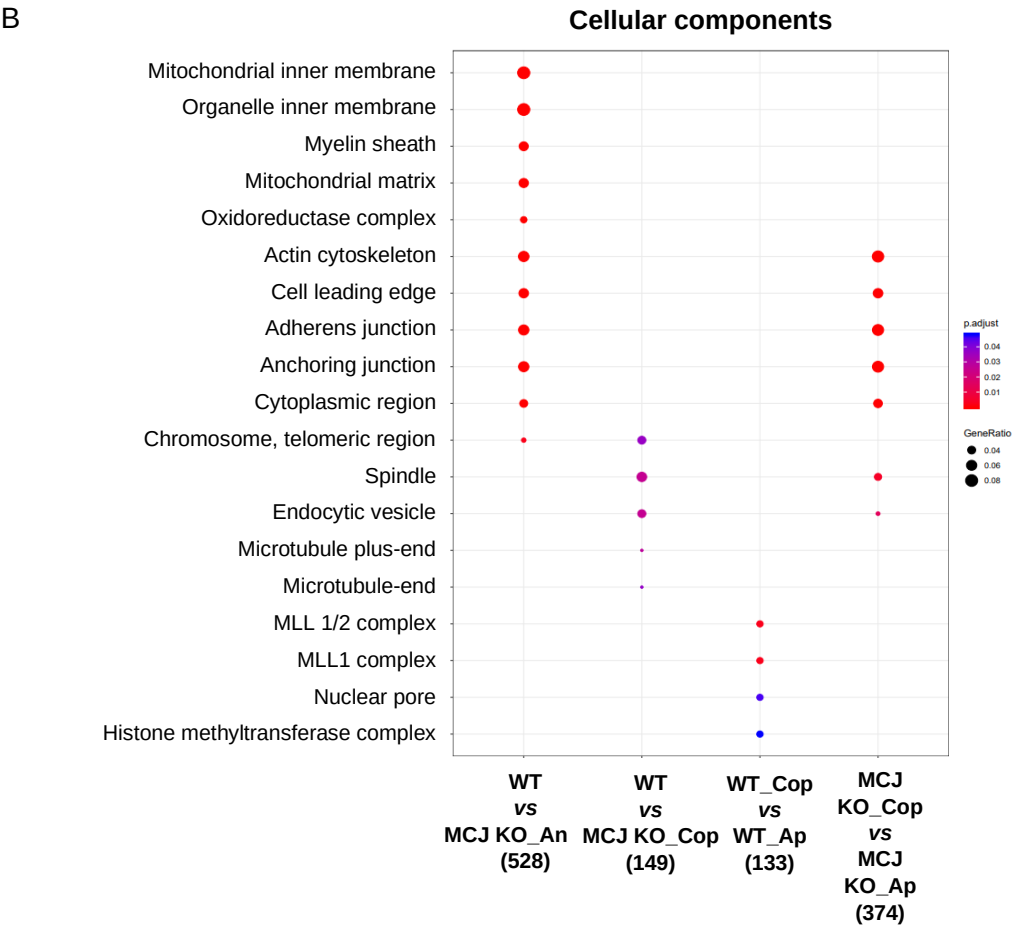
Cellular components
Mitochondrial inner membrane
Organelle inner membrane
Myelin sheath
Mitochondrial matrix
Oxidoreductase complex
Actin cytoskeleton
Cell leading edge
Adherens junction
Anchoring junction
Cytoplasmic region
Chromosome, telomeric region
Spindle
Endocytic vesicle
Microtubule plus-end
Microtubule-end
MLL 1/2 complex
MLL1 complex
Nuclear pore
Histone methyltransferase complex
p.adjust
0.04
0.03
0.02
0.01
GeneRatio
0.04
0.06
0.08
WT vs MCJ KO_An (528)
WT vs MCJ KO_Cop (149)
WT_Cop vs WT_Ap (133)
MCJ KO_Cop vs MCJ KO_Ap (374)

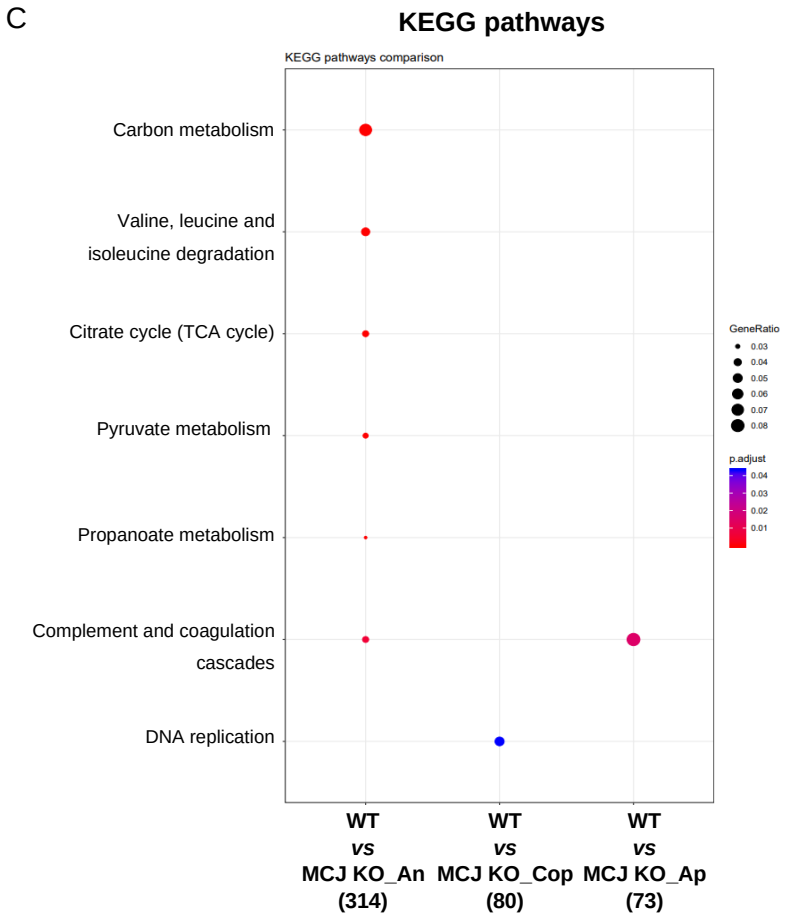

Figure 38. The impact of cohousing on host proteome. Dot plot shows upregulated proteins associated with the GO terms (FDR <0.05) of (**A**) biological processes, (**B**) cellular components and (**C**) KEGG pathways identified under the different contrasts. Dot size reflects gene count enrichment, and dot color displays pathway enrichment significance (p.adj < 0.05), being red color the most significant.

We performed a Spearman correlation analysis to identify associations between proteins significantly different between WT and MCJ-deficient colitis colon tissue with specific microbial OTUs (Figure 39). Interestingly, *A. muciniphila,* which was augmented in the MCJ-deficient mice, was strongly associated with AP1M2 protein, a master regulator of intestinal epithelial cell polarization that is required for maintenance of immune homeostasis. Furthermore, *A. muciniphila* was associated with increased mitochondrial protein translation by tRNA synthetase RARS2 protein, and is also linked to the appropriate degradation of damaged proteins and cells by PSMC6 and RIP3K proteins. *A. muciniphila* was also related to C3, a central component of the complement cascade and part of the innate immune system that plays a key role in defense against pathogens. The *S24-7* family, which was generally increased in MCJ-deficient mice, also correlated positively with histone-related proteins, such as PSMC6, RIP3K and C3. Select *Lactobacillus* OTUs also strongly correlated with histone-related proteins, suggesting that some *Lactobacillus* strains could be involved in the epigenetic reprogramming of immune cells, for example in the process of innate immune memory acquisition. On the contrary, the *Bacteroides* genus and commensal *B. acidifaciens* showed a negative correlation with histone-related proteins. Collectively, our data indicate that microbiota-host interactions are critical for the development and function of the host immune system in UC.

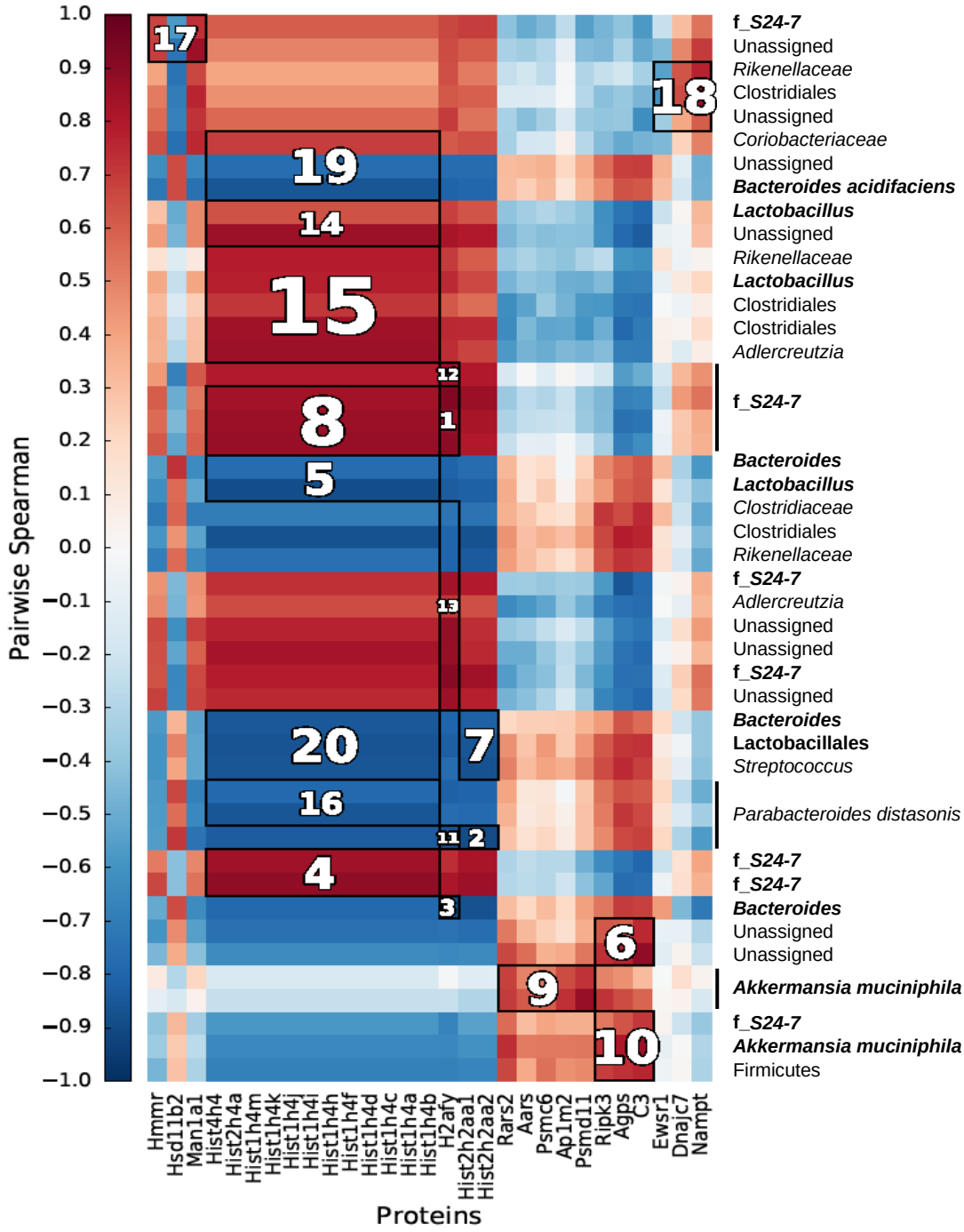

Figure 39. Heatmap of Spearman's rank correlation coefficients between the gut microbiota and host proteome. Associations were determined between bacterial OTUs from WT and MCJ KO mice treated with DSS and proteins enriched in the colon tissue. To identify significant associations, hierarchical all against all association (HAIIA) testing was performed.

In summary, transmission of microbiota between distinct genotypes underscores the reciprocal interactions between microbiota and host intestinal tissues, which regulate diverse host functions and responses. Our results support the further application of proteomics to human IBD to discover novel biomarkers for predicting disease progression or therapeutic responsiveness.

3.1.3 IgA-SEQ identifies potentially drivers of ulcerative colitis within MCJ deficiency

Previous work in either DSS-induced experimental mice or IBD patients suggested that disease-driving bacteria are highly coated with IgA. Therefore, we sought to determine whether bacterial IgA coating would identify a potential microbial signature associated with mitochondrial dysfunction and increased susceptibility to IBD development. We used magnetic activated cell sorting and 16S sequencing to characterize taxa-specific coating of the intestinal microbiota with immunoglobulin A (IgA-SEQ). We achieved good taxonomic resolution with a mean read count of 37.502 ± 8.773 sequences per sample and a Good´s coverage percentage of 100%. First, we studied alpha diversity indices of IgA coated bacteria including Observed species, Chao1 and Shannon (Figure 40A). IgA coated intestinal bacteria from MCJ-deficient mice after DSS treatment exhibited the lowest diversity indices as compared to IgA coated bacteria in DSS-treated WT mice (*p* value = 0.055) within Observed species and Chao1 indexes. Notably, IgA coated bacteria in MCJ-deficient mice upon DSS treatment displayed significantly reduced gut microbial diversity compared to those of healthy MCJ-deficient mice (*p* value = 0.019). *Proteobacteria* were the major phylum coated with IgA in all experimental groups (Figure 40B). Nonetheless, after induction of colitis (not previously at day 0), MCJ-deficient IgA coated taxa displayed significantly higher abundance of this phylum compared to WT group (*p* value = 0.0458). In homeostatic conditions, IgA coating of Actinobacteria was significantly decreased in MCJ-deficient mice compared to WT mice (*p* value = 0.0352).

To compare IgA coating levels between taxa, the IgA coating index score (ICI) for each taxon (relative abundance (IgA+) / relative abundance (IgA−)) was used. In homeostasis, WT mice showed increased IgA coating and relative abundance of *Bifidobacterium* and *Akkermansia* genera (Figure 40C). On the contrary, the segmented filamentous bacteria (SFB) *Candidatus Arthromitus*, *Elizabethkingia* and *Ochromobactrum* were highly coated in the MCJ-deficient mice whereas they had similar relative abundance in both genotypes, except *C. Arthromitus* that presented higher abundance in WT mice (Figure 40D). During intestinal inflammation, members of *Pasteurellaceae* (ICI 18.47) and *Veillonellaceae* (ICI 2.51) family, and *Achromobacter* (ICI 6.36) genus were more abundant and coated with IgA in MCJ-deficient mice microbiota.

Next, we used DESeq to identify statistically different OTUs abundance within IgA coated bacteria between genotypes. Prior to DSS-induced colitis, OTUs belonging to *Faecalibacterium* and *Streptococcus* genera were enriched in MCJ-deficient mice compared to WT, which instead exhibited increased abundance of *Bifidobacterium*, *Acidaminococcus* and *C. Arthromitus* (Figure 40D). After DSS administration, genera linked to colitogenic members such as *Achromobacter*, *Prevotella, Staphylococcus* and *Veillonella* were augmented in the MCJ-deficient mice, although putatively beneficial *Lactobacillus* and *Lactococcus* genera were also increased in this group (Figure 40E). Conversely, members of *Alistipes, Corynebacterium, Clostridium and Sutterella* were decreased in MCJ-deficient mice after DSS.

In summary, specific taxa were found to be of higher abundance and IgA coating in MCJ-deficient mice community and suggest that IgA-SEQ highlights a potential microbial signature linked to mitochondrial dysfunction.

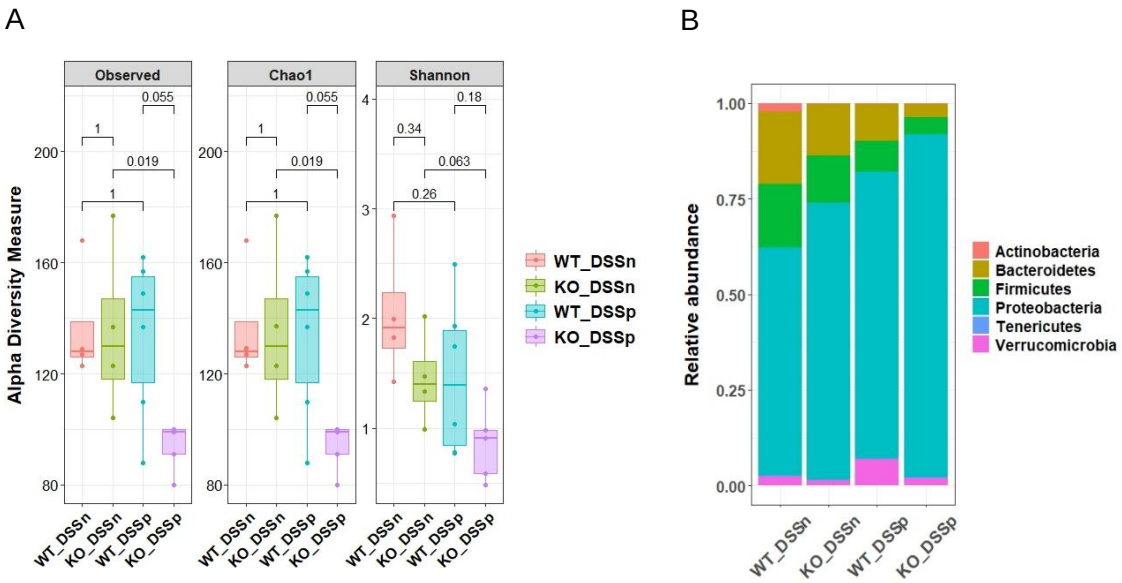

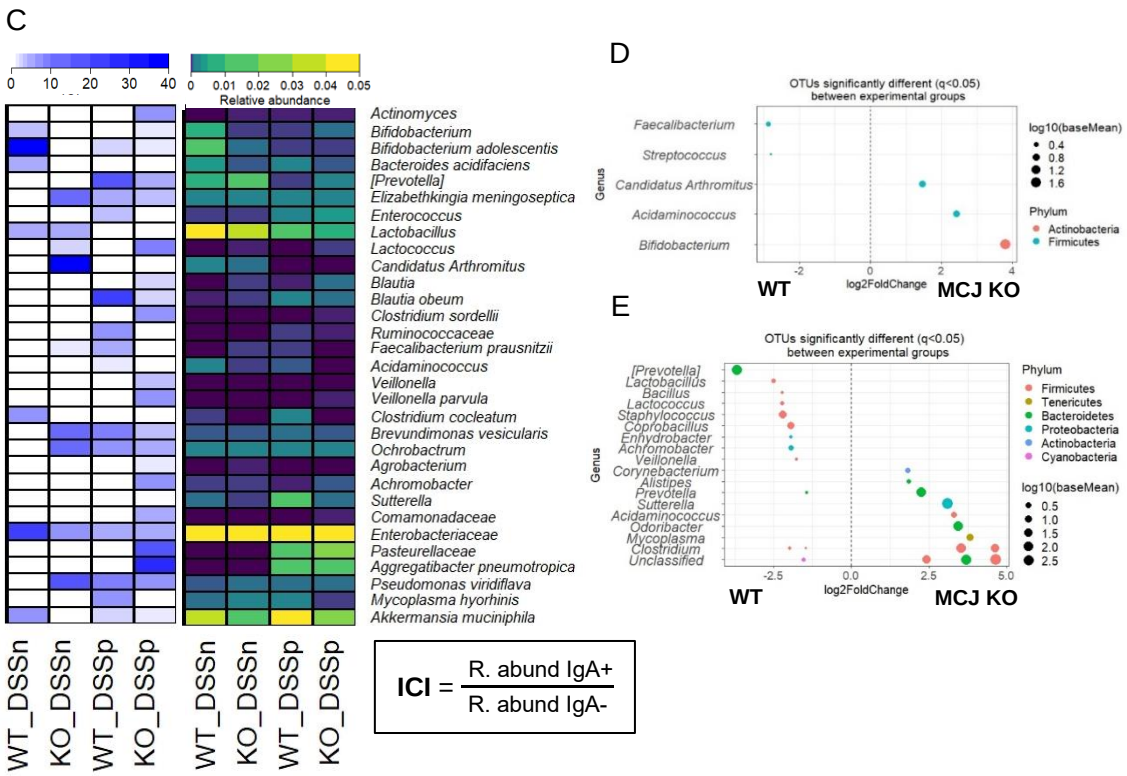

Figure 40. Differential IgA coating of WT and MCJ-deficient mice intestinal microbiota. IgA-SEQ technology was performed to identify specific taxa coated with IgA. (**A**) Observed OTUs, Chao1 and Shannon alpha diversity indices of bacteria coated with IgA (IgA+). The nonparametric Wilcoxon rank sum test was used for the statistical analysis. (**B**) Taxa bar plot at phylum level of intestinal bacteria coated with IgA in all experimental groups. In healthy conditions, WT mice displayed a significant enrichment of gut bacteria from Actinobacteria phylum coated with IgA compared to MCJ-deficient mice (*p* value = 0.0352). After colitis induction, MCJ-deficient mice exhibited a moderate enrichment of bacteria coated with IgA from Proteobacteria phylum (*p* value = 0.0458). (**C**) Heatmap representation of IgA coating index (ICI) score and relative abundances of specific bacterial families, genera and species coated with IgA. To calculate the ICI score, the relative abundance of the IgA+ fraction was divided by the IgA- fraction. In the ICI score heatmap, dark blue represents the highest ICI value and in the relative abundance heatmap, yellow color shows the highest relative abundance. Differentially abundant OTUs identified through DESeq2 testing (p.adj < 0.05) between WT and MCJ-deficient mice gut bacteria coated with IgA (**D**) in homeostasis (WT_DSSn *vs* KO_DSSn) and (**E**) in intestinal inflammation (WT_DSSp *vs* KO_DSSp). Each point represents a single OTU colored by phylum and grouped by taxonomic genus, and point´s size reflect the mean abundance of the sequenced data. KO: MCJ KO.

3.2 Discussion

Bidirectional mitochondria-microbiota interactions appear to be critical in numerous diseases including obesity, diabetes, intestinal inflammation and cancer (Vezza et al., 2020; Jackson and Theiss, 2020). We found that the colitis-prone phenotype of MCJ-deficient mice was transferable to GF mice after microbiota transplantation. Then, mice with altered mitochondrial function improved after cohousing with WT mice, suggesting the acquisition of protective microbial taxa by MCJ-deficient mice during cohousing. Finally, we sought to identify highly IgA coated bacteria that might contribute to intestinal disease in a mouse model of mitochondrial dysfunction. Notably, microbiome alterations also had dramatic impacts on the host colonic proteome.

Although most previously described colitogenic bacteria do not induce overt pathology in WT mice, they can trigger pathogenic inflammatory responses in genetically or environmentally predisposed animals (Palm et al., 2014). This is consistent with our finding that *Ruminococcus* and *Prevotella* are enriched in GF mice colonized with MCJ-deficient microbiota after DSS induction. Strikingly, *R. gnavus* was previously found to be enriched in IBD patients with increased disease activity, and high abundance of this bacterium has been associated with lack of response to anti-TNF treatment (Hall et al., 2017; Dovrolis et al., 2020). *Prevotellaceae* species were reported to exacerbate DSS-induced colitis (Elinav et al., 2011, Brinkman et al., 2013, Iljazovic et al., 2020) and to be highly IgA coated in dysbiotic mice (Palm et al., 2014). In agreement, *Prevotella* correlated positively with the DAI in our microbial transplantation experiment. The reduced *Oscillospira* and *Prevotella* abundance detected in MCJ-deficient mice after cohousing, suggested that decreased levels of specific microorganisms might be linked to a better prognosis. Low IgA coating of *Oscillospira* has been recently associated with earlier resection and has been considered a potential pathobiont that may exacerbate disease in the absence of a potent IgA response (Shapiro et al., 2021). In agreement with our results, gnotobiotic mice colonized with a community of organisms isolated from IBD patients that included *Oscillospira,* were more susceptible to DSS colitis (Palm et al., 2014). Furthermore, the high levels of *Il1b, Tnfr1* and *Myd88* expression detected in MCJ-deficient mice housed alone significantly decreased in cohoused MCJ-deficient mice after colitis induction, indicating that specific members of MCJ-deficient microbiota might be responsible for inducing increased pro-inflammatory cytokine production. Based on this data we confirmed a potential connection between mitochondrial function and microbiota composition by showing that MCJ-deficient mice exhibit a distinct microbial signature opening new venues for the prediction of disease outcome.

After cohousing with WT mice, we found that MCJ-deficient mice acquired many OTUs belonging to the *Lactobacillus* genus. Probiotics, including *Lactobacillus* have been suggested to maintain and induce remission within UC patients, although the efficacy of probiotics in IBD is still inconclusive (Derwa et al., 2017). Nonetheless, VSL#3 probiotic mixture (*Bifidobacterium*, *Lactobacillus*, and *Streptococcus*) has been demonstrated to have beneficial effects when inducing remission in active UC patients (56.2% failed to achieve remission with VSL#3 *versus* 75.2% in patients receiving placebo) (Tursi et al., 2010; Derwa et al., 2017). Furthermore, multiple OTUs belonging to *Lactobacillus* genera correlated negatively with DAI. Therefore, the augmented *Lactobacillus* taxa might explain the improvement seen in cohoused MCJ-deficient mice. Conversely, the positive correlation observed between *A. muciniphila* and the DAI, suggested that *A. muciniphila* might play a therapeutic role to ameliorate the elevated damage produced by DSS-induced colitis (Bian et al. 2019). Even though WT mice acquired some colitogenic members of the MCJ-deficient microbial community, including *Oscillospira* and *R. gnavus*, this did not affect the progression of colitis. In this case, the gut microbial ecosystem is complex and well-established, therefore the presence of defective mitochondria and the derived environment effect may be needed to develop a severe disease, pointing to an essential bidirectional interaction between gut microbiota and mitochondria in mucosal, epithelial and immune cells. However, FMT in GF mice had a stronger effect due to the less effective immune responses and defects in metabolism (Round and Mazmanian, 2009). Hence, due to the high heterogeneity observed in UC patients, assessment of mitochondrial function in patients has the potential to be an early indicator of course of the disease, leading to early prognosis, helping to choose the best therapy in order to obtain better outcome.

On the other hand, increasing knowledge of the proteome has the potential to improve our understanding in disease pathophysiology and promote personalized medicine. Importantly, we found that cohousing of animals was sufficient to alter the host proteome likely due to changes promoted by specific bacteria and their metabolites in the intestinal ecosystem. Many pathways affected by cohousing were related to tight junction dynamics that link tissue repair to the innate immune response (Banan et al., 2000; Binker et al., 2007; Vasileva and Citi, 2018). Collectively, our data suggests that specific members of the gut microbiota such as *Lactobacillus* might play an important role in modifying immune responses and consequently the proteome of subjects with altered mitochondria function.

Specific members of human intestinal microbiota have been demonstrated to be potentially involved in the development of chronic inflammatory responses. The low diversity of IgA coated taxa observed in MCJ-deficient mice during intestinal inflammation suggested that IgA coating could be linked to a high affinity, pathogen-specific and T-cell dependent response (Palm et al., 2014). Remarkably, we identified *Achromobacter* genus and bacteria belonging to *Pasteurellaceae* and *Veillonellaceae* families with higher abundance and higher IgA coating in MCJ-deficient mice after colitis induction. While IgA responses can protect against bacterially-driven intestinal inflammation, highly IgA coated bacteria have been shown to drive inflammatory disease indicating that the host IgA responses to select intestinal bacteria may be insufficient to fully neutralize or clear potentially pathogenic species (Palm et al., 2014). Furthermore, IgA coating can also sometimes facilitate bacterial colonization through antibody-enhanced biofilm formation (Bollinger et al., 2003; Shapiro et al., 2021). In agreement with our results, a study using a large cohort of pediatric UC patients reported enrichment of *Enterobacteriaceae*, *Pasteurellaceae*, *Veillonellaceae*, and *Fusobacteriaceae* families in patients with augmented inflammation (Gevers et al., 2014). Furthermore, *Achromobacter* and *Elizabethkingia* genera have been previously observed in UC patients with active disease (Walujkar et al., 2018). Interestingly, in homeostasis, we found that *Candidatus Arthromitus* and *Elizabethkingia* genera were highly coated in MCJ-deficient mice. *C. Arthromitus,* also known as SFB, is a potent inducer of the IgA response and Th17 cells, and have been suggested to drive intestinal inflammation in UC (Stepankova et al., 2007; Morgan et al., 2012; Flannigan et al., 2018). Of note, SFB appeared to be highly IgA coated in both colitis-induced, and dysbiosis- and colitis-induced specific pathogen-free mice (Palm et al., 2014). Collectively, we conclude that disturbed mitochondrial activity may critically impact microbial composition and host IgA responses, augmenting susceptibility to UC.

In conclusion, our study complements previous findings about the role of the microbiome in UC. Germ-free mice colonization demonstrated that the dysbiotic microbiota from MCJ-deficient mice can confer disease susceptibility. Mitochondrial dysfunction due to MCJ deficiency in UC was associated with increased *Oscillospira* and *Prevotella*, and decreased *Lactobacillus* abundances. However, we demonstrated that microbial transplant through cohousing with WT mice improved disease outcomes in MCJ-deficient mice. Finally, we identified Proteobacteria as the major phylum coated with IgA and significantly increased in MCJ deficient groups. Therefore, results from the present study suggest that microbiota-targeted treatment may be a valuable option in patients with mitochondrial dysfunction.

In summary, our findings support the use of therapies to eliminate specific pro-inflammatory bacteria and the use of probiotic supplementation therapy to restore gut homeostasis. However, the identification of colitis-associated microbial signatures continues to be a challenge and more biomarkers are needed to support microbial-based diagnostic and therapeutic approaches.

Chronic model of ulcerative colitis in MCJ-deficient mice

Publication

Peña-Cearra A, Castelo J, Pascual-Itoiz MA, Lavín JL, Fuertes M, Martín-Ruiz I, Barriales D, Palacios Araujo S, Fullaondo A, Aransay AM, Rodriguez H, Anguita J, Abecia L**.** MCJ deficiency increases TACE activity in chronic ulcerative colitis. *In preparation.*

4.1 Results

Whereas acute models of IBD have been widely used to analyze the onset of the disease characterized by a higher contribution of the innate immune system, human IBD is a chronic, relapsing and remitting intestinal inflammatory disorder. Therefore, we used a mouse model of chronic colitis to assess MCJ contribution in the chronic phases of the disease, which is more associated with the adaptive immune responses.

HYPOTHESIS	MCJ deficiency might be also an important player in the perpetuation of chronic inflammatory processes

4.1.1 Phenotypic evaluation of MCJ impact on chronic DSS-induced colitis

To examine MCJ contribution to chronic colitis, disease severity parameters were first assessed. Significant differences between genotypes in DAI were detected in the first cycle of DSS (days 3-6, 12, 15 and 16) and only at days 24 and 26 of the second cycle (Figure 41A). Strikingly, no differences were observed during the third cycle of DSS. Sustained WL was only detected on certain days of the first cycle (days 7, 13 and 16) (Figure 41B). At the end of the experimental period histological score, colonic length, intestinal permeability, neutrophil infiltration (MPO) and goblet cells quantity only changed due to DSS treatment (Figures 41C-G). Spleen weights also augmented after DSS treatment, albeit MCJ-deficient mice had significantly smaller spleen weights than WT mice (Figure 41H). Altogether, these data indicate that MCJ plays a key role in acute colitis, impacting the innate immune system response but its effect fades over the course of disease.

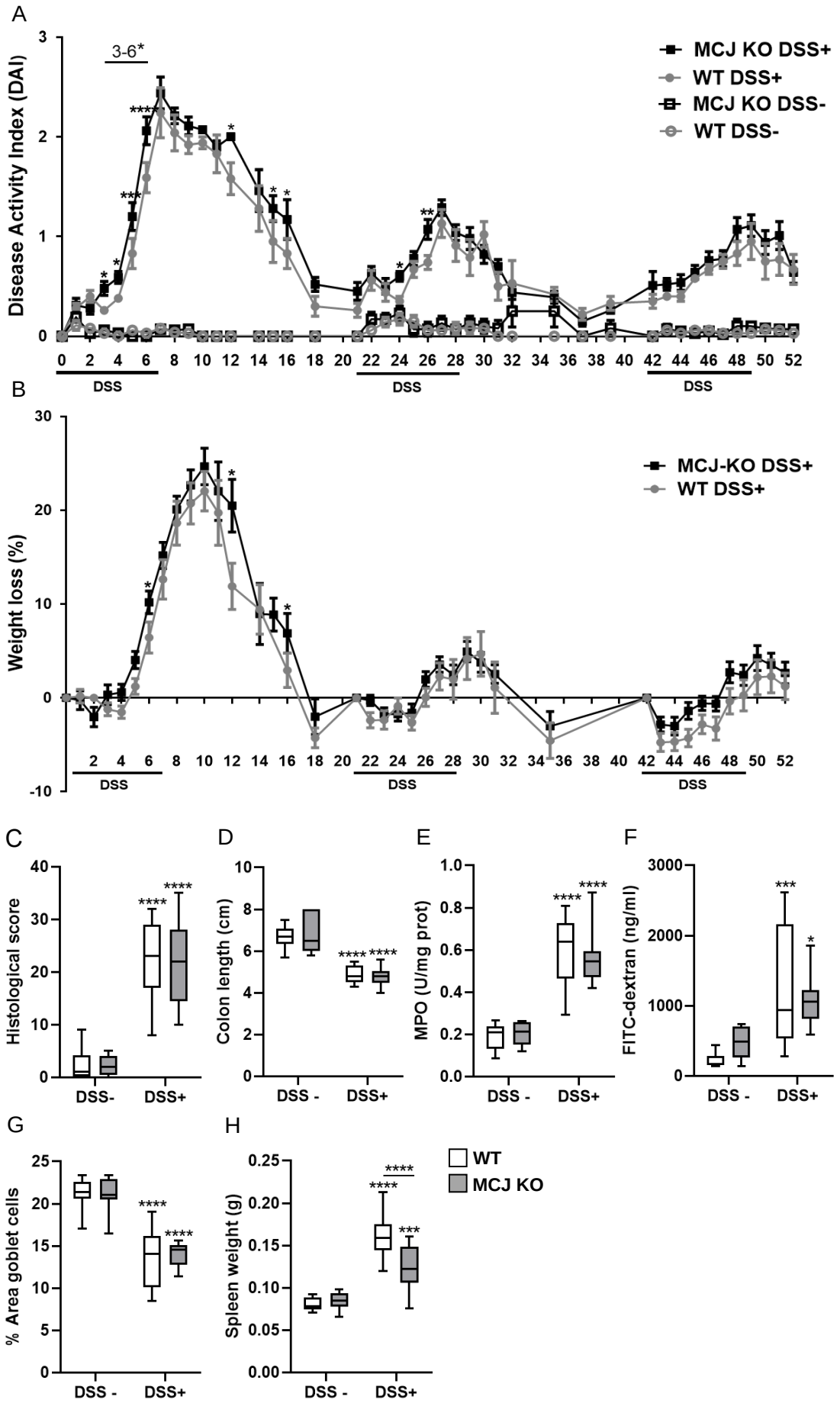
A
Disease Activity Index (DAI)
3-6*
MCJ KO DSS+
WT DSS+
MCJ KO DSS-
WT DSS-
DSS
DSS
DSS
B
Weight loss (%)
MCJ-KO DSS+
WT DSS+
DSS
DSS
DSS
C
Histological score
DSS-
DSS+
D
Colon length (cm)
DSS -
DSS+
E
MPO (U/mg prot)
DSS -
DSS+
F
FITC-dextran (ng/ml)
DSS -
DSS+
G
% Area goblet cells
DSS -
DSS+
H
Spleen weight (g)
DSS -
DSS+
WT
MCJ KO

Figure 41. Characterization of DSS-induced chronic colitis effect in MCJ-deficient mice. Experimental design: to induce chronic colitis, mice received 3 cycles of 2% DSS during 7 days with 15 days with water in between. After the last cycle of DSS mice were let 3 days with water to recover. (**A**) DAI and (**B**) WL percentage; data are means ± SEM. (**C**) Histological score. (**D**) Colon length (cm). (**E**) Permeability to the tracer FITC-dextran (ng/ml). (**F**) MPO activity (U/mg prot). (**G**) Goblet cells: % of positive cells stained with PAS. (**H**) Spleen weight (g). Grey lines and white boxplots indicate WT and black lines and grey boxplots MCJ KO mice. Box whisker plots of median, quartiles and range with at least 9 mice per group. For statistical analysis, two-way ANOVA was used as. In line graphs, an asterisk or asterisks "*" above the line for MCJ-KO DSS-induced chronic colitis (KO_P) *versus* WT DSS-induced chronic colitis (WT_P). In boxplots, an asterisk or asterisks above boxes *versus* control genotype (DSS+ *vs* DSS-), and asterisks above line *versus* different genotypes in the same experimental group.

4.1.2 Colonic gene expression analysis in chronic colitis

Next, we tested whether MCJ levels during chronic inflammation influence the inflammatory output and the TNF pathway modified due to MCJ deficiency. Of note, gene expression levels of *Tnf* substantially increased in the absence of MCJ in chronic inflammation compared to WT genotype (Figure 42A). Moreover, the metalloprotease TACE, involved in the cleavage of membrane-bound TNF to produce soluble TNF, also increased after chronic colitis induction in MCJ-deficient mice compared to WT, suggesting a higher sTNF/mTNF ratio (Figure 42B). In addition, no differences were observed between genotypes regarding *Timp3* levels (TACE inhibitor) in healthy controls and chronic DSS-induced colitis groups, and decreased expression of *Timp3* was detected after chronic colitis induction in both genotypes (Figure 42C). Although gene expression of *Tnfr1* did not significantly increase under chronic inflammatory conditions, MCJ-deficient DSS-treated group of mice showed higher *Tnfr1* levels than WT mice (Figure 42D). Importantly, gene expression levels of *Lcn2,* the biomarker of intestinal inflammation released by immune cells, and *Il1b,* the potent pro-inflammatory cytokine induced during colitis, were highly affected by MCJ levels when mice were treated with DSS (Figure 42E). Notably, MCJ-deficient mice displayed higher amount of IL-6 in chronic colitis compared to WT (Figure 42F). Regarding IL-10, lower levels were observed under inflammatory conditions in both WT and MCJ-deficient mice compared to healthy animals (Figure 42G). Remarkably, expression of the antimicrobial *Reg3b* was only increased in MCJ-deficient mice after induction of chronic colitis suggesting a more protective environment (Figure 42H).

Although *Tlr9* expression was increased in MCJ-deficient mice within chronic colitis, no significant differences were detected between genotypes and the expression of *Myd88* was not affected, suggesting that the *Myd88*-*Tlr9* signaling pathway might be critically regulated in the innate immune response, but not in chronic responses (Figure 42I). Additionally, *Tlr4* and *Tlr5* remained unchanged in colon tissue (Figure 42J). Next, we confirmed that DSS administration did not affect *Mcj* gene expression (Figure 42K). However, the expression of *Ifng*, which is known to act as an inhibitor of *Mcj* gene transcription, was highly increased in WT mice upon intestinal inflammation compared to MCJ-deficient mice (Figures 42L). Collectively, these results indicated that genes involved in the TNF pathway were significantly influenced by MCJ deficiency during chronic inflammation. Nevertheless, an opposite gene regulation of TACE and *Timp3* compared to acute colitis was found, which suggested an impact also on both forms of TNF (sTNF and mTNF).

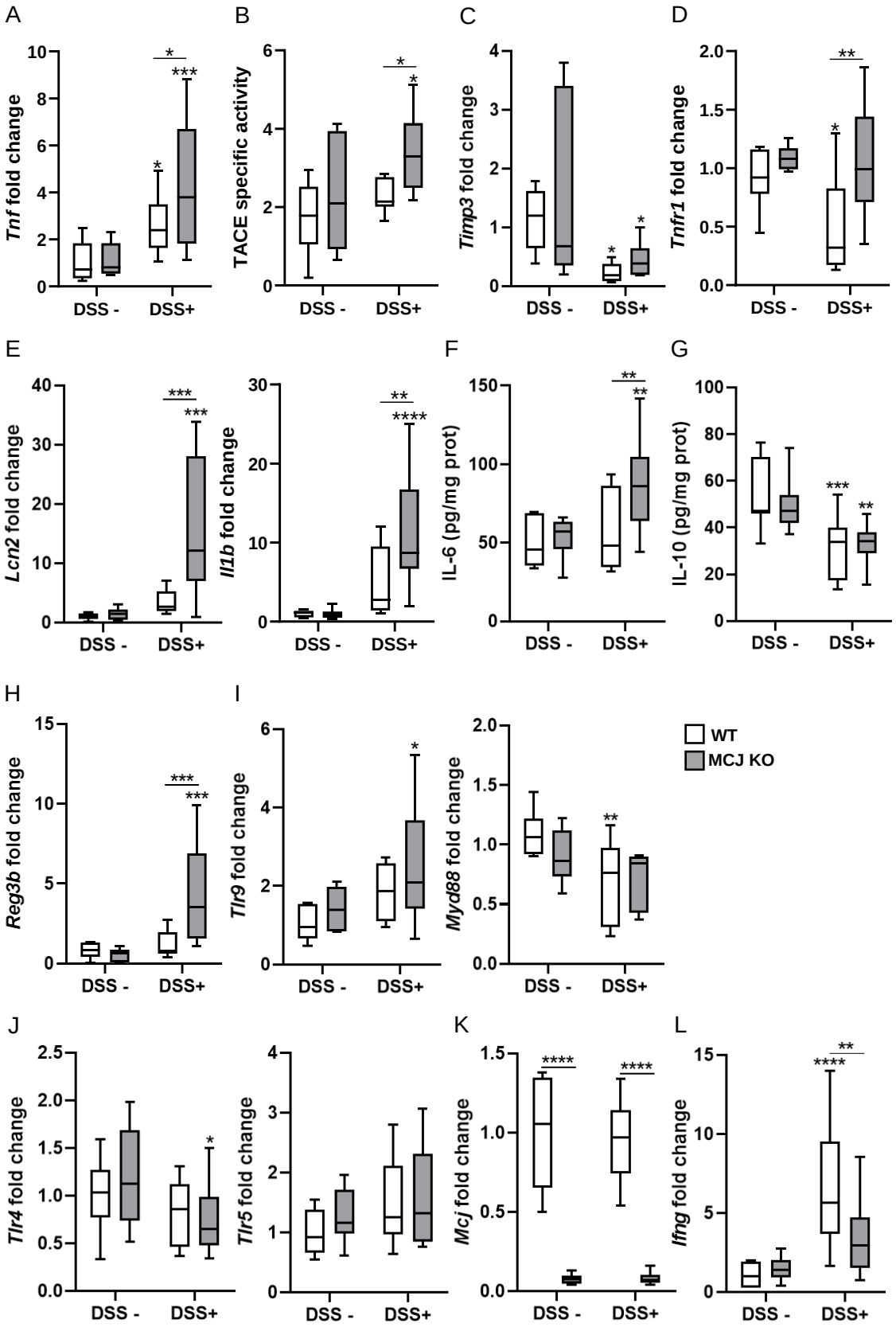
A
Tnf fold change
B
TACE specific activity
C
Timp3 fold change
D
Tnfr1 fold change
E
Lcn2 fold change
F
Il1b fold change
G
IL-6 (pg/mg prot)
H
IL-10 (pg/mg prot)
I
Reg3b fold change
J
Tlr9 fold change
K
Myd88 fold change
L
Tlr4 fold change
Tlr5 fold change
Mcj fold change
Ifng fold change
DSS -
DSS+
WT
MCJ KO

Figure 42. Evaluation of relevant genes and proteins during chronic colitis. Gene expression analysis from mice colon tissue of (**A**) *Tnf*, (**C**) *Timp3*, (**D**) *Tnfr1*, (**E**) *Lcn2* and *Il1b*, (**H**) *Reg3b*, (**I**) *Tlr9* and *Myd88*, and (**J**) *Tlr4* and *Tlr5*, (**K**) *Mcj* and (**L**) *Ifng* shown as mean fold change of treated experimental groups versus untreated WT group (DSS-) (n=9 mice per group at minimum). (**B**) TACE specific activity (n=7). (**F**) IL-6 and (**G**) IL-10 ELISA (pg/mg prot). White boxplots indicate wild-type and grey boxplots MCJ-deficient mice. Box and whisker plots of median, quartiles and range. For statistical analysis two-way ANOVA was used. An asterisk or asterisks "*" above boxes *versus* control genotype (DSS- *vs* DSS+), and an asterisk or asterisks above line *versus* different genotypes in the same experimental group.

4.1.3 Characterization of cellular immune responses in a murine model of experimental chronic colitis

Then, we sought to clarify the role of MCJ in innate and adaptive immune responses in a DSS-induced chronic colitis. Therefore, we determined the number and activation status of innate and adaptive cells in the MLNs. Within macrophages, significantly higher percentages of F4/80+CD11b+ cells were observed in mice administered with DSS compared to untreated mice regardless of the genotype (Figure 43A). However, the percentage of CD103+ dendritic cells increased in the absence of MCJ upon DSS treatment, being significantly different from WT mice (Figure 43B).

We also analyzed markers of T cell activation in the MLNs. The treatment with DSS resulted in a decreased percentage of MHC II+ cells (Figure 43C). However, even though there were also reduced compared to non-treated controls, the percentage of MHC II+ cells was significantly higher in MCJ-deficient mice, compared to controls (Figure 43C). Furthermore, the percentage of CD44+ cells in both the CD4+ and CD8+ T cell compartments were significantly higher in the absence of MCJ than in WT mice, albeit with a significant reduction in both genotypes compared to untreated animals (Figures 43D, E), probably as a result of T cell mobilization from the MLN to the lamina propria.

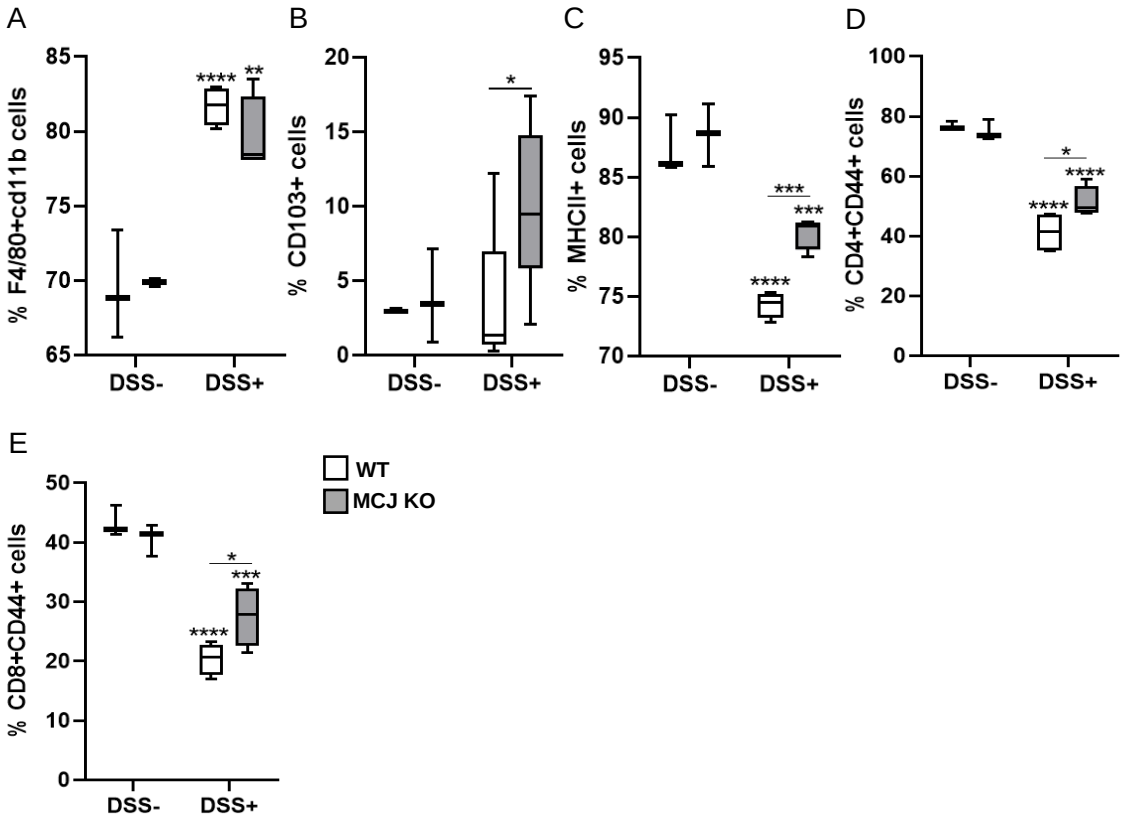

Figure 43. Characterization of cellular immune responses in a murine DSS-induced chronic colitis model. Flow cytometry analysis of lymphoid populations in MLNs, shown as percentage. (**A**) F4/80+CD11b macrophages, (**B**) CD103+ dendritic cells, (**C**) MHCII+ antigen presenting cells, and (**D**) CD4+CD44+ and (**E**) CD8+CD44+ T cells. Statistical differences. Box and whisker plots of median, quartiles and range. For statistical analysis two-way ANOVA was used. An asterisk or asterisks "*" above boxes *versus* control genotype (DSS- versus DSS+), an asterisk or asterisks above line *versus* different genotypes in the same experimental group.

4.1.4 Composition of host microbiome in a chronic DSS-induced colitis model

Secretory IgA provides protection against pathogens and toxins through immune exclusion and binds to bacteria regulating the composition and function of gut microbiota. Therefore, IgA levels were measured and a marked increase of IgA was found in chronic colitis-induced MCJ-deficient mice compared to WT animals (Figure 44A). Increased IgA responses in the absence of MCJ could be associated with changes in the intestinal microbiota. Then, bacterial *16S rRNA* gene was evaluated. A high taxonomic resolution was obtained with mean read counts of 97.954 ± 19.769 sequences per sample and a Good´s coverage percentage of 99%. First, microbial alpha diversity analysis revealed microbiota stabilization after 3 cycles of DSS, in fact, diversity indices did not show a substantial reduction due to DSS administration, which is typically observed in acute colitis (Figure 44B). Remarkably, the alpha diversity indices (Observed species and Chao1) significantly increased in MCJ-deficient mice when mice were treated with DSS. PCoA of the gut microbiome based on the non-parametric statistical method ANOSIM, showed not significant differences between WT and MCJ-deficient mice microbial communities either in homeostasis or chronic colitis (Figure 44C). Nevertheless, WT and MCJ-deficient mice exhibited distinct microbial composition differences in homeostasis at the phylum level (Figure 44D). Untreated MCJ-deficient mice presented higher Actinobacteria (8.4% *vs* 4.4%) and Bacteroidetes (31.1% *vs* 12.6%) compared to healthy WT. Moreover, we observed a significant enrichment of the phylum Verrucomicrobia in WT mice compared to MCJ-deficient mice (21.8% *vs* 4.8%). Of note, among all the significant differences identified at the phylum level in homeostasis, after chronic colitis induction only the differences observed at Bacteroidetes level persisted. To determine the OTUs that were statistically different between WT and MCJ-deficient gut microbial communities, DESeq2 tool was used. Without DSS administration, WT mice displayed increased levels of *Akkermansia*, *Clostridium*, *Coprococcus* and *Turicibacter* genera whereas MCJ-deficient mice showed higher levels of *Anaerobacillus*, *Bifidobacterium*, *Coprobacillus* and *Listeria* (Figure 44E). After chronic colitis induction, *R. gnavus*, commonly found in the absence of MCJ during acute inflammation, and the *Allobaculum* genus were significantly enriched in WT animals, compared to MCJ-deficient mice (Figure 44F). Nonetheless, MCJ-deficient mice exhibited enriched abundance of many genera upon chronic inflammation, including *Bacteroides*, *Coprobacillus*, *Coprococcus*, *Desulfuvibrio*, *Dorea*, *Lactobacillus*, *Oscillospira*, *Prevotella* and *Suterella*. Altogether, these data suggest that induction of chronic colitis diminished microbial composition

differences between genotypes, in which the high levels of IgA observed in the absence of MCJ could be partially responsible for the shifts in bacterial composition.

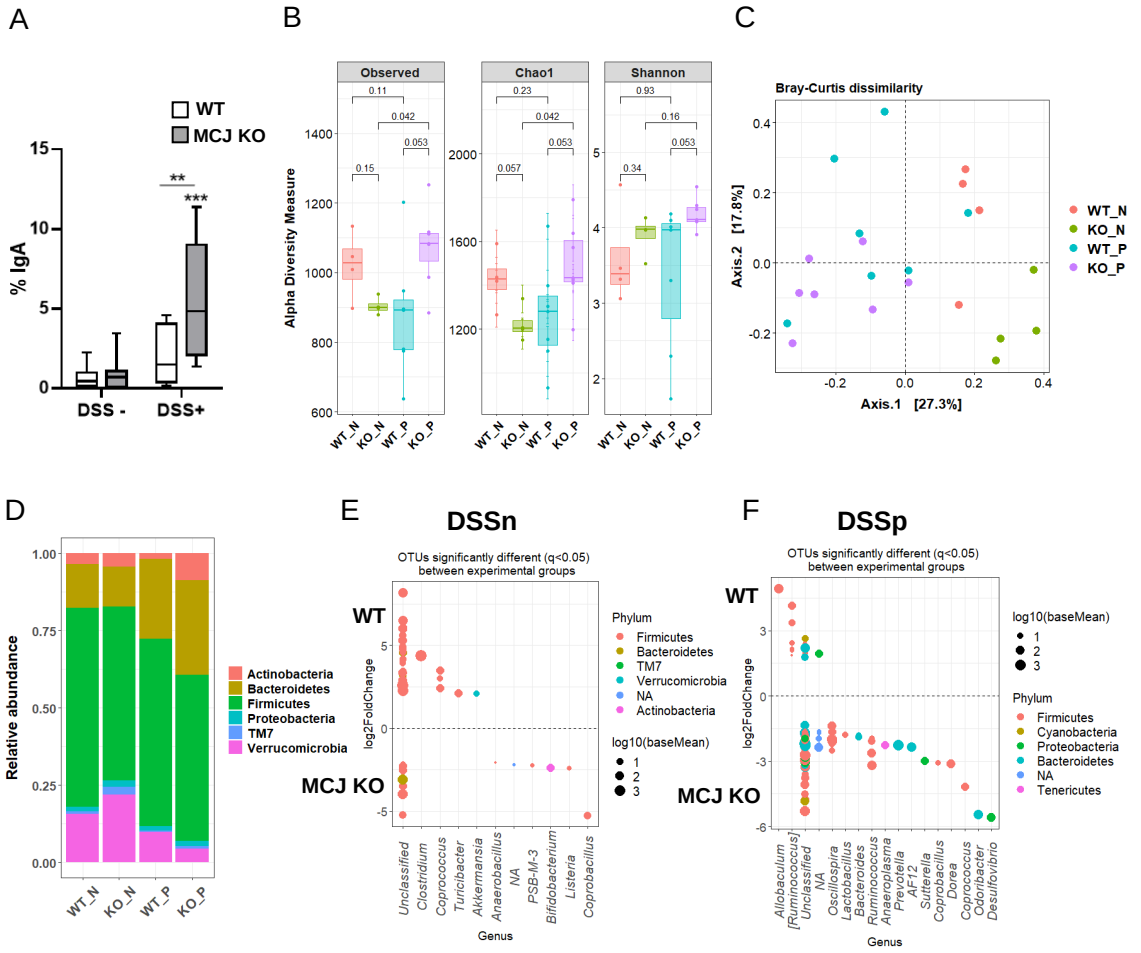

Figure 44. Impact of DSS-induced chronic colitis on the composition of host microbiome. (**A**) Quantification of IgA levels in colon tissue by immunohistochemistry. Box and whisker plots of median, quartiles and range, n=8 mice per group at a minimum. For statistical analysis two-way ANOVA was used. Asterisks "*" above boxes *versus* control genotype (DSS- *vs* DSS+), and asterisks above line *versus* different genotypes in the same experimental group. (**B**) Alpha diversity (total observed taxonomic units, Chao1 and Shannon diversity indices) in mice fecal microbiota. The non-parametric Wilcoxon rank sum test was used for the statistical analysis. (**C**) PCoA plot of bacterial beta-diversity based on Bray-Curtis dissimilarities. (**D**) Stacked bar plots showing the average relative abundance of bacterial phyla in the different experimental groups. Representation of OTUs that significantly (p.adj < 0.05) differ in colon content at genus level between (**E**) WT and MCJ-deficient controls and (**F**) WT and MCJ-deficient chronic colitis groups. Each point represents a single OTU colored by phylum and grouped by taxonomic genus, and point´s size reflect the mean abundance of the sequenced data.

4.2 Discussion

Acute models of IBD have been widely used to reduce the heterogeneity observed in humans and to analyze the onset of the disease characterized by a higher contribution of the innate immune system. However, human IBD is a chronic relapsing and remitting disorder that involves chronic inflammation of the gastrointestinal tract. Therefore, a mouse model of chronic colitis was used to assess the contribution of MCJ contribution in adaptive immunity.

In our previous work, the MCJ-deficient murine model of DSS-induced acute colitis showed inhibited TACE activity and increased *Timp3* expression levels, which effectively prevented the shedding of TNF from the plasma membrane. Thus, the loss of MCJ resulted in increased transmembrane TNF, which could lead to a higher disease severity (Pascual-Itoiz et al., 2020). Conversely, within chronic inflammation we observed an augmented TACE activity in MCJ-deficient mice and *Timp3* depleted in both genotypes. Therefore, our results suggested a higher sTNF/tmTNF ratio in MCJ-deficient mice in this condition. Despite being both forms of TNF detrimental for the course of colitis, the expression of mTNF by CD14+ macrophages has been reported to be relevant in IBD (Atreya et al., 2011) and mTNF signaling has been implicated in the development of granulomas in CD patients (Perrier et al., 2013). Furthermore, inflammation could not be reduced by neutralization of sTNF, which suggested that the development and maintenance of inflammation might be dependent on mTNF (Perrier et al., 2013). Besides the strong evidence of TNF as a pro-inflammatory cytokine, TNF has also immunosuppressive functions that might play a beneficial role in IBD. In this regard, sTNF has been shown to sensitize activated T cells for apoptosis during the priming phase, thereby attenuating the extent and duration of T-cell reactivity, and consequently limiting T-cell-mediated inflammation (Müller et al., 2009). Collectively, our data suggest that the form of TNF highly affects disease severity during chronic colitis, and that sTNF could be linked to the amelioration of the MCJ-deficient phenotype reported in acute colitis.

The high levels of IL-1β secreted by colon lamina propria monocytes have been associated with disease activity and the high expression of *LCN2* by gut epithelial cells has been found in the inflamed areas of patients with IBD (Ligumsky et al., 1990; Reinecker et al., 1993; Stallhofer et al., 2015). Thus, both proteins serve as valuable indicators of inflammation. In agreement with our results, either *Il1b* or *Lcn2* were increased in MCJ-deficient mice upon chronic inflammation. Indeed, results agreed with augmented *Il1b* reported in acute colitis due to MCJ deficiency (Pascual-Itoiz et al.,

2020). Nevertheless, we did not observe the increased expression of the *Tlr9*/*Myd88* pathway shown within acute colitis due to MCJ deficiency compared to WT (Pascual-Itoiz et al., 2020). In this regard, *Tlr9* can respond to mtDNA, which is commonly released during active IBD, contributing to inflammation (Boyapati et al., 2018). Hence, although expression of pro-inflammatory cytokines was affected by MCJ level in colon tissue, it was not strong enough to show an increase in disease severity.

Changes in gut microbiota composition due to mitochondrial dysfunction is a hallmark in the pathogenesis of UC. Nevertheless, the differences observed in gut microbiota composition from healthy to colitis or between genotypes during acute colitis disappeared in the chronic model of ulcerative colitis. Despite being dysbiosis characterized by increased levels of Proteobacteria, both genotypes showed low quantities of Proteobacteria upon chronic inflammation. It seems that DSS-induced chronic colitis mice might become partially adapted to the inflammatory environment independently of the initial level of MCJ. Furthermore, it was demonstrated that the expression of *Mcj* in macrophages could be regulated in order to adapt metabolically to new conditions, as it could be the case in a chronic inflammation (Navasa et al., 2015a).

Host microbial-interactions are critical in the disease. Therefore, some of the shifts observed due to MCJ deficiency including increased *Lcn2*, *Reg3b* and IgA, could be implicated in the regulation of gut microbial composition mirroring microbiota in the control group (WT). Among the diverse physiological functions of LCN2, one is to limit bacterial growth and REG3B modulates host defense processes via bactericidal activity on Gram-positive bacteria. In addition, augmented levels of IgA could be associated with a higher binding to gut microbiota that regulates its composition and function (Yang and Palm, 2020). Hence, these shifts could have shaped microbiota composition in the absence of MCJ, resulting in decreased *R. gnavus* levels compared to WT animals and improving the disease outcome.

Antigen presenting dendritic cells and macrophages are inducers and regulators of immune responses. Although we did not detect differences between genotypes regarding macrophage infiltration upon chronic inflammation, it was observed a significant influx of dendritic cells into the MLN in MCJ-deficient mice, which could be involved in the interaction with B cells and initiate antigen-specific antibody responses (Hall et al., 2011). Even though DSS colitis is caused primarily by disruption of the epithelium and activation of macrophages and neutrophils, T-cell responses affect the inflammatory response at later phases of the disease. During chronic DSS-induced colitis T cells might play an important role and interfere with colonic healing (Dieleman et al.,

1998). Remarkably, it was found a decline in both activated (CD44+) T CD4 and T CD8 cells in the MLN of mice with chronic colitis compared to controls, suggesting their mobilization to the lamina propria. However, after induction of chronic inflammation, MCJ-deficient mice displayed a higher percentage of these cells. Not only CD44 is a marker of T cell activation and is a property of long-lived memory cells, but also it is involved in T cell trafficking and adhesion, activation and differentiation (Guan et al., 2009; Mitchell and Wiliams, 2010). These T-cell responses can result in effector cytokine production that contributes to the high levels of TNF and IL-6 produced by innate cells in both forms (acute and chronic) of DSS colitis. Although IL-6 is linked to the initiation of pro-inflammatory responses, recent evidence also suggests its involvement in healing processes (Sommer et al., 2014). Moreover, IL-6 has a large impact on antigen-specific B cell responses, that could result in a large number of plasma cells in the lamina propria leading to higher IgA levels (Eto et al., 2011). In this regard, a recent study showed that the altered microbiota of mice deficient in the kinase TAK1, promoted both IL-1β and IL-6 signaling pathways that are needed for the induction of protective intestinal Th17 cells (Xing et al., 2021). Overall, a higher production of IL-6 and IL-1β in MCJ-deficient mice could indicate a higher presence of protective T cells, and therefore, resistance to colitis.

Collectively, results from the present work provide evidence of the dynamic adaptation of the colon tissue to changes in the environment as a way to adapt metabolically to new conditions. MCJ/DnaJC15 is emerging as an important regulator of mitochondrial activity in experimental colitis. Therefore, the control of MCJ levels which impact on *Timp3* gene transcription and consequently alter TACE activity constitutes a mechanism to regulate cellular responses to environmental changes during chronic ulcerative colitis. Overall, it can be hypothesized that the deficiency of *Mcj* expression, results in a more efficient elimination of translocated bacteria without a concomitant increase in the chronic inflammatory damage.

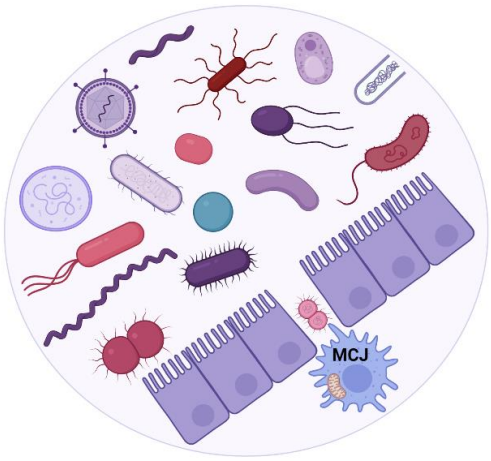

General discussion

IBD are complex and multifactorial disorders with unknown etiology. Although, a great progress has been made in terms of IBD pathogenesis, it is still out of reach and, consequently, efficient treatments and the implementation of precision medicine is far from being achieved. It seems that a causative combination of inherited susceptibility factors and environmental factors alter the epithelial barrier function, allowing the translocation of commensal bacteria and microbial products from the gut into the lumen wall, leading to immune cell activation and cytokine production (Neurath, 2014). Increasing evidence suggest that dysbiosis may play a pivotal role in the pathogenesis of IBD (Nishida et al., 2018). In addition, although the role that mitochondria dysfunction plays in IBD is not well understood, there is a significant connection between intestinal inflammation and mitochondrial function. In fact, numerous studies have pointed mitochondrial function as a key factor in both the onset and recurrence of disease (Novak and Mollen, 2015). In particular, a study conducted with UC mucosal transcriptomes found a decreased mitochondrial electron transport chain complex I activity, underlying disease severity and treatment response in IBD patients (Haberman et al., 2019).

To determine the possible contribution of the mitochondrial gene *Mcj* during acute colitis we used an experimental murine colitis model to overcome the clinical heterogeneity present in IBD patients (Imhann et al., 2018). Our first objective was to shed light on the role that mitochondrial function plays in the pathogenesis of IBD. Based on the previous knowledge generated in our lab (Navasa et al., 2015a), we confirmed that MCJ deficiency not only in bone marrow macrophages but also when cells are integrated in the colon tissue, affected TNF signaling pathway. At gut level, loss of MCJ also resulted in the upregulation of the TACE inhibitor *Timp3*, which prevents the shedding of TNF from the membrane. These data indicated that MCJ deficiency might contribute to disease severity at least partly due to the regulation of membrane TNF and its ability to signal through TNFR1. Importantly, our MCJ-deficient murine model resembled human disease, presenting UC patients similar gene expression levels of *MCJ* and *TIMP3*. This finding validated the use of our mouse model to study microbiota-mitochondria interaction during UC. Then, to know if the impact of MCJ was primarily limited to immune cells, we examined the effect of MCJ deficiency on epithelial cells´ colonic gene expression and we observed that epithelial cells were not affected by the loss of MCJ. Therefore, we focused our study on macrophages and by using colon samples from human colectomies we could determine the co-localization of MCJ within macrophages in IBD patients. Due to the difficulty that implies the acquisition and processing of human samples to isolate macrophages from colonic tissues obtained during surgery, we conducted a murine colon macrophage transcriptome to assess the

role of MCJ in this cell type. Our data showed that MCJ deficiency in murine macrophages had a strong impact on the expression of susceptibility genes identified in UC. In addition, Fc gamma receptors which are critical in the recognition of IgG coated targets showed elevated expression, including IgG coated bacteria that play a critical role in the intestinal homeostasis. Nevertheless, the differences observed between both genotypes in microbiota composition during acute colitis, indicated a regulatory relationship between microbiota and mitochondrial function. Alteration of microbiota composition regulated by MCJ levels might favour a potentially pathogenic and pro-inflammatory luminal environment through the production of specific metabolites that compromises the growth of commensal bacteria in UC (Rolhion and Chassaing, 2016, Parada Venegas et al., 2019). In this regard, we performed a metabolomics profiling approach to determine significant changes in the metabolome associated with mitochondrial dysfunction. Notably, we found increased levels of conjugated primary BAs that could have resulted from lumen environment perturbation due to MCJ deficiency in the host. Since BAs are antibacterial compounds, the microbiota from MCJ-deficient mice might be characterized by intestinal bacteria resistant to augmented levels of bile acids (Urdaneta and Casadesús, 2017). A good example could be *R. gnavus* that its abundance was augmented in colitis-induced MCJ-deficient mice. This bacterium expresses bile salt hydrolases indicating tolerance to bile acids (Begley et al., 2005; Zheng et al., 2017). Moreover, the elevated levels of *R. gnavus* found in IBD patients suggested its ability to tolerate the increased oxidative stress of the gut (Hall et al., 2017). Both parameters, BA metabolism (Lloyd-Price 2019) and *R gnavus* abundance, an important member of the altered gut microbiome in IBD (Hall et al., 2017), were described previously in different cohorts of IBD patients. Additionally, BAs concentration might influence consistency of stools, one of the three indicators measured to obtain the disease activity index, leading to a more severe disease (Duboc et al., 2012).

In this project we have shown that the bidirectional interaction between mitochondria and microbiota is crucial in the progression of the disease. Changes in the gut microbiota composition regulated by MCJ levels seem to be the principal hallmark of our experimental model of colitis. TNF inhibitors (anti-TNFs) are used routinely to induce clinical remission in patients with severe disease. However, a roughly one third of the IBD patients receiving anti-TNF agents may not respond (primary failure), and another third of the patients may lose response over time (secondary failure) (Singh et al., 2018). Thus, specific microbial signatures are being investigated as predictors of anti-TNF treatment outcomes. In addition, after the induction of acute colitis, the elevated expression of genes from the FcγR signaling observed in MCJ-deficient mice colon

macrophages together with the high colonic IgG levels, suggested MCJ deficiency to be associated with the lack of response to the anti-TNF treatment. To test our hypothesis, we used infliximab (anti-TNF agent), a chimeric human-murine anti-TNF monoclonal antibody proven to be effective for UC and able to bind both murine and human TNF (Lopetuso et al., 2013). As predicted, MCJ-deficient mice did not respond to IFX treatment, even after fecal microbial transplant by cohousing with WT mice indicating that the presence of defective mitochondria was enough for treatment failure. Noteworthy, WT mice did not respond to the treatment after microbiota transplantation from MCJ-deficient mice, suggesting that transmitted bacteria might induce pro-inflammatory cytokine production counteracting the effect of anti-TNF therapy. Therefore, our data reflects that either dysfunctional mitochondria or the presence of specific pro-inflammatory bacteria such as *R. gnavus*, *Prevotella* or *Oscillospira* might be valuable biomarkers for prediction of poor treatment response. In this regard, a blood biomarker to detect mitochondrial dysfunction in IBD patients will be very useful in clinical practice. Although c-reactive protein is the most widely used serum indicator of inflammation in IBD, based on results from this project and taking into account that monocytes are the precursors of colon macrophages, it would be desirable to identify non-invasive and rapid biomarkers to use in clinic in order to detect patients with mitochondrial perturbations. Currently, there is a growing need to personalize therapies to foster accurate clinical decision-making via enhanced use of existing biomarkers for the early detection and prevention of disease (Borg-Bartolo et al., 2020). In addition, implementation of personalized medicine has the potential to significantly contribute to a better quality of life and life extension of the patient, thereby minimizing the harmful side effects and guaranteeing a more successful result (Mathur and Sutton, 2017). This approach delays or prevents the need to apply more severe treatments and reduces healthcare costs associated with inappropriate treatments as well as hospitalizations for serious adverse drug reactions (Kasztura et al., 2019).

Based on our data, gut microbiota is a determinant player in the disease. Furthermore, there is growing evidence that certain members of the intestinal microbiota predispose individuals to disease, although the identification of disease-driving bacteria is still a major challenge (Palm et al., 2014). To identify a gut microbial signature linked to perturbed mitochondria with a potential role to predict disease progression, different approaches such as microbial colonization of GF mice, fecal microbiota transplantation by cohousing and IgA-SEQ were used. For the first time, we detected specific colitogenic members including *Oscillospira*, *Prevotella* and *R. gnavus* linked to mitochondrial malfunctioning due to MCJ deficiency by using microbial colonization of GF mice and

FMT. Furthermore, we found that high IgA coating identified different intestinal bacteria in MCJ-deficient mice with a potential role in disease progression and a higher proportion of IgA coated bacteria in the gut microbiota of this group of mice were Proteobacteria. Notably, we discovered that it was possible to transfer the mitochondrial dysfunction phenotype to GF mice and revert it by FMT. Mitochondrial perturbations have shown to promote substantial shifts in the colonic microbiota composition that are sufficient to cause increased susceptibility to DSS-induced colitis in GF mice. However, FMT did not affect WT phenotype, although it acquired some potential disease-driver bacteria of the MCJ-deficient microbial community, including *Oscillospira* and *R. gnavus* (Hall et al., 2017; Shapiro et al., 2021). In the case of FMT by cohousing in WT mice, the interaction of specific microorganisms with defective mitochondria seems to be necessary to develop a severe disease, pointing to an essential bidirectional interaction between gut microbiota and mitochondria function from mucosal, epithelial and immune cells. In this regard, FMT in GF mice probably had a stronger effect due to the less effective immune responses and defects in metabolism they present. In fact, these mice are susceptible to infections (Round and Mazmanian, 2009). Nevertheless, transfer of MCJ-deficient gut microbes and associated environment by cohousing may be more complicated as long as these mice display a complex and well-established gut microbial ecosystem in addition to a developed and antigen experienced immune system with increased reactivity to intestinal microbiota and increased serum antibody levels (Round and Mazmanian, 2009). Hence, in this thesis we propose some microbiota-targeted biomarkers to predict disease severity in patients with dysfunctional mitochondria. However, the identification of colitis-associated microbial signatures continues to be a challenge and more non-invasive biomarkers are needed to support microbial-based diagnostic and therapeutic approaches. In addition, variation in the microbiological environment of laboratory mice between research institutes or commercial breeding facilities may influence the composition of the gut microbiota and might contribute to the lack of reproducibility of animal model experiments between institutes (Laukens et al., 2016). Exposure to physical stress and differences in animal feeding can also change the composition of gut microbiome and influence experimental outcome. Furthermore, differences in the human gut microbiota composition might be associated with different factors, including host genetic, diet, age, mode of birth, smoking, antibiotics and lifestyle habits, among others, which influences biomarkers discovery (Hasan and Yang, 2019). In this regard, although advances in next-generation sequencing technologies have allowed comprehensive investigations of complex microbial communities, the lack of consensus and standardization in procedures from sampling to data analysis (handling and storage, nucleic acid extraction, *16S rRNA* gene primer selection, length, variable

regions, depth of sequencing, taxonomic reference databases and bioinformatics analyses) hinders comparisons of large microbiome datasets which are critical to find consistent microbial signatures of disease (Osman et al., 2018). Each methodological stage can introduce biases that can lead to changes in the relative abundances observed and affect the perception of community diversity (Pollock et al., 2018). Nevertheless, in this thesis consistent methodology was used in all stages of the gut microbiome analysis to minimize potential biases and prevent erroneous results.

Our findings support the use of therapies to eliminate specific pro-inflammatory bacteria and the use of probiotic supplementation therapy in order to restore gut homeostasis in patients with perturbed mitochondrial function. Although we used a broad-spectrum antibiotic that diminished microbial differences related to MCJ effect, *R. gnavus* survived in the gut of MCJ-deficient mice. Antibiotic administration resulted in increased disease activity, showing MCJ-deficient mice the highest DAI. The use of a broad-spectrum antibiotic was unable to remove some of the disease-driving members linked to MCJ deficiency. Thus, we suggest the implementation of targeted and personalized antimicrobial therapies that selectively eliminate harmful bacteria without killing of commensal bacteria (Xu et al., 2020). Regarding the use of probiotics, we conducted a microbiota transplantation approach by cohousing. In this approach we detected statistically higher *Lactobacillus* abundance in cohoused MCJ-deficient mice after colitis induction compared to MCJ-deficient mice housed alone. The *Lactobacillus* abundance correlated with disease severity improvement. Hence, our data provide an alternative treatment to anti-TNF agent based on probiotics supplementation with *Lactobacillus* in case of mitochondrial dysfunction. However, further studies are required to prove the effectiveness of this approach in the context of IBD patients with disrupted mitochondrial function.

Another interesting point studied in this thesis was the use of a chronic colitis model to mimic human IBD, which is characterized by chronic inflammatory responses and multiple exacerbations during disease progression. While acute colitis is based on short-lasting barrier alterations that involve mainly the innate immune system, chronic colitis may provide a greater understanding of the adaptive immune response (Wirtz et al., 2017). Indeed, this model is characterized by prominent regenerations of the colonic mucosa including dysplasia and frequent formation of lymphoid follicles (Okayasu et al., 1990). Although we obtained relevant information about the pathogenesis of IBD with the MCJ-deficient mouse model of acute colitis, we sought to identify the effect of MCJ on a chronic DSS-induced colitis model. Notably, in the first cycle of DSS, WT and MCJ-

deficient mice displayed differences in DAI that completely disappeared in the third cycle of DSS treatment. In both genotypes, the DAI decreased in the second and third cycles compared to the first one, suggesting a healing effect during the chronic phases that could be promoted by the mobilization of “antigen-experienced” T cells from the MLN to the lamina propria or by the presence of regulatory T cells. Moreover, MCJ deficiency in chronic colitis displayed an opposite regulation of some of the proteins and genes involved in the TNF signaling pathway compared to acute colitis, including TACE and *Timp3*. This modification might be linked to a higher production of sTNF rather than mTNF, thereby altering the susceptibility to DSS. In this regard, several studies have reported the importance of mTNF in the development and maintenance of inflammation (Perrier et al., 2013), whereas sTNF has been shown to be related to immunosuppressive functions (Müller et al., 2009). Regarding gut microbiota composition between WT and MCJ-deficient animals after the induction of chronic colitis, we did not observe important changes. Surprisingly, low quantities of Proteobacteria were detected in both genotypes, indicating that these mice might become partially adapted to the inflammatory environment generated by chronic DSS-induced colitis, independently of the initial level of MCJ. Nevertheless, specific microbial modifications in the MCJ-deficient mice may promote IL-1β and IL-6 signaling pathways, which are required for induction of protective intestinal Th17 cells and may be associated with the improved disease outcome (Xing et al., 2021).

Despite the informative potential of metagenomics and the valuable information obtained by this approach, we only focused our research on gut bacteria and not on fungi (mycobiota), viruses, archaea or eukaryotic parasites, although some members of these populations are known to be involved in IBD pathogenesis. In this regard, apart from bacteria, intestinal fungi are the most well-studied microorganisms. Therefore, relevant information regarding fungal dysbiosis and its interaction with mitochondrial function was lost in the present work. Thus, it would be very interesting to investigate the impact of dysbiosis in all microbial populations in our murine model deficient in MCJ. With regard to fungal dysbiosis, IBD patients are likely to have increased *C. albicans* abundances associated with active disease and delays in healing (Zwolińska-Wcisło et al., 2006; Zwolińska-Wcisło et al., 2009; Sokol et al., 2017). In these cases, antifungal therapy during *Candida* infection improved UC activity index (Zwolińska-Wcisło et al., 2006). Hence, in future studies we should elucidate the possible connection between mitochondrial dysfunction and the distinct gut microbial populations to find effective treatments, such as antifungal therapies in IBD patients with defective mitochondria.

Gene knockout in transgenic mice has been traditionally used to provide valuable insights into the physiological roles of gene products. While powerful, this approach has several limitations. The principal limitation encountered in the use of a murine model deficient in MCJ is that the target gene is ablated in all tissues and consequently gene deletion is not tissue-specific. Thus, it may be difficult to distinguish direct cell or tissue specific effects from secondary impacts arising through indirect actions in other organs. We should consider that both, direct or indirect consequences of gene products may contribute to observed phenotypes (Davey and MacLean, 2006). To avoid the problems usually observed in conventional knockout models, tissue specific gene knockout models have been developed. In tissue-specific knockouts, the phenotype tends to be closely related to the inactivation of the target gene in a specific location without secondary interferences. Therefore, by using this knockout model we could obtain information about tissue-specific function of the mitochondrial gene *Mcj* and it could be possible to detect associations and investigate causality.

In recent years, the advent of high-throughput processes and the utilization of omics-based techniques has allowed the rapid discovery of many candidate biomarkers. However, few of them have entered the clinic (Quezada et al., 2017). To study the complex biological processes and to identify a potential biomarker, an integrative approach that combines multi-omics data is needed. Omics integration permits determining the interrelationships of the involved biomolecules and their functions to obtain an accurate modeling of complex diseases (Subramanian et al., 2020). However, truly integrated multi-omics analyses have not been widely applied due to the challenging task that integrating different 'omics' datasets mean. In fact, omics integration relies heavily on data mining and machine learning algorithms that requires appropriate mathematical and statistical methodologies to describe causal links between different subcomponents (Alyass et al., 2015). Therefore, it would be very helpful to integrate multiomics datasets obtained from the experiments performed during this thesis (genomics, transcriptomics, metabolomics and proteomics) in order to have a greater understanding of the studied system. Nevertheless, additional efforts are needed to develop an analytical infrastructure that could be easily applied to the different types of omics and that could analyze data effectively (Olivier et al., 2019).

Another limitation found in the elaboration of the thesis was the unavailability of a primary antibody against murine MCJ and the limited number of immune cells obtained from colon tissue. Although we showed MCJ expression in human macrophages, we did not detect the specific location of MCJ in the mouse during DSS-induced experimental

colitis. Thus, it was not possible to determine the specific cell or tissue with the highest contribution. Moreover, the animal model we used mimics some typical histopathological and certain immunological characteristics of patients with IBD, but the model is not fully representative of the complex features of the disease. Despite all these limitations, the use of a mouse model deficient in MCJ was useful to illuminate host-microbial interactions during acute colitis.

In summary, the present thesis demonstrates the usefulness of the MCJ-deficient murine model to study UC pathogenesis. We provided a deep insight into the regulatory role of mitochondrial dysfunction on both forms of TNF (bound to membrane and soluble), macrophages transcriptome and microbiota composition in the gut, which are critical in the development of UC. MCJ-deficiency in colon macrophages affected many UC susceptibility genes, including genes from FCGR signaling pathway. The impact on this pathway was crucial to predict the failure of response to anti-TNF therapy. Furthermore, we identified specific groups of bacteria related to disease progression and impaired mitochondrial function, which might lead to changes in the luminal content favoring a pro-inflammatory environment. Thus, our findings point to specific microbial-based therapies as a promising strategy to control IBD. Collectively, our results open new avenues to the identification of potential biomarkers able to predict mitochondrial dysfunction and consequently, disease progression and anti-TNF response. Biomarkers permit the stratification of patients into distinct clinical entities of UC spectrum offering personalized therapies.

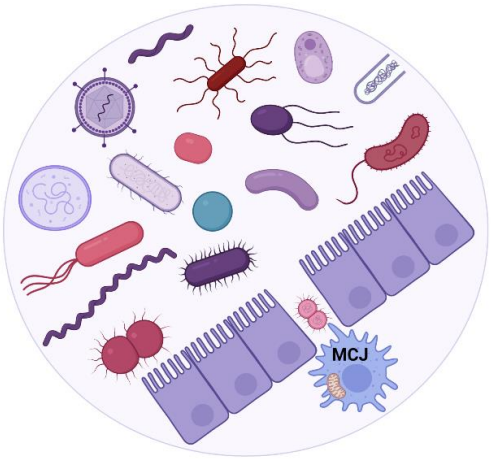

Conclusions

The results obtained in this thesis work, despite the limitations, offer valuable insights into the involvement of mitochondrial dysfunction in ulcerative colitis, leading to the following conclusions:

1. The loss of MCJ during acute experimental colitis highly increased the levels of *Timp3* resulting in the inhibition of TACE activity, which prevented the shedding of TNF from the cell membrane. The regulation of membrane TNF and its ability to signal through TNFR1 might contribute to a sustained disease progression.
2. MCJ-deficient murine model resembled human disease presenting similar gene expression levels of *MCJ* and *TIMP3* in the colon of ulcerative colitis patients. Therefore, validate the usefulness of this mouse model to study disease pathogenesis.
3. DSS-induced colitis in MCJ-deficient mice modified gut microbiota composition including augmented *R. gnavus* abundance and alteration in bile acid metabolism, showing a regulatory relationship between gut microbiota and mitochondrial function, which is critical for the development of ulcerative colitis.
4. MCJ expression was localized in gut macrophages from IBD patients suggesting that its effect was principally linked to macrophages. Indeed, colon macrophages´ transcriptome showed that MCJ deficiency impacted on several confirmed susceptibility-related genes for UC, including the expression of genes belonging to the FcγR signaling.
5. The failure of response of MCJ-deficient mice to anti-TNF treatment, even after fecal microbiota transplantation by cohousing, indicated that the mitochondrial dysfunction plays a critical role in the response to treatment. Thus, the identification of prognostic biomarkers for anti-TNF response based on mitochondrial-related genes would allow physicians to choose the best therapies for each individual patient.
6. The use of a broad-spectrum antibiotic diminished microbial differences related to MCJ deficiency. However, the abundance of *R. gnavus* persisted in the gut of MCJ-deficient mice contributing to the higher severity of the disease. Additionally, other disease-driving bacteria such as *Oscillospira* and *Prevotella* were related to MCJ deficiency in germ-free mice microbial colonization and fecal microbial transplantation approaches. Thus, the implementation of targeted and personalized antimicrobial therapies that selectively eliminate colitogenic bacteria would be of clinical value in IBD.

7. Microbial environment modified by mitochondrial dysfunction was transferred to germ-free mice (without mitochondrial impairment), which contributed to the development of the disease. However, MCJ-deficient disease phenotype was reverted by fecal microbiota transplantation after the acquisition of members of the microbiota such as *Lactobacillus*. Results corroborate the use of probiotic supplementation in patients presenting mitochondrial dysfunction.
8. The induction of chronic colitis showed a similar phenotype in MCJ-deficient and WT animals. In this regard, the augmented TACE activity observed in MCJ-deficient mice supported the association of the soluble form of TNF with a milder phenotype. Furthermore, microbial differences between genotypes were reduced and the higher production of cytokines such as IL-6 and IL-1β in MCJ-deficient mice indicated a higher presence of protective T cells.

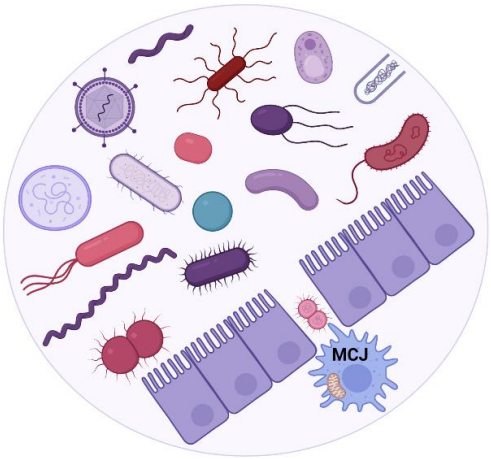

Conclusiones

Los resultados obtenidos a lo largo de este trabajo de tesis, ofrecen valiosos conocimientos sobre la implicación de la disfunción mitocondrial en la colitis ulcerosa a pesar de las limitaciones, llegando a las siguientes conclusiones:

1. La pérdida de MCJ tras la inducción de la colitis experimental aguda aumentó los niveles de *Timp3*, inhibiendo la actividad de TACE y evitando la liberación del TNF unido a la membrana celular. La regulación del TNF unido a membrana y su capacidad de señalización a través del TNFR1 podría contribuir al aumento de la gravedad de la enfermedad.
2. El modelo murino deficiente en MCJ se parece a la enfermedad humana, ya que los niveles de expresión génica de *MCJ* y *TIMP3* fueron similares en el colon de pacientes con colitis ulcerosa, lo que valida el uso de este modelo de ratón para estudiar la patogénesis de la enfermedad.
3. La colitis inducida por DSS en ratones deficientes en MCJ modificó la composición de la microbiota intestinal y el metabolismo de los ácidos biliares, aumentando la abundancia de *R. gnavus*. Lo que demuestra que existe una interacción bidireccional entre las mitocondrias y la microbiota intestinal, jugando un papel fundamental para el desarrollo de la colitis ulcerosa.
4. La expresión de MCJ en el colon de pacientes con EII se localizó en los macrófagos, lo que sugiere que su efecto está principalmente relacionado con estas células. De hecho, el estudio del transcriptoma de los macrófagos del colon mostró que la deficiencia de MCJ afectó a varios genes de susceptibilidad para la colitis ulcerosa, incluida la expresión de genes pertenecientes a la ruta de señalización de los FcγR.
5. Los ratones deficientes en MCJ no respondieron a los agentes anti-TNF, incluso después del trasplante de microbiota fecal por cohabitación, lo que indica que la disfuncionalidad mitocondrial juega un papel crítico en la respuesta al tratamiento. Por lo tanto, la identificación de biomarcadores de pronóstico para la respuesta a agentes anti-TNF basados en genes mitocondriales permitiría a los médicos elegir las mejores terapias para cada paciente.

6. El uso de antibióticos de amplio espectro previo a la colitis experimental disminuyó las diferencias microbianas relacionadas con la expresión de MCJ. Sin embargo, la abundancia de *R. gnavus* persistió en el intestino de dichos ratones contribuyendo a una mayor gravedad de la enfermedad. Mediante la colonización de ratones libres de microorganismos o el trasplante de microbiota fecal por cohabitación, otras bacterias con potencial colitogénico como *Oscillospira* y *Prevotella* también fueron asociadas con la deficiencia de MCJ. Por ello, la implementación de terapias antimicrobianas dirigidas y personalizadas que eliminen selectivamente las bacterias diana sería de valor clínico en la EII.
7. El ambiente microbiano modificado por la disfunción mitocondrial fue transferido a ratones libres de microorganismos (sin daño mitocondrial), contribuyendo a una peor progresión de la enfermedad. Sin embargo, el fenotipo de la enfermedad asociado a la deficiencia de MCJ se revirtió mediante el trasplante de microbiota fecal, a través de la adquisición de miembros comensales de la microbiota intestinal como *Lactobacillus*. Estos resultados corroboran el uso de suplementos probióticos en pacientes con alteraciones mitocondriales.
8. La inducción de la colitis crónica mostró un fenotipo similar entre los ratones deficientes en MCJ y los WT. El aumento de la actividad TACE en dichos ratones, relacionó la forma soluble de TNF con un fenotipo más leve. Además, la disminución de las diferencias microbianas entre genotipos, y el aumento de la producción de citocinas como IL-6 e IL-1β en ratones deficientes en MCJ podría estar asociado con una mayor presencia de células T protectoras.

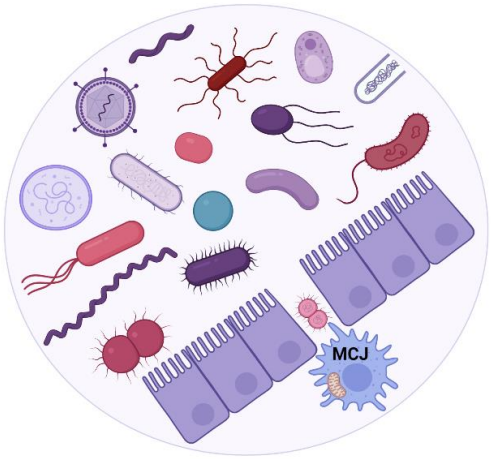

Bibliography

Alam MT, Amos GCA, Murphy ARJ, Murch S, Wellington EMH, Arasaradnam RP. Microbial imbalance in inflammatory bowel disease patients at different taxonomic levels. Gut Pathog. 2020;12:1.

Allaire JM, Crowley SM, Law HT, Chang SY, Ko HJ, Vallance BA. The Intestinal Epithelium: Central Coordinator of Mucosal Immunity. Trends Immunol. 2018;39:677-96.

Alyass A, Turcotte M, Meyre D. From big data analysis to personalized medicine for all: challenges and opportunities. BMC Med Genomics. 2015;8:33.

Al-Asmakh M, Zadjali F. Use of Germ-Free Animal Models in Microbiota-Related Research. J Microbiol Biotechnol. 2015;25:1583-8

Amarante-Mendes GP, Adjemian S, Branco LM, Zanetti LC, Weinlich R, Bortoluci KR. Pattern Recognition Receptors and the Host Cell Death Molecular Machinery. Front Immunol. 2018;9:2379.

Ananthakrishnan AN, Bernstein CN, Iliopoulos D, Macpherson A, Neurath MF, Ali RAR, et al. Environmental triggers in IBD: a review of progress and evidence. Nat Rev Gastroenterol Hepatol. 2018;15:39-49.

Angajala A, Lim S, Phillips JB, Kim JH, Yates C, You Z, et al. Diverse Roles of Mitochondria in Immune Responses: Novel Insights Into Immuno-Metabolism. Front Immunol. 2018;9:1605.

Aratani Y. Myeloperoxidase: Its role for host defense, inflammation, and neutrophil function. Arch Biochem Biophys. 2018;640:47-52.

Arumugam M, Raes J, Pelletier E, Le Paslier D, Yamada T, Mende DR, et al. Enterotypes of the human gut microbiome. Nature. 2011;473:174-80.

Ashaolu TJ. Immune boosting functional foods and their mechanisms: A critical evaluation of probiotics and prebiotics. Biomed Pharmacother. 2020;130:110625.8;102:443-79.

Atreya R, Zimmer M, Bartsch B, Waldner MJ, Atreya I, Neumann H, et al. Antibodies against tumor necrosis factor (TNF) induce T-cell apoptosis in patients with inflammatory bowel diseases via TNF receptor 2 and intestinal $CD14^+$ macrophages. Gastroenterology. 2011;141:2026-38.

Banan A, Fields JZ, Talmage DA, Zhang Y, Keshavarzian A. PKC-beta1 mediates EGF protection of microtubules and barrier of intestinal monolayers against oxidants. Am J Physiol Gastrointest Liver Physiol. 2001;281:G833-47.

Barbier-Torres L, Iruzubieta P, Fernández-Ramos D, Delgado TC, Taibo D, Guitiérrez-de-Juan V, et al. The mitochondrial negative regulator MCJ is a therapeutic target for acetaminophen-induced liver injury. Nat Commun. 2017;8:2068.

Begley M, Gahan CG, Hill C. The interaction between bacteria and bile. FEMS Microbiol Rev. 2005;29:625-51.

Belkaid Y, Hand TW. Role of the microbiota in immunity and inflammation. Cell. 2014;157:121-41.

Benharush D, Cohen MJ, Kasirer Y, Turner D. Short chain fatty acids (butyrate) for induction of remission in ulcerative colitis. Cochrane Database Syst Rev. 2019;2019:CD008730.

Bian X, Wu W, Yang L, Lv L, Wang Q, Li Y, et al. Administration of Akkermansia muciniphila Ameliorates Dextran Sulfate Sodium-Induced Ulcerative Colitis in Mice. Front Microbiol. 2019;10:2259.

Bindea G, Mlecnik B, Hackl H, Charoentong P, Tosolini M, Kirilovsky A, et al. ClueGO: a Cytoscape plug-in to decipher functionally grouped gene ontology and pathway annotation networks. Bioinformatics. 2009;25:1091-3.

Binker MG, Zhao DY, Pang SJ, Harrison RE. Cytoplasmic linker protein-170 enhances spreading and phagocytosis in activated macrophages by stabilizing microtubules. J Immunol. 2007;179(6):3780-91.

Biron CA. Chapter 4 - Innate immunity: recognizing and responding to foreign invaders—no training needed. In: Viral Pathogenesis. From Basics to Systems Biology 3er edn. Elsevier, 2016:41-55.

Bjerrum JT, Wang Y, Hao F, Coskun M, Ludwig C, Günther U, et al. Metabonomics of human fecal extracts characterize ulcerative colitis, Crohn's disease and healthy individuals. Metabolomics. 2015;11:122-33.

Black RA. TIMP3 checks inflammation. Nat Genet. 2004;36:934-5.

Bolisetty S, Jaimes EA. Mitochondria and reactive oxygen species: physiology and pathophysiology. Int J Mol Sci. 2013;14:6306-44.

Bollinger RR, Everett ML, Palestrant D, Love SD, Lin SS, Parker W. Human secretory immunoglobulin A may contribute to biofilm formation in the gut. Immunology. 2003;109:580-7.

Borg-Bartolo SP, Boyapati RK, Satsangi J, Kalla R. Precision medicine in inflammatory bowel disease: concept, progress and challenges. F1000Res. 2020;9:F1000 Faculty Rev-54.

Boyapati RK, Dorward DA, Tamborska A, Kalla R, Ventham NT, Doherty MK, et al. Mitochondrial DNA Is a Pro-Inflammatory Damage-Associated Molecular Pattern Released During Active IBD. Inflamm Bowel Dis. 2018;24:2113-22.

Brenner D, Blaser H, Mak TW. Regulation of tumour necrosis factor signalling: live or let die. Nat Rev Immunol. 2015;15:362-74.

Brinkman BM, Becker A, Ayiseh RB, Hildebrand F, Raes J, Huys G, et al. Gut microbiota affects sensitivity to acute DSS-induced colitis independently of host genotype. Inflamm Bowel Dis. 2013;19:2560-7.

Brodmann T, Endo A, Gueimonde M, Vinderola G, Kneifel W, de Vos WM, et al. Safety of Novel Microbes for Human Consumption: Practical Examples of Assessment in the European Union. Front Microbiol. 2017;8:1725.

Busquets D, Mas-de-Xaxars T, López-Siles M, Martínez-Medina M, Bahí A, Sàbat M, et al. Anti-tumour Necrosis Factor Treatment with Adalimumab Induces Changes in the Microbiota of Crohn's Disease. J Crohns Colitis. 2015;9:899-906.

Camuesco D, Comalada M, Rodríguez-Cabezas ME, Nieto A, Lorente MD, Concha A, et al. The intestinal anti-inflammatory effect of quercitrin is associated with an inhibition in iNOS expression. Br J Pharmacol. 2004;1

Caporaso JG, Kuczynski J, Stombaugh J, Bittinger K, Bushman FD, Costello EK, et al. QIIME allows analysis of high-throughput community sequencing data. Nat Methods. 2010;7:335-6.

Caporaso JG, Lauber CL, Walters WA, Berg-Lyons D, Lozupone CA, Turnbaugh PJ, et al. Global patterns of 16S rRNA diversity at a depth of millions of sequences per sample. Proc Natl Acad Sci U S A. 2011;108 Suppl 1:4516-22.

Cardinale CJ, Wei Z, Li J, Zhu J, Gu M, Baldassano RN, et al. Transcriptome profiling of human ulcerative colitis mucosa reveals altered expression of pathways enriched in genetic susceptibility loci. PLoS One. 2014;9:e96153.

Cario E. Toll-like receptors in inflammatory bowel diseases: a decade later. Inflamm Bowel Dis. 2010;16:1583-97.

Caruso R, Ono M, Bunker ME, Núñez G, Inohara N. Dynamic and Asymmetric Changes of the Microbial Communities after Cohousing in Laboratory Mice. Cell Rep. 2019;27:3401-3412.e3.

Castro-Dopico T, Dennison TW, Ferdinand JR, Mathews RJ, Fleming A, Clift D, et al. Anti-commensal IgG Drives Intestinal Inflammation and Type 17 Immunity in Ulcerative Colitis. Immunity. 2019;50:1099-1114.e10.

Champagne DP, Hatle KM, Fortner KA, D'Alessandro A, Thornton TM, Yang R, et al. Fine-Tuning of CD8(+) T Cell Mitochondrial Metabolism by the Respiratory Chain Repressor MCJ Dictates Protection to Influenza Virus. Immunity. 2016;44:1299-311.

Chan SN, Low END, Raja Ali RA, Mokhtar NM. Delineating inflammatory bowel disease through transcriptomic studies: current review of progress and evidence. Intest Res. 2018;16:374-83.

Changbumrung S, Tungtrongchitr R, Migasena P, Chamroenngan S. Serum unconjugated primary and secondary bile acids in patients with cholangiocarcinoma and hepatocellular carcinoma. J Med Assoc Thai. 1990;73:81-90.

Chassaing B, Aitken JD, Malleshappa M, Vijay-Kumar M. Dextran sulfate sodium (DSS)-induced colitis in mice. Curr Protoc Immunol. 2014;104:15.25.1-15.25.14.

Chen J, Bardes EE, Aronow BJ, Jegga AG. ToppGene Suite for gene list enrichment analysis and candidate gene prioritization. Nucleic Acids Res. 2009;37:W305-11.

Cheng FS, Pan D, Chang B, Jiang M, Sang LX. Probiotic mixture VSL#3: An overview of basic and clinical studies in chronic diseases. World J Clin Cases. 2020;8:1361-84.

Chhibba T, Ma C. Is there room for immunomodulators in ulcerative colitis? Expert Opin Biol Ther. 2020;20:379-390.

Cho JH, Brant SR. Recent insights into the genetics of inflammatory bowel disease. Gastroenterology. 2011;140:1704-12.

Chong J, Xia J. Computational Approaches for Integrative Analysis of the Metabolome and Microbiome. Metabolites. 2017;7:62.

Clark A, Mach N. The Crosstalk between the Gut Microbiota and Mitochondria during Exercise. Front Physiol. 2017;8:319.

Cohen RD, Yu AP, Wu EQ, Xie J, Mulani PM, Chao J. Systematic review: the costs of ulcerative colitis in Western countries. Aliment Pharmacol Ther. 2010;31:693-707.

Cohen LJ, Cho JH, Gevers D, Chu H. Genetic Factors and the Intestinal Microbiome Guide Development of Microbe-Based Therapies for Inflammatory Bowel Diseases. Gastroenterology. 2019;156:2174-2189.

Corthësy B. Secretory immunoglobulin A: well beyond immune exclusion at mucosal surfaces. Immunopharmacol Immunotoxicol. 2009;31:174-9.

Cosnes J. What is the link between the use of tobacco and IBD? Inflamm Bowel Dis. 2008;14 Suppl 2:S14-5.

Costello SP, Hughes PA, Waters O, Bryant RV, Vincent AD, Blatchford P, et al. Effect of Fecal Microbiota Transplantation on 8-Week Remission in Patients With Ulcerative Colitis: A Randomized Clinical Trial. JAMA. 2019;321:156-64.

Cui B, Feng Q, Wang H, Wang M, Peng Z, Li P, et al. Fecal microbiota transplantation through mid-gut for refractory Crohn's disease: safety, feasibility, and efficacy trial results. J Gastroenterol Hepatol. 2015;30:51-8.

Czarnewski P, Parigi SM, Sorini C, Diaz OE, Das S, Gagliani N, et al. Conserved transcriptomic profile between mouse and human colitis allows unsupervised patient stratification. Nat Commun. 2019;10:2892.

Darnaud M, Dos Santos A, Gonzalez P, Augui S, Lacoste C, Desterke C, et al. Enteric Delivery of Regenerating Family Member 3 alpha Alters the Intestinal Microbiota and Controls Inflammation in Mice With Colitis. Gastroenterology. 2018;154:1009-1023.e14.

Davani-Davari D, Negahdaripour M, Karimzadeh I, Seifan M, Mohkam M, Masoumi SJ, et al. Prebiotics: Definition, Types, Sources, Mechanisms, and Clinical Applications. Foods. 2019;8:92.

Davey RA, MacLean HE. Current and future approaches using genetically modified mice in endocrine research. Am J Physiol Endocrinol Metab. 2006;291:E429-38.

David LA, Maurice CF, Carmody RN, Gootenberg DB, Button JE, Wolfe BE, et al. Diet rapidly and reproducibly alters the human gut microbiome. Nature. 2014;505:559-63.

Dawson PA, Karpen SJ. Intestinal transport and metabolism of bile acids. J Lipid Res. 2015;56:1085-99.

De Filippo C, Cavalieri D, Di Paola M, Ramazzotti M, Poullet JB, Massart S, et al. Impact of diet in shaping gut microbiota revealed by a comparative study in children from Europe and rural Africa. Proc Natl Acad Sci U S A. 2010;107:14691-6.

De Preter V. Metabolomics in the Clinical Diagnosis of Inflammatory Bowel Disease. Dig Dis. 2015;33 Suppl 1:2-10.

Depommier C, Everard A, Druart C, Plovier H, Van Hul M, Vieira-Silva S, et al. Supplementation with Akkermansia muciniphila in overweight and obese human volunteers: a proof-of-concept exploratory study. Nat Med. 2019;25:1096-1103.

Derrien M, Vaughan EE, Plugge CM, de Vos WM. Akkermansia muciniphila gen. nov., sp. nov., a human intestinal mucin-degrading bacterium. Int J Syst Evol Microbiol. 2004;54:1469-1476.

Derwa Y, Gracie DJ, Hamlin PJ, Ford AC. Systematic review with meta-analysis: the efficacy of probiotics in inflammatory bowel disease. Aliment Pharmacol Ther. 2017;46:389-400.

Devkota S, Chang EB. Diet-induced expansion of pathobionts in experimental colitis: implications for tailored therapies. Gut Microbes. 2013;4:172-4.

Dieleman LA, Palmen MJ, Akol H, Bloemena E, Peña AS, Meuwissen SG, et al. Chronic experimental colitis induced by dextran sulphate sodium (DSS) is characterized by Th1 and Th2 cytokines. Clin Exp Immunol. 1998;114:385-91.

Ding NS, McDonald JAK, Perdones-Montero A, Rees DN, Adegbola SO, Misra R, et al. Metabonomics and the Gut Microbiome Associated With Primary Response to Anti-TNF Therapy in Crohn's Disease. J Crohns Colitis. 2020;14:1090-1102.

Dobin A, Davis CA, Schlesinger F, Drenkow J, Zaleski C, Jha S, et al. STAR: ultrafast universal RNA-seq aligner. Bioinformatics. 2013;29:15-21.

Dorrington MG, Fraser IDC. NF-κB Signaling in Macrophages: Dynamics, Crosstalk, and Signal Integration. Front Immunol. 2019;10:705.

Dovrolis N, Michalopoulos G, Theodoropoulos GE, Arvanitidis K, Kolios G, Sechi LA, et al. The Interplay between Mucosal Microbiota Composition and Host Gene-Expression is Linked with Infliximab Response in Inflammatory Bowel Diseases. Microorganisms. 2020;8:438.

Du Z, Hudcovic T, Mrazek J, Kozakova H, Srutkova D, Schwarzer M, et al. Development of gut inflammation in mice colonized with mucosa-associated bacteria from patients with ulcerative colitis. Gut Pathog. 2015;7:32.

Duarte TT, Spencer CT. Personalized Proteomics: The Future of Precision Medicine. Proteomes. 2016;4:29.

Dubinsky M, Braun J. Diagnostic and Prognostic Microbial Biomarkers in Inflammatory Bowel Diseases. Gastroenterology. 2015;149:1265-1274.e3.

Duboc H, Rainteau D, Rajca S, Humbert L, Farabos D, Maubert M, et al. Increase in fecal primary bile acids and dysbiosis in patients with diarrhea-predominant irritable bowel syndrome. Neurogastroenterol Motil. 2012;24:513-20, e246-7.

Duboc H, Rajca S, Rainteau D, Benarous D, Maubert MA, Quervain E, et al. Connecting dysbiosis, bile-acid dysmetabolism and gut inflammation in inflammatory bowel diseases. Gut. 2013;62:531-9.

Duerr RH, Taylor KD, Brant SR, Rioux JD, Silverberg MS, Daly MJ, et al. A genome-wide association study identifies IL23R as an inflammatory bowel disease gene. Science. 2006;314:1461-3.

Edgar RC. Search and clustering orders of magnitude faster than BLAST. Bioinformatics. 2010;26:2460-1.

Ehrlich M, Jiang G, Fiala E, Dome JS, Yu MC, Long TI, et al. Hypomethylation and hypermethylation of DNA in Wilms tumors. Oncogene. 2002;21:6694-702.

Ek WE, D'Amato M, Halfvarson J. The history of genetics in inflammatory bowel disease. Ann Gastroenterol. 2014;27:294-303.

Elinav E, Strowig T, Kau AL, Henao-Mejia J, Thaiss CA, Booth CJ, et al. NLRP6 inflammasome regulates colonic microbial ecology and risk for colitis. Cell. 2011;145:745-57.

Elten M, Benchimol EI, Fell DB, Kuenzig ME, Smith G, Chen H, et al. Ambient air pollution and the risk of pediatric-onset inflammatory bowel disease: A population-based cohort study. Environ Int. 2020;138:105676.

Esteban-Fernández A, Ibañez C, Simó C, Bartolomé B, Moreno-Arribas MV. An Ultrahigh-Performance Liquid Chromatography-Time-of-Flight Mass Spectrometry Metabolomic Approach to Studying the Impact of Moderate Red-Wine Consumption on Urinary Metabolome. J Proteome Res. 2018;17:1624-35.

Eto D, Lao C, DiToro D, Barnett B, Escobar TC, Kageyama R, et al. IL-21 and IL-6 are critical for different aspects of B cell immunity and redundantly induce optimal follicular helper CD4 T cell (Tfh) differentiation. PLoS One. 2011;6:e17739.

Everard A, Belzer C, Geurts L, Ouwerkerk JP, Druart C, Bindels LB, et al. Cross-talk between Akkermansia muciniphila and intestinal epithelium controls diet-induced obesity. Proc Natl Acad Sci U S A. 2013;110:9066-71.

Everard A, Geurts L, Caesar R, Van Hul M, Matamoros S, Duparc T, et al. Intestinal epithelial MyD88 is a sensor switching host metabolism towards obesity according to nutritional status. Nat Commun. 2014;5:5648.

Fan Y, Liu B. Expression of Toll-like receptors in the mucosa of patients with ulcerative colitis. Exp Ther Med. 2015;9:1455-9.

Feagan BG, Rutgeerts P, Sands BE, Hanauer S, Colombel JF, Sandborn WJ, et al. Vedolizumab as induction and maintenance therapy for ulcerative colitis. N Engl J Med. 2013;369:699-710.

Feakins RM; British Society of Gastroenterology. Inflammatory bowel disease biopsies: updated British Society of Gastroenterology reporting guidelines. J Clin Pathol. 2013;66:1005-26.

Feerick CL, McKernan DP. Understanding the regulation of pattern recognition receptors in inflammatory diseases - a 'Nod' in the right direction. Immunology. 2017;150:237-47.

Fitzgerald KA, Chen ZJ. Sorting out Toll signals. Cell. 2006;125:834-6.

Flannigan KL, Denning TL. Segmented filamentous bacteria-induced immune responses: a balancing act between host protection and autoimmunity. Immunology. 2018;154:537–46.

Fritz JV, Desai MS, Shah P, Schneider JG, Wilmes P. From meta-omics to causality: experimental models for human microbiome research. Microbiome. 2013;1:14.

Fukata M, Arditi M. The role of pattern recognition receptors in intestinal inflammation. Mucosal Immunol. 2013;6:451-63.

Fűri I, Sipos F, Germann TM, Kalmár A, Tulassay Z, Molnár B, et al. Epithelial toll-like receptor 9 signaling in colorectal inflammation and cancer: clinico-pathogenic aspects. World J Gastroenterol. 2013;19:4119-26.

Gajendran M, Loganathan P, Jimenez G, Catinella AP, Ng N, Umapathy C, et al. A comprehensive review and update on ulcerative colitis. Dis Mon. 2019;65:100851

GBD 2017 Inflammatory Bowel Disease Collaborators. The global, regional, and national burden of inflammatory bowel disease in 195 countries and territories, 1990-2017: a systematic analysis for the Global Burden of Disease Study 2017. Lancet Gastroenterol Hepatol. 2020;5:17-30.

Geerling BJ, Dagnelie PC, Badart-Smook A, Russel MG, Stockbrügger RW, Brummer RJ. Diet as a risk factor for the development of ulcerative colitis. Am J Gastroenterol. 2000;95:1008-13.

Gerriets V, Bansal P, Goyal A, Khaddour K. Tumor Necrosis Factor Inhibitors. StatPearls [Internet] StatPearls Publishing; Treasure Island (FL). 2021.

Gevers D, Kugathasan S, Denson LA, Vázquez-Baeza Y, Van Treuren W, Ren B, et al. The treatment-naive microbiome in new-onset Crohn's disease. Cell Host Microbe. 2014;15:382-92.

Ghoreschi K, Laurence A, Yang XP, Tato CM, McGeachy MJ, Konkel JE, et al. Generation of pathogenic T(H)17 cells in the absence of TGF-β signalling. Nature. 2010;467:967-71.

Gisbert JP, Chaparro M. Clinical Usefulness of Proteomics in Inflammatory Bowel Disease: A Comprehensive Review. J Crohns Colitis. 2019;13:374-84.

Gorkiewicz G, Moschen A. Gut microbiome: a new player in gastrointestinal disease. Virchows Arch. 2018;472:159-72.

Gouba N, Hien YE, Guissou ML, Fonkou MDM, Traoré Y, Tarnagda Z. Digestive tract mycobiota and microbiota and the effects on the immune system. Human Microbiome Journal. 2019;12:100056.

Goyal A, Yeh A, Bush BR, Firek BA, Siebold LM, Rogers MB, et al. Safety, Clinical Response, and Microbiome Findings Following Fecal Microbiota Transplant in Children With Inflammatory Bowel Disease. Inflamm Bowel Dis. 2018;24:410-21.

Grüner N, Mattner J. Bile Acids and Microbiota: Multifaceted and Versatile Regulators of the Liver-Gut Axis. Int J Mol Sci. 2021;22:1397.

Guan H, Nagarkatti PS, Nagarkatti M. Role of CD44 in the differentiation of Th1 and Th2 cells: CD44-deficiency enhances the development of Th2 effectors in response to sheep RBC and chicken ovalbumin. J Immunol. 2009;183:172-80.

Guan Q. A Comprehensive Review and Update on the Pathogenesis of Inflammatory Bowel Disease. J Immunol Res. 2019;2019:7247238.

Guarner F. What is the role of the enteric commensal flora in IBD? Inflamm Bowel Dis. 2008;14 Suppl 2:S83-4.

Haberman Y, Karns R, Dexheimer PJ, Schirmer M, Somekh J, Jurickova I, et al. Ulcerative colitis mucosal transcriptomes reveal mitochondriopathy and personalized mechanisms underlying disease severity and treatment response. Nat Commun. 2019;10:38.

Hall LJ, Faivre E, Quinlan A, Shanahan F, Nally K, Melgar S. Induction and activation of adaptive immune populations during acute and chronic phases of a murine model of experimental colitis. Dig Dis Sci. 2011;56:79-89.

Hall AB, Yassour M, Sauk J, Garner A, Jiang X, Arthur T, et al. A novel Ruminococcus gnavus clade enriched in inflammatory bowel disease patients. Genome Med. 2017;9:103.

Hampe J, Cuthbert A, Croucher PJ, Mirza MM, Mascheretti S, Fisher S, et al. Association between insertion mutation in NOD2 gene and Crohn's disease in German and British populations. Lancet. 2001;357:1925-8.

Hardy H, Harris J, Lyon E, Beal J, Foey AD. Probiotics, prebiotics and immunomodulation of gut mucosal defences: homeostasis and immunopathology. Nutrients. 2013;5:1869-912.

Hasan N, Yang H. Factors affecting the composition of the gut microbiota, and its modulation. PeerJ. 2019;7:e7502.

Hatle KM, Gummadidala P, Navasa N, Bernardo E, Dodge J, Silverstrim B, et al. MCJ/DnaJC15, an endogenous mitochondrial repressor of the respiratory chain that controls metabolic alterations. Mol Cell Biol. 2013;33:2302-14.

Heinz S, Benner C, Spann N, Bertolino E, Lin YC, Laslo P, et al. Simple combinations of lineage-determining transcription factors prime cis-regulatory elements required for macrophage and B cell identities. Mol Cell. 2010;38:576-89.

Henao-Mejia J, Elinav E, Jin C, Hao L, Mehal WZ, Strowig T, et al. Inflammasome-mediated dysbiosis regulates progression of NAFLD and obesity. Nature. 2012;482:179-85.

Henke MT, Kenny DJ, Cassilly CD, Vlamakis H, Xavier RJ, Clardy J. Ruminococcus gnavus, a member of the human gut microbiome associated with Crohn's disease, produces an inflammatory polysaccharide. Proc Natl Acad Sci U S A. 2019;116:12672-12677.

Herst PM, Rowe MR, Carson GM, Berridge MV. Functional Mitochondria in Health and Disease. Front Endocrinol (Lausanne). 2017;8:296.

Hill C, Guarner F, Reid G, Gibson GR, Merenstein DJ, Pot B, et al. Expert consensus document. The International Scientific Association for Probiotics and Prebiotics consensus statement on the scope and appropriate use of the term probiotic. Nat Rev Gastroenterol Hepatol. 2014;11:506-14.

Holbrook J, Lara-Reyna S, Jarosz-Griffiths H, McDermott M. Tumour necrosis factor signalling in health and disease. F1000Res. 2019;8:F1000 Faculty Rev-111.

Hou JK, Kramer JR, Richardson P, Mei M, El-Serag HB. The incidence and prevalence of inflammatory bowel disease among U.S. veterans: a national cohort study. Inflamm Bowel Dis. 2013;19:1059-64.

Hu C, Shu L, Huang X, Yu J, Li L, Gong L, et al. OPA1 and MICOS Regulate mitochondrial crista dynamics and formation. Cell Death Dis. 2020;11:940.

Huang da W, Sherman BT, Lempicki RA. Systematic and integrative analysis of large gene lists using DAVID bioinformatics resources. Nat Protoc. 2009;4:44-57.

Hughes CS, Moggridge S, Müller T, Sorensen PH, Morin GB, Krijgsveld J. Single-pot, solid-phase-enhanced sample preparation for proteomics experiments. Nat Protoc. 2019;14:68-85.

Hviid A, Svanström H, Frisch M. Antibiotic use and inflammatory bowel diseases in childhood. Gut. 2011;60:49-54.

Icaza-Chávez ME. Microbiota intestinal en la salud y la enfermedad [Gut microbiota in health and disease]. Rev Gastroenterol Mex. 2013;78:240-8.

Iheozor-Ejiofor Z, Kaur L, Gordon M, Baines PA, Sinopoulou V, Akobeng AK. Probiotics for maintenance of remission in ulcerative colitis. Cochrane Database Syst Rev. 2020;3:CD007443.

Iljazovic A, Roy U, Gálvez EJC, Lesker TR, Zhao B, Gronow A, et al. Perturbation of the gut microbiome by Prevotella spp. enhances host susceptibility to mucosal inflammation. Mucosal Immunol. 2021;14:113-24.

Imhann F, Vich Vila A, Bonder MJ, Fu J, Gevers D, Visschedijk MC, et al. Interplay of host genetics and gut microbiota underlying the onset and clinical presentation of inflammatory bowel disease. Gut. 2018;67:108-19.

Ip WKE, Hoshi N, Shouval DS, Snapper S, Medzhitov R. Anti-inflammatory effect of IL-10 mediated by metabolic reprogramming of macrophages. Science. 2017;356:513-9.

Iurescia S, Fioretti D, Rinaldi M. The Innate Immune Signalling Pathways: Turning RIG-I Sensor Activation Against Cancer. Cancers (Basel). 2020;12:3158.

Jackson DN, Theiss AL. Gut bacteria signaling to mitochondria in intestinal inflammation and cancer. Gut Microbes. 2020;11:285-304.

Jalanka J, Cheng J, Hiippala K, Ritari J, Salojärvi J, Ruuska T, et al. Colonic Mucosal Microbiota and Association of Bacterial Taxa with the Expression of Host Antimicrobial Peptides in Pediatric Ulcerative Colitis. Int J Mol Sci. 2020;21:6044.

Jiang Y, Yu M, Hu X, Han L, Yang K, Ba H, et al. STAT1 mediates transmembrane TNF-alpha-induced formation of death-inducing signaling complex and apoptotic signaling via TNFR1. Cell Death Differ. 2017;24:660-71.

Johansson ME, Larsson JM, Hansson GC. The two mucus layers of colon are organized by the MUC2 mucin, whereas the outer layer is a legislator of host-microbial interactions. Proc Natl Acad Sci U S A. 2011;108 Suppl 1:4659-65.

Johnston I, Nolan J, Pattni SS, Walters JR. New insights into bile acid malabsorption. Curr Gastroenterol Rep. 2011;13:418-25.

Kaimal V, Bardes EE, Tabar SC, Jegga AG, Aronow BJ. ToppCluster: a multiple gene list feature analyzer for comparative enrichment clustering and network-based dissection of biological systems. Nucleic Acids Res. 2010;38:W96-102.

Kalliolias GD, Ivashkiv LB. TNF biology, pathogenic mechanisms and emerging therapeutic strategies. Nat Rev Rheumatol. 2016;12:49-62.

Kaplan GG. The global burden of IBD: from 2015 to 2025. Nat Rev Gastroenterol Hepatol. 2015;12:720-7.

Kaplan GG, Bernstein CN, Coward S, Bitton A, Murthy SK, Nguyen GC, et al. The Impact of Inflammatory Bowel Disease in Canada 2018: Epidemiology. J Can Assoc Gastroenterol. 2019;2:S6-S16.

Kasztura M, Richard A, Bempong NE, Loncar D, Flahault A. Cost-effectiveness of precision medicine: a scoping review. Int J Public Health. 2019;64:1261-71.

Kaunitz J, Nayyar P. Bugs, genes, fatty acids, and serotonin: Unraveling inflammatory bowel disease? F1000Res. 2015;4:F1000 Faculty Rev-1146.

Kennedy RJ, Hoper M, Deodhar K, Erwin PJ, Kirk SJ, Gardiner KR. Interleukin 10-deficient colitis: new similarities to human inflammatory bowel disease. Br J Surg. 2000;87:1346-51.

Kennedy EA, King KY, Baldridge MT. Mouse Microbiota Models: Comparing Germ-Free Mice and Antibiotics Treatment as Tools for Modifying Gut Bacteria. Front Physiol. 2018;9:1534.

Kennedy NA, Heap GA, Green HD, Hamilton B, Bewshea C, Walker GJ, et al; UK Inflammatory Bowel Disease Pharmacogenetics Study Group. Predictors of anti-TNF treatment failure in anti-TNF-naive patients with active luminal Crohn's disease: a prospective, multicentre, cohort study. Lancet Gastroenterol Hepatol. 2019;4:341-53.

Kim JM. Antimicrobial proteins in intestine and inflammatory bowel diseases. Intest Res. 2014;12:20-33.

Kim S, Covington A, Pamer EG. The intestinal microbiota: Antibiotics, colonization resistance, and enteric pathogens. Immunol Rev. 2017a;279:90-105.

Kim D, Hofstaedter CE, Zhao C, Mattei L, Tanes C, Clarke E, et al. Optimizing methods and dodging pitfalls in microbiome research. Microbiome. 2017b;5:52.

Klebanoff SJ, Kettle AJ, Rosen H, Winterbourn CC, Nauseef WM. Myeloperoxidase: a front-line defender against phagocytosed microorganisms. J Leukoc Biol. 2013;93:185-98.

Knights D, Silverberg MS, Weersma RK, Gevers D, Dijkstra G, Huang H, et al. Complex host genetics influence the microbiome in inflammatory bowel disease. Genome Med. 2014;6:107.

Knoop KA, McDonald KG, Kulkarni DH, Newberry RD. Antibiotics promote inflammation through the translocation of native commensal colonic bacteria. Gut. 2016;65:1100-9.

Kobayashi T, Siegmund B, Le Berre C, Wei SC, Ferrante M, Shen B, et al. Ulcerative colitis. Nat Rev Dis Primers. 2020;6:74.

Koelink PJ, Wildenberg ME, Stitt LW, Feagan BG, Koldijk M, van 't Wout AB, et al. Development of Reliable, Valid and Responsive Scoring Systems for Endoscopy and Histology in Animal Models for Inflammatory Bowel Disease. J Crohns Colitis. 2018;12:794-803.

Kondadi AK, Anand R, Reichert AS. Functional Interplay between Cristae Biogenesis, Mitochondrial Dynamics and Mitochondrial DNA Integrity. Int J Mol Sci. 2019;20:4311.

Kruis W, Fric P, Pokrotnieks J, Lukás M, Fixa B, Kascák M, et al. Maintaining remission of ulcerative colitis with the probiotic Escherichia coli Nissle 1917 is as effective as with standard mesalazine. Gut. 2004;53:1617-23.

Kumar M, Garand M, Al Khodor S. Integrating omics for a better understanding of Inflammatory Bowel Disease: a step towards personalized medicine. J Transl Med. 2019;17:419.

Landy J, Ronde E, English N, Clark SK, Hart AL, Knight SC, et al. Tight junctions in inflammatory bowel diseases and inflammatory bowel disease associated colorectal cancer. World J Gastroenterol. 2016;22:3117-26.

Langille MG, Zaneveld J, Caporaso JG, McDonald D, Knights D, Reyes JA. Predictive functional profiling of microbial communities using 16S rRNA marker gene sequences. Nat Biotechnol. 2013;31:814-21.

Laukens D, Brinkman BM, Raes J, De Vos M, Vandenabeele P. Heterogeneity of the gut microbiome in mice: guidelines for optimizing experimental design. FEMS Microbiol Rev. 2016;40:117-32.

Legaki E, Gazouli M. Influence of environmental factors in the development of inflammatory bowel diseases. World J Gastrointest Pharmacol Ther. 2016;7:112-25.

Lepage P, Häsler R, Spehlmann ME, Rehman A, Zvirbliene A, Begun A, et al. Twin study indicates loss of interaction between microbiota and mucosa of patients with ulcerative colitis. Gastroenterology. 2011;141:227-36.

Leung S, Liu X, Fang L, Chen X, Guo T, Zhang J. The cytokine milieu in the interplay of pathogenic Th1/Th17 cells and regulatory T cells in autoimmune disease. Cell Mol Immunol. 2010;7:182-9.

Levy M, Blacher E, Elinav E. Microbiome, metabolites and host immunity. Curr Opin Microbiol. 2017;35:8-15.

Li XV, Leonardi I, Iliev ID. Gut Mycobiota in Immunity and Inflammatory Disease. Immunity. 2019;50:1365-79.

Liao Y, Smyth GK, Shi W. The Subread aligner: fast, accurate and scalable read mapping by seed-and-vote. Nucleic Acids Res. 2013;41:e108.

Ligumsky M, Simon PL, Karmeli F, Rachmilewitz D. Role of interleukin 1 in inflammatory bowel disease--enhanced production during active disease. Gut. 1990;31:686-9.

Linden SK, Sutton P, Karlsson NG, Korolik V, McGuckin MA. Mucins in the mucosal barrier to infection. Mucosal Immunol. 2008;1:183-97.

Lindsay JO, Whelan K, Stagg AJ, Gobin P, Al-Hassi HO, Rayment N, et al. Clinical, microbiological, and immunological effects of fructo-oligosaccharide in patients with Crohn's disease. Gut. 2006;55:348-55.

Lindsey JC, Lusher ME, Strathdee G, Brown R, Gilbertson RJ, Bailey S, et al. Epigenetic inactivation of MCJ (DNAJD1) in malignant paediatric brain tumours. Int J Cancer. 2006;118:346-52.

Lissner D, Schumann M, Batra A, Kredel LI, Kühl AA, Erben U, et al. Monocyte and M1 Macrophage-induced Barrier Defect Contributes to Chronic Intestinal Inflammation in IBD. Inflamm Bowel Dis. 2015;21:1297-305.

Liu TC, Stappenbeck TS. Genetics and Pathogenesis of Inflammatory Bowel Disease. Annu Rev Pathol. 2016;11:127-48.

Livak KJ, Schmittgen TD. Analysis of relative gene expression data using real-time quantitative PCR and the 2(-Delta Delta C(T)) Method. Methods. 2001;25:402-8.

Lloyd-Price J, Arze C, Ananthakrishnan AN, Schirmer M, Avila-Pacheco J, Poon TW, et al. Multi-omics of the gut microbial ecosystem in inflammatory bowel diseases. Nature. 2019;569:655-62.

Lo Presti A, Zorzi F, Del Chierico F, Altomare A, Cocca S, Avola A, et al. Fecal and Mucosal Microbiota Profiling in Irritable Bowel Syndrome and Inflammatory Bowel Disease. Front Microbiol. 2019;10:1655.

Loddo I, Romano C. Inflammatory Bowel Disease: Genetics, Epigenetics, and Pathogenesis. Front Immunol. 2015;6:551.

Looijer-van Langen MA, Dieleman LA. Prebiotics in chronic intestinal inflammation. Inflamm Bowel Dis. 2009;15:454-62.

Lopetuso LR, Petito V, Cufino V, Arena V, Stigliano E, Gerardi V, et al. Locally injected Infliximab ameliorates murine DSS colitis: differences in serum and intestinal levels of drug between healthy and colitic mice. Dig Liver Dis. 2013;45:1017-21.

Lopez J, Grinspan A. Fecal Microbiota Transplantation for Inflammatory Bowel Disease. Gastroenterol Hepatol (N Y). 2016;12:374-9.

Lord JD, Long SA, Shows DM, Thorpe J, Schwedhelm K, Chen J, et al. Circulating integrin alpha4/beta7+ lymphocytes targeted by vedolizumab have a pro-inflammatory phenotype. Clin Immunol. 2018;193:24-32.

Love MI, Huber W, Anders S. Moderated estimation of fold change and dispersion for RNA-seq data with DESeq2. Genome Biol. 2014;15:550.

Low D, Nguyen DD, Mizoguchi E. Animal models of ulcerative colitis and their application in drug research. Drug Des Devel Ther. 2013;7:1341-57.

Lu Y, Li X, Liu S, Zhang Y, Zhang D. Toll-like Receptors and Inflammatory Bowel Disease. Front Immunol. 2018;9:72.

Ma J, Coarfa C, Qin X, Bonnen PE, Milosavljevic A, Versalovic J, et al. mtDNA haplogroup and single nucleotide polymorphisms structure human microbiome communities. BMC Genomics. 2014;15:257.

Machiels K, Joossens M, Sabino J, De Preter V, Arijs I, Eeckhaut V, et al. A decrease of the butyrate-producing species Roseburia hominis and Faecalibacterium prausnitzii defines dysbiosis in patients with ulcerative colitis. Gut. 2014;63:1275-83.

Macpherson AJ, Uhr T. Induction of protective IgA by intestinal dendritic cells carrying commensal bacteria. Science. 2004;303:1662-5.

Magnusson MK, Strid H, Sapnara M, Lasson A, Bajor A, Ung KA, et al. Anti-TNF Therapy Response in Patients with Ulcerative Colitis Is Associated with Colonic Antimicrobial Peptide Expression and Microbiota Composition. J Crohns Colitis. 2016;10:943-52.

Maier E, Anderson RC, Roy NC. Understanding how commensal obligate anaerobic bacteria regulate immune functions in the large intestine. Nutrients. 2014;7:45-73.

Manichanh C, Reeder J, Gibert P, Varela E, Llopis M, Antolin M, et al. Reshaping the gut microbiome with bacterial transplantation and antibiotic intake. Genome Res. 2010;20:1411-9.

Martini GA, Brandes JW. Increased consumption of refined carbohydrates in patients with Crohn's disease. Klin Wochenschr. 1976;54:367–71.

Maslowski KM, Vieira AT, Ng A, Kranich J, Sierro F, Yu D, et al. Regulation of inflammatory responses by gut microbiota and chemoattractant receptor GPR43. Nature. 2009;461:1282-6.

Mathur S, Sutton J. Personalized medicine could transform healthcare. Biomed Rep. 2017;7:3-5.

Matsuoka K, Kanai T. The gut microbiota and inflammatory bowel disease. Semin Immunopathol. 2015;37:47-55.

Mayberry JF, Rhodes J, Newcombe RG. Increased sugar consumption in Crohn's disease. Digestion. 1980;20:323-6.

Mayer FL, Wilson D, Hube B. Candida albicans pathogenicity mechanisms. Virulence. 2013;4:119-28.

McBride HM, Neuspiel M, Wasiak S. Mitochondria: more than just a powerhouse. Curr Biol. 2006;16:R551-60.

McClure R, Massari P. TLR-Dependent Human Mucosal Epithelial Cell Responses to Microbial Pathogens. Front Immunol. 2014;5:386.

McDonald D, Price MN, Goodrich J, Nawrocki EP, DeSantis TZ, Probst A, et al. An improved Greengenes taxonomy with explicit ranks for ecological and evolutionary analyses of bacteria and archaea. ISME J. 2012;6:610-8.

McGeachy MJ, Bak-Jensen KS, Chen Y, Tato CM, Blumenschein W, McClanahan T, et al. TGF-beta and IL-6 drive the production of IL-17 and IL-10 by T cells and restrain T(H)-17 cell-mediated pathology. Nat Immunol. 2007; 8:1390-7.

McGeachy MJ, Chen Y, Tato CM, Laurence A, Joyce-Shaikh B, Blumenschein WM, et al. The interleukin 23 receptor is essential for the terminal differentiation of interleukin 17-producing effector T helper cells in vivo. Nat Immunol. 2009;10:314-24.

Meier F, Beck S, Grassl N, Lubeck M, Park MA, Raether O, et al. Parallel Accumulation-Serial Fragmentation (PASEF): Multiplying Sequencing Speed and Sensitivity by Synchronized Scans in a Trapped Ion Mobility Device. J Proteome Res. 2015;14:5378-87.

Meier F, Brunner AD, Koch S, Koch H, Lubeck M, Krause M, et al. Online Parallel Accumulation-Serial Fragmentation (PASEF) with a Novel Trapped Ion Mobility Mass Spectrometer. Mol Cell Proteomics. 2018;17:2534-45.

Metwaly A, Haller D. Multi-omics in IBD biomarker discovery: the missing links. Nat Rev Gastroenterol Hepatol. 2019;16:587-8.

Mirpuri J, Raetz M, Sturge CR, Wilhelm CL, Benson A, Savani RC, et al. Proteobacteria-specific IgA regulates maturation of the intestinal microbiota. Gut Microbes. 2014;5:28-39.

Mitchell DM, Williams MA. An activation marker finds a function. Immunity. 2010;32:9-11.

Mizoguchi E, Low D, Ezaki Y, Okada T. Recent updates on the basic mechanisms and pathogenesis of inflammatory bowel diseases in experimental animal models. Intest Res. 2020;18:151-67.

Moayyedi P, Surette MG, Kim PT, Libertucci J, Wolfe M, Onischi C, et al. Fecal Microbiota Transplantation Induces Remission in Patients With Active Ulcerative Colitis in a Randomized Controlled Trial. Gastroenterology. 2015;149:102-109.e6.

Monteleone G, Monteleone I, Fina D, Vavassori P, Del Vecchio Blanco G, Caruso R, et al. Interleukin-21 enhances T-helper cell type I signaling and interferon-gamma production in Crohn's disease. Gastroenterology. 2005;128:687-94.

Moreno-Lastres D, Fontanesi F, García-Consuegra I, Martín MA, Arenas J, Barrientos A, et al. Mitochondrial complex I plays an essential role in human respirasome assembly. Cell Metab. 2012;15:324-35.

Morgan XC, Tickle TL, Sokol H, Gevers D, Devaney KL, Ward DV, et al. Dysfunction of the intestinal microbiome in inflammatory bowel disease and treatment. Genome Biol. 2012;13:R79.

Mottawea W, Chiang CK, Mühlbauer M, Starr AE, Butcher J, Abujamel T, et al. Altered intestinal microbiota-host mitochondria crosstalk in new onset Crohn's disease. Nat Commun. 2016;7:13419.

Mukherjee S, Hooper LV. Antimicrobial defense of the intestine. Immunity. 2015;42:28-39.

Müller S, Rihs S, Schneider JM, Paredes BE, Seibold I, Brunner T, et al. Soluble TNF-alpha but not transmembrane TNF-alpha sensitizes T cells for enhanced activation-induced cell death. Eur J Immunol. 2009;39:3171-80.

Muniz LR, Knosp C, Yeretssian G. Intestinal antimicrobial peptides during homeostasis, infection, and disease. Front Immunol. 2012;3:310.

Murphy MP. How mitochondria produce reactive oxygen species. Biochem J. 2009;417:1-13.

Muthusamy V, Duraisamy S, Bradbury CM, Hobbs C, Curley DP, Nelson B, et al. Epigenetic silencing of novel tumor suppressors in malignant melanoma. Cancer Res. 2006;66:11187-93.

Na YR, Stakenborg M, Seok SH, Matteoli G. Macrophages in intestinal inflammation and resolution: a potential therapeutic target in IBD. Nat Rev Gastroenterol Hepatol. 2019;16:531-43.

Navasa N, Martín I, Iglesias-Pedraz JM, Beraza N, Atondo E, Izadi H, et al. Regulation of oxidative stress by methylation-controlled J protein controls macrophage responses to inflammatory insults. J Infect Dis. 2015a;211:135-45.

Navasa N, Martin-Ruiz I, Atondo E, Sutherland JD, Angel Pascual-Itoiz M, Carreras-González A, et al. Ikaros mediates the DNA methylation-independent silencing of MCJ/DNAJC15 gene expression in macrophages. Sci Rep. 2015b;5:14692.

Neurath MF. Cytokines in inflammatory bowel disease. Nat Rev Immunol. 2014;14:329-42.

Nicholson MR, Mitchell PD, Alexander E, Ballal S, Bartlett M, Becker P, et al. Efficacy of Fecal Microbiota Transplantation for Clostridium difficile Infection in Children. Clin Gastroenterol Hepatol. 2020;18:612-619.e1.

Nie YF, Hu J, Yan XH. Cross-talk between bile acids and intestinal microbiota in host metabolism and health. J Zhejiang Univ Sci B. 2015;16:436-46.

Nie JY, Zhao Q. Beverage consumption and risk of ulcerative colitis: Systematic review and meta-analysis of epidemiological studies. Medicine (Baltimore). 2017;96:e9070.

Nishida A, Inoue R, Inatomi O, Bamba S, Naito Y, Andoh A. Gut microbiota in the pathogenesis of inflammatory bowel disease. Clin J Gastroenterol. 2018;1:1-10.

Novak EA, Mollen KP. Mitochondrial dysfunction in inflammatory bowel disease. Front Cell Dev Biol. 2015;3:62.

Ohbuchi A, Kono M, Takenokuchi M, Imoto S, Saigo K. Acetate moderately attenuates the generation of neutrophil extracellular traps. Blood Res. 2018;53:177-80.

Ohtsuka Y, Lee J, Stamm DS, Sanderson IR. MIP-2 secreted by epithelial cells increases neutrophil and lymphocyte recruitment in the mouse intestine. Gut. 2001;49:526-33.

Okayasu I, Hatakeyama S, Yamada M, Ohkusa T, Inagaki Y, Nakaya R. A novel method in the induction of reliable experimental acute and chronic ulcerative colitis in mice. Gastroenterology. 1990;98:694-702.

Olivier M, Asmis R, Hawkins GA, Howard TD, Cox LA. The Need for Multi-Omics Biomarker Signatures in Precision Medicine. Int J Mol Sci. 2019;20:4781.

Opstelten JL, Beelen RMJ, Leenders M, Hoek G, Brunekreef B, van Schaik FDM, et al. Exposure to Ambient Air Pollution and the Risk of Inflammatory Bowel Disease: A European Nested Case-Control Study. Dig Dis Sci. 2016;61:2963-71.

Ordás I, Eckmann L, Talamini M, Baumgart DC, Sandborn WJ. Ulcerative colitis. Lancet. 2012;380:1606-19.

Osakunor DNM, Munk P, Mduluza T, Petersen TN, Brinch C, Ivens A, et al. The gut microbiome but not the resistome is associated with urogenital schistosomiasis in preschool-aged children. Commun Biol. 2020;3:155.

Osman MA, Neoh HM, Ab Mutalib NS, Chin SF, Jamal R. 16S rRNA Gene Sequencing for Deciphering the Colorectal Cancer Gut Microbiome: Current Protocols and Workflows. Front Microbiol. 2018;9:767.

Pabst O, Slack E. IgA and the intestinal microbiota: the importance of being specific. Mucosal Immunol. 2020;13:12-21.

Palm NW, de Zoete MR, Cullen TW, Barry NA, Stefanowski J, Hao L, et al. Immunoglobulin A coating identifies colitogenic bacteria in inflammatory bowel disease. Cell. 2014;158:1000-10.

Parada Venegas D, De la Fuente MK, Landskron G, González MJ, Quera R, Dijkstra G, et al. Short Chain Fatty Acids (SCFAs)-Mediated Gut Epithelial and Immune Regulation and Its Relevance for Inflammatory Bowel Diseases. Front Immunol. 2019;10:277.

Paramsothy S, Paramsothy R, Rubin DT, Kamm MA, Kaakoush NO, Mitchell HM, et al. Faecal Microbiota Transplantation for Inflammatory Bowel Disease: A Systematic Review and Meta-analysis. J Crohns Colitis. 2017a;11:1180-99.

Paramsothy S, Kamm MA, Kaakoush NO, Walsh AJ, van den Bogaerde J, Samuel D, et al. Multidonor intensive faecal microbiota transplantation for active ulcerative colitis: a randomised placebo-controlled trial. Lancet. 2017b;389:1218-28.

Parks DH, Tyson GW, Hugenholtz P, Beiko RG. STAMP: statistical analysis of taxonomic and functional profiles. Bioinformatics. 2014;30:3123-4.

Parsi MA, Achkar JP, Richardson S, Katz J, Hammel JP, Lashner BA, et al. Predictors of response to infliximab in patients with Crohn's disease. Gastroenterology. 2002;123:707-13.

Pascal V, Pozuelo M, Borruel N, Casellas F, Campos D, Santiago A, et al. A microbial signature for Crohn's disease. Gut. 2017;66:813-22.

Pascual-Itoiz MA, Peña-Cearra A, Martín-Ruiz I, Lavín JL, Simó C, Rodríguez H, et al. The mitochondrial negative regulator MCJ modulates the interplay between microbiota and the host during ulcerative colitis. Sci Rep. 2020;10:572.

Peloquin JM, Goel G, Villablanca EJ, Xavier RJ. Mechanisms of Pediatric Inflammatory Bowel Disease. Annu Rev Immunol. 2016;34:31-64.

Perrier C, de Hertogh G, Cremer J, Vermeire S, Rutgeerts P, Van Assche G, et al. Neutralization of membrane TNF, but not soluble TNF, is crucial for the treatment of experimental colitis. Inflamm Bowel Dis. 2013;19:246-53.

Perše M, Cerar A. Dextran sodium sulphate colitis mouse model: traps and tricks. J Biomed Biotechnol. 2012;2012:718617.

Pickard JM, Zeng MY, Caruso R, Núñez G. Gut microbiota: Role in pathogen colonization, immune responses, and inflammatory disease. Immunol Rev. 2017;279:70-89.

Pietrzak B, Tomela K, Olejnik-Schmidt A, Mackiewicz A, Schmidt M. Secretory IgA in Intestinal Mucosal Secretions as an Adaptive Barrier against Microbial Cells. Int J Mol Sci. 2020;21:9254.

Piovani D, Danese S, Peyrin-Biroulet L, Nikolopoulos GK, Lytras T, Bonovas S. Environmental Risk Factors for Inflammatory Bowel Diseases: An Umbrella Review of Meta-analyses. Gastroenterology. 2019;157:647-59.e4.

Pluskal T, Castillo S, Villar-Briones A, Oresic M. MZmine 2: modular framework for processing, visualizing, and analyzing mass spectrometry-based molecular profile data. BMC Bioinformatics. 2010;11:395.

Png CW, Lindén SK, Gilshenan KS, Zoetendal EG, McSweeney CS, Sly LI, et al. Mucolytic bacteria with increased prevalence in IBD mucosa augment in vitro utilization of mucin by other bacteria. Am J Gastroenterol. 2010;105:2420-8.

Pollock J, Glendinning L, Wisedchanwet T, Watson M. The Madness of Microbiome: Attempting To Find Consensus "Best Practice" for 16S Microbiome Studies. Appl Environ Microbiol. 2018;84:e02627-17.

Quezada H, Guzmán-Ortiz AL, Díaz-Sánchez H, Valle-Rios R, Aguirre-Hernández J. Omics-based biomarkers: current status and potential use in the clinic. Bol Med Hosp Infant Mex. 2017;74:219-26.

Rajca S, Grondin V, Louis E, Vernier-Massouille G, Grimaud JC, Bouhnik Y, et al. Alterations in the intestinal microbiome (dysbiosis) as a predictor of relapse after infliximab withdrawal in Crohn's disease. Inflamm Bowel Dis. 2014;20:978-86.

Rautava S, Walker WA. Commensal bacteria and epithelial cross talk in the developing intestine. Curr Gastroenterol Rep. 2007;9:385-92.

Redza-Dutordoir M, Averill-Bates DA. Activation of apoptosis signalling pathways by reactive oxygen species. Biochim Biophys Acta. 2016;1863:2977-92.

Reinecker HC, Steffen M, Witthoeft T, Pflueger I, Schreiber S, MacDermott RP, et al. Enhanced secretion of tumour necrosis factor-alpha, IL-6, and IL-1 beta by isolated lamina propria mononuclear cells from patients with ulcerative colitis and Crohn's disease. Clin Exp Immunol. 1993;94:174-81.

Renga B, Mencarelli A, Cipriani S, D'Amore C, Carino A, Bruno A, et al. The bile acid sensor FXR is required for immune-regulatory activities of TLR-9 in intestinal inflammation. PLoS One. 2013;8:e54472.

Ridaura VK, Faith JJ, Rey FE, Cheng J, Duncan AE, Kau AL, et al. Gut microbiota from twins discordant for obesity modulate metabolism in mice. Science. 2013;341:1241214.

Ridlon JM, Kang DJ, Hylemon PB, Bajaj JS. Bile acids and the gut microbiome. Curr Opin Gastroenterol. 2014;30:332-8.

Ro S, Ma HY, Park C, Ortogero N, Song R, Hennig GW, et al. The mitochondrial genome encodes abundant small noncoding RNAs. Cell Res. 2013;23:759-74.

Roediger WE. The colonic epithelium in ulcerative colitis: an energy-deficiency disease? Lancet. 1980;2:712-5.

Rolhion N, Chassaing B. When pathogenic bacteria meet the intestinal microbiota. Philos Trans R Soc Lond B Biol Sci. 2016;371:20150504.

Rossen NG, Fuentes S, van der Spek MJ, Tijssen JG, Hartman JH, Duflou A, et al. Findings From a Randomized Controlled Trial of Fecal Transplantation for Patients With Ulcerative Colitis. Gastroenterology. 2015;149:110-8.e4.

Round JL, Mazmanian SK. The gut microbiota shapes intestinal immune responses during health and disease. Nat Rev Immunol. 2009;9:313-23.

Rovedatti L, Kudo T, Biancheri P, Sarra M, Knowles CH, Rampton DS, et al. Differential regulation of interleukin 17 and interferon gamma production in inflammatory bowel disease. Gut. 2009;58:1629-36.

Saito R, Smoot ME, Ono K, Ruscheinski J, Wang PL, Lotia S, et al. A travel guide to Cytoscape plugins. Nat Methods. 2012;9:1069-76.

Salice M, Rizzello F, Calabrese C, Calandrini L, Gionchetti P. A current overview of corticosteroid use in active ulcerative colitis. Expert Rev Gastroenterol Hepatol. 2019;13:557-61.

Sánchez-Muñoz F, Fonseca-Camarillo G, Villeda-Ramírez MA, Miranda-Pérez E, Mendivil EJ, Barreto-Zúñiga R, et al. Transcript levels of Toll-Like Receptors 5, 8 and 9 correlate with inflammatory activity in Ulcerative Colitis. BMC Gastroenterol. 2011;11:138.

Sanchis-Artero L, Martínez-Blanch JF, Manresa-Vera S, Cortés-Castell E, Rodriguez-Morales J, Cortés-Rizo X. Evaluation of Changes in Gut Microbiota in Patients with Crohn's Disease after Anti-Tnfα Treatment: Prospective Multicenter Observational Study. Int J Environ Res Public Health. 2020;17:5120.

Sands BE. Biomarkers of Inflammation in Inflammatory Bowel Disease. Gastroenterology. 2015;149:1275-85.e2.

Sawant KV, Poluri KM, Dutta AK, Sepuru KM, Troshkina A, Garofalo RP, et al. Chemokine CXCL1 mediated neutrophil recruitment: Role of glycosaminoglycan interactions. Sci Rep. 2016;6:33123.

Schreiner P, Neurath MF, Ng SC, El-Omar EM, Sharara AI, Kobayashi T, et al. Mechanism-Based Treatment Strategies for IBD: Cytokines, Cell Adhesion Molecules, JAK Inhibitors, Gut Flora, and More. Inflamm Intest Dis. 2019;4:79-96.

Schusdziarra C, Blamowska M, Azem A, Hell K. Methylation-controlled J-protein MCJ acts in the import of proteins into human mitochondria. Hum Mol Genet. 2013;22:1348-57.

Segata N, Izard J, Waldron L, Gevers D, Miropolsky L, Garrett WS, et al. Metagenomic biomarker discovery and explanation. Genome Biol. 2011;12:R60.

Sena LA, Chandel NS. Physiological roles of mitochondrial reactive oxygen species. Mol Cell. 2012;48:158-67.

Shapiro JM, de Zoete MR, Palm NW, Laenen Y, Bright R, Mallette M, et al. Immunoglobulin A Targets a Unique Subset of the Microbiota in Inflammatory Bowel Disease. Cell Host Microbe. 2021;29:83-93.e3.

Shen ZH, Zhu CX, Quan YS, Yang ZY, Wu S, Luo WW, et al. Relationship between intestinal microbiota and ulcerative colitis: Mechanisms and clinical application of probiotics and fecal microbiota transplantation. World J Gastroenterol. 2018;24:5-14.

Shimizu H, Suzuki K, Watanabe M, Okamoto R. Stem cell-based therapy for inflammatory bowel disease. Intest Res. 2019;17:311-6.

Shindo R, Katagiri T, Komazawa-Sakon S, Ohmuraya M, Takeda W, Nakagawa Y, et al. Regenerating islet-derived protein (Reg)3β plays a crucial role in attenuation of ileitis and colitis in mice. Biochem Biophys Rep. 2020;21:100738.

Shridhar V, Bible KC, Staub J, Avula R, Lee YK, Kalli K, et al. Kaufmann SH, Smith DI. Loss of expression of a new member of the DNAJ protein family confers resistance to chemotherapeutic agents used in the treatment of ovarian cancer. Cancer Res. 2001;61:4258-65.

Sifroni KG, Damiani CR, Stoffel C, Cardoso MR, Ferreira GK, Jeremias IC, et al. Mitochondrial respiratory chain in the colonic mucosal of patients with ulcerative colitis. Mol Cell Biochem. 2010;342:111-5.

Silva FA, Rodrigues BL, Ayrizono ML, Leal RF. The Immunological Basis of Inflammatory Bowel Disease. Gastroenterol Res Pract. 2016;2016:2097274.

Sina C, Gavrilova O, Förster M, Till A, Derer S, Hildebrand F, et al. G protein-coupled receptor 43 is essential for neutrophil recruitment during intestinal inflammation. J Immunol. 2009;183:7514-22.

Singh S, George J, Boland BS, Vande Casteele N, Sandborn WJ. Primary Non-Response to Tumor Necrosis Factor Antagonists is Associated with Inferior Response to Second-line Biologics in Patients with Inflammatory Bowel Diseases: A Systematic Review and Meta-analysis. J Crohns Colitis. 2018;12:635-43.

Sinha SR, Haileselassie Y, Nguyen LP, Tropini C, Wang M, Becker LS, et al. Dysbiosis-Induced Secondary Bile Acid Deficiency Promotes Intestinal Inflammation. Cell Host Microbe. 2020;27:659-70.e5.

Smith PD, Janoff EN, Mosteller-Barnum M, Merger M, Orenstein JM, Kearney JF, et al. Isolation and purification of CD14-negative mucosal macrophages from normal human small intestine. J Immunol Methods. 1997;202:1-11.

Smith MI, Turpin W, Tyler AD, Silverberg MS, Croitoru K. Microbiome analysis - from technical advances to biological relevance. F1000Prime Rep. 2014;6:51.

Sokol H, Seksik P, Rigottier-Gois L, Lay C, Lepage P, Podglajen I, et al. Specificities of the fecal microbiota in inflammatory bowel disease. Inflamm Bowel Dis. 2006;12:106-11.

Sokol H, Pigneur B, Watterlot L, Lakhdari O, Bermúdez-Humarán LG, Gratadoux JJ, et al. Faecalibacterium prausnitzii is an anti-inflammatory commensal bacterium identified by gut microbiota analysis of Crohn disease patients. Proc Natl Acad Sci U S A. 2008;105:16731-6.

Sokol H, Leducq V, Aschard H, Pham HP, Jegou S, Landman C, et al. Fungal microbiota dysbiosis in IBD. Gut. 2017;66:1039-48.

Sokol H, Landman C, Seksik P, Berard L, Montil M, Nion-Larmurier I, et al. Fecal microbiota transplantation to maintain remission in Crohn's disease: a pilot randomized controlled study. Microbiome. 2020;8:12.

Sommer J, Engelowski E, Baran P, Garbers C, Floss DM, Scheller J. Interleukin-6, but not the interleukin-6 receptor plays a role in recovery from dextran sodium sulfate-induced colitis. Int J Mol Med. 2014;34:651-60.

Sood A, Midha V, Makharia GK, Ahuja V, Singal D, Goswami P, et al. The probiotic preparation, VSL#3 induces remission in patients with mild-to-moderately active ulcerative colitis. Clin Gastroenterol Hepatol. 2009;7:1202-9, 1209.e1.

Staley C, Weingarden AR, Khoruts A, Sadowsky MJ. Interaction of gut microbiota with bile acid metabolism and its influence on disease states. Appl Microbiol Biotechnol. 2017;101:47-64.

Stallhofer J, Friedrich M, Konrad-Zerna A, Wetzke M, Lohse P, Glas J, et al. Lipocalin-2 Is a Disease Activity Marker in Inflammatory Bowel Disease Regulated by IL-17A, IL-22, and TNF-α and Modulated by IL23R Genotype Status. Inflamm Bowel Dis. 2015;21:2327-40.

Stenman LK, Holma R, Korpela R. High-fat-induced intestinal permeability dysfunction associated with altered fecal bile acids. World J Gastroenterol. 2012;18:923-9.

Stepankova R, Powrie F, Kofronova O, Kozakova H, Hudcovic T, Hrncir T, et al. Segmented filamentous bacteria in a defined bacterial cocktail induce intestinal inflammation in SCID mice reconstituted with CD45RBhigh CD4+ T cells. Inflamm Bowel Dis. 2007;13:1202-11.

Stojanov S, Berlec A, Štrukelj B. The Influence of Probiotics on the Firmicutes/Bacteroidetes Ratio in the Treatment of Obesity and Inflammatory Bowel disease. Microorganisms. 2020;8:1715.

Strober W, Fuss IJ. Proinflammatory cytokines in the pathogenesis of inflammatory bowel diseases. Gastroenterology. 2011;140:1756-67.

Subramanian I, Verma S, Kumar S, Jere A, Anamika K. Multi-omics Data Integration, Interpretation, and Its Application. Bioinform Biol Insights. 2020;14:1177932219899051.

Swidsinski A, Weber J, Loening-Baucke V, Hale LP, Lochs H. Spatial organization and composition of the mucosal flora in patients with inflammatory bowel disease. J Clin Microbiol. 2015;43:3380-9.

Tahrir FG, Langford D, Amini S, Mohseni Ahooyi T, Khalili K. Mitochondrial quality control in cardiac cells: Mechanisms and role in cardiac cell injury and disease. J Cell Physiol. 2019;234:8122-33.

Tang JX, Thompson K, Taylor RW, Oláhová M. Mitochondrial OXPHOS Biogenesis: Co-Regulation of Protein Synthesis, Import, and Assembly Pathways. Int J Mol Sci. 2020;21:3820.

Tiratterra E, Franco P, Porru E, Katsanos KH, Christodoulou DK, Roda G. Role of bile acids in inflammatory bowel disease. Ann Gastroenterol. 2018;31:266-72.

Tursi A, Brandimarte G, Papa A, Giglio A, Elisei W, Giorgetti GM, et al. Treatment of relapsing mild-to-moderate ulcerative colitis with the probiotic VSL#3 as adjunctive to a standard pharmaceutical treatment: a double-blind, randomized, placebo-controlled study. Am J Gastroenterol. 2010;105:2218-27.

Tyanova S, Temu T, Sinitcyn P, Carlson A, Hein MY, Geiger T, et al. The Perseus computational platform for comprehensive analysis of (prote)omics data. Nat Methods. 2016;13:731-40.

Tyler AD, Kirsch R, Milgrom R, Stempak JM, Kabakchiev B, Silverberg MS. Microbiome Heterogeneity Characterizing Intestinal Tissue and Inflammatory Bowel Disease Phenotype. Inflamm Bowel Dis. 2016;22:807-16.

Urdaneta V, Casadesús J. Interactions between Bacteria and Bile Salts in the Gastrointestinal and Hepatobiliary Tracts. Front Med (Lausanne). 2017;4:163.

Uzbay T. Germ-free animal experiments in the gut microbiota studies. Curr Opin Pharmacol. 2019;49:6-10.

van Eeden SF, Tan WC, Suwa T, Mukae H, Terashima T, Fujii T, et al. Cytokines involved in the systemic inflammatory response induced by exposure to particulate matter air pollutants (PM(10)). Am J Respir Crit Care Med. 2001;164:826-30.

Vasileva E, Citi S. The role of microtubules in the regulation of epithelial junctions. Tissue Barriers. 2018;6:1539596.

Vaughn BP, Vatanen T, Allegretti JR, Bai A, Xavier RJ, Korzenik J, et al. Increased Intestinal Microbial Diversity Following Fecal Microbiota Transplant for Active Crohn's Disease. Inflamm Bowel Dis. 2016;22:2182-90.

Vermeire S, Joossens M, Verbeke K, Wang J, Machiels K, Sabino J, et al. Donor Species Richness Determines Faecal Microbiota Transplantation Success in Inflammatory Bowel Disease. J Crohns Colitis. 2016;10:387-94.

Vezza T, Abad-Jiménez Z, Marti-Cabrera M, Rocha M, Víctor VM. Microbiota-Mitochondria Inter-Talk: A Potential Therapeutic Strategy in Obesity and Type 2 Diabetes. Antioxidants (Basel). 2020;9:848.

Wajant H, Pfizenmaier K, Scheurich P. Tumor necrosis factor signaling. Cell Death Differ. 2003;10:45-65.

Waldner MJ, Neurath MF. Chemically induced mouse models of colitis. Curr Protoc Pharmacol. 2009;Chapter 5:Unit 5.55.

Walujkar SA, Kumbhare SV, Marathe NP, Patangia DV, Lawate PS, Bharadwaj RS, et al. Molecular profiling of mucosal tissue associated microbiota in patients manifesting acute exacerbations and remission stage of ulcerative colitis. World J Microbiol Biotechnol. 2018;34:76.

Wang D, Dubois RN, Richmond A. The role of chemokines in intestinal inflammation and cancer. Curr Opin Pharmacol. 2009;9:688-96.

Wang Y, Xu L, Gu YQ, Coleman-Derr D. MetaCoMET: a web platform for discovery and visualization of the core microbiome. Bioinformatics. 2016;32:3469-70.

Wang F, Feng J, Gao Q, Ma M, Lin X, Liu J, et al. Carbohydrate and protein intake and risk of ulcerative colitis: Systematic review and dose-response meta-analysis of epidemiological studies. Clin Nutr. 2017;36:1259-65.

Wang Y, Gao X, Ghozlane A, Hu H, Li X, Xiao Y, et al. Characteristics of Faecal Microbiota in Paediatric Crohn's Disease and Their Dynamic Changes During Infliximab Therapy. J Crohns Colitis. 2018;12:337-46.

Wang Y, Gao X, Zhang X, Xiao F, Hu H, Li X, et al. Microbial and metabolic features associated with outcome of infliximab therapy in pediatric Crohn's disease. Gut Microbes. 2021;13:1-18.

Welters CF, Heineman E, Thunnissen FB, van den Bogaard AE, Soeters PB, Baeten CG. Effect of dietary inulin supplementation on inflammation of pouch mucosa in patients with an ileal pouch-anal anastomosis. Dis Colon Rectum. 2002;45:621-7.

West NR, Hegazy AN, Owens BMJ, Bullers SJ, Linggi B, Buonocore S, et al. Oncostatin M drives intestinal inflammation and predicts response to tumor necrosis factor-neutralizing therapy in patients with inflammatory bowel disease. Nat Med. 2017;23:579-89.

Whisner CM, Castillo LF. Prebiotics, Bone and Mineral Metabolism. Calcif Tissue Int. 2018;102:443-79.

Windsor JW, Kaplan GG. Evolving Epidemiology of IBD. Curr Gastroenterol Rep. 2019;21:40.

Wirtz S, Neurath MF. Mouse models of inflammatory bowel disease. Adv Drug Deliv Rev. 2007;59:1073-83.

Wirtz S, Popp V, Kindermann M, Gerlach K, Weigmann B, Fichtner-Feigl S, et al. Chemically induced mouse models of acute and chronic intestinal inflammation. Nat Protoc. 2017;12:1295-09.

Woodland DL, Kohlmeier JE. Migration, maintenance and recall of memory T cells in peripheral tissues. Nat Rev Immunol. 2009;9:153-61.

Xia J, Wishart DS. Using MetaboAnalyst 3.0 for Comprehensive Metabolomics Data Analysis. Curr Protoc Bioinformatics. 2016;55:14.10.1-14.10.91.

Xing C, Wang M, Ajibade AA, Tan P, Fu C, Chen L, et al. Microbiota regulate innate immune signaling and protective immunity against cancer. Cell Host Microbe. 2021;29:959-74.e7.

Xu L, Shao C, Li G, Shan A, Chou S, Wang J, et al. Conversion of Broad-Spectrum Antimicrobial Peptides into Species-Specific Antimicrobials Capable of Precisely Targeting Pathogenic Bacteria. Sci Rep. 2020;10:944.

Yadav PK, Chen C, Liu Z. Potential role of NK cells in the pathogenesis of inflammatory bowel disease. J Biomed Biotechnol. 2011;2011:348530.

Yang ZW, Meng XX, Xu P. Central role of neutrophil in the pathogenesis of severe acute pancreatitis. J Cell Mol Med. 2015;19:2513-20.

Yang B, Wang Y, Qian PY. Sensitivity and correlation of hypervariable regions in 16S rRNA genes in phylogenetic analysis. BMC Bioinformatics. 2016;17:135.

Yang Y, Palm NW. Immunoglobulin A and the microbiome. Curr Opin Microbiol. 2020;56:89-96.

Yardeni T, Tanes CE, Bittinger K, Mattei LM, Schaefer PM, Singh LN, et al. Host mitochondria influence gut microbiome diversity: A role for ROS. Sci Signal. 2019;12:eaaw3159.

Yu G, Wang LG, Han Y, He QY. clusterProfiler: an R package for comparing biological themes among gene clusters. OMICS. 2012;16:284-7.

Yuk JM, Yoshimori T, Jo EK. Autophagy and bacterial infectious diseases. Exp Mol Med. 2012;44:99-108.

Zhai R, Xue X, Zhang L, Yang X, Zhao L, Zhang C. Strain-Specific Anti-inflammatory Properties of Two Akkermansia muciniphila Strains on Chronic Colitis in Mice. Front Cell Infect Microbiol. 2019;9:239.

Zhan K, Zheng H, Li J, Wu H, Qin S, Luo L, et al. Gut Microbiota-Bile Acid Crosstalk in Diarrhea-Irritable Bowel Syndrome. Biomed Res Int. 2020;2020:3828249.

Zhang YZ, Li YY. Inflammatory bowel disease: pathogenesis. World J Gastroenterol. 2014;20:91-9.

Zhao RZ, Jiang S, Zhang L, Yu ZB. Mitochondrial electron transport chain, ROS generation and uncoupling (Review). Int J Mol Med. 2019;44:3-15.

Zheng X, Huang F, Zhao A, Lei S, Zhang Y, Xie G, et al. Bile acid is a significant host factor shaping the gut microbiome of diet-induced obese mice. BMC Biol. 2017;15:120.

Zhou Y, Zhi F. Lower Level of Bacteroides in the Gut Microbiota Is Associated with Inflammatory Bowel Disease: A Meta-Analysis. Biomed Res Int. 2016;2016:5828959.

Zhou Y, Xu ZZ, He Y, Yang Y, Liu L, Lin Q, et al. Gut Microbiota Offers Universal Biomarkers across Ethnicity in Inflammatory Bowel Disease Diagnosis and Infliximab Response Prediction. mSystems. 2018;3:e00188-17.

Zhuang X, Tian Z, Feng R, Li M, Li T, Zhou G, et al. Fecal Microbiota Alterations Associated With Clinical and Endoscopic Response to Infliximab Therapy in Crohn's Disease. Inflamm Bowel Dis. 2020;26:1636-47.

Zoetendal EG, von Wright A, Vilpponen-Salmela T, Ben-Amor K, Akkermans AD, de Vos WM. Mucosa-associated bacteria in the human gastrointestinal tract are uniformly distributed along the colon and differ from the community recovered from feces. Appl Environ Microbiol. 2002;68:3401-7.

Zwolińska-Wcisło M, Budak A, Trojanowska D, Mach T, Rudnicka-Sosin L, Galicka-Latała D, et al. [The influence of Candida albicans on the course of ulcerative colitis]. Przegl Lek. 2006;63:533-8.

Zwolinska-Wcislo M, Brzozowski T, Budak A, Kwiecien S, Sliwowski Z, Drozdowicz D, et al. Effect of Candida colonization on human ulcerative colitis and the healing of inflammatory changes of the colon in the experimental model of colitis ulcerosa. J Physiol Pharmacol. 2009;60:107-18.

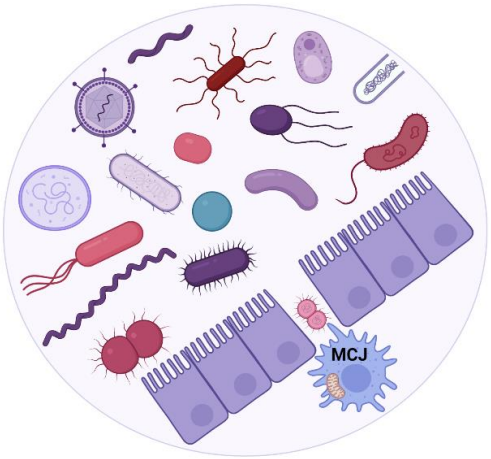

Annex

Supplementary material

1. **Chapter 1:** MCJ impact on host-gut microbiota crosstalk during acute ulcerative colitis

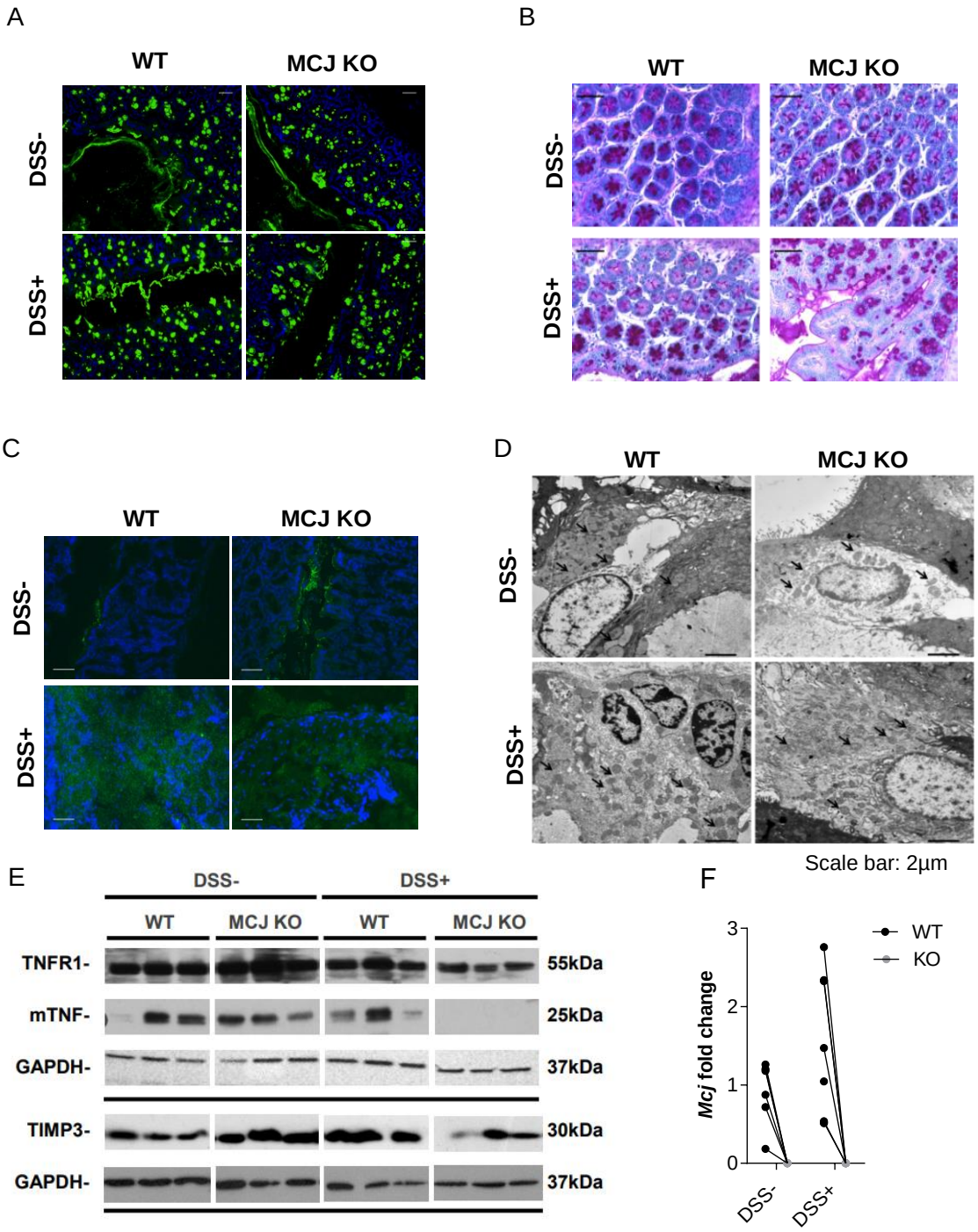

Supplementary Figure 1. Additional data of DSS-induced colitis experiment. (**A**) Representative immunostaining of Muc2 (green) and mucus layer thickness (µm) in the distal mouse colon. (**B**) Representative image of the goblet cell numbers in the distal colon. (**C**). Permeability to the tracer FITC-dextran (ng/ml). Representative images are shown. (**D**) Electron microscopy showing mitochondrial morphology in DSS induced colitis groups (Scale bar: 2µm). (**E**) Western blot refecting TIMP3, TNFR1 and TNF bound to membrane protein levels in colon tissue using GAPDH as reference. (**F**) *Mcj* gene expression levels in whole colonic tissue presented as fold change nomalized to *Rpl19* houskeeping gene. Black dots indicate WT and grey dots MCJ KO.

2. **Chapter 2:** MCJ deficiency and antibiotic-induced gut dysbiosis in colon macrophages transcriptome

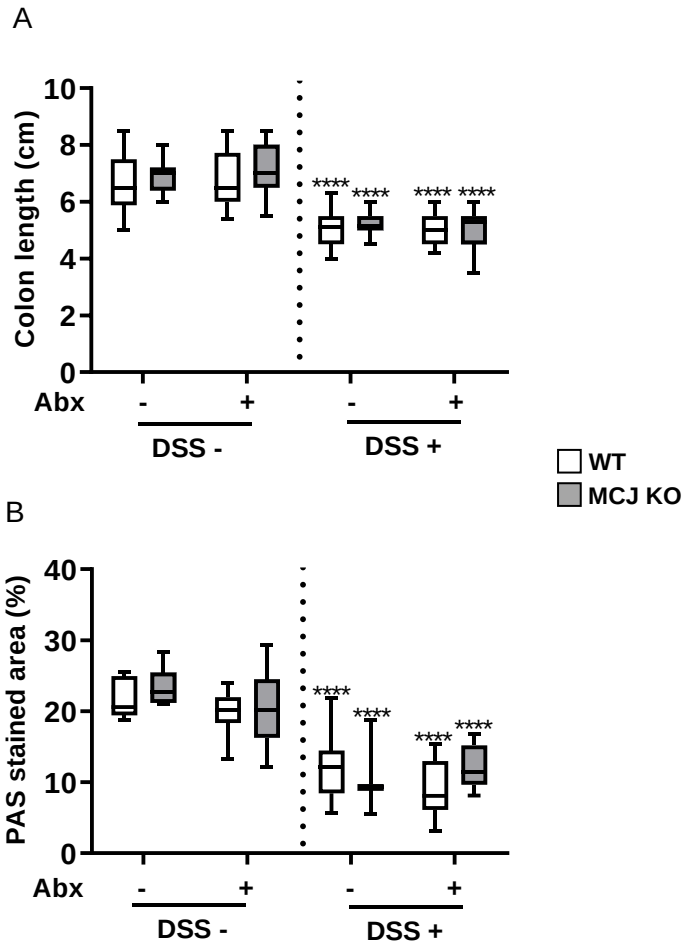

Supplementary Figure 2. Additional data of antibiotic-induced dysbiosis experiment prior to colitis induction. Experimental design: antibiotic or water were administered to WT and MCJ-deficient mice one week before DSS administration which lasted 6 days. (**A**) Colon length (cm) (n=20). (**B**) Goblet cells: % of positive cells stained with PAS (n=10). For statistical analysis two-way ANOVA was used. Statistical significance is shown by asterisks above boxes *versus* control genotype (Abx-DSS+ *vs* Abx-DSS- and Abx+DSS+ *vs* Abx+DSS-). Abx: antibiotic.

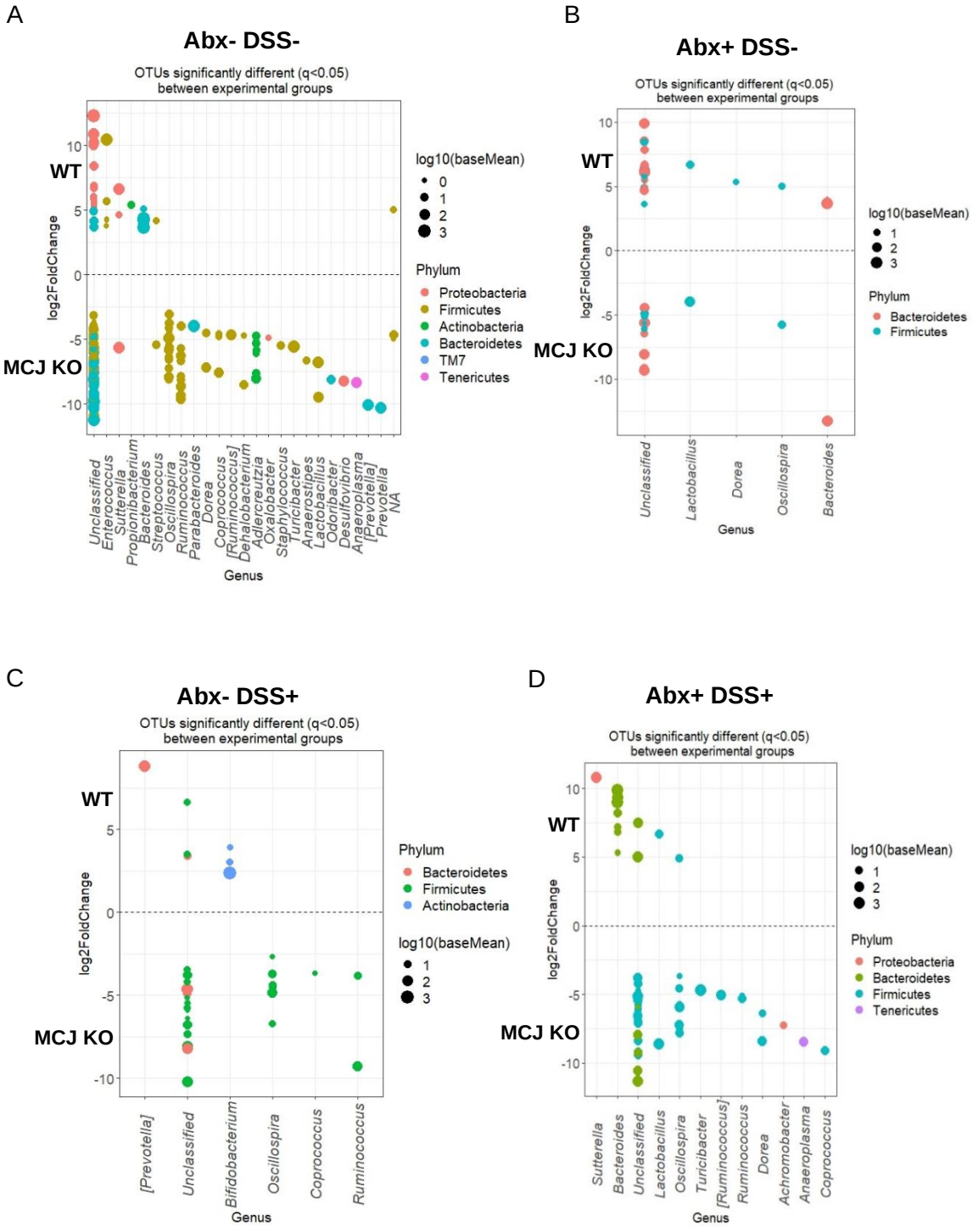
A
Abx- DSS-
OTUs significantly different (q<0.05) between experimental groups
WT
MCJ KO
log2FoldChange
log10(baseMean)
Phylum
Proteobacteria
Firmicutes
Actinobacteria
Bacteroidetes
TM7
Tenericutes
Unclassified
Enterococcus
Sutterella
Propionibacterium
Bacteroides
Streptococcus
Oscillospira
Ruminococcus
Parabacteroides
Dorea
Coprococcus
[Ruminococcus]
Dehalobacterium
Adlercreutzia
Oxalobacter
Staphylococcus
Turicibacter
Anaerostipes
Lactobacillus
Odoribacter
Desulfovibrio
Anaeroplasma
[Prevotella]
Prevotella
NA
Genus
B
Abx+ DSS-
OTUs significantly different (q<0.05) between experimental groups
WT
MCJ KO
log2FoldChange
log10(baseMean)
Phylum
Bacteroidetes
Firmicutes
Unclassified
Lactobacillus
Dorea
Oscillospira
Bacteroides
Genus
C
Abx- DSS+
OTUs significantly different (q<0.05) between experimental groups
WT
MCJ KO
log2FoldChange
log10(baseMean)
Phylum
Bacteroidetes
Firmicutes
Actinobacteria
[Prevotella]
Unclassified
Bifidobacterium
Oscillospira
Coprococcus
Ruminococcus
Genus
D
Abx+ DSS+
OTUs significantly different (q<0.05) between experimental groups
WT
MCJ KO
log2FoldChange
log10(baseMean)
Phylum
Proteobacteria
Bacteroidetes
Firmicutes
Tenericutes
Sutterella
Bacteroides
Unclassified
Lactobacillus
Oscillospira
Turicibacter
[Ruminococcus]
Ruminococcus
Dorea
Achromobacter
Anaeroplasma
Coprococcus
Genus

E

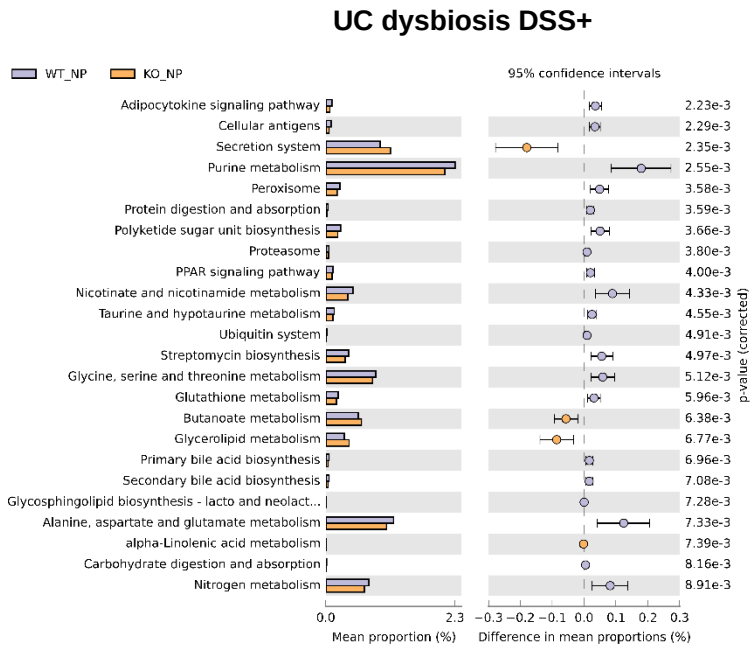

G

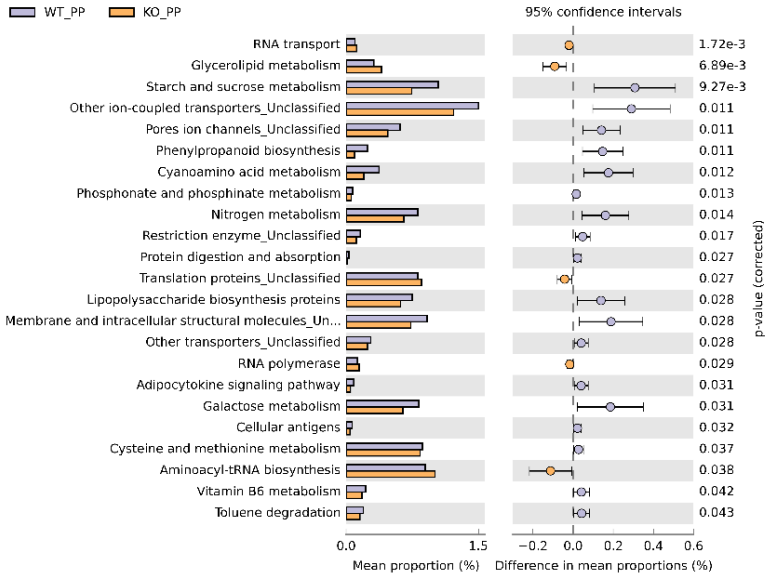

Supplementary Figure 3. Composition of host microbiome at genus level. Differential representation of OTUs (p.adj < 0.05) between WT and MCJ-deficient at genus level of (**A**) healthy (Abx-DSS-), (**B**) antibiotic-induced dysbiosis (Abx+DSS-), (**C**) colitis (Abx-DSS+) and (**D**) antibiotic-induced dysbiosis and colitis (Abx+DSS+) groups. Each point represents a single OTU colored by phylum, grouped by genus and point´s size reflect the mean abundance of the sequenced data. PICRUSt analysis for predicted metabolic function between (**E**) WT and MCJ-deficient Abx-DSS+ (NP) and (**G**) WT and MCJ-deficient Abx+DSS+ (PP). Purple represents WT and Orange MCJ KO. Abx: antibiotic; OUT: operational taxonomic unit.

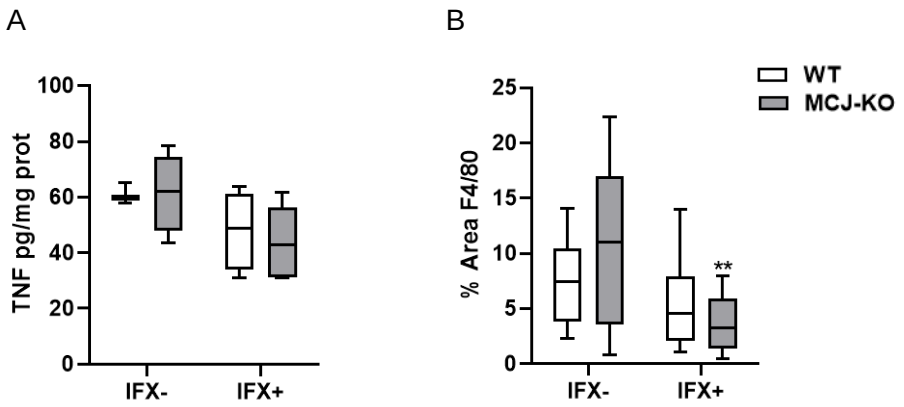

Supplementary Figure 4. Additional data of anti-TNF in vivo experiment. (**A**) TNF quantity (pg/mg prot) in colon protein extracts. (**B**) Macrophage infiltration within colonic tissue of mice treated (IFX+) or not with Infliximab (IFX-) (%). White boxplots indicate wild-type and grey boxplots indicate MCJ-deficient mice. For statistical analysis two-way ANOVA was used. Asterisks "*" above boxes *versus* control genotype (IFX+ versus IFX-).

3. **Chapter 3:** Role of the gut microbiota modulated by MCJ deficiency in the pathogenesis of UC

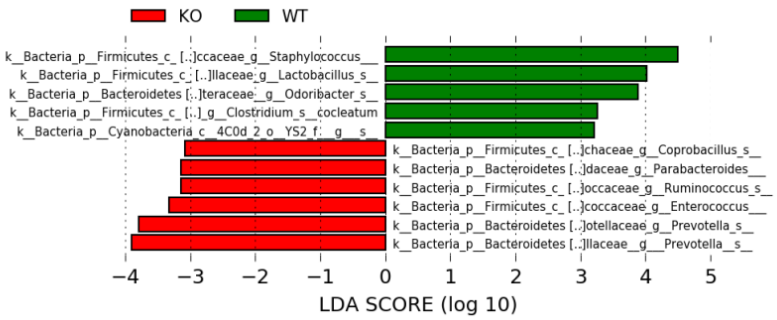

Supplementary Figure 5. LEfSe analysis from GF mice experiment. Histogram of linear discriminant analysis (LDA) effect size (LEfSe) representing statistically differential abundance between GF mice colonized with WT (shown in green) and MCJ-deficient mice (shown in red) microbial communities after colitis induction.

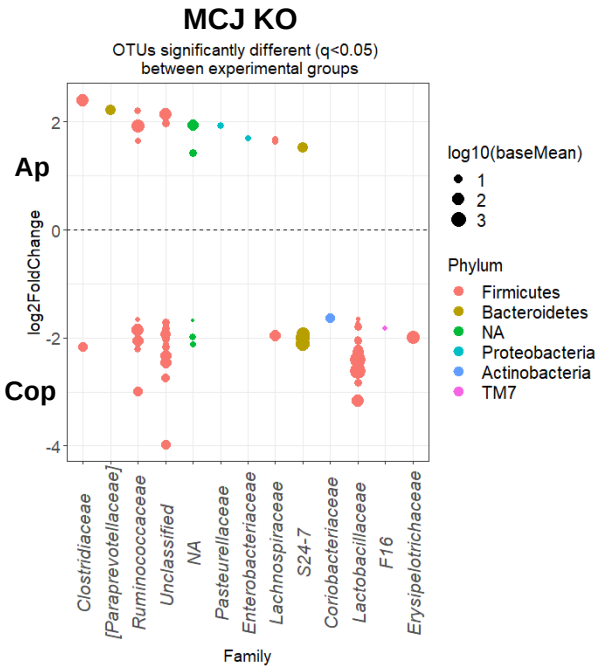

Supplementary Figure 6. Composition of host microbiome family level. Differential abundance (p.adj < 0.05) of OTUs at family level between MCJ-deficient housed alone and cohoused. Each point represents a single OTU colored by phylum, grouped by family and point´s size reflect the mean abundance of the sequenced data.